JSCSEN 86(10)901–1011(2021)

ISSN 1820-7421(Online)

Journal of the Serbian Chemical Society

Electronic version

VOLUME 86

No 10

BELGRADE 2021

Available on line at

www.shd.org.rs/JSCS/

The full search of JSCS is available through

DOAJ DIRECTORY OF OPEN ACCESS JOURNALS

www.doaj.org

The **Journal of the Serbian Chemical Society** (formerly Glasnik Hemijskog društva Beograd), one volume (12 issues) per year, publishes articles from the fields of chemistry. The **Journal** is financially supported by the **Ministry of Education, Science and Technological Development of the Republic of Serbia.**

Articles published in the **Journal** are indexed in **Clarivate Analytics products: Science Citation Index-Expanded™** – accessed *via* **Web of Science®** and **Journal Citation Reports®**.

Impact Factor announced 2020: **1.097; 5-year Impact Factor**: **1.023**.

Articles appearing in the **Journal** are also abstracted by: **Scopus, Chemical Abstracts Plus (CAplus℠), Directory of Open Access Journals, Referativnii Zhurnal (VINITI), RSC Analytical Abstracts, EuroPub, Pro Quest** and **Asian Digital Library.**

Publisher:	**Serbian Chemical Society**, Karnegijeva 4/III, P. O. Box 36, 1120 Belgrade 35, Serbia tel./fax: +381–11–3370–467, E-mails: **Society** – shd@shd.org.rs; **Journal** – jscs@shd.org.rs Home Pages: **Society** – http://www.shd.org.rs/, **Journal** – http://www.shd.org.rs/JSCS/
Internet Service:	Contents, Abstracts and full papers (from Vol 64, No. 1, 1999) are available in the electronic form at the Web Site of the **Journal** (http://www.shd.org.rs/JSCS/).
Former Editors:	**Nikola A. Pušin** (1930–1947), **Aleksandar M. Leko** (1948–1954), **Panta S. Tutundžić** (1955**–**1961), **Miloš K. Mladenović** (1962–1964), **Đorđe M. Dimitrijević** (1965–1969), **Aleksandar R. Despić** (1969–1975), **Slobodan V. Ribnikar** (1975–1985), **Dragutin M. Dražić** (1986–2006).
Editor-in-Chief:	BRANISLAV Ž. **NIKOLIĆ**, Serbian Chemical Society (E-mail: jscs-ed@shd.org.rs)
Deputy Editor:	DUŠAN **SLADIĆ**, Faculty of Chemistry, University of Belgrade
Sub editors:	
Organic Chemistry	DEJAN **OPSENICA**, Institute of Chemistry, Technology and Metallurgy, University of Belgrade JÁNOS **CSANÁDI**, Faculty of Science, University of Novi Sad
Biochemistry and Biotechnology	OLGICA **NEDIĆ**, INEP – Institute for the Application of Nuclear Energy, University of Belgrade
Inorganic Chemistry	MILOŠ **ĐURAN**, Serbian Chemical Society
Theoretical Chemistry	IVAN **JURANIĆ**, Serbian Chemical Society
Physical Chemistry	LJILJANA **DAMJANOVIĆ-VASILIĆ**, Faculty of Physical Chemistry, University of Belgrade
Electrochemistry	SNEŽANA **GOJKOVIĆ**, Faculty of Technology and Metallurgy, University of Belgrade
Analytical Chemistry	SLAVICA **RAŽIĆ**, Faculty of Pharmacy, University of Belgrade
Polymers	BRANKO **DUNJIĆ**, Faculty of Technology and Metallurgy, University of Belgrade
Thermodynamics	MIRJANA **KIJEVČANIN**, Faculty of Technology and Metallurgy, University of Belgrade
Chemical Engineering	TATJANA **KALUĐEROVIĆ RADOIČIĆ**, Faculty of Technology and Metallurgy, University of Belgrade
Materials	RADA **PETROVIĆ**, Faculty of Technology and Metallurgy, University of Belgrade
Metallic Materials and Metallurgy	NENAD **RADOVIĆ**, Faculty of Technology and Metallurgy, University of Belgrade
Environmental and Geochemistry	VESNA **ANTIĆ**, Faculty of Agriculture, University of Belgrade
History of and Education in Chemistry	DRAGICA **TRIVIĆ**, Faculty of Chemistry, University of Belgrade
English Language Editors:	LYNNE **KATSIKAS**, Serbian Chemical Society VLATKA **VAJS**, Serbian Chemical Society JASMINA **NIKOLIĆ**, Faculty of Technology and Metallurgy, University of Belgrade
Technical Editors:	VLADIMIR **PANIĆ**, ALEKSANDAR **DEKANSKI**, VUK **FILIPOVIĆ**, Institute of Chemistry, Technology and Metallurgy, University of Belgrade
Journal Manager & Web Master:	ALEKSANDAR **DEKANSKI,** Institute of Chemistry, Technology and Metallurgy, University of Belgrade
Office:	VERA **ĆUŠIĆ**, Serbian Chemical Society

Editorial Board

From abroad: **R. Adžić**, Brookhaven National Laboratory (USA); **A. Casini**, University of Groningen (The Netherlands); **G. Cobb**, Baylor University (USA); **D. Douglas**, University of British Columbia (Canada); **G. Inzelt**, Etvos Lorand University (Hungary); **N. Katsaros**, NCSR "Demokritos", Institute of Physical Chemistry (Greece); **J. Kenny**, University of Perugia (Italy); **Ya. I. Korenman**, Voronezh Academy of Technology (Russian Federation); **M. D. Lechner**, University of Osnabrueck (Germany); **S. Macura**, Mayo Clinic (USA); **M. Spiteller**, INFU, Technical University Dortmund (Germany); **M. Stratakis**, University of Crete (Grecce); **M. Swart**, University de Girona (Cataluna, Spain); **G. Vunjak-Novaković**, Columbia University (USA); **P. Worsfold**, University of Plymouth (UK); **J. Zagal**, Universidad de Santiago de Chile (Chile).

From Serbia: **B. Abramović**, **V. Antić, V. Beškoski**, **J. Csanadi**, **Lj. Damjanović-Vasilić**, **A. Dekanski**, **V. Dondur**, **B. Dunjić**, **M. Đuran, S. Gojković**, **I. Gutman**, **B. Jovančićević**, **I. Juranić**, **L. Katsikas**, **M. Kijevčanin**, **V. Leovac**, **S. Milonjić**, **V.B. Mišković-Stanković, O. Nedić**, **B. Nikolić**, **J. Nikolić, D. Opsenica**, **V. Panić**, **M. Petkovska**, **R. Petrović**, **I. Popović**, **B. Radak**, T. **Kaluđerović Radiočić, N. Radović**, **S. Ražić**, **D. Sladić**, **S. Sovilj**, **S. Šerbanović**, **B. Šolaja**, **Ž. Tešić**, **D. Trivić, V. Vajs**.

Subscription: The annual subscription rate is **150.00 €** including postage (surface mail) and handling. For Society members from abroad rate is **50.00 €**. For the proforma invoice with the instruction for bank payment contact the Society Office (E-mail: shd@shd.org.rs) or see JSCS Web Site: http://www.shd.org.rs/JSCS/, option Subscription.

Godišnja pretplata: Za članove SHD: **2.500,00 RSD**, za penzionere i studente: **1000,00 RSD**, a za ostale: **3.500,00 RSD**:za organizacije i ustanove: **16.000,00 RSD**. Uplate se vrše na tekući račun Društva: **205-13815-62**, poziv na broj **320**, sa naznakom "pretplata za JSCS".

Nota: Radovi čiji su svi autori članovi SHD prioritetno se publikuju.

Odlukom Odbora za hemiju Republičkog fonda za nauku Srbije, br. 66788/1 od 22.11.1990. godine, koja je kasnije potvrđena odlukom Saveta Fonda, časopis je uvršten u kategoriju međunarodnih časopisa (**M-23**). Takođe, aktom Ministarstva za nauku i tehnologiju Republike Srbije, 413-00-247/2000-01 od 15.06.2000. godine, ovaj časopis je proglašen za publikaciju od posebnog interesa za nauku. **Impact Factor** časopisa objavljen 2020. godine iznosi **1,097**, a petogodišnji **Impact Factor 1,023**.

INSTRUCTIONS FOR AUTHORS (2021)

GENERAL

The *Journal of the Serbian Chemical Society* (the *Journal* in further text) is an international journal publishing papers from all fields of chemistry and related disciplines. Twelve issues are published annually. The Editorial Board expects the editors, reviewers, and authors to respect the well-known standard of professional ethics.

Types of Contributions

Original scientific papers	(up to 15 typewritten pages, including Figures, Tables and References) report original research which must not have been previously published.
Short communications	(up to 8 pages) report unpublished preliminary results of sufficient importance to merit rapid publication.
Notes	(up to 5 pages) report unpublished results of short, but complete, original research
Authors' reviews	(up to 40 pages) present an overview of the author's current research with comparison to data of other scientists working in the field
Reviews[a]	(up to 40 pages) present a concise and critical survey of a specific research area. Generally, these are prepared at the invitation of the Editor
Surveys	(about 25 pages) communicate a short review of a specific research area.
Book and Web site reviews	(1 - 2 pages)
Extended abstracts	(about 4 pages) of Lectures given at meetings of the Serbian Chemical Society Divisions
Letters to the Editor	report miscellaneous topics directed directly to the Editor

[a]Generally, Authors' reviews, Reviews and Surveys are prepared at the invitation of the Editor.

Submission of manuscripts

Manuscripts should be submitted using the **OnLine Submission Form**, available on the JSCS Web Site (**http://www.shd-pub.org.rs/index.php/JSCS**). The manuscript must be uploaded as a Word.doc or .rtf file, with tables and figures (including the corresponding captions – above Tables and below Figures), placed within the text to follow the paragraph in which they were mentioned for the first time.

Please note that **Full Names (**First Name, Last Name), **Full Affiliation** and **Country** (from drop down menu) of **ALL OF AUTHORS** (written in accordance with English spelling rules - the first letter capitalized) must be entered in the manuscript Submission Form (Step 3). Manuscript Title, authors' names and affiliations, as well as the Abstract, **WILL APPEAR** in the article listing, as well as in **BIBLIOGRAPHIC DATABASES (WoS, SCOPUS...)**, in the form and in the order entered in the author details

Graphical abstract

Graphical abstract is a one-image file containing the main depiction of the authors work and/or conclusion and must be supplied along with the manuscript. It must enable readers to quickly gain the main message of the paper and to encourage browsing, help readers identify which papers are most relevant to their research interests. Authors must provide an image that clearly represents the research described in the paper. The most relevant figure from the work, which summarizes the content, can also be submitted. The image should be submitted as a separate file in **Online Submission Form - Step 2**.

Specifications: The graphical abstract should have a clear start and end, reading from top to bottom or left to right. Please omit unnecessary distractions as much as possible.

- **Image size:** minimum of 500×800 pixels (W×H) and a minimum resolution of 300 dpi. If a larger image is sent, then please use the same ratio: 16 wide × 9 high. Please note that your image will be scaled proportionally to fit in the available window in TOC; a 150x240 pixel rectangle. Please be sure that the quality of an image cannot be increased by changing the resolution from lower to higher, but only by rescanning or exporting the image with a higher resolution, which can be set in usual "settings" option.
- **Font:** Please use Calibri and Symbol font with a large enough font size, so it is readable even from the image of a smaller size (150 × 240 px) in TOC.
- **File type:** JPG and PNG only.

No additional text, outline or synopsis should be included. Please do not use white space or any heading within the image.

Cover Letter

Manuscripts must be accompanied by a cover letter (strictly uploaded in **Online Submission Step 2**) in which the type of the submitted manuscript and a warranty as given below are given. The Author(s) has(have) to warranty that the manuscript submitted to the *Journal* for review is original, has been written by the stated author(s) and has not been published elsewhere; is currently not being considered for publication by any other journal and will not be submitted for such a review while under review by the *Journal*; the manuscript contains no libellous or other unlawful statements and does not contain any materials that violate any personal or proprietary rights of any other person or entity. All manuscripts will be acknowledged on receipt (by e-mail).

Illustrations

Illustrations (Figs, schemes, photos…) in TIF or EPS format (JPG format is acceptable for colour and greyscale photos, only), must be additionally uploaded (Online Submission Step 2) as a separate file or one archived (.zip, .rar or .arj) file. Figures and/or Schemes should be prepared according to the **Artwork Instructions -** http://www.shd.org.rs/JSCS/jscs-pdf/Artwork_Instructions.pdf!

For any difficulties and questions related to **OnLine Submission Form -** https://www.shd-pub.org.rs/index.php/JSCS/submission/wizard, please refer to **User Guide -** https://openjournal-systems.com/ojs-3-user-guide/ , Chapter **Submitting an Article -** https://openjournalsystems.com/ojs-3-user-guide/submitting-an-article/. If difficulties still persist, please contact JSCS Editorial Office at **JSCS@shd.org.rs**

A manuscript not prepared according to these instructions will be returned for resubmission without being assigned a reference number.

Conflict-of-Interest Statement*: Public trust in the peer review process and the credibility of published articles depend in part on how well a conflict of interest is handled during writing, peer review, and editorial decision making. A conflict of interest exists when an author (or the author's institution), reviewer, or editor has financial or personal relationships that inappropriately influence (bias) his or her actions (such relationships are also known as dual commitments, competing interests, or competing loyalties). These relationships vary from those with negligible potential to those with great potential to influence judgment, and not all relationships represent true conflict of interest. The potential for a conflict of interest can exist whether or not an individual believes that the relationship affects his or her scientific judgment. Financial relationships (such as employment, consultancies, stock ownership, honoraria, paid expert testimony) are the most easily identifiable conflicts of interest and the most likely to undermine the credibility of the journal, the authors, and of science itself. However, conflicts can occur for other reasons, such as personal relationships, academic competition, and intellectual passion.

Informed Consent Statement*: Patients have a right to privacy that should not be infringed without informed consent. Identifying information, including patients' names, initials, or hospital numbers, should not be published in written descriptions, photographs, and pedigrees unless the information is essential for scientific purposes and the patient (or parent or guardian) gives written informed consent for publication. Informed consent for this purpose requires that a patient who is identifiable be shown the manuscript to be published. Authors should identify Individuals who provide writing assistance and disclose the funding source for this assistance. Identifying details should be omitted if they are not essential. Complete anonymity is difficult to achieve, however, and informed consent should be obtained if there is any doubt. For example, masking the eye region in photographs of patients is inadequate protection of anonymity. If identifying characteristics are altered to protect anonymity, such as in genetic pedigrees, authors should provide assurance that alterations do not distort scientific meaning and editors should so note. The requirement for informed consent should be included in the journal's instructions for authors. When informed consent has been obtained it should be indicated in the published article.

Human and Animal Rights Statement* When reporting experiments on human subjects, authors should indicate whether the procedures followed were in accordance with the ethical standards of the responsible committee on human experimentation (institutional and national) and with the Helsinki Declaration of 1975, as revised in 2000 (5). If doubt exists whether the research was conducted in accordance with the Helsinki Declaration, the authors must explain the rationale for their approach, and demonstrate that the institutional review body explicitly approved the doubtful aspects of the study. When reporting experiments on animals, authors should be asked to indicate whether the institutional and national guide for the care and use of laboratory animals was followed.

---

*International Committee of Medical Journal Editors ("Uniform Requirements for Manuscripts Submitted to Biomedical Journals"), February 2006

PROCEDURE

All contributions will be peer reviewed and only those deemed worthy and suitable will be accepted for publication. The Editor has the final decision. To facilitate the reviewing process, authors are encouraged to suggest up to three persons competent to review their manuscript. Such suggestions will be taken into consideration but not always accepted. If authors would prefer a specific person not be a reviewer, this should be announced. The Cover Letter must be accompanied by these suggestions. Manuscripts requiring revision should be returned according to the requirement of the Editor, within 60 days upon reception of the reviewing comments by e-mail.

The *Journal* maintains its policy and takes the liberty of correcting the English as well as false content of manuscripts **provisionally accepted** for publication in the first stage of reviewing process. In this second stage of manuscript preparation by JSCS Editorial Office, the author(s) may be required to supply some **additional clarifications and corrections**. This procedure will be executed during copyediting actions, with a demand to author(s) to perform corrections of unclear parts before the manuscript would be published OnLine as **finally accepted manuscript (OLF Section of the JSCS website)**. Please note that the manuscript can receive the status of **final rejection** if the author's corrections would not be satisfactory.

When finally accepted manuscript is ready for printing, the corresponding author will receive a request for proof reading, which should be performed within 2 days. Failure to do so will be taken as the authors agree with any alteration which may have occurred during the preparation of the manuscript for printing.

Accepted manuscripts of active members of the Serbian Chemical Society (all authors) have publishing priority.

MANUSCRIPT PRESENTATION

Manuscripts should be typed in English (either standard British or American English, but consistent throughout) with 1.5 spacing (12 points Times New Roman; Greek letters in the character font Symbol) in A4 format leaving 2.5 cm for margins. For Regional specific, non-standard characters that may appear in the text, save documents with Embed fonts Word option: *Save as -> (Tools) -> Save Options… -> Embed fonts in the text.*

The authors are requested to seek the assistance of competent English language expert, if necessary, to ensure their English is of a reasonable standard. The Serbian Chemical Society can provide this service in advance of submission of the manuscript. If this service is required, please contact the office of the Society by e-mail (jscs-info@shd.org.rs).

Tables, figures and/or schemes must be embedded in the main text of the manuscript and should follow the paragraph in which they are mentioned for the first time. **Tables** must be prepared with the aid of the **WORD table function**, without vertical lines. The minimum size of the font in the tables should be **10 pt**. Table columns must not be formatted using multiple spaces. Table rows must not be formatted using any returns (enter key; ↵ key) and are **limited to 12 cm width**. Tables should not be incorporated as graphical objects. **Footnotes to Tables** should follow them and are to be indicated consequently (in a single line) in superscript letters and separated by semi-column.

Table caption must be placed above corresponding Table, while **Captions of the Illustrations** (Figs. Schemes...) must follow the corresponding item. **The captions, either for Tables or Illustrations**, should make the items comprehensible without reading of the main text (but clearly referenced in), must follow numerical order (Roman for Tables, Arabic for Illustrations), and should not be provided on separate sheets or as separate files.

High resolution Illustrations (named as Fig. 1, Fig. 2… and/or Scheme 1, Scheme 2…) in **TIF or EPS format** (JPG format is acceptable for photos, only) **must be additionally uploaded as a separate files or one archived (.zip, .rar) file.**

Illustrations should be prepared according to the ARTWORK INSTRUCTIONS - http://www.shd.org.rs/JSCS/jscs-pdf/Artwork_Instructions.pdf. **!**

All pages of the manuscript must be numbered continuously.

DESIGNATION OF PHYSICAL QUANTITIES AND UNITS

IUPAC recommendations for the naming of compounds should be followed. SI units, or other permissible units, should be employed. The designation of physical quantities must be in italic throughout the text (including figures, tables and equations), whereas the units and indexes (except for indexes having the meaning of physical quantities) are in upright letters. They should be in Times New Roman font. In graphs and tables, a slash should be used to separate the designation of a physical quantity from the unit

(example: p / kPa, j / mA cm^{-2}, t / °C, T_0 / K, τ / h, ln (j / mA cm^{-2})…). Designations such as: p (kPa), t [min]…, are not acceptable. However, if the full name of a physical quantity is unavoidable, it should be given in upright letters and separated from the unit by a comma (example: Pressure, kPa; Temperature, K; Current density, mA cm^{-2}…). Please do not use the axes of graphs for additional explanations; these should be mentioned in the figure captions and/or the manuscript (example: "pressure at the inlet of the system, kPa" should be avoided). The axis name should follow the direction of the axis (the name of y-axis should be rotated by 90°). Top and right axes should be avoided in diagrams, unless they are absolutely necessary.

Latin words, as well as the names of species, should be in *italic*, as for example: *i.e.*, *e.g.*, *in vivo*, *ibid*, *Calendula officinalis* L., *etc*. The branching of organic compound should also be indicated in *italic*, for example, *n*-butanol, *tert*-butanol, *etc*.

Decimal numbers must have decimal points and not commas in the text (except in the Serbian abstract), tables and axis labels in graphical presentations of results. Thousands are separated, if at all, by a comma and not a point.

Mathematical and chemical equations should be given in separate lines and must be numbered, Arabic numbers, consecutively in parenthesis at the end of the line. All equations should be embedded in the text Complex equations (fractions, integrals, matrix…) should be prepared with the aid of the **Microsoft Equation 3.0** (or higher) or **MathType** (Do not use them to create simple equations and labels). **Using the Insert -> Equation option, integrated in MS Office 2010 and MS Office 2013, as well as insertion of equation objects within paragraph text IS NOT ALLOWED.**

ARTICLE STRUCTURE

- TITLE PAGE;
- MAIN TEXT – including Tables and Illustrations with corresponding captions;
- SUPPLEMENTARY MATERIAL (optional**)**

Title page

- **Title** in bold letters, should be clear and concise, preferably 12 words or less. The use of non-standard abbreviations, symbols and formulae is discouraged.
- AUTHORS' NAMES in capital letters with the full first name, initials of further names separated by a space and surname. Commas should separate the author's names except for the last two names when 'and' is to be used. In multi-affiliation manuscripts, the author's affiliation should be indicated by an Arabic number placed in superscript after the name and before the affiliation. Use * to denote the corresponding author(s).
- *Affiliations* should be written in italic. The e-mail address of the corresponding author should be given after the affiliation(s).
- *Abstract:* A one-paragraph abstract written of 150 – 200 words in an impersonal form indicating the aims of the work, the main results and conclusions should be given and clearly set off from the text. Domestic authors should also submit, on a separate page, an Abstract - Izvod, the author's name(s) and affiliation(s) in Serbian (Cyrillic letters). (Домаћи аутори морају доставити Извод (укључујући имена аутора и афилијацију) на српском језику, исписане ћирилицом, иза Захвалнице, а пре списка референци.) For authors outside Serbia, the Editorial Board will provide a Serbian translation of their English abstract.
- *Keywords:* Up to 6 keywords should be given. Do not use words appearing in the manuscript title
- RUNNING TITLE: A one line (maximum five words) short title in capital letters should be provided.

Main text – should have the form:

- **INTRODUCTION,**
- **EXPERIMENTAL (RESULTS AND DISCUSSION),**
- **RESULTS AND DISCUSSION (EXPERIMENTAL),**
- **CONCLUSIONS,**
- **NOMENCLATURE (optional) and**
- ***Acknowledgements*: If any.**
- REFERENCES (Citation of recent papers published in chemistry journals that highlight the significance of work to the general readership is encouraged.)

The sections should be arranged in a sequence generally accepted for publication in the respective fields. They subtitles should be in capital letters, centred and NOT numbered.

- The INTRODUCTION should include the aim of the research and a concise description of background information and related studies directly connected to the paper.
- The EXPERIMENTAL section should give the purity and source of all employed materials, as well as details of the instruments used. The employed methods should be described in sufficient detail to enable experienced persons to repeat them. Standard procedures should be referenced and only modifications described in detail. On no account should results be included in the experimental section.

Chemistry

Detailed information about instruments and general experimental techniques should be given in all necessary details. If special treatment for solvents or chemical purification were applied that must be emphasized.

Example: Melting points were determined on a Boetius PMHK or a Mel-Temp apparatus and were not corrected. Optical rotations were measured on a Rudolph Research Analytical automatic polarimeter, Autopol IV in dichloromethane (DCM) or methanol (MeOH) as solvent. IR spectra were recorded on a Perkin-Elmer spectrophotometer FT-IR 1725X. ^{1}H and ^{13}C NMR spectra were recorded on a Varian Gemini-200 spectrometer (at 200 and 50 MHz, respectively), and on a Bruker Ultrashield Advance III spectrometer (at 500 and 125 MHz, respectively) employing indicated solvents (*vide infra*) using TMS as the internal standard. Chemical shifts are expressed in ppm (δ / ppm) values and coupling constants in Hz (J / Hz). ESI-MS spectra were recorded on Agilent Technologies 6210 Time-Of-Flight LC-MS instrument in positive ion mode with CH_3CN/H_2O 1/1 with 0.2 % HCOOH as the carrying solvent solution. Samples were dissolved in CH_3CN or MeOH (HPLC grade purity). The selected values were as follows: capillary voltage = 4 kV, gas temperature = 350 °C, drying gas flow 12 L min^{-1}, nebulizer pressure = 310 kPa, fragmentator voltage = 70 V.The elemental analysis was performed on the Vario EL III- C,H,N,S/O Elemental Analyzer (Elementar Analysensysteme GmbH, Hanau-Germany). Thin-layer chromatography (TLC) was performed on precoated Merck silica gel 60 F254 and RP-18 F254 plates. Column chromatography was performed on Lobar LichroPrep Si 60 (40-63 μm), RP-18 (40-63 μm) columns coupled to a Waters RI 401 detector, and on Biotage SP1 system with UV detector and FLASH 12+, FLASH 25+ or FLASH 40+ columns pre packed with KP-SIL [40-63 μm, pore diameter 6 nm (60 Å)], KP-C18-HS (40-63 μm, pore diameter 9 nm (90 Å) or KP-NH [40-63 μm, pore diameter 10 nm (100 Å)] as adsorbent. Compounds were analyzed for purity (HPLC) using a Waters 1525 HPLC dual pump system equipped with an Alltech, Select degasser system, and dual λ 2487 UV-VIS detector. For data processing, Empower software was used (methods A and B). Methods C and D: Agylent Technologies 1260 Liquid Chromatograph equipped with Quat Pump (G1311B), Injector (G1329B) 1260 ALS, TCC 1260 (G1316A) and Detector 1260 DAD VL+ (G1315C). For data processing, LC OpenLab CDS ChemStation software was used. For details, see Supporting Information.

1. Synthesis experiments

Each paragraph describing a synthesis experiment should begin with the name of the product and any structure number assigned to the compound in the Results and Discussions section. Thereafter, the compound should be identified by its structure number. Use of standard abbreviations or unambiguous molecular formulas for reagents and solvents, and of structure numbers rather than chemical names to identify starting materials and intermediates, is encouraged.

When a new or improved synthetic method is described, the yields reported in key experimental examples, and yields used for comparison with existing methods, should represent amounts of isolated and purified products, rather than chromategraphically or spectroscopically determined yields. Reactant quantities should be reported in weight and molar units and for product yields should be reported in weight units; percentage yields should only be reported for materials of demonstrated purity. When chromatography is used for product purification, both the support and solvent should be identified.

2. Microwave experiments

Reports of syntheses conducted in microwave reactors must clearly indicate whether sealed or open reaction vessels were used and must document the manufacturer and model of the reactor, the method of monitoring the reaction mixture temperature, and the temperature-time profile. Reporting a wattage rating or power setting is not an acceptable alternative to providing temperature data. Manuscripts describing work done with domestic (kitchen) microwave ovens will not be accepted except for studies where the unit is used for heating reaction mixtures at atmospheric pressure.

3. Compound characterization

The Journal upholds a high standard for compound characterization to ensure that substances being added to the chemical literature have been correctly identified and can be synthesized in known yield and purity by the reported preparation and isolation methods. For **all new** compounds, evidence adequate to establish both **identity** and **degree of purity** (homogeneity) must be provided.

Identity *- Melting point.* All homogeneous solid products (*e.g.* not mixtures of isomers) should be characterized by melting or decomposition points. The colors and morphologies of the products should also be noted.

Specific rotations. Specific rotations based on the equation $[\alpha]^t; D = (100\ \alpha) / (l\ c)$ should be reported as unitless numbers as in the following example: $[\alpha]^{20}$; D = -25.4 (c 1.93, $CHCl_3$), where c / g mL^{-1} is concentration and l / dm is path length. The units of the specific rotation, (deg mL) / (g dm), are implicit and are not included with the reported value.

Spectra/*Spectral Data.* Important IR adsorptions should be given.

For all new diamagnetic substances, NMR data should be reported (^1H, ^{13}C, and relevant heteronuclei). ^1H NMR chemical shifts should be given with two digits after the decimal point. Include the number of protons represented by the signal, signal multiplicity, and coupling constants as needed (*J* italicized, reported with up to one digit after the decimal). The number of bonds through which the coupling is operative, ^xJ, may be specified by the author if known with a high degree of certainty. ^{13}C NMR signal shifts should be rounded to the nearest 0.01 ppm unless greater precision is needed to distinguish closely spaced signals. Field strength should be noted for each spectrum, not as a comment in the general experimental section. Hydrogen multiplicity (C, CH, CH_2, CH_3) information obtained from routine DEPT spectra should be included. If detailed signal assignments are made, the type of NOESY or COSY methods used to establish atom connectivity and spatial relationships should be identified in the Supporting Information. Copies of spectra should also be included where structure assignments of complex molecules depend heavily on NMR interpretation. Numbering system used for assignments of signals should be given in the Supporting Information with corresponding general structural formula of named derivative.

HPLC/LCMS can be substituted for biochemistry papers where the main focus is not on compound synthesis.

HRMS/*elemental analysis.* To support the molecular formula assignment, HRMS data accurate within 5 ppm, or combustion elemental analysis [carbon and hydrogen (and nitrogen, if present)] data accurate within 0.5 %, should be reported for new compounds. HRMS data should be given in format as is usually given for combustion analysis: calculated mass for given formula following with observed mass: (+)ESI-HRMS *m*/*z*: [molecular formula + H]$^+$ calculated mass, observed mass. Example: (+)ESI-HRMS *m*/*z*: calculated for [$C_{13}H_8BrCl_2N + H^+$] 327.92899, observed 327.92792.

NOTE: in certain cases, a crystal structure may be an acceptable substitute for HRMS/elemental analysis.

Biomacromolecules. The structures of biomacromolecules may be established by providing evidence about sequence and mass. Sequences may be inferred from the experimental order of amino acid, saccharide, or nucleotide coupling, from known sequences of templates in enzyme-mediated syntheses, or through standard sequencing techniques. Typically, a sequence will be accompanied by MS data that establish the molecular weight.

Example: Product was isolated upon column chromatography [dry flash (SiO_2, eluent EA, EA/MeOH gradient 95/5 → 9/1, EA/MeOH/NH_3 gradient 18/0.5/0.5 → 9/1/1, and flash chromatography (Biotage SP1, RP column, eluent MeOH/H_2O gradient 75/25 → 95/5, N-H column, eluent EA/Hex gradient 6/3 → EA). was obtained after flash column chromatography (Biotage SP NH column, eluent hexane/EA 4:6 → 2:6). Yield 968.4 mg (95 %). Colorless foam softens at 96-101 °C. $[\alpha]^{20}$; D = +0,163 (c =2.0×10^{-3} g/mL, CH_2Cl_2). IR (ATR): 3376w, 2949m, 2868w, 2802w, 1731s, 1611w, 1581s, 1528m, 1452m, 1374s, 1331w, 1246s, 1171m, 1063w, 1023m, 965w, 940w, 881w, 850w, 807w, cm^{-1}. ^1H NMR (500 MHz, $CDCl_3$, δ): 8.46 (*d*, 1H, J = 5.4, H-2'), 7.89 (*s*, 1H, J = 2.0, H-8'), 7.71 (*d*, 1H, J = 8.9, H-5'), 7.30 (*dd*, 1H, J_1 = 8.8, J_2 = 2.1, H-6'), 6.33 (*d*, 1H, J = 5.4, H-3'), 6.07 (*s*, HN-Boc, exchangeable with D_2O), 5.06 (*s*, 1H, H-12), 4.92-4.88 (*m*, 1H, H-7), 4.42 (*bs*, H-3), 3.45 (*s*,CH_3-N), 3.33 (*bs*, H-9'), 3.05-2.95 (*m*, 2H, H-11'), 2.70-2.43 (*m*, 2H, H-24) and HN, exchangeable with D_2O), 2.07 (*s*, CH_3COO), 2.04 (*s*, CH_3COO), 1.42 (*s*, 9H, $(CH_3)_3$C-N(Boc)), 0.88 (*s*, 3H, CH_3-10), 0.79 (*d*, 3H,J = 6.6, CH_3-20), 0.68 (*s*, 3H, CH_3-13). ^{13}C NMR (125 MHz, $CDCl_3$, δ): 170.34, 170.27, 151.80, 149.92, 148.87, 134.77, 128.36, 125.11, 121.43, 117.29, 99.98, 75.41, 70.82, 50.43, 49.66, 47.60, 47.33, 44.97, 43.30, 41.83, 41.48, 37.65, 36.35, 35.44, 34.89,

34.19, 33.23, 31.24, 28.79, 28.35, 27.25, 26.45, 25.45, 22.74, 22.63, 21.57, 21.31, 17.85, 12.15. (+)ESI-HRMS (*m/z*): calculated for $[C_{45}H_{67}ClN_4O_6 + H]^+$ 795.48219, observed 795.48185. Combustion analysis for $C_{45}H_{67}ClN_4O_6$: Calculated. C 67.94, H 8.49, N 7.04; found C 67.72, H 8.63, N 6.75. HPLC purity: method A: RT 1.994, area 99.12 %; method C: RT 9.936, area 98.20 %.

Purity **-** Evidence for documenting compound purity should include one or more of the following:

a) Well-resolved high field 1D ^{1}H NMR spectrum showing at most only trace peaks not attributable to the assigned structure and a standard 1D proton-decoupled ^{13}C NMR spectrum. Copies of the spectra should be included as figures in the Supporting Information.
b) Quantitative gas chromatographic analytical data for distilled or vacuum-transferred samples, or quantitative HPLC analytical data for materials isolated by column chromatography or separation from a solid support. HPLC analyses should be performed in two diverse systems. The stationary phase, solvents (HPLC), detector type, and percentage of total chromatogram integration should be reported; a copy of the chromatograms may be included as a figure in the Supporting Information.
c) Electrophoretic analytical data obtained under conditions that permit observing impurities present at the 5 % level.

HRMS data may be used to support a molecular formula assignment **but cannot be used as a criterion of purity**.

4. Biological Data

Quantitative biological data are required for all tested compounds. Biological test methods must be referenced or described in sufficient detail to permit the experiments to be repeated by others. Detailed descriptions of biological methods should be placed in the experimental section. Standard compounds or established drugs should be tested in the same system for comparison. Data may be presented as numerical expressions or in graphical form; biological data for extensive series of compounds should be presented in tabular form. Tables consisting primarily of negative data will not usually be accepted; however, for purposes of documentation they may be submitted as supporting information. Active compounds obtained from combinatorial syntheses should be resynthesized and retested to verify that the biology conforms to the initial observation.

Statistical limits (statistical significance) for the biological data are usually required. If statistical limits cannot be provided, the number of determinations and some indication of the variability and reliability of the results should be given. References to statistical methods of calculation should be included. Doses and concentrations should be expressed as molar quantities (*e.g.*, mol/kg, μmol/kg, M, mM). The routes of administration of test compounds and vehicles used should be indicated, and any salt forms used (hydrochlorides, sulfates, *etc.*) should be noted. The physical state of the compound dosed (crystalline, amorphous; solution, suspension) and the formulation for dosing (micronized, jet-milled, nanoparticles) should be indicated. For those compounds found to be inactive, the highest concentration (*in vitro*) or dose level (*in vivo*) tested should be indicated.

- The RESULTS AND DISCUSSION should include concisely presented results and there significance discussed and compared to relevant literature data. The results and discussion may be combined or kept separate.
- The inclusion of a CONCLUSION section, which briefly summarizes the principal conclusions, is recommended.
- NOMENCLATURE is optional but, if the authors wish, a list of employed symbols may be included.
- REFERENCES should be numbered sequentially as they appear in the text. Please note that any reference numbers appearing in the Illustrations and/or Tables and corresponding captions must follow the numbering sequence of the paragraph in which they appear for the first time. When cited, the reference number should be superscripted in Font 12, following any punctuation mark. In the reference list, they should be in normal position followed by a full stop. Reference entry must not be formatted using Carriage returns (enter key; ↵ key) or multiple space key. The formatting of references to published work should follow the *Journal'*s style as follows:

Journals[a]:	A. B. Surname1, C. D. Surname2, *J. Serb. Chem. Soc.* **Vol** (Year) first page Number (https://doi.org/doi)[b]
Books:	A. B. Surname1, C. D. Surname2, *Name of Book*, Publisher, City, Year, pp. 100-101 (https://doi.org/doi)[b]
Compilations:	A. B. Surname1, C. D. Surname2, in *Name of Compilation*, A. Editor1, C. Editor2, Ed(s)., Publisher, City, Year, p. 100 (https://doi.org/doi)[b]
Proceedings:	A. B. Surname1, C. D. Surname2, in *Proceedings of Name of the Conference or Symposium*, (Year), Place of the Conference, Country, *Title of the Proceeding*, Publisher, City, Year, p. or Abstract No. 100
Patents:	A. B. Inventor1, C. D. Inventor2, (Holder), Country Code and patent number (registration year)
Chemical Abstracts:	A. B. Surname1, C. D. Surname2, *Chem. Abstr*. CA 234 567a; For non-readily available literature, the Chemical Abstracts reference should be given in square brackets: [C.A. 139/2003 357348t] after the reference
Standards:	EN ISO 250: *Name of the Standard* (Year)
Websites:	Title of the website, URL in full (date accessed)

[a] When citing Journals, the International Library Journal abbreviation is required. Please consult, *e.g.*, https://images.webofknowledge.com/WOK46/help/WOS/A_abrvjt.html

[b] doi should be replaced by doi number of the Article, for example: http://dx.doi.org/10.2298/JSC161212085B (as active link). If doi do not exist, provide the link to the online version of the publication.

Only the last entry in the reference list should end with a full stop.

The names of all authors should be given in the list of references; the abbreviation *et al.* may only be used in the text. The original journal title is to be retained in the case of publications published in any language other than English (please denote the language in parenthesis after the reference). Titles of publications in non-Latin alphabets should be transliterated. Russian references are to be transliterated using the following transcriptions:

ж→zh, х→kh, ц→ts, ч→ch, ш→sh, щ→shch, ы→y, ю→yu, я→ya, э→e, й→i, ь→’.

Supplementary material

Authors are encouraged to presentthe information and results non-essential to the understanding of their paper as SUPPLEMENTARY MATERIAL (can be uploaded inStep 4 of Online Submission). This material may include as a rule, but is not limited to, the presentation of analytical and spectral data demonstrating the identity and purity of synthesized compounds, tables containing raw data on which calculations were based, series of figures where one example would remain in the main text, etc. The Editorial Board retain the right to assign such information and results to the Supplementary material when deemed fit. Supplementary material does not appear in printed form but can be downloaded from the web site of the JSCS.

Mathematical and chemical equations should be given in separate lines and must be numbered, Arabic numbers, consecutively in parenthesis at the end of the line. All equations should be embedded in the text Complex equations (fractions, integrals, matrix…) should be prepared with the aid of the Microsoft Equation 3.0 (or higher) or MathType (Do not use them to create simple equations and labels). Using the Insert -> Equation option, integrated in MS Office 2010 and MS Office 2013, as well as insertion of equation objects within paragraph text IS NOT ALLOWED.

Deposition of crystallographic data

Prior to submission, the crystallographic data included in a manuscript presenting such data should be deposited at the appropriate database. Crystallographic data associated with organic and metal-organic structures should be deposited at the Cambridge Crystallographic Data Centre (CCDC) by e-mail to **deposit@ccdc.cam.ac.uk**

Crystallographic data associated with inorganic structures should be deposited with the Fachinformationszentrum Karlsruhe (FIZ) by e-mail to **crysdata@fiz-karlsruhe.de**. A deposition number will then be provided, which should be added to the reference section of the manuscript.

For detailed instructions please visit the JSCS website:
https://www.shd-pub.org.rs/index.php/JSCS/Instructions

ARTWORK INSTRUCTIONS

JSCS accepts only **TIFF** or **EPS** formats, as well as **JPEG** format (only for colour and greyscale photographs) for electronic artwork and graphic files. **MS files** (Word, PowerPoint, Excel, Visio) **NOT acceptable**. Generally, scanned instrument data sheets should be avoided. Authors are responsible for the quality of their submitted artwork. Every single Figure or Scheme, as well as any part of the Figure (A, B, C…) should be prepared according to following instructions (every part of the figure, A, B, C…, must be submitted as an independent single graphic file):

TIFF

Virtually all common artwork and graphic creation software is capable of saving files in TIFF format. This 'option' can normally be found under 'the 'Save As...' or 'Export...' commands in the 'File' menu.

TIFF (Tagged Image File Format) is the recommended file format for bitmap, greyscale and colour images.

- Colour images should be in the RGB mode
- When supplying TIFF files, please ensure that the files are supplied at the correct resolution:
    1. Line artwork: minimum of 1000 dpi
    2. RGB image: minimum of 300 dpi
    3. Greyscale image: minimum of 300 dpi
    4. Combination artwork (line/greyscale/RGB): minimum of 500 dpi
- Images should be tightly cropped, without frame and any caption.
- If applicable please re-label artwork with a font supported by JSCS (Arial, Helvetica, Times, Symbol) and ensure it is of an appropriate font size.
- Save an image in TIFF format with LZW compression applied.
- It is recommended to remove Alpha channels before submitting TIFF files.
- It is recommended to flatten layers before submitting TIFF files.

Please be sure that quality of an image cannot be increased by changing the resolution from lower to higher, but only by rescanning or exporting the image with higher resolution, which can be set in usual "settings" facilities.

EPS

Virtually all common artwork creation software, such as Canvas, ChemDraw, CorelDraw, SigmaPlot, Origin Lab…, are capable of saving files in EPS format. This 'option' can normally be found under the 'Save As...' or 'Export...' commands in the 'File' menu.

For vector graphics, EPS (Encapsulated PostScript) files are the preferred format as long as they are provided in accordance with the following conditions:

- when they contain bitmap images, the bitmaps should be of good resolution (see instructions for TIFF files)
- when colour is involved, it should be encoded as RGB
- an 8-bit preview/header at a resolution of 72 dpi should always be included
- embed fonts should always included and only the following fonts should be used in artwork: Arial, Helvetica, Times, Symbol
- the vertical space between the parts of an illustration should be limited to the bare necessity for visual clarity
- no data should be present outside the actual illustration area
- line weights should range from 0.35 pt to 1.5 pt
- when using layers, they should be reduced to one layer before saving the image (Flatten Artwork)

JPEG

Virtually all common artwork and graphic creation software is capable of saving files in JPEG format. This 'option' can normally be found under 'the 'Save As...' or 'Export...' commands in the 'File' menu.

JPEG (Joint Photographic Experts Group) is the acceptable file format **only for colour and greyscale photographs**. JPEG can be created with respect to photo quality (low, medium, high; from 1 to 10), ensuring file sizes are kept to a minimum to aid easy file transfer. Images should have a minimum resolution of 300 dpi. Image width: minimum 3.0 cm; maximum 12.0 cm.

Please be sure that quality of an image cannot be increased by changing the resolution from lower to higher, but only by rescanning or exporting the image with higher resolution, which can be set in usual "settings" facilities.

SIZING OF ARTWORK

- JSCS aspires to have a uniform look for all artwork contained in a single article. Hence, it is important to be aware of the style of the journal.
- Figures should be submitted in black and white or, if required, colour (charged). If coloured figures or photographs are required, this must be stated in the cover letter and arrangements made for payment through the office of the Serbian Chemical Society.
- As a general rule, the lettering on an artwork should have a finished, printed size of 11 pt for normal text and no smaller than 7 pt for subscript and superscript characters. Smaller lettering will yield a text that is barely legible. This is a rule-of-thumb rather than a strict rule. There are instances where other factors in the artwork, (for example, tints and shadings) dictate a finished size of perhaps 10 pt. Lines should be of at least 1 pt thickness.
- When deciding on the size of a line art graphic, in addition to the lettering, there are several other factors to address. These all have a bearing on the reproducibility/readability of the final artwork. Tints and shadings have to be printable at the finished size. All relevant detail in the illustration, the graph symbols (squares, triangles, circles, *etc*.) and a key to the diagram (to explain the explanation of the graph symbols used) must be discernible.
- The sizing of halftones (photographs, micrographs,...) normally causes more problems than line art. It is sometimes difficult to know what an author is trying to emphasize on a photograph, so you can help us by identifying the important parts of the image, perhaps by highlighting the relevant areas on a photocopy. The best advice that can be given to graphics suppliers is not to over-reduce halftones. Attention should also be paid to magnification factors or scale bars on the artwork and they should be compared with the details inside. If a set of artwork contains more than one halftone, again please ensure that there is consistency in size between similar diagrams.

General sizing of illustrations which can be used for the Journal of the Serbian Chemical Society:

- Minimum fig. size: 30 mm width
- Small fig. size - 60 mm width
- Large fig. size - 90 mm width
- Maximum fig. size - 120 mm width

Pixel requirements (width) per print size and resolution for bitmap images:

	Image width	A	B	C
Minimal size	30 mm	**354**	**591**	**1181**
Small size	60 mm	**709**	**1181**	**2362**
Large size	90 mm	**1063**	**1772**	**3543**
Maximal size	120 mm	**1417**	**2362**	**4724**

A: 300 dpi > RGB or Greyscale image
B: 500 dpi > Combination artwork (line/greyscale/RGB)
C: 1000 dpi> Line artwork

The designation of physical quantities and graphs formatting

The designation of physical quantities on figures must be in italic, whereas the units are in upright letters. They should be in Times New Roman font. In graphs a slash should be used to separate the designation of a physical quantity from the unit (example: p / kPa, t °C, T_0 / K, τ / h, ln (j / mA cm^{-2})…). Designations such as: p (kPa), t [min]…, are not acceptable. However, if the full name of a physical quantity is unavoiable, it should be given in upright letters and separated from the unit by a comma (example: Pressure, kPa, Temperature, K…). Please do not use the axes of graphs for additional explanations; these should be mentioned in the figure captions and/or the manuscript (example: "pressure at the inlet of the system, kPa" should be avoided). The axis name should follow the direction of the axis (the name of y-axis should be rotated by 90°). Top and right axes should be avoided in diagrams, unless they are absolutely necessary. Decimal numbers must have decimal points and not commas in the axis labels in graphical presentations of results. Thousands are separated, if at all, by a comma and not a point.

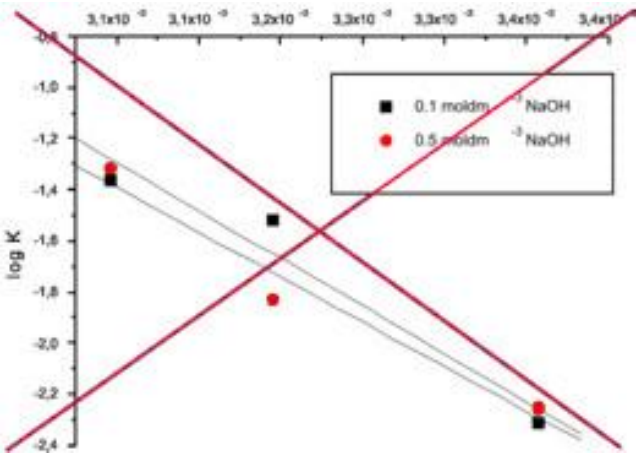

INCORRECT

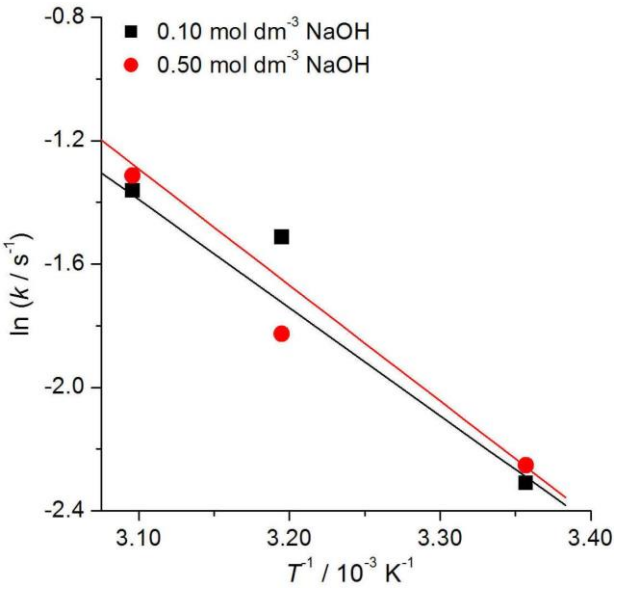

CORRECT

Journal of the Serbian Chemical Society
JSCS-info@shd.org.rs • www.shd.org.rs/JSCS

J. Serb. Chem. Soc. Vol. 86, No. 10 (2021)

CONTENTS*

Published by the Serbian Chemical Society
Karnegijeva 4/III, P.O. Box 36, 11120 Belgrade, Serbia
Printed by the Faculty of Technology and Metallurgy
Karnegijeva 4, P.O. Box 35-03, 11120 Belgrade, Serbia

* For colored figures in this issue please see electronic version at the Journal Home Page: http://www.shd.org.rs/JSCS/

Journal of the Serbian Chemical Society
JSCS@tmf.bg.ac.rs • www.shd.org.rs/JSCS
J. Serb. Chem. Soc. *86* (10) 901–915 (2021)
JSCS–5471
Original scientific paper
Published 9 September 2021

Synthesis and properties of new fused pyrrolo-1,10-phenanthroline type derivatives

CRISTINA M. AL-MATARNEH[1,2]*, IRINA ROSCA[1], SERGIU SHOVA[1] and RAMONA DANAC[2]**

[1]*"Petru Poni" Institute of Macromolecular Chemistry of Romanian Academy, 41A Grigore Ghica Voda Alley, Iasi 700487, Romania and* [2]*Chemistry Department, Faculty of Chemistry, "Al. I. Cuza" University of Iasi, 11 Carol I, Iasi 700506, Romania*

(Received 19 August 2020, revised 10 July, accepted 13 July 2021)

Abstract: New fused pyrrolo-phenanthroline type derivatives were synthesized, in two steps, from 1,10-phenanthroline and evaluated for antimicrobial activity and fluorescence properties. Our synthetic approach involved a 3+2 dipolar-cycloaddition of some selected *N*-substituted 1,10-phenanthrolin-1-ium ylides, (m)ethoxycarbonyl and cyano (1,2-di)substituted acetylenes and alkenes, respectively. The structures of compounds were supported by analytical and spectroscopic data. The molecular structures of four selected compounds have also been also determined by monocrystal XRD analyses. All synthesized compounds were then evaluated for their potential antimicrobial activity against *Staphylococcus aureus* ATCC25923, *Escherichia coli* ATCC25922 and *Candida albicans* ATCC10231. Two of the compounds demonstrated significant activity against the above tested strains.

Keywords: azahetarenes; 1,3-dipolar-cycloaddition; antimicrobial activity; fluorescence; phenanthrolinium-*N*-ylides.

INTRODUCTION

1,10-Phenanthroline is, "traditionally", a privileged moiety, being endowed with a series of significant properties such as the convenient placement of the nitrogen atoms which make it a valuable chelating bidentate ligand used for the detection or removal of metal ions, and the rigid planar structure with an extended π-conjugation, thus conferring challenging semiconducting and emissive properties. Moreover, due its specific structure, 1,10-phenanthroline has a good intercalation ability with DNA base pairs, being an excellent scaffold of choice in the generation of unique bioactive compounds.[1–3]

*,** Corresponding authors. E-mail: (*)almatarneh.cristina@icmpp.ro; (**)rdanac@uaic.ro
https://doi.org/10.2298/JSC200819057A

1,10-Phenanthroline derivatives have found various uses in domains like solid-state device technology, particularly organic light emitting diodes (OLEDs),[4,5] luminescence[6] or pharmacology.[7–10]

However, the main drawback of using 1,10-phenanthroline derivatives as drugs consists of their toxicity given by its intrinsic chelating nitrogen atoms that can inhibit diverse metalloenzymes.[8] Therefore, an adopted strategy for the reduction of the toxicity, without affecting the planar geometry of 1,10-phenanthroline mandatory for the DNA intercalation, is the "locking" of one of the nitrogen atoms. This can involve, for example, the quaternization of one of the nitrogen atoms by forming monoquaternary salts,[7,8] or the synthesis of fused 1,10-phenanthroline compounds in which just one nitrogen atom is bridgehead.[7]

On the other hand, the fusion of two or more heterocyclic rings is a well-known strategy leading to new classes of condensed heterosystems, many of them providing different properties against to the initial ones.

On the other hand, pyrrole is equally an important nitrogen containing heterocycle, largely documented in pharmaceuticals, agrochemicals, solar batteries, OLED's and organic semiconductors chemistry.[11–13]

Fluorine incorporation into biologically active molecules confers modifications in their chemical, physical, and biological properties. From the medicinal point of view, this is an important motif because of its stereoelectronic properties.[14] The trifluoromethyl group can increase lipophilicity of a molecule to improve its *in vivo* transport. Also, the formation of secondary metabolites is reduced because of the strength of the C-F bond.[15]

Using some structural combination strategies, several series of fused pyrrolophenanthroline derivatives were so far reported to possess not only bio-impact, but also other interesting properties, in order to increase the structural diversity of the potential biological active compounds.[16-18]

From the synthetic point of view, the methods for obtaining pyrrolo[1,2-*a*]-[1,10]phenanthrolines are very limited. 1,3-Dipolar cycloaddition reactions of phenanthrolinium *N*-ylides to π-deficient alkynes or alkenes is one of the most useful strategies to afford pyrrolo-phenanthroline derivatives.[19–22] Multicomponent condensation reactions,[23-24] different cyclization reactions including domino-Knoevenagel-cyclization,[22,25] or one pot four component microwave-assisted reactions[18,26] are the additional reported pathways to form pyrrolo[1,2-*a*]-[1,10]phenanthroline fused system.

As a continuation of our research focused on phenanthrolines fused systems[27–30] and as part of our concern in the field of biologically active compounds,[31–35] the purpose of our present study was to synthesize new 1,10-phenanthroline derivatives having one of its *N*-atoms locked in order to ensure a potential bio-activity (by maintaining the rings coplanarity and reducing the toxicity due to *N*-atoms internal chelating propensity). Thus, herein we report the syn-

thesis, structure, fluorescence and the *in vitro* antimicrobial evaluation of several new 1,10-phenanthroline derivatives.

EXPERIMENTAL

Chemistry

Melting points were recorded on an A. Krüss Optronic melting point meter KSPI and are uncorrected. 1D-, 2D-, ^{1}H- and ^{13}C-NMR spectra were recorded on a Bruker Avance III 500 instrument operating at 500 or 125 MHz for ^{1}H- and ^{13}C nuclei, respectively. All chemical shifts (δ values) are given in parts per million (ppm); all homo- and heterocoupling patterns (^{n}J values) are given in Hertz (Hz). No TMS was added, chemical shifts were measured against the solvent peak. IR spectra were recorded on a FTIR Shimadzu or Jasco 660 plus FTIR spectrophotometer. Thin layer chromatography (TLC) was carried out on Merck silica gel 60F_{254} plates. Visualization of the plates was achieved using a UV lamp (λ_{max} = 254 or 365 nm). UV–Vis spectra were recorded on a Lambda 35, Perkin Elmer spectrometer. Fluorescence measurements were carried out using a Fluoromax 4, Horiba fluorescence spectrophotometer. All commercially available products were used without further purification unless otherwise specified.

*General procedure for synthesis of salts **3***

To an acetone (5mL) solution containing 1,10-phenanthroline (1 mmol), the corresponding 4-(tri)fluoro(methyl)phenacyl bromide (1.1 mmol) was added. The reaction mixture was stirred at room temperature over the night. After this period, the resulted suspension was filtered off and the solid was washed with acetone to give the desired product.

The following compounds were synthesized:

- 1-[2-(4-Fluorophenyl)-2-oxoethyl]-1,10-phenanthrolin-1-ium bromide (**3a**);
- 1-[2-(4-Trifluoromethylphenyl)-2-oxoethyl]-1,10-phenanthrolin-1-ium bromide (**3b**).

*General procedure for synthesis of compounds **4**–**7***

At room temperature and under inert atmosphere, to a dichloromethane (5 mL) suspension containing the cycloimmonium salt (1 mmol) and dipolarophile (dimethylacetylene dicarboxylate (DMAD), ethyl propiolate (EP), acrylonitrile or fumarodinitrile, 1.1 mmol) triethylamine (TEA, 3 mmol) was added dropwise over 1 h with vigorous stirring. The reaction mixture was then stirred over the night at room temperature (rt). Methanol (5 mL) was added and the resulting mixture was kept over the night without stirring. The resulted suspension was filtered off to give a solid that was washed with methanol. The crude product was then crystallized from an appropriate solvent (reported in Supplementary material to this paper for each compound).

The following compounds were synthesized:

- Dimethyl 11-(4-fluorobenzoyl)-10,11-dihydropyrrolo[1,2-*a*][1,10]phenanthroline-9,10--dicarboxylate (**4a**);
- Dimethyl 11-[4-(trifluoromethyl)benzoyl]-10,11-dihydropyrrolo[1,2-*a*][1,10]phenanthroline-9,10-dicarboxylate (**4b**);
- Ethyl 11-(4-fluorobenzoyl) pyrrolo[1,2-a][1,10]phenanthroline-9-carboxylate (**5a**);
- Ethyl 11-[4-(trifluoromethyl)benzoyl]pyrrolo[1,2-a][1,10]phenanthroline-9-carboxylate (**5b**);
- 11-(4-Fluorobenzoyl)-10,11-dihydropyrrolo[1,2-a][1,10]phenanthroline-9-carbonitrile (**6a**);
- 11-[4-(Trifluoromethyl)benzoyl]-10,11-dihydropyrrolo[1,2-a][1,10]phenanthroline-9--carbonitrile (**6b**);

• 11-(4-Fluorobenzoyl)-8a,9-dihydropyrrolo[1,2-a][1,10]phenanthroline-9,10-dicarbonitrile (**7a**);

• 11-[4-(Trifluoromethyl)benzoyl]-8a,9,10,11-tetrahydropyrrolo[1,2-a][1,10]phenanthroline-9-carbonitrile (**7b**).

The physical and spectral data for compounds **3**–**7** are provided in the Supplementary material of this paper.

X-Ray crystallography

X-ray diffraction measurements were carried out with a Rigaku Oxford-Diffraction Xcalibur E CCD diffractometer equipped with graphite-monochromated MoKα radiation. Single crystals were positioned at 40 mm from the detector and 325 frames were measured each for 30 s over 1° scan width. The unit cell determination and data integration were carried out using the CrysAlis package of Oxford Diffraction.[36] The structures were solved by Intrinsic Phasing using Olex2[37] software with the SHELXT[38] structure solution program and refined by the full-matrix least-squares on F^2 with SHELXL-2015[39] using an anisotropic model for non-hydrogen atoms. All H atoms were introduced in idealized positions (d_{CH} = 0.96 Å) using the riding model with their isotropic displacement parameters fixed at 120 % of their riding atom. The molecular plots were obtained using the Olex2 program. The crystallographic data and the refinement details are given in Table S-I (Supplementary material to this paper) as CCDC 2056678 (for **4b**), 2015662 (for **6a**), 2056679 (for **6b**) and 2056680 (for **7b**). These data can be obtained free of charge from the Cambridge Crystallographic Data Centre *via* www.ccdc.cam.ac.uk/data_request/cif.

Photophysical investigations (UV–Vis and fluorescence spectra)

Spectroscopic grade solvents were used for the photophysical characterization of the synthesized derivatives. UV–Vis measurements were performed on a Lambda 35 device (Perkin Elmer, USA). The absorption spectra were measured in the 270–700 nm range for identical sample volumes (3 mL) with the following parameters: slit width 1 nm, scan speed 480 nm/ /min and data interval 1 nm. The spectra of the samples were measured at room temperature using 1 cm path length quartz cuvettes. The UV–Vis absorption and the emission spectra of 1,10-phenanthroline derivatives employed in this study were recorded in dilute solution (2×10^{-7} mol/L) using dimethylsulfoxide (DMSO). Fluorescence measurements were carried out using a FluoroMax-4 spectrophotometer (Horiba, Kyoto, Japan). The emission spectra were collected using an excitation wavelength of 292 nm.

Antimicrobial activity

The antimicrobial activity was determined by disk diffusion assay against three different reference strains: *Staphylococcus aureus* ATCC25923, *Escherichia coli* ATCC25922 and *Candida albicans* ATCC10231. All microorganisms were stored at –80 °C in 20 % glycerol. The bacterial strains (*S. aureus* and *E. coli*) were refreshed in Mueller-Hinton broth at 36±1 °C, and the yeast strain (*C. albicans*) was refreshed on Sabouraud dextrose broth at 36±1 °C. Microbial suspensions were prepared with these cultures in sterile solution in order to obtain the turbidity optically comparable to that of 0.5 McFarland standards (yielding a suspension containing 10^8 CFU mL^{-1} for all the microorganisms).

Volumes of 0.4 mL from each inoculum were spread onto Mueller–Hinton agar and Sabouraud dextrose agar and all the tested samples were added after the medium surface dried. The sterilized paper discs (6 mm) were placed on the plate and an aliquot (20 μL) of the tested compounds (concentration 100 mg/mL, dissolved in DMSO) was added on the paper discs. As controls it was used Trimethoprim 98 % (TMP, Acros Organics, New Jersey, USA)

against the bacterial strains and nystatin 85+ % (NS) (Acros Organics, New Jersey, USA) against the yeast strain at the same concentrations as the tested compounds. To evaluate the antimicrobial properties, the growth inhibition was measured under standard conditions after 24 h of incubation at 36±1 °C. After the incubation, the diameters of inhibition zones were measured by using Image-J software. Minimum inhibitory concentration (*MIC*) was determined from a 10-dilution series starting from 100 mg/mL.

RESULTS AND DISCUSSION

Synthesis and characterization

Our strategy to access the pyrrolo[1,2-*a*][1,10]phenanthroline skeleton involved a two steps sequence including first the monoquaternization of 1,10-phenanthroline, and second, the 3+2 dipolar-cycloaddition of the azomethine ylides, generated *in situ* from the monoquaternary salts, to different dipolarophiles.

Thus, monoquaternary salts **3a** and **b** were obtained with excellent yields by an *N*-alkylation reaction of 1,10-phenanthroline **1** with 2-bromo-4'-fluoroacetophenone **2a** or 2-bromo-4'-trifluoromethylacetophenone **2b** (Scheme 1). Compound **3a** was previously reported, the analytical data being in accordance to the literature.[40]

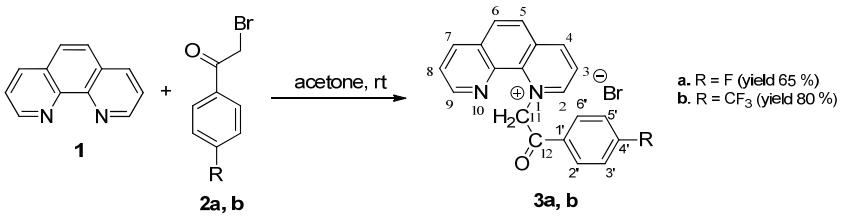

1 **2a, b** **3a, b**

Scheme 1. Synthesis of monoquaternary salts **3a** and **b**.

Next step was the dipolar cycloaddition of the ylides **4'a** and **b** (generated *in situ* upon triethylamine treatment from the corresponding salts **3a** and **b**) to dimethylacetylene dicarboxylate (DMAD) and ethyl propiolate (EP), respectively (Scheme 2).

An earlier insight concerning the cycloadditions of the *N*-ylide **3'a** to DMAD and EP was previously reported by Dumitrascu *et al*., using similar reaction conditions.[41] While, from the reaction of **3'a** with EP, only one single regioisomer of the expected aromatic pyrrolo[1,2-*a*][1,10]phenanthroline **5a** has been isolated in accordance with the reported data,[41] the reaction of **3'a** with DMAD, led, to the new 10,11-dihydropyrrolo[1,2-*a*][1,10]phenanthroline derivative **4a** (Scheme 2) in a moderate yield. The compound **4a** was different with respect to the those reported in Ref 41 (a mixture of similar substituted 8*a*,9-dihydropyrrolo[1,2-*a*][1,10]phenanthroline and pyrrolo[1,2-*a*][1,10]phenan-throline derivatives) by the position of the double bond in the pyrrole ring. Thus, our NMR data of compound **4a** clearly revealed that the double bond was, in fact,

located between C-3 and C-3a atoms of the fused pyrrole ring. Similarly, the compounds **4b** and **5b** were also obtained in the reaction between *N*-ylide **3'b** with DMAD and EP, respectively.

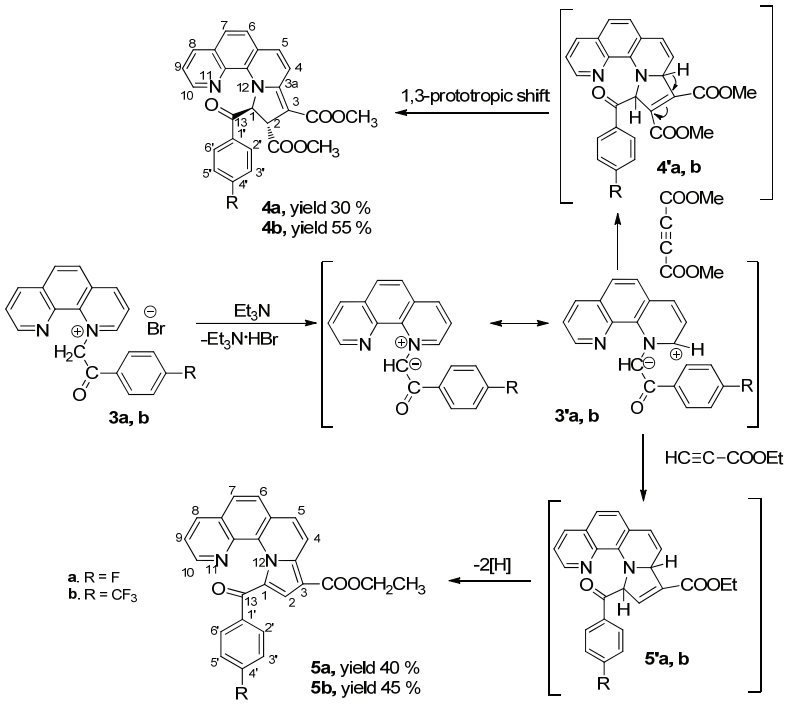

Scheme 2. Proposed reaction pathways for the synthesis of compounds **4a** and **b** and **5a** and **b**.

Thus, it was assumed that the cycloaddition resulted initially in the formation of no isolable 8*a*,11-dihydropyrrolo[1,2-*a*][1,10]phenanthroline intermediates **4'a** and **b** and **5'a** and **b**, respectively, which next underwent different pathways: an oxidative aromatization in case of **5'a** and **b** (converting them into the more stable aromatic compounds, **5a** and **b**) and a 1,3-protopropic shift (initiated by the excess of TEA) in the case of **4'a** and **b** leading to the compounds **4a** and **b** (Scheme 2).

By comparing the magnitude of the coupling pattern $^{3}J_{H,H}$(H-1/H-2), exhibited by compound **4a** (5.0 Hz), with the ones reported for other similar compounds (4.8 Hz), whose X-ray molecular structure displayed the geometry of the dihydropyrrole ring,[40] it was clear that substituents at C-1 and C-2 were located in a *trans*-configuration, *i.e.*, 1S*, 2S*. Next, spectral data (IR, NMR) of compound **5a** were in accordance with those reported in the literature.[40]

Next, the similar conditions were created (dichloromethane as solvent at room temperature) for the cycloaddition of the *N*-ylide **3'a** and **b** to acrylonitrile

and fumarodinitrile, respectively (Scheme 3). Each reaction afforded just a single regioisomeric (**3a** and **b** → **6a** and **b**) or diastereomeric (**3a** → **6a**, but **3b** → **7b**) product. Thus, in the case of salt **3a**, the both compounds obtained **6a** and **7a** proved to possess a 10,11-dihydropyrrolo[1,2-*a*][1,10]phenanthroline structure (Scheme 3). In the case of salt **3b** (issued from the reaction with fumarodinitrile), the compound **6b** with 8a,9,10,11-tetrahydropyrrolo[1,2-*a*][1,10]phenanthroline structure was produced, while in the case of reaction with acrylonitrile, the compound **7b** with 10,11-dihydropyrrolo[1,2-*a*][1,10]phenanthroline structure was isolated (Scheme 3). Compounds **6a** and **b** and **7a** were formed during the subsequent partial oxidation of a tetrahydropyrrolo[1,2-*a*][1,10] phenanthroline type intermediates, which is supposed to be formed in the first stage.[20]

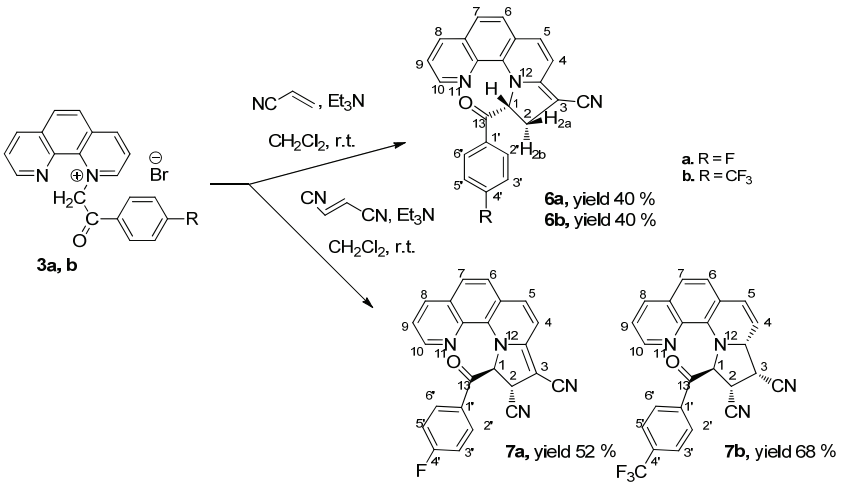

Scheme 3. Synthesis of compounds **6a** and **b** and **7a** and **b**.

As for compound **4a** and also in the case of compound **7a**, we re-found the same size of the coupling pattern, namely $^{3}J_{H,H}$(H-1/H-2) = 5.0 Hz, that we assigned, once again, to a *trans*-arrangement (1S*, 2S*) of the ligands –CN and 4-fluorobenzoyl.

All (poly)chiral compounds **4a, b**, **7a** and **7b** were obtained as major racemates.

The results of X-ray diffraction study for compounds **4b**, **6a**, **6b** and **7b** are shown in Fig. 1. The selected bond distances and angles are summarized in Table S-I of trhe Supplementary material. According to X-ray crystallography, all the compounds crystallized with one molecule in the asymmetric part. There is no co-crystallized solvent molecule in all the crystals. As it was expected, due to steric hindrance, all the molecules exhibit essentially non-planar conformation. The dihedral angle between two sets of co-planar atoms were found to be of 74.83(8), 87.88(16), 99.1(3) and 110.2(1) for **4b**, **6a**, **6b** and **7b**, respectively.

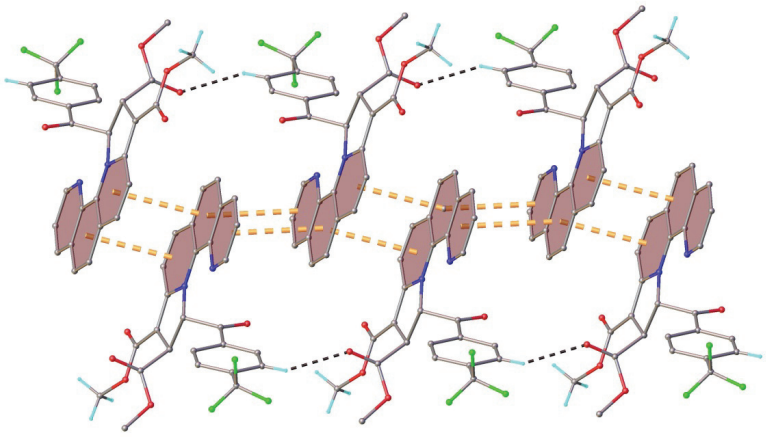

Fig. 1. X-ray molecular structure of compounds: **4b** (a) as (14S, 15S), **6a** (b) as (15R), **6b** (c) as (15S) and **7b** (d) as (12R, 13R, 14S, 15S) enantiomers with atom labelling and thermal ellipsoids at 50 % level.

Further investigation of the crystal structures packing revealed the presence of one-dimensional arrays of the neutral molecules determined by C–H···O intermolecular hydrogen bonding along with π–π stacking interactions in **4b** and **6a** (Figs. 2 and 3). In the absence of π–π stacking, the supramolecular chains in **6b** and **7b** (Figs. 4 and 5) were formed due to C–H···N (for **6b**) and C–H···N and C–H···O hydrogen bonds (for **7b**), respectively.

Photophysical investigations

The electronic absorption spectra of 1,10-phenanthroline derivatives exhibited three main absorption bands located in the following domains: 350–410 nm (α band), 295–325 nm (p band) and 250–280 nm (β band), Fig. 6. All electronic absorption spectra kept still up the fine structure, specific for the phenanthrene spectrum.[42] The nature of the (di-, tetra)hydropyrrole ring together with that if its substituents exerted an important influence on the position of the absorption and the emission bands of phenanthroline derivatives. Thus, the presence of CN or COOMe groups in position C-3 of the pyrrole like moiety resulted in a blue shift of the absorption and emission bands of phenanthroline derivatives (**4** and **7**). Moreover, the unique insertion of a CN group at C-3 position only, or in duplicate, in C-2 and C-3 positions of the (di-, tetra)hydropyrrole ring of compounds **7a** and **b** promoted the appearance of a new absorption band at 530 nm. The replacement of fluorine atom in compounds **3a**–**7a** with trifluoromethyl group in compounds **3b**–**7b** led to an increase as tenfold of the absorbance.

The fluorescence spectra of 1,10-phenanthroline derivatives **3**–**7** in DMSO displayed two emission bands located around 230 and 335 nm (Fig. 7).

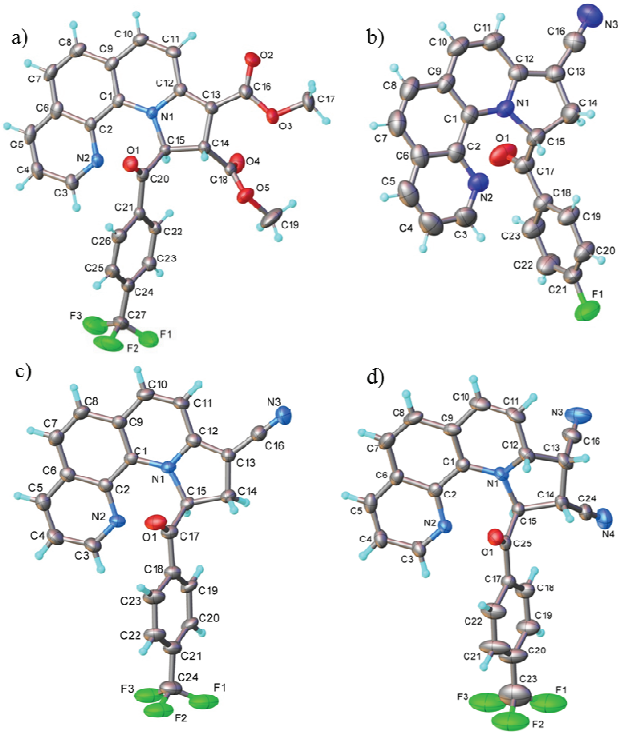

Fig. 2. The role of π-π stacking and H-bonds in the formation of 1D homochiral supramolecular array in the crystal structure of compound **4b**. H-bonds and centroid-to-centroid distances are shown as dashed black and orange lines, respectively. H-bonds parameters: 254–H···O4 [C25–H 0.95 Å, H···O4 2.47 Å, C25···O4(x, y – 1, z) 3.3295(6) Å, ∠C25HO4 145.6°].

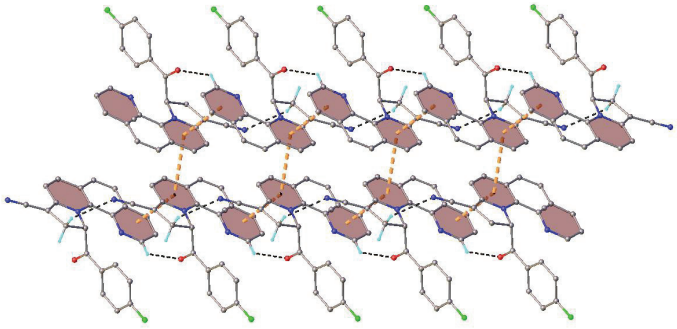

Fig. 3. The role of π-π stacking and H-bonds in the formation of 1D homochiral supramolecular array in the crystal structure of compound **6a**. H-bonds and centroid-to-centroid distances are shown as dashed black and orange lines, respectively. H-bonds parameters: C3–H···O1 [C3–H 0.93 Å, H···O1 2.43 Å, C3···O1(x, 1 + y, z) 3.166(4) Å, ∠C3HO1 135.8°]; C20–H···N3 [C20–H 0.93 Å, H···N3 2.65 Å, C20···N3(0.5 - x, 1.5 + y, 0.5 - z) 3.571(4) Å, ∠C20HN3 171.1°].

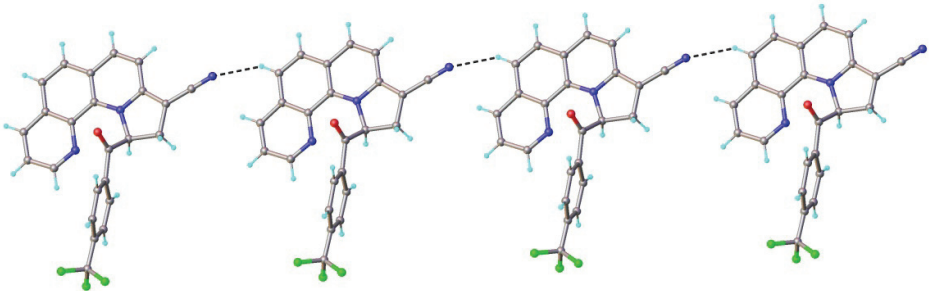

Fig. 4. One-dimensional homochiral supramolecular architecture in the crystal structure of compound **6b**. H-bond parameters: C7–H···N3 [C7–H 0.95 Å, H···N3 2.60 Å, C7···N3(*x*- 1,*y* - 1, *z*) 3.453(5) Å, ∠C7HN3 150.1°].

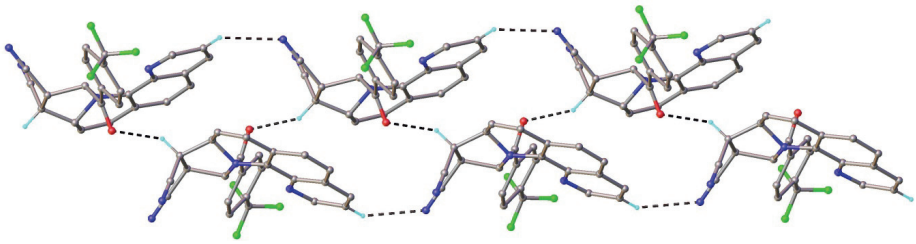

Fig. 5. One-dimensional homochiral supramolecular architecture in the crystal structure of compound **7b**. H-bonds parameters: C4–H···N4 [C4–H 0.95 Å, H···N4 2.60 Å, C4···N4(*x*, *y* – 1, *z*) 3.392(6) Å, ∠C4HN4 130.1°]; C13–H···O1 [C13–H 1.00 Å, H···O1 2.21 Å, C13···O1(-*x*, 0.5 + *y*, 0.5 - *z*) 3.042(5) Å, ∠C13HN4 139.4°].

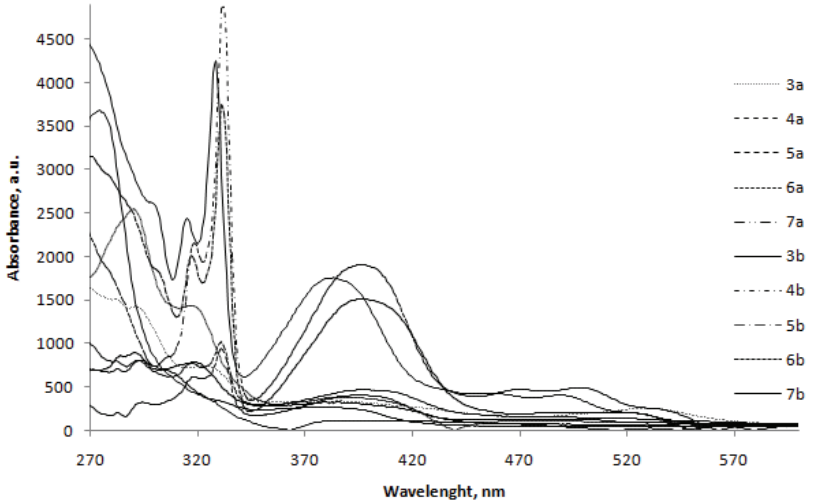

Fig. 6. UV–Vis absorption spectra in DMSO of pyrrolo[1,2-*a*][1,10]phenanthroline compounds **3**–**7**.

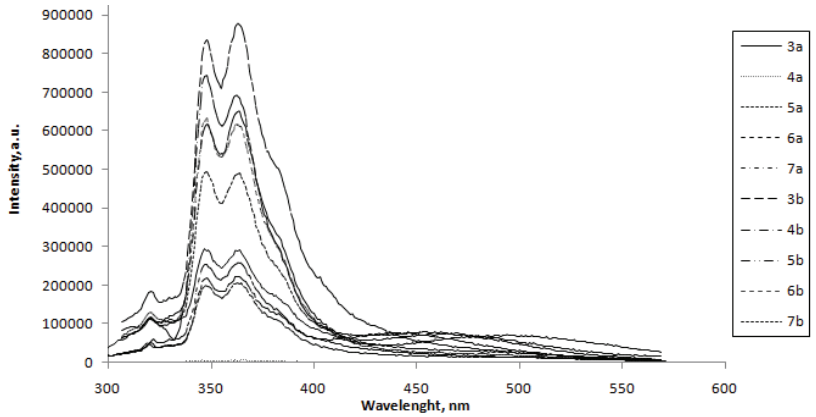

Fig. 7. Fluorescence spectra of substituted pyrrolo[1,2-*a*][1,10]phenanthroline derivatives **3**-**7a**, **b** in DMSO.

These emission bands were broad and structureless. In the case of compounds **7a** and **7b**, the appearance of a third band at about 445 nm, was also observed. As shown in Fig. 4, compound **4a** displayed no emissive properties. Usually, the fluorescence spectra of compounds with similar skeleton are substituent dependent, and in this case small differences were registered for the investigated compounds. Finally, we note the fluorescence emission being threefold increased when fluorine from compound **3-7a** was replaced with trifluoromethyl group in compounds **3**–**7**.

Antimicrobial activity

Our group has previously reported several 1,10-phenanthrolinium monoquaternary salts[7], possessing antibacterial and antifungal activities. Within this context, we tested all synthesized compounds **3**–**7** against both Gram-positive *S. Aureus* and Gram-negative *E. coli* strains, but also against *C. albicans* fungus. The antimicrobial evaluation revealed that only compounds **3a, b** proved antimicrobial activity, especially compound **3b** against the yeast strain represented by *C. Albicans* (up to 45 mm of inhibition zone). The minimum inhibitory concentration (*MIC*) values for compound **3b** were 3.125 mg/ml against *S. Aureus* and *C. Albicans* and 6.25 mg/ml against *E. coli*, respectively.

When compared with the control specimens, even if they proved to be efficient against *S.aureus* and *E. coli*, their activity was not better than the known antibiotic trimethoprim (TMP). In the same time compound **3b** proved to be by far more efficient in fighting *C. albicans* than the ordinary antifungal drug represented by nystatin (NS). Data on the average diameters of the inhibition zones for the tested compounds are presented in Table I. These results suggests that the chemical modification of 1,10-phenanthroline by locking one nitrogen atom *via* quaternization with *p*-(tri)fluoro(methyl)phenacyl moiety can be beneficial for

the antimicrobial activity (as we reported earlier[7]), while the locking by bridging a nitrogen atom into fused pyrrolo[1,2-*a*][1,10]phenanthroline leaded to the loss of antibacterial properties.

TABLE I. Antimicrobial activity of the controls and compounds **3a** and **b** against the references strains; **3a** did not show activity against *C. albicans* ATCC10231

c mg mL^{-1}	Diameter of inhibition zone ± *SD*, mm							
	S. aureus ATCC25923			*E. coli* ATCC25922			*C. albicans* ATCC10231	
	TMP	**3a**	**3b**	TMP	**3a**	**3b**	NS	**3b**
100	41.15±0.01	25.0±0.1	31±2	41.42±0.03	25.0±0.2	23.5±0.9	29.77±0.06	46±1
50	40.17±0.01	23.48±0.05	28.4±0.1	40.3±0.2	22.0±0.2	23.4±0.1	29.3±0.1	36.0±0.6
25	38.33±0.06	22.0±0.2	21.4±0.6	40.3±0.2	13.69±0.05	19.8±0.6	28.6±0.6	31.3±0.8
12.5	36.7±0.1	17.3±0.1	16.4±0.9	40.24±0.01	11.60±0.13	16.5±0.5	28.6±0.2	25.6±0.4
6.25	35.89±0.01	15.1±0.2	11±1	39.38±0.01	–	11±1	27.30±0.05	22.1±0.4
3.125	32.5±0.2	–	8.2±0.6	38.3±0.2	–	–	26.8±0.1	14.3±0.1

CONCLUSION

The synthesis and structure of novel fused 10,11-dihydropyrrolo[1,2-*a*]-[1,10]phenanthroline were presented. The cycloadducts were obtained *via* 3+2 dipolar-cycloaddition reactions to (un)symmetrically substituted π-deficient alkynes and alkenes as dipolarophiles. The cycloadditions to unsymmetrically substituted dipolarophiles (acrylonitrile and ethyl propiolate) occurred with complete regioselectivity, under charge control. The monocrystal X-ray diffraction analysis of (poly)chiral compounds **4b**, **6a** and **b** and **7b** proved unambiguously the compounds structure and the configuration of the (di-, tetra)hydropyrrole ring and brings remarkable information concerning lattice structure.

The absorption and emissive properties of (di)hydropyrrolo[1,2-*a*][1,10]phenanthroline derivatives in DMSO were substituent dependent and the introduction of trifluoromethyl substituent in benzoyl *para*-position led to a significant increase of both absorbance and emission properties. The antimicrobial activity of the synthesized compounds was measured, the salt **3b** proved to be very efficient against *S. aureus* and *C. Albicans*, with *MIC* values of 3.125 and 6.25 mg/ml, respectively.

SUPPLEMENTARY MATERIAL

Additional data and information are available electronically at the pages of journal website: https://www.shd-pub.org.rs/index.php/JSCS/article/view/9813, or from the corresponding author on request.

Acknowledgement. We thank the POSCCE-O 2.2.1, SMIS-CSNR 13984-901, Project no. 257/28.09.2010, CERNESIM, for the NMR experiments.

ИЗВОД

СИНТЕЗА И ОСОБИНЕ НОВИХ КОНДЕНЗОВАНИХ ДЕРИВАТА ПИРОЛ-1,10-ФЕНАНТРОЛИНА

CRISTINA M. AL MATARNEH[1,2], IRINA ROSCA[1], SERGIU SHOVA[1] и RAMONA DANAC[2]

[1]*"PetruPoni" Institute of Macromolecular Chemistry of Romanian Academy, 41A Grigore Ghica Voda Alley, Iasi 700487, Romania* и [2]*Chemistry Department, Faculty of Chemistry, "Al. I. Cuza" University of Iasi, 11 Carol I, Iasi 700506, Romania*

Синтетисана је нова серија деривата пирол-1,10-фенантролина у два реакциона корака, полазећи од 1,10-фенантролина и испитана је њихова антимикробна активност и флуоресцентне карактеристике. Описан синтетички приступ укључује 3+2 диполарну циклоадицију одабраних *N*-супституисаних-1,10-фенантролин-1-иум-илида, (m)етоксикарбонил и циано(1,2-ди)супституисаних ацетилена и алкена, редом. Структура синтетисаних једињења је потврђена аналитичким и спектроскопским подацима. Осим тога, молекулска структура четири одабрана једињења је одређена XRD анализом монокристала. Испитана је антимикробна активност свих синтетисаних једињења према *Staphylococcus aureus* ATCC25923, *Escherichia coli* ATCC25922 и *Candida albicans* ATCC10231.

(Примљено 19. августа 2020, ревидирано 10. јула, прихваћено 13. јула 2021)

REFERENCES

1. W. Huang, L. Wang, H. Tanaka, T. Ogawa, *Eur. J. Inorg. Chem*. **10** (2009) 1321 (https://doi.org/10.1002/ejic.200801131)
2. L. Ming, L. Xiu-Liang, W. Li-Rong, H. Zhi-Qiang, *Org. Lett.* **15** (2013) 1262 (https://doi.org/10.1021/ol400191b)
3. E. Szajdzinska-Pietek, M. Pinteala, S. Schlick, *Polymer* **45** (2004) 4113 (https://doi.org/10.1016/j.polymer.2004.03.101)
4. L. Leontie, I. Druta, R. Danac, G.I. Rusu, *Synth. Met.* **155** (2005) 138 (https://doi.org/10.1016/j.synthmet.2005.07.342)
5. M. Prelipceanu, O. S. Prelipceanu, L. Leontie, R, Danac, *Phys. Lett. A***368** (2007) 331 (http://dx.doi.org/10.1016/j.physleta.2007.04.013)
6. G. Accorsi, A. Listorti, K. Yoosaf, N. Armaroli, *Chem. Soc. Rev.* **38** (2009) 1690 (https://doi.org/10.1039/B806408N)
7. I. Druta, R. Danac, M. Ungureanu, G. Grosu, G. Drochioiu, *Ann. Pharm. Fr.* **60** (2002) 348 (https://pubmed.ncbi.nlm.nih.gov/12378146/)
8. A. Abebe, M. Atlabachew, M. Liyew, E. Ferede, *Cogent Chemistry* **4** (2018) 1476077 (https://doi.org/10.1080/23312009.2018.1476077)
9. L. Viganor, O. Howe, P. Mc Carron, M. Mc Cann, M. Devereux, *Curr. Top. Med. Chem.* **17** (2017) 1280 (https://doi.org/10.2174/1568026616666161003143333)
10. D. Wesselinova, M. Neykov, N. Kaloyanov,R.Toshkova, G. Dimitrov, *Eur. J. Med. Chem.* **44** (2009) 2720 (https://doi.org/10.1016/j.ejmech.2009.01.036)
11. L. Leontie, I. Druta, R. Danac, M. Prelipceanu, G.I. Rusu, *Prog. Org. Coat*. **54** (2005) 175 (https://doi.org/10.1016/j.porgcoat.2005.06.003)
12. A. Rotaru, R. Danac, I. Druta, G. Drochioiu, I. Cretescu, *Rev. Chim*. **56** (2005) 179 (https://revistadechimie.ro/Articles.asp?ID=570)
13. O. Gunaydin, L. Toppare, Y. Yagci, V. Harabagiu, M. Pinteala, B.C. Simionescu, *Polym. Bull.* **47(6)** (2002) 501 (https://doi.org/10.1007/s002890200014)

14. E.Maftei, C. V. Maftei, P. G. Jones, M. Freytag, M. H. Franz, G.Kelter, H.-H.Fiebig, M.Tamm, I. Neda, *Helv. Chim. Acta* **99** (2016) 469 (https://doi.org/10.1002/hlca.201500529)
15. C. V. Maftei, E. Fodor, P. G. Jones, C. G. Daniliuc, M. H. Franz, G. Kelter, H.-H. Fiebig, M. Tamm, I. Neda, *Tetrahedron* **72** (2016) 1185 (https://doi.org/10.1016/j.tet.2016.01.011)
16. L. Leontie, R. Danac, N. Apetroaei, G.I. Rusu, *Mater. Chem. Phys*. **127** (2011) 471 (https://doi.org/10.1016/j.matchemphys.2011.02.040)
17. R. Danac, L. Leontie, A. Carlescu, G. I. Rusu, *Mater. Chem. Phys*. **134** (2012) 1042 (https://doi.org/10.1016/j.matchemphys.2012.03.110)
18. I. Dhinamkaran, V. Padmini, K. Ganesan, K. Selvarasu, *Chemistry Select* **2** (2017) 6154 (https://doi.org/10.1002/slct.201700819)
19. R. Danac, A. Rotaru, G. Drochioiu, I. Druta, *J. Heterocycl. Chem.* **40** (2003) 283 (https://doi.org/10.1002/jhet.5570400213)
20. R. Danac, M. Constantinescu, A. Rotaru, A. Vlahovici, I. Cretescu, I. Druta, *Rev. Chim*. **56** (2005) 85 (https://revistadechimie.ro/Articles.asp?ID=546)
21. F. Dumitrascu, C. I. Mitan, *Tetrahedron Lett.* **42** (2001) 8379 (https://doi.org/10.1016/S0040-4039(01)01803-2)
22. M. Li, X.L. Lv, L. R. Wen, Z.Q. Hu, *Chem. Res. Chin. Univ.* **29** (2013) 1089 (https://doi.org/10.1007/s40242-013-3224-2)
23. G. Marandi, N. Hazeri, M. T. Maghsoodlou, S. M. Habibi-Khorassani, N. Akbarzadeh Torbati, F. Rostami Charati, B. W. Skelton, M. Makhad, *J. Heterocyclic Chem.* **50** (2013) 568 (https://doi.org/10.1002/jhet.1532)
24. Y. Kitahara, T. Mizuno, A. Kubo, *Tetrahedron* **60** (2004) 4283 (https://doi.org/10.1016/j.tet.2004.03.057)
25. R. Heydari, B. Tahamipour, *Chin. Chem. Lett.* **22** (2011) 1281 (https://doi.org/10.1016/j.cclet.2011.05.035)
26. C. M. Al-Matarneh, C. Ciobanu, V. Mangalagiu, G. Zbancioc, R. Danac, *Rev. Chim.* **71** (2020) 287 (https://doi.org/10.37358/RC.20.3.7998)
27. C. M. Al-Matarneh, M. O. Apostu, I. I. Mangalagiu, R. Danac, *Tetrahedron* **72** (2016) 4230 (https://doi.org/10.1016/j.tet.2016.05.061)
28. C. M. Al-Matarneh, C. Ciobanu, M. O. Apostu, I. I. Mangalagiu, R. Danac, *C. R. Chim.* **21** (2018) 1 (https://doi.org/10.1016/j.crci.2017.11.003)
29. C. M. Al-Matarneh, D.L. Isac, R. Tigoianu, R. Danac, A. Airinei, *J. Lumin.* **199** (2018) 6 (https://doi.org/10.1016/j.jlumin.2018.03.005)
30. C. M. Al-Matarneh, R. Danac, L. Leontie, F. Tudorache, I. Petrila, F. Iacomi, A. Carlescu, G. Nedelcu, I. I. Mangalagiu, *Environ. Eng. Manage. J.* **14** (2015) 420 (https://doi.org/10.30638/eemj.2015.044)
31. C. M. Al-Matarneh, S. Shova, I. I. Mangalagiu, R. Danac, *J. Enz. Inhib. Med. Chem.* **31** (2016) 470 (https://doi.org/10.3109/14756366.2015.1039530)
32. C. M. Al-Matarneh, M. C. Sardaru, M. O. Apostu, I. Rosca, C. Ciobanu, I. I. Mangalagiu, R. Danac, *Studia UBB Chemia* **LXIV** (2019) 67 (https://doi.org/10.24193/subbchem.2019.3.06)
33. C. M. Al-Matarneh, R. M. Amarandi, A. M. Craciun, I. I. Mangalagiu, G. Zbancioc, R. Danac, *Molecules* **25** (2020) 527 (https://doi.org/10.3390/molecules25030527)
34. A. Rotaru, G. Pricope, T. N. Plank, L. Clima, E. L. Ursu, M. Pinteala, J. T. Davis, M. Barboiu, *Chem. Comm.* **53** (2013) 12668 (https://doi.org/10.1039/C7CC07806D)

35. M. C. Sardaru, A. M. Craciun, C. M. Al Matarneh, I. A. Sandu, R. M. Amarandi, L. Popovici, C. I. Ciobanu, D. Peptanariu, M. Pinteala, I. I. Mangalagiu, R. Danac, *J. Enz. Inhib. Med. Chem.* **35** (2020) 1581 (https://doi.org/10.1080/14756366.2020.1801671)
36. *Rigaku Oxford Diffraction*, CrysAlisPro software system version 1.171.38.46, Rigaku Corporation, Oxford, 2015
37. O. V. Dolomanov, L. J. Bourhis, R. J. Gildea, J. A. K. Howard, H. J. Pushmann, *Appl. Crystallogr.* **42** (2009) 339 (https://doi.org/10.1107/S0021889808042726)
38. G. M. Sheldrick, *Acta Crystallogr., A* **71** (2015) 3 (https://doi.org/10.1107/S2053273314026370)
39. G. M. Sheldrick, *Acta Crystaalogr*., *C* **71** (2015) 3 (http://dx.doi.org/10.1107/S2053229614024218)
40. F. Dumitrascu, C. Draghici, M. R. Caira, L. Barbu, *Rev. Chim*. **56** (2005) 521 (https://revistadechimie.ro/Articles.asp?ID=649)
41. F. Dumitrascu, M. R. Caira, C. Draghici, M. T. Caproiu, L. Barbu, *Rev. Chim.* **60** (2009) 851 (https://revistadechimie.ro/Articles.asp?ID=2338)
42. N. S. Kozlov, K. N. Gusak, V. A. Serzhanina, L. F. Gladchenko, N. A. Krot, K. Getorotsikl, *Chem. Heterocycl. Compd*. **23** (1987) 1329 (https://doi.org/10.1007/BF00472258).

Journal of the Serbian Chemical Society
JSCS@tmf.bg.ac.rs • www.shd.org.rs/JSCS
J. Serb. Chem. Soc. 86 (10) S175–S185 (2021) *Supplementary material*

SUPPLEMENTARY MATERIAL TO

Synthesis and properties of new fused pyrrolo-1,10-phenanthroline type derivatives

CRISTINA M. AL-MATARNEH[1,2]*, IRINA ROSCA[1], SERGIU SHOVA[1] and RAMONA DANAC[2]**

[1]*"Petru Poni" Institute of Macromolecular Chemistry of Romanian Academy, 41A Grigore Ghica Voda Alley, Iasi 700487, Romania and* [2]*Chemistry Department, Faculty of Chemistry, "Al. I. Cuza" University of Iasi, 11 Carol I, Iasi 700506, Romania*

J. Serb. Chem. Soc. 86 (10) (2021) 901–915

PHYSICAL AND SPECTRAL DATA FOR THE SYNTHESIZED COMPOUNDS

*1-(2-(4-fluorophenyl)-2-oxoethyl)-1,10-phenanthrolin-1-ium bromide (**3a**)*

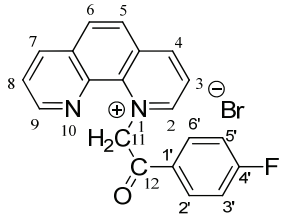

Pink powder, mp = 277-279 ºC, yield: 65%. Spectral data are in accordance to the literature.[40] Obtained by general procedure, at room temperature in acetone. Pink powder, mp = 277-279 ºC, yield: 65 %. IR (KBr): 3062, 3027; 2986, 2916 1687 1595, 1531, 1230 cm^{-1}. ^1H NMR (500 MHz, DMSO-d6, δ(ppm)): 9.66 (1H, dd, J = 6.0, 1.0 Hz, H-2), 9.61 (1H, dd, J = 8.5, 1.0 Hz, H-4), 8.78 (1H, dd, J = 8.0, 1.5 Hz, H-9), 8.63 (1H, dd, J = 8.5, 6.0 Hz, H-3), 8.50 (3H, m, H-7, H-5, H-6,), 8.30 (2H, m, H-2', 6'), 7.91 (1H, dd, J = 8.0, 4.0 Hz, H-8), 7.60 (2H, m, H-3', 5'), 7.29 (2H, as, H-11). ^{13}C RMN (125 MHz, DMSO-d6, δ(ppm)): 189.4 C-12, 165.5 (d, $J_{C,F}$ = 251.0 Hz, C-4'), 152.1 C-2, 148.8 C-9, 148.2 C-4, 138.4 C-10a, 138.0 C-7, 136.2 C-10b, 132.0 C-4a, 131.5 C-6a, 131.3 (d, $J_{C,F}$ = 10 Hz, C-2', C-6'), 131.0 (d, $J_{C,F}$ = 2.5 Hz, C-1'), 130.7 C-5, 127.0 C-6, 125.5 C-8, 124.3 C-3, 116.4 (d, $J_{C,F}$= 22.5 Hz, C-3', C-5'), 69.5 C-11. Combustion analysis for $C_{20}H_{14}BrFN_2O$: Calculated. C 60.47, H 3.55, N 7.05; found C 60.49, H 3.53, N 7.08.

*,** Corresponding authors. E-mail: (*)almatarneh.cristina@icmpp.ro; (**)rdanac@uaic.ro

*1-(2-oxo-2-(4-(trifluoromethyl)phenyl)ethyl)-1,10-phenanthrolin-1-ium bromide (**3b**)*

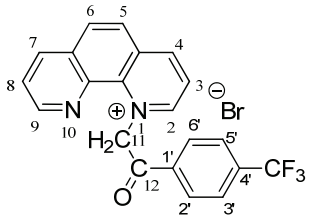

Obtained by general procedure, at room temperature in acetone. Pink powder, mp = 212-215 ºC, yield: 80 %. IR (KBr): 2988, 2918, 1691, 1630, 1585, 1321, 1230, 1175, 1126, 1065 cm^{-1}. ^1H NMR (500 MHz, DMSO-d6, δ(ppm)): 9.65 (1H, d, *J* = 5.5 Hz, H-2), 9.62 (1H, dd, *J* = 8.5, 1.0 Hz, H-4), 9.20 (1H, dd, *J* = 4.5, 1.5 Hz, H-9), 8.80 (1H, dd, *J* = 8.5, 1.5 Hz, H-7), 8.64 (1H, dd, *J* = 8.5, 6.0 Hz, H-3), 8.51 (1H, d, *J* = 9.0 Hz, H-6), 8.49 (1H, d, *J* = 9.0 Hz, H-5), 8.40 (2H, d, *J* = 8.0 Hz, H-2', 6'), 8.13 (2H, d, *J* = 8.0 Hz, H-3', 5'), 8.00 (1H, dd, *J* = 8.5, 4.5 Hz, H-8), 7.30 (2H, bs, H-11). ^{13}C RMN (125 MHz, DMSO-d6, δ(ppm)): 190.0 C-12, 152.1 C-2, 148.7 C-9, 148.3 C-4, 138.2 C-10a, 138.1 C-7, 137.6 C-1', 136.1 C-10b, 133.3 (q, $J_{C,F}$ = 31.3 Hz, C-4'), 132.1 C-4a, 131.5 C-6a, 130.8 C-5, 129.1 (C-2', C-6'), 127.1 C-6, 124.9 C-3, 124.6 C-8, 123.8 (q, $J_{C,F}$ = 270.0 Hz, CF_3), 126.4 (q, $J_{C,F}$= 3.8 Hz, C-3',C-5'), 69.6 C-11. Combustion analysis for $C_{21}H_{14}BrF_3N_2O$: Calculated. C 56.39, H 3.16, N 6.26; found C 56.40, H 3.14, N 6.28.

*Dimethyl 11-(4-fluorobenzoyl)-10,11-dihydropyrrolo[1,2-a][1,10]phenanthroline-9,10-dicarboxylate (**4a**)*

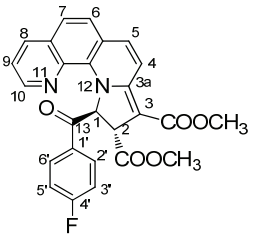

Crystallized from methanol-chloroform 1:1, (v/v). Red crystals, mp = 235-237 ºC, yield: 30 %. IR (KBr): 3070, 2954, 2920, 1749, 1688, 1627, 1592, 1566, 1497, 1230, 1119, 1047 cm^{-1}. ^1H-NMR (500 MHz, $CDCl_3$, δ(ppm)): 8.13 (2H, m, H-2', H-6'), 7.96 (1H, d, *J* = 4.5 Hz, H-10), 7.92 (1H, d, *J* =7.5 Hz, H-4), 7.79 (1H, d, *J* = 8.5 Hz, H-8), 7.56 (1H, d, *J* = 5.0 Hz, H-1), 7.26 (1H, d, *J* = 7.5 Hz, H-5), 7.25 (2H, bs, H-6, H-7), 7.19 (2H, m, H-3', H-5'), 7.13 (1H, dd, *J* = 8.5; 4.5 Hz, H-9), 4.00 (1H, d, *J*= 5.0 Hz, H-2), 3.72 (3H, s, CH_3), 3.62 (3H, s, CH_3). ^{13}C-RMN (125 MHz, $CDCl_3$, δ(ppm)): 189.3 C-13, 173.9 CO_{ester}, 166.1 CO_{ester}, 166.0 (d, $J_{C,F}$= 253.75 Hz, C-4'), 155.3 C-3a, 146.5 C-10, 137.6 C-7, 136.6 C-4, 135.8 C-11b, 132.0 (d, $J_{C,F}$= 8.75 Hz, C-2', C-6'), 130.1 (d,

$J_{C,F}$= 3.75 Hz, C-1'), 126.9 C-6, 126.1 C-7a, C-11a, 125.6 C-5a, 122.0 C-9, 121.0 C-5, 119.7 C-8, 116.2 (d, J_{C-F}= 21.25 Hz, C-3', C-5'), 88.2 C-3, 71.3 C-1, 52.9 CH_3, 50.6 CH_3, 49.6 C-2. Combustion analysis for $C_{26}H_{19}FN_2O_5$: Calculated. C 68.12, H 4.18. N 6.11; found C 68.15, H 4.15, N 6.14.

*Dimethyl 11-(4-(trifluoromethyl)benzoyl)-10,11-dihydropyrrolo[1,2-a][1,10]phenanthroline-9,10-dicarboxylate (**4b**)*

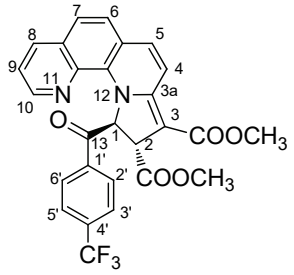

Crystallized from methanol-chloroform 1:1, (v/v). Red crystals, mp = 225-226 ºC, yield: 55 %. IR (KBr): 3022, 2953, 1728, 1690, 1630, 1585, 1547, 1463, 1230, 1115, 1065 cm^{-1}. ^{1}H-NMR (500 MHz, $CDCl_3$, δ(ppm)): 8.29 (2H, d, *J* = 8.0 Hz, H-2', H-6'), 8.02 (1H, d, *J* = 8.0 Hz, H-4), 7.97 (1H, d, *J* = 4.5 Hz, H-10), 7.85-7.89 (3H, overlapped signals, H-3', H-5', H-8), 7.62 (1H, d, *J* = 4.0 Hz, H-1), 7.44-7.48 (2H, overlapped signals, H-6, H-7), 7.37 (1H, d, *J* = 8.5 Hz, H-5), 7.23 (1H, dd, *J* = 7.5; 4.0 Hz, H-9), 4.07 (1H, d, *J* = 4.5 Hz, H-2), 3.79 (s, 3H, CH_3), 3.70 (s, 3H, CH_3). ^{13}C-RMN (125 MHz, $CDCl_3$, δ(ppm)): 189.23 C-13, 173.7 CO_{ester}, 166.0 CO_{ester}, 155.1 C-3a, 146.5 C-10, 137.4 C-7, 136.8 C-4, 136.6 (C-1'), 135.6 C-11b, 134.8 (q, $J_{C,F}$= 31.3 Hz, C-4'), 130.5 C-7a, 129.8 (C-2', C-6'), 127.0 (C-6, C-5a), 126.0 (C-3', C-5', C-11a), 122.1 C-9, 123.76 (q, $J_{C,F}$= 271.3 Hz, CF_3), 121.1 C-5, 119.8 C-8, 88.2 C-3, 71.3 C-1, 53.0 CH_3, 50.6 CH_3, 49.5 C-2. Combustion analysis for $C_{27}H_{19}F_3N_2O_5$: Calculated. C 63.78, H 3.77, N 5.51; found C 63.80, H 3.76, N 5.53.

*Ethyl 11-(4-fluorobenzoyl) pyrrolo[1,2-a][1,10]phenanthroline-9-carboxylate (**5a**)*

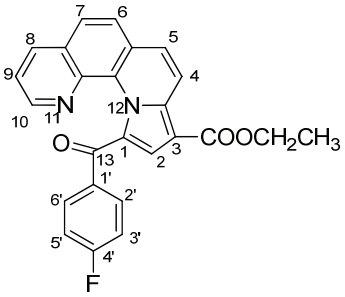

Crystallized from methanol-chloroform 1:1, (v/v). Yellow crystals, mp = 162-164 °C, yield: 40 %. IR (KBr): 2981, 1697, 1645, 1596, 1226, 1121 cm^{-1}.

^{1}H-NMR (500 MHz, $CDCl_3$, δ(ppm)): 8.58 (1H, d, J = 9.5 Hz, H-4), 8.33 (1H, bs, H-8), 8.44 (1H, bs, H-10), 8.15 (2H, bs, H-2', H-6'), 7.94 (1H, d, J = 8.5 Hz, H-7), 7.87 (1H, d, J = 8.5 Hz, H-6), 7.72 (1H, d, J = 9.5 Hz, H-5), 7.50 (1H, m, H-9), 7.53 (1H, s, H-2), 7.21 (2H, at, J = 8.5 Hz, H-3', H-5'), 4.40 (2H, q, J = 7.0 Hz, CH_2), 1.42 (3H, t, J = 7.0 Hz, CH_3). ^{13}C-RMN (125 MHz, $CDCl_3$, δ(ppm)): 191.4 C-13, 164.6 CO_{ester}, 165.2 (d, $J_{C,F}$ = 252.5 Hz, C-4'), 157.4 C-3a, 145.9 C-10, C-11b, 137.4 C-8, 134.9 (d, $J_{C,F}$ = 3.75 Hz, C-1'), 131.9 (d, $J_{C,F}$ = 8.75 Hz, C-2', C-6'), 127.4 C-7, 127.9 C-7a, C-11a, 125.7 C-5, 125.1 C-5a, 125.0 C-6, 122.8 C-9, 121.0 C-4, C-2, 115.7 (d, J_{C-F} = 21.25 Hz, C-3', C-5'), 107.3 C-1, 104.5 C-3, 60.3 CH_2, 14.7 CH_3. Combustion analysis for $C_{25}H_{17}FN_2O_3$: Calculated. C 72.81, H 4.15, N 6.79; found C 72.83, H 4.12, N 6.81.

*Ethyl 11-(4-(trifluoromethyl)benzoyl)pyrrolo[1,2-a][1,10]phenanthroline-9-carboxylate (**5b**)*

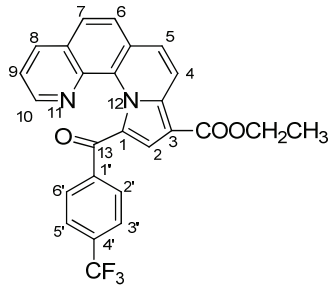

Crystallized from methanol-chloroform 1:1, (v/v). Yellow powder, mp = 220-221 °C, yield: 45 %. IR (KBr): 3072, 2986, 1697, 1651, 1584, 1236, 1126 cm^{-1}. ^{1}H-NMR (500 MHz, $CDCl_3$, δ(ppm)): 8.60 (1H, d, J = 9.0 Hz, H-4), 8.25-8.33 (4H, overlapped signals, H-8, H-10, H-2', H-6'), 7.93 (1H, d, J = 8.5 Hz, H-7), 7.82-7.85 (3H, overlapped signals, H-6, H-3', H-5'), 7.75 (1H, d, J = 9.0 Hz, H-5), 7.54 (1H, s, H-2), 7.43 (1H, dd, J = 7.5; 5.5 Hz, H-9), 4.40 (2H, m, CH_2), 1.42 (3H, t, J = 7.0 Hz, CH_3). ^{13}C-RMN (125 MHz, $CDCl_3$, δ(ppm)): 192.9 C-13, 164.6 CO_{ester}, 157.4 C-3a, 146.1 C-10, 141.2 C-11b, 138.4 (C-1'), 136.9 C-8, 133.8 (q, $J_{C,F}$ = 31.3 Hz, C-4'), 130.3 (C-2', C-6'), 128.0 C-7a, C-11a, 127.1 C-7, 125.8 C-5a, 125.7 C-5, 125.6 (q, $J_{C,F}$ = 2.5 Hz, C-3', C-5'), 125.2 C-6, 124.0 (q, $J_{C,F}$ = 271.3 Hz, CF_3), 122.8 C-9, 121.6 C-2, 120.6 C-4, 106.9 C-1, 104.4 C-3, 60.3 CH_2, 14.7 CH_3. Combustion analysis for $C_{26}H_{17}F_3N_2O_3$: Calculated. C 67.53, H 3.71, N 6.06; found: C 67.56, H 3.68, N 6.05.

*11-(4-fluorobenzoyl)-10,11-dihydropyrrolo[1,2-a][1,10]phenanthroline-9-carbonitrile (**6a**)*

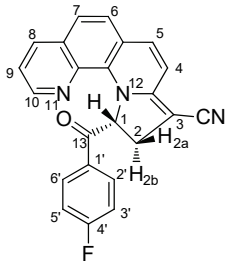

Crystallized from ethanol-chloroform 1:1, (v/v). Red solid, mp = 213-215 °C, yield: 40 %. IR (KBr): 3060, 2962, 2917, 2160, 1695, 1594, 1458, 1192 cm^{-1}. ^{1}H-NMR (500 MHz, $CDCl_3$, δ(ppm)): 7.99 (2H, m, H-2', H-6'), 7.88 (2H, overlapped signals, H-10, H-8), 7.12-7.27 (7H, overlapped signals, H-5, H-3', H-5', H-4, H-6, H-1, H-9), 6.77 (1H, s, H-7), 3.38 (1H, t, J = 13.5; 11.5 Hz, H-2a), 2.85 (1H, dd, J = 15.0; 6.0 Hz, H-2b). ^{13}C-RMN (125 MHz, $CDCl_3$, δ(ppm)): 190.2 C-13, 165.9 (d, $J_{C,F}$ = 253.75 Hz, C-4'), 157.4 C-11a, 146.4 C-10, 137.1 C-3a, 136.6 C-11b, 136.4 C-8, 135.8 C-7a, 131.5 (d, $J_{C,F}$ = 8.75 Hz, C-2', C-6'), 130.6 (d, $J_{C,F}$ = 3.75 Hz, C-1'), 126.9 C-6, C-5, C-5a, 122.1 C-9, 120.6 C-4, 120.2 CN, 118.0 C-7, 116.3 (d, J_{C-F} = 21.25 Hz, C-3', C-5'), 69.4 C-3, 68.0 C-1, 33.0 C-2. Combustion analysis for $C_{23}H_{14}FN_3O$: Calculated. C 75.19, H 3.84, N 11.44; found C 75.18, H 3.81, N 11.46.

*11-(4-(trifluoromethyl)benzoyl)-10,11-dihydropyrrolo[1,2-a][1,10]phenanthroline-9-carbonitrile (**6b**)*

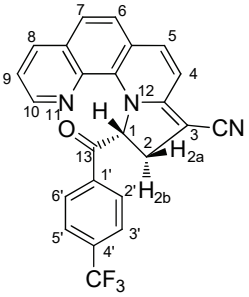

Crystallized from methanol-chloroform 1:1, (v/v). Red crystals, mp = 240-242 °C, yield: 40 %. IR (KBr): 2995, 2943, 2243, 2172, 1680, 1639, 1595, 1452, 1128 cm^{-1}. ^{1}H-NMR (500 MHz, $CDCl_3$, δ(ppm)): 8.15 (2H, d, J = 7.5 Hz, H-2', H-6'), 7.99 (1H, d, J = 7.5 Hz, H-8), 7.85-7.88 (3H, overlapped signals, H-10, H-3', H-5'), 7.20-7.37 (5H, overlapped signals, H-5, H-4, H-6, H-1, H-9), 6.86 (1H, bs, H-7), 3.47 (1H, t, J = 14.0 Hz, H-2a), 2.93 (1H, dd, J = 14.5; 6.5 Hz, H-2b). ^{13}C-RMN (125 MHz, $CDCl_3$, δ(ppm)): 190.1 C-13, 157.4 C-11a, 155.1 C-3a, 146.3 C-10, 136.8 C-8, 135.8 C-11b, 130.6 C-7a, 129.3 (C-2', C-6'), 137.4 (C-1'), 134.79 (q, $J_{C,F}$ = 31.3 Hz, C-4'), 126.9 C-6, C-5, C-5a, 126.2 (C-3',

C-5'), 123.7 (q, $J_{C,F}$ = 271.3 Hz, CF_3), 122.2 C-9, 120.9 C-4, 120.7 CN, 118.0 C-7, 67.9 C-1, 66.8 C-3, 32.9 C-2. Combustion analysis for $C_{24}H_{14}F_3N_3O$: Calculated. C 69.06, H 3.38, N 10.07; Found C 69.08, H 3.35, N 10.09.

*11-(4-fluorobenzoyl)-8a,9-dihydropyrrolo[1,2-a][1,10]phenanthroline-9,10-dicarbonitrile (**7a**)*

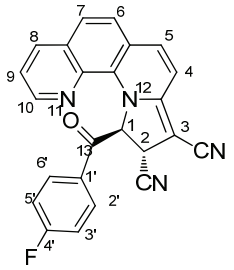

Crystallized from ethanol-chloroform 1:1, (v/v). Orange solid, mp = 238-240 °C, yield: 52 %. IR (KBr): 3062, 2978, 2925, 2225, 2175, 1691, 1596, 1460, 1153cm^{-1}. ^{1}H-NMR (500 MHz, $CDCl_3$, δ(ppm)): 8.17 (2H, m, H-2', H-6'), 8.05-8.09 (2H, overlapped signals, H-10, H-8), 7.74 (1H, d, J = 5.0 Hz, H-1), 7.50-7.53 (2H, overlapped signals, H-4, H-7), 7.34 (2H, t, J = 8.5 Hz, H-3', H-5'), 7.30 (1H, dd, J = 8.5; 4.5 Hz, H-9), 7.26 (1H, d, J = 9.5 Hz, H-5), 6.99 (1H, d, J = 8.5 Hz, H-6), 4.13 (1H, d, J = 5.0 Hz, H-2). ^{13}C-RMN (125 MHz, $CDCl_3$, δ(ppm)): 187.2 C-13, 166.6 (d, $J_{C,F}$ = 253.75 Hz, C-4'), 158.2 C-3a, 147.2 C-10, 137.8 C-7, 137.0 C-8, C-11b, 135.2 C-11a, 131.8 (d, $J_{C,F}$ = 10.0 Hz, C-2', C-6'), 130.7 C-7a, 129.1 (d, $J_{C,F}$ = 3.75 Hz, C-1'), 127.0 C-4, 125.9 C-5a, 122.6 C-9, 122.2 C-6, 122.1 C-5, 118.0 CN, 117.5 CN, 117.0 (d, $J_{C\text{-}F}$= 22.5 Hz, C-3', C-5'), 71.2 C-1, 63.0 C-3, 35.6 C-2. Combustion analysis for $C_{24}H_{13}FN_4O$: Calculated. C 73.46, H 3.34, N 14.28; found C 73.44, H 3.31, N 14.30.

*11-(4-(trifluoromethyl)benzoyl)-8a,9,10,11-tetrahydropyrrolo[1,2-a][1,10]phenanthroline--9,10-dicarbonitrile (**7b**)*

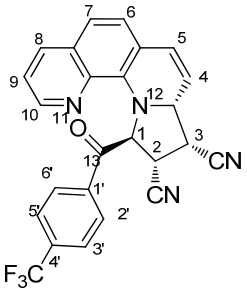

Crystallized from methanol-chloroform 1:1, (v/v). Orange solid, mp = 230-232 °C, yield: 68 %. IR (KBr): 2996, 2914, 2365, 2249, 1688, 1647, 1454, 1126 cm^{-1}. ^{1}H-NMR (500 MHz, DMSO-d6, δ(ppm)): 8.36 (2H, d, J = 8.0 Hz,

H-2', H-6'), 8.09 (1H, dd, *J* = 8.0; 1.5 Hz, H-8), 8.04 (2H, d, *J* =8.0 Hz, H-3', H-5'), 7.53 (1H, dd, *J* = 4.5; 1.5 Hz, H-10), 7.28 (1H, d, *J* = 8.5 Hz, H-6), 7.18-7.21 (2H, overlapped signals, H-7, H-9), 6.72-6.77 (2H, overlapped signals, H-5, H-1), 5.88 (1H, dd, *J* = 10.0; 2.0 Hz, H-4), 5.40 (1H, dd, *J* = 4.5; 1.5 Hz, H-3a), 4.33 (1H, dd, *J* = 7.0; 5.0 Hz, H-3), 4.08 (1H, t, *J* = 7.0 Hz, H-2). ^{13}C-RMN (125 MHz, DMSO-d6, δ(ppm)): 192.6 C-13, 145.0 C-10, 138.3 C-1', 137.3 C-11b, 136.5 C-8, 136.3 C-11a, 132.6 (q, $J_{C,F}$= 32.5 Hz, C-4'), 129.8 (C-2', C-6'), 129.5 C-7a, 128.3 C-5, 126.8 C-6, 126.0 (d, J_{C-F}= 3.8 Hz, C-3', C-5'), 123.5 (q, $J_{C,F}$= 271.3 Hz, CF_3), 121.1 C-7, 119.9 C-4, 118.7 C-5a, 117.8 CN, 117.3 CN, 116.8 C-9, 65.7 C-1, 63.6 C-3a, 39.5 C-3, 32.9 C-2. Combustion analysis for $C_{25}H_{15}F_3N_4O$: Calculated. C 67.57, H 3.40, N 12.61; found C 67.59, H 3.38, N 12.62.

TABLE S-I. Crystallographic data and refinement details

Compound	**4b** (4719)	**6a** (4665)	**6b** (4819)	**7b** (4833)
Empirical formula	$C_{27}H_{19}F_3N_2O_5$	$C_{23}H_{14}FN_3O$	$C_{24}H_{14}F_3N_3O$	$C_{25}H_{15}F_3N_4O$
Formula weight	508.44	367.37	417.38	444.41
Temperature/K	200	293	200	140
Crystal system	triclinic	monoclinic	triclinic	monoclinic
Space group	*P*-1	*C*2/*c*	*P*-1	$P2_1/c$
a / Å	7.5236(5)	26.468(2)	5.4429(5)	9.2761(4)
b / Å	9.5486(7)	6.2708(4)	9.7038(8)	11.1990(4)
c / Å	17.3690(12)	22.8898(19)	18.6668(14)	20.0050(9)
α / °	77.052(6)	90	75.239(7)	90
β / °	87.591(6)	113.351(11)	82.490(7)	91.083(4)
γ / °	70.374(6)	90	80.305(7)	90
Volume, Å^3	1144.66(15)	3488.0(5)	935.77(14)	2077.81(15)
Z	2	8	2	4
ρ_{calc}g / cm^3	1.475	1.399	1.481	1.421
μ / mm^{-1}	0.119	0.095	0.113	0.108
Crystal size, mm^3	0.3×0.15 0.15	0.15×0.10×0.10	0.3×0.15×0.15	0.30×0.25×0.20
2*θ* / °	4.646 to 50.046	3.352 to 57.404	4.384 to 50.052	4.072 to 50.038
Reflections collected	9201	9862	8106	11269
Independent reflections	4009 [R_{int}= 0.0361]	3942 [R_{int}= 0.0735]	3306 [R_{int}= 0.0311]	3668 [R_{int}= 0.0409]
Data/restraints/parameters	4009/0/336	3942/0/253	3306/81/277	3668/70/299
R_1[a]	0.0667	0.0671	0.0841	0.050
R_2[b]	0.1561	0.1827	0.2286	0.2300
GOF[c]	1.091	0.994	1.050	1.055
Largest diff. peak/hole, e Å^{-3}	0.28/-0.29	0.17/-0.23	0.82/-0.79	0.50/-0.48

[a]$R_1=\Sigma||F_o| - |F_c||/\Sigma|F_o|$. [b]$wR_2=\{\Sigma[w(F_o^2-F_c^2)^2]/\Sigma[w(F_o^2)^2]\}^{1/2}$. [c]$GOF=\{\Sigma[w(F_o^2-F_c^2)^2]/(n-p)\}^{1/2}$, where *n* is the number of reflections and *p* is the total number of parameters refined.

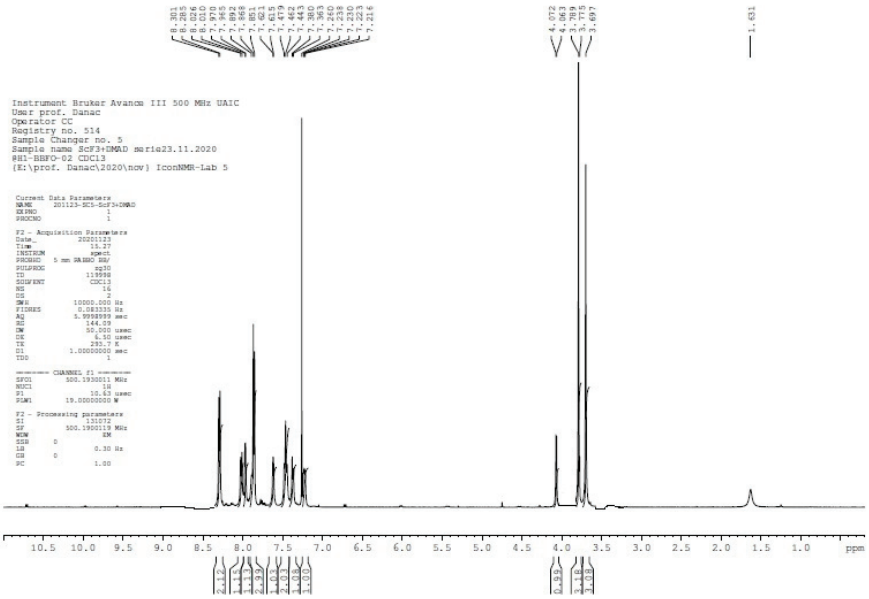

Fig. S-1. ^{1}H NMR spectrum of compound **4b**.

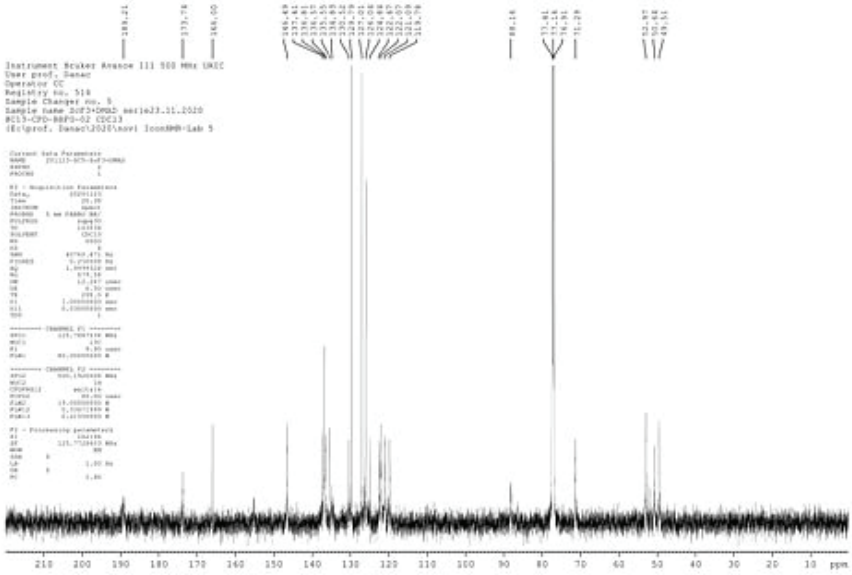

Fig. S-2. ^{13}C NMR spectrum of compound ^{13}C NMR of **4b**.

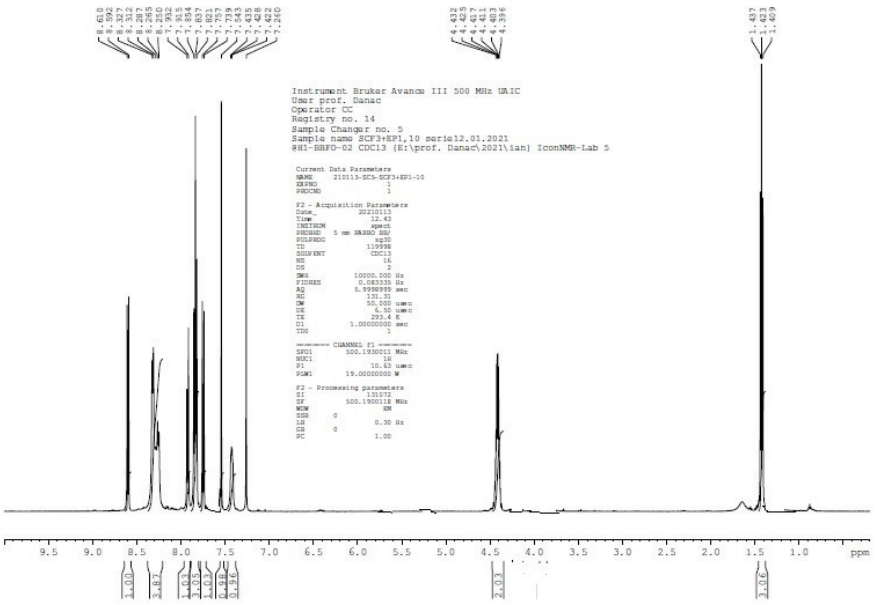

Fig. S-3. ^{1}H NMR spectrum of compound **5b**.

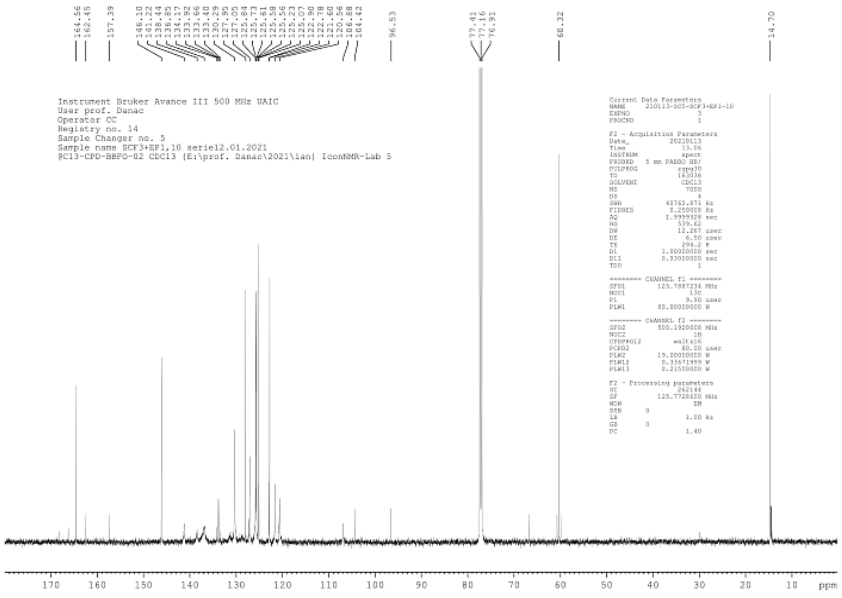

Fig. S-4. ^{13}C NMR spectrum of compound ^{13}C NMR of **5b**.

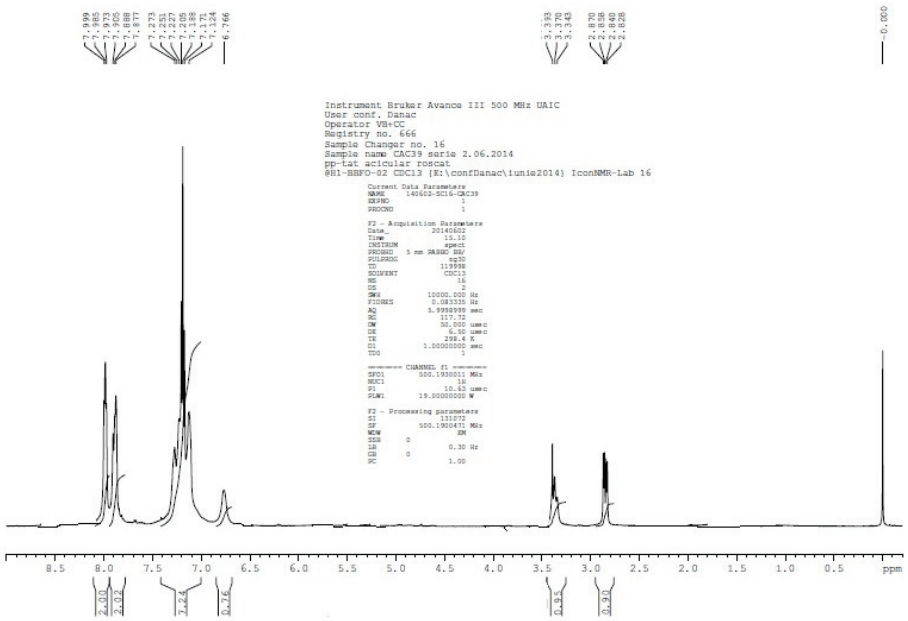

Fig. S-5. ^{1}H NMR spectrum of compound **6a**.

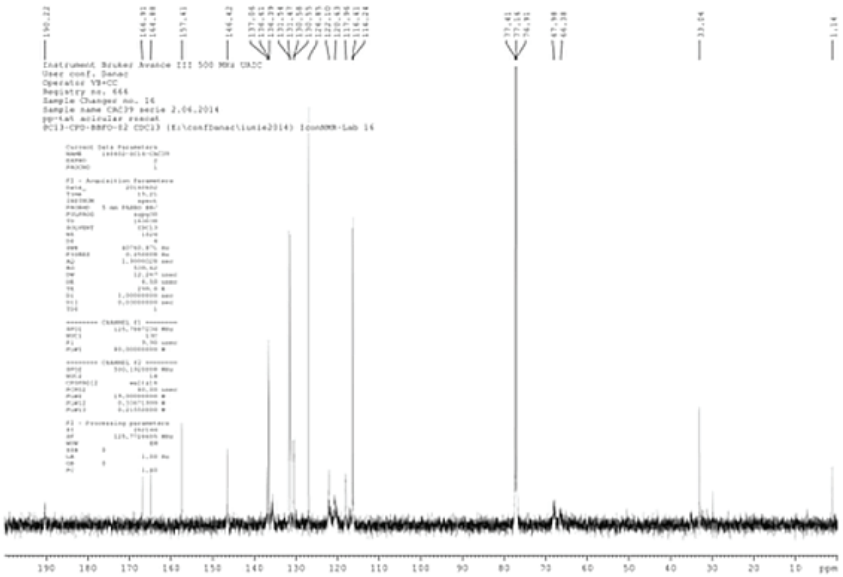

Fig. S-6. ^{13}C NMR spectrum of compound ^{13}C NMR of **6a**.

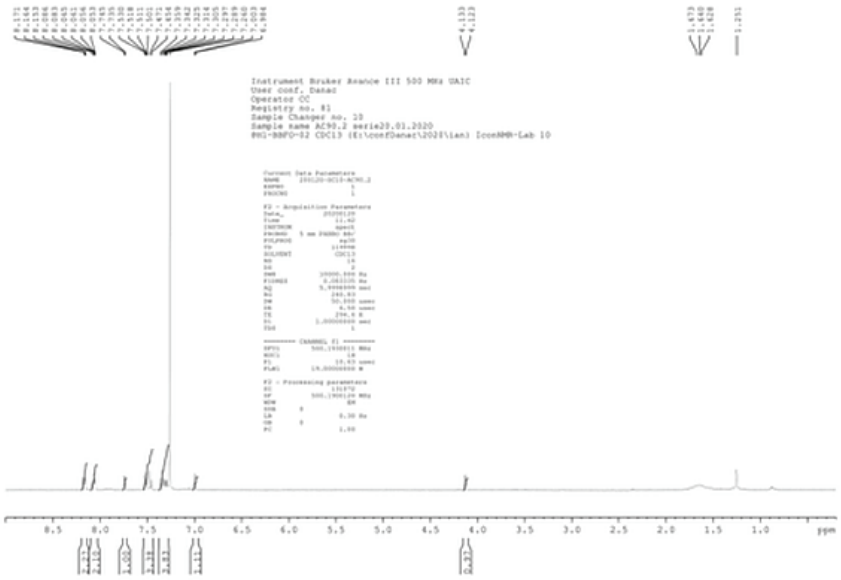

Fig. S-7. ^{1}H NMR spectrum of compound **7a**.

Journal of the Serbian Chemical Society
JSCS@tmf.bg.ac.rs • www.shd.org.rs/JSCS
J. Serb. Chem. Soc. *86* (10) 917–925 (2021)
JSCS–5472
Original scientific paper
Published 10 September 2021

Synthesis of new derivatives of alepterolic acid *via* click chemistry

XIN JIN[1,2], JIANGUO CAO[3], QINGJIE ZHAO[4], QI WANG[3], HONGMEI GUO[1,2], HAJI AKBER AISA[1]* and GUOZHENG HUANG[1,5]**

[1]*Key Laboratory of Plant Resources and Chemistry of Arid Zone, Xinjiang Technical Institute of Physics and Chemistry, Chinese Academy of Sciences, Urumqi, 830011, P.R. China,* [2]*University of Chinese Academy of Sciences, Beijing, 100049, P.R. China,* [3]*College of Life Sciences, Shanghai Normal University, Shanghai, 201418, P.R. China,* [4]*CAS Key Laboratory for Receptor Research, Shanghai Institute of Materia Medica, Chinese Academy of Sciences, Shanghai 201203, P. R. China and* [5]*College of Chemistry and Chemical Engineering, Anhui University of Technology, Ma'anshan, 243002, P. R. China*

(Received 16 March, revised 30 May, accepted 14 June 2021)

Abstract: Alepterolic acid is a natural diterpenoid isolated from *Aleuritopteris argentea* (S. G. Gmél.) Fée, a fern with potential medicinal activity, used in China as a folk medicine to regulate menstruation and prevent cancer. Nevertheless, there are few reports about the structural modification of this natural product. With the wide application of 1,2,3-triazole derivatives in medicines, pesticides, functional materials, the synthesis of 1,2,3-triazoles derivatives has attracted the attention of synthetic chemists. In this article, 23 new derivatives of alepterolic acid combined with 1,2,3-triazole were designed and synthesized by esterification and click chemistry reaction in a fast, conventional and efficient way. All the products were obtained in good yields (72 to 97 %). The structure of these compounds was confirmed by ^{1}H-, ^{13}C-NMR and mass spectral data. The use of the easily available reactants and the common reaction conditions furnish an efficient method for the synthesis of alepterolic acid derivatives. The preparation of these compounds would enable further biological evaluation in the future.

Keywords: diterpenoid; 1,2,3-triazole; structural modification.

INTRODUCTION

Aleuritopteris argentea (S. G. Gmél.) Fée, also known as *Cheilanthes argentea* (S. G. Gmél.) Kunze, is a kind of medicinal fern plant growing in China, Japan, the Korean Peninsula and Russia. Extracts from the fern possess a wide range of medicinal values, such as promoting blood circulation, regulating mens-

*,** Corresponding authors. E-mail: (*)haji@ms.xjb.ac.cn; (**)guozheng.huang@ahut.edu.cn
https://doi.org/10.2298/JSC210316045J

truation, tonifying asthenia and relieving cough. In 1962, Ageta *et al.* isolated a diterpenoid compound from *A. argentea* for the first time, namely alepterolic acid (Fig. 1).[1] Later, it was found that alepterolic acid was produced in specimens of *A. argentea* from Japan and mainland Asia, while *ent*-anti-copalic acid was present (Fig. 1) in specimens from Taiwan island. Thus, the types and content of metabolites of this fern are different according to the geographical distribution.[2] These two diterpenoids share the same labdane frame, with a hydroxy group at 3-positon in the molecule of alepterolic acid. Recently, Idippily *et al.* reported the structural modification of *ent*-anti-copalic acid by amination and esterification reactions. Compared to that of *ent*-anti-copalic, the anticancer activity of those semi-synthesized derivatives against LNCaP cell line considerably increased.[3] However, the modification of alepterolic acid was less investigated.

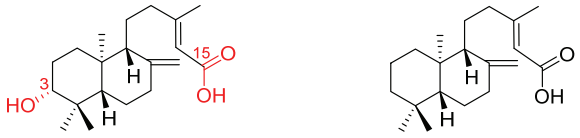

Alepterolic acid **ent-anti-Copalic acid**

Fig. 1. Structure of alepterolic acid and *ent*-anti-copalic acid.

1,2,3-Triazole, as one of the most important heterocycles, can form various non-covalent interactions such as hydrophobic interactions, hydrogen bonds, van der Waals forces with different biological targets.[4] Accordingly, the compounds with 1,2,3-triazole moiety possess diverse pharmaceutical properties such as antibacterial,[5] antimalarial,[6] antifungal,[7] antiviral,[8] antitubercular[9] and anticancer[10] activities. The combination of 1,2,3-triazole with other bioactive drug molecules or natural products may produce hybrid molecules with better biological activity performance.[11,12] Previously, our group reported the structural modification of rupestonic acid (Fig. 2) by the introduction of the 1,2,3-triazole. The synthesized derivatives displayed interesting potency against influenza A viruses.[13] Carnosic acid (Fig. 2), a diterpenoid, exhibited potential antiproliferative and antifungal activities after combination with 1,2,3-triazole by Pertino *et al.*[14] Acanthoic acid (Fig. 2), also a kind of diterpenoid compound, was recently modified by Kasemsuk, with the results demonstrating that the triazole ring and nitro group on the benzyl ring play a pivotal role in the cytotoxic activity against cholangiocarcinoma.[15] It was reported that hybrids of oleanolic acid (Fig. 2) and 1,2,3-triazole possess considerable anticancer activity and could inhibit the proliferation of a variety of tumor cells.[16] Based on the above-mentioned studies, the introduction of 1,2,3-triazole moiety into alepterolic acid is supposed to be a prospective derivatization method to acquire or enhance the bioactivities.

Our group recently isolated grams of alepterolic acid from *A. argentea*. A pioneer derivation was achieved by incorporation of amino moiety to the 15-carboxy group.[17] The obtained compounds showed improved cytotoxic activity against HeLa cell lines compared to alepterolic acid itself. Taking these factors into account, we intended to further modify alepterolic acid by introducing 1,2,3--triazole moiety.

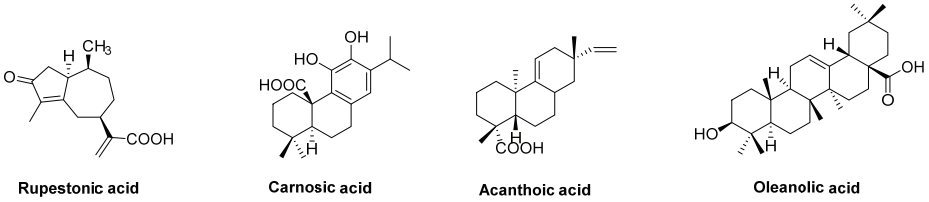

Fig. 2. Structures of rupestonic acid, carnosic acid, acanthoic acid and oleanolic acid.

EXPERIMENTAL

Visualization on TLC was achieved by use of UV light (254 nm) or iodine. NMR spectra were recorded on a Varian Inova-400 MHz spectrometer (400 MHz for ^{1}H, 100 MHz ^{13}C). The spectra were recorded in $CDCl_3$ as solvent at room temperature, ^{1}H- and ^{13}C-NMR chemical shifts are reported in ppm relative to either the residual solvent peak (^{13}C, δ = 77.16 ppm or ^{1}H, δ = 7.26 ppm) as an internal standard. Data for ^{1}H-NMR are reported as follows: chemical shift (δ / ppm), multiplicity, integration, coupling constant (Hz) and assignment. The melting point of the product was determined by Buchi M-560 melting point apparatus.

Propargyl bromide, NaN_3, $CuSO_4 \cdot 5H_2O$, substitued benzyl bromides and anilines are purchased from Adamas Reagent, Co. Ltd. (Shanghai, China) and were used without further purification.

*Synthesis of prop-2-yn-1-yl (*E*)-5-((1*R*,4a*S*,6*R*,8a*S*)-6-hydroxy-5,5,8a-trimethyl-2-methylene-decahydronaphthalen-1-yl)-3-methylpent-2-enoate (**3**)*

To the solution of alepterolic acid (960.7 mg, 3.0 mmol) in 10 mL of DMF was added potassium carbonate (621.9 mg, 4.5 mmol) and propargyl bromide (428.3 mg, 3.6 mmol). The reaction was stirred at room temperature for 12 hours. Then the mixture was quenched with water and extracted with ethyl acetate (3×10 mL). Combined organic layers were washed with water (3×20 mL), brine (20 mL), and dried over Na_2SO_4. After the solvent was removed in vacuum, the crude product was purified by column chromatography (petroleum ether:ethyl acetate, 4:1 to 1:1 volume ratios) to afford 969.1 mg of desired product as a yellow solid (yield 90 %).

*General procedure for the synthesis of substituted phenyl azides **4a**–**n***

To a stirred solution of substituted aniline (1.0 mmol) in 2 mL of 6 N HCl at 0 °C was added $NaNO_2$ (103.5 mg, 1.5 mmol) in H_2O (2 mL). After stirring for 15 min, a solution of NaN_3 (78 mg, 1.2 mmol) in H_2O (1 mL) was cautiously added dropwise. The reaction was left to stir for 1 h at room temperature, followed by extraction with ethyl acetate (3×5 mL). The combined organic layers were dried over Na_2SO_4, and carefully concentrated under reduced pressure to give corresponding phenyl azide. The crude product was used directly without purification.

*General procedure for the synthesis of substituted benzyl azides **4o**–**w***

To a stirred solution of substituted benzyl bromide (1.0 mmol) in 4 mL of acetone was added NaN_3 (96 mg, 1.50 mmol) in 1 mL of water. After stirring for 12 h, the reaction mixture was extracted with ethyl acetate (3×10 mL), washed with brine, dried over Na_2SO_4, and concentrated carefully under reduced pressure to give corresponding benzyl azide. The crude product was used directly without purification.

*General procedure for the synthesis of 1,2,3-triazoles derivations of alepterolic acid **5a**–**w***

To the solution of compound **3** (30.0 mg, 0.083 mmol) and corresponding azide (0.10 mmol) in 4 mL of DMF/H_2O (1:1 volume ratio) was added sodium ascorbate (6.5 mg, 0.033 mmol) and $CuSO_4 \cdot 5H_2O$ (3.8 mg, 0.014 mmol). The reaction was stirred at 60 °C for 6 h and monitored by thin layer chromatography to ensure that compound **3** had been completely consumed. Then the mixture was quenched with ice-cold water and extracted with ethyl acetate (3×5 mL). Combined organic layers were washed with water (3×5 mL), brine (10 mL), and dried over Na_2SO_4. After the solvent was removed in vacuum, the crude product was purified by column chromatography (petroleum ether:ethyl acetate, 1:1 to 1:4 volume ratios) to afford the desired products **5a**–**w**.

The detailed spectral data of synthetic compounds are presented in the Supplemental material to this paper.

RESULTS AND DISCUSSION

Click chemistry is applied to all aspects of drug discovery to form 1,2,3-triazole compounds. The copper-(I)-catalyzed 1,2,3-triazole formation from azides and terminal acetylenes is a very useful route to create a library of new compounds for the screening of activity, due to its high degree of dependability, complete specificity and the biocompatibility of the reactants.[18] With that in mind, we used classical click reaction conditions to prepare a series of 1,2,3-triazole derivatives of alepterolic acid, taking copper sulfate pentahydrate and sodium ascorbate as the source of catalytic copper (I).

At the beginning, the substrate of the click reaction, propargyl alepterolate (**3**) was prepared by simple derivatization on alepterolic acid in yield of 90 % by mixing alepterolic acid (**1**) and 3-bromoprop-1-yne (**2**) with potassium carbonate in *N*,*N*-dimethylformamide for 12 h (Scheme 1).[19]

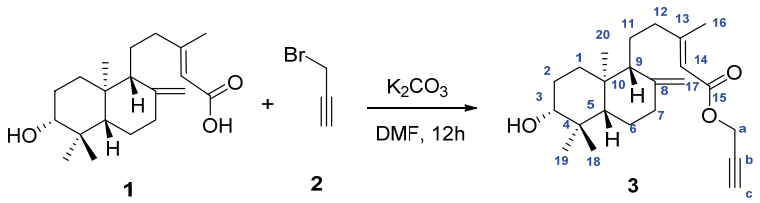

Scheme 1. Synthesis of propargyl alepterolate. Reaction condition: propargyl bromide, alepterolic acid, K_2CO_3, *N*,*N*-dimethylformamide, r.t.

Other components of the click reaction substrate, are phenyl azides and benzyl azides. Phenyl azides **4a**–**n** were synthesized by firstly mixing the corres-

ponding aniline, sodium nitrite and concentrated hydrochloride at 0 °C for 15 min, then adding sodium azide to the system and stirring at room temperature for 1 h.[20] The resulting products are listed in Table I. Benzyl azides **4o**–**w** were synthesized by mixing the corresponding benzyl bromide and sodium azide in a mixed solvent of acetone and water and reacting overnight.[21] The resulting products are listed in Table II. All the azides were obtained in high yields after simple work-up and directly used in the next step without further purification.

TABLE I. Preparation of phenyl azides **4a**–**n**; [a]reaction conditions: 1) $NaNO_2$, aniline, 6 M HCl, H_2O, 0 °C; 2) NaN_3, r.t., H_2O

$$\mathbf{R}NH_2 \xrightarrow[(2)\ NaN_3]{(1)\ HCl\ NaNO_2} \mathbf{R}N_3$$

Entry	Azide	R	Yield[a], %
1	**4a**	Ph	91
2	**4b**	2-MePh	75
3	**4c**	3-MePh	85
4	**4d**	4-MePh	90
5	**4e**	4-FPh	67
6	**4f**	4-ClPh	92
7	**4g**	4-BrPh	85
8	**4h**	4-MeOPh	77
9	**4i**	4-CNPh	93
10	**4j**	4-CF_3Ph	90
11	**4k**	4-NO_2Ph	62
12	**4l**	2,4-2ClPh	93
13	**4m**	3,4-2ClPh	80
14	**4n**	1-Nap	81

[a]Isolated yield

TABLE II. Preparation of benzyl azides 4o–4w; reaction conditions: NaN_3, benzyl bromide, acetone/ H_2O, r.t.

$$\mathbf{R}Br \xrightarrow[acetone\ /\ H_2O]{NaN_3} \mathbf{R}N_3$$

Entry	Azides	R	Yield[a], %
1	**4o**	Bn	95
2	**4p**	4-MeBn	94
3	**4q**	4-FBn	85
4	**4r**	4-ClBn	90
5	**4s**	4-BrBn	88
6	**4t**	4-MeOBn	88
7	**4u**	4-CNBn	85
8	**4v**	4-CF_3Bn	92
9	**4w**	4-NO_2Ph	95

[a]Isolated yield

The preparation of 1,2,3-triazoles derivatives of alepterolic acid **5a**–**w** were achieved as depicted in Scheme 2. All the products were prepared in good yields

as displayed. It is worth mentioning that when *ortho* substituted phenyl azides participated in the reactions such as **4b** or **4l**, the yields were relatively lower than with the other substrates, which implied that steric hindrance affected and limited the scope of the reaction to some extent similar to that previously reported.[22] Due to the existence of the ester group, most of the products stayed oily at room temperature.

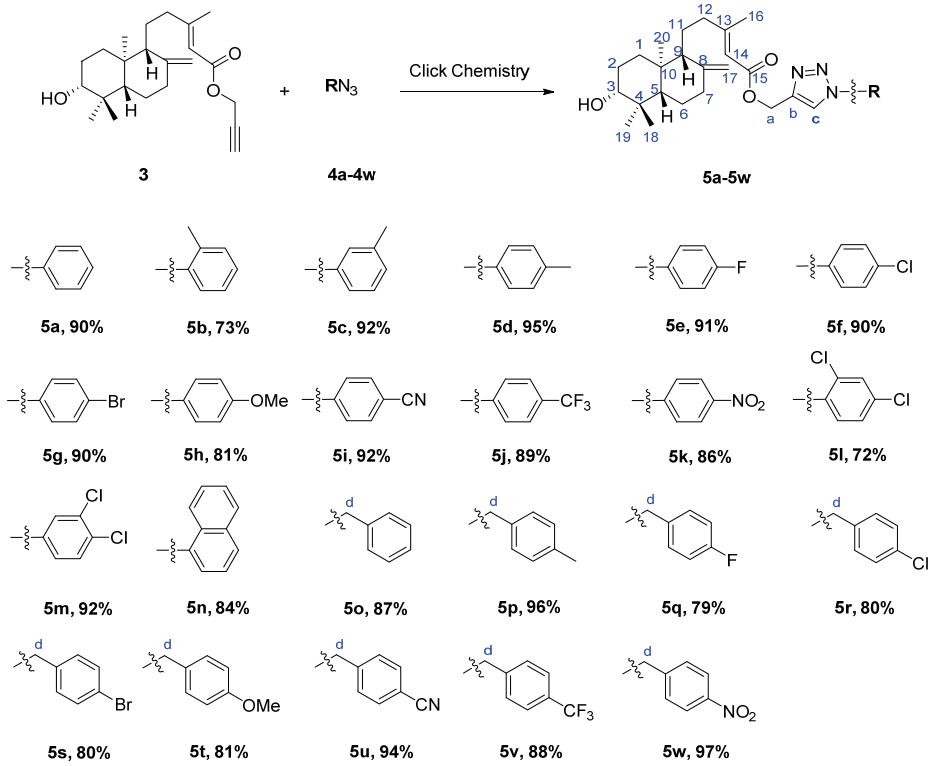

Scheme 2. Synthesis of 1,2,3-triazoles derivtives of alepterolic acid. Reaction conditions: propargyl alepterolate, azides, sodium ascorbate, $CuSO_4 \cdot 5H_2O$, *N*,*N*-dimethylformamide/H_2O, 60 °C; isolated yield.

The structures of obtained compounds were analyzed by NMR and HRMS. The assignments of ^1H and ^{13}C spectra to the peak positions of the synthesized derivatives **5a**–**w** were attained by comparison with the signals to the original NMR data of alepterolic acid.[2,17] Compared with the ^1H-NMR of propargyl alepterolate, the terminal alkyne hydrogen signal disappeared, and the aromatic hydrogen atom signals appeared, while no obvious change was observed in the signal of methylene at the α-position of the ester group. The ^1H-NMR revealed the signal of hydrogen atom fluctuating from $\delta \approx 8.19$ to 7.51 ppm in the newly formed five-membered 1,2,3-triazole rings. The signal of 3-OH in the target com-

pounds appeared at $\delta \approx 3.24$ or 3.23 ppm, usually as a doublet of doublets, just like that of alepterolic acid, indicating that 3-OH was left untouched in the reactions. The signals of 14-H and 17-H on the NMR spectra were similar to those of alepterolic acid, which revealed the double-bond was tolerable for click chemistry. The signals of the four methyl groups stayed the same as those in alepterolic acid. From the information provided by ^{1}H-NMR, it can be concluded that the frame of alepterolic acid other than the carboxyl group was not affected during the whole process of the reactions. The ^{13}C-NMR data also consisted to the related structures, which tallied with previous literature reports.[2,17] The mass of the products showed molecular ion peaks corresponding to the molecular weight of the acquired structures.

CONCLUSIONS

Alepterolic acid, as the main metabolite of the fern plant *A. argentea*, is a diterpenoid worthy of structural modification. In this work, we have successfully developed a rapid and efficient process for the synthesis of 1,2,3-triazole derivatives through the application of click reaction. Twenty-three derivatives were synthesized in good yields and characterized by spectral analysis. These compounds would be evaluated with regard to their biological activities, such as anticancer or antiviral activities for future drug discovery.

SUPPLEMENTARY MATERIAL

Additional data and information are available electronically at the pages of journal website: https://www.shd-pub.org.rs/index.php/JSCS/article/view/10525, or from the corresponding author on request.

Acknowledgement. This work was financially supported by the start-up fund from Anhui University of Technology and "Personalized Medicines–Molecular Signature-Based Drug Discovery and Development", Strategic Priority Research Program of the Chinese Academy of Sciences (No. XDA12040322).

ИЗВОД

СИНТЕЗА НОВИХ ДЕРИВАТА АЛЕПТЕРОЛИЧНЕ КИСЕЛИНЕ ПРИМЕНОМ КЛИК-ХЕМИЈЕ

XIN JIN[1,2], JIANGUO CAO[3], QINGJIE ZHAO[4], QI WANG[2], HONGMEI GUO[1,2], HAJI AKBER AISA[1] и GUOZHENG HUANG[1,5]

[1]Key Laboratory of Plant Resources and Chemistry of Arid Zone, Xinjiang Technical Institute of Physics and Chemistry, Chinese Academy of Sciences, Urumqi, 830011, P.R. China; [2]University of Chinese Academy of Sciences, Beijing, 100049, P.R. China; [3]College of Life Sciences, Shanghai Normal University, Shanghai, 201418, P.R. China, [4]CAS Key Laboratory for Receptor Research, Shanghai Institute of Materia Medica, Chinese Academy of Sciences, Shanghai 201203, P. R. China, [5]College of Chemistry and Chemical Engineering, Anhui University of Technology, Ma'anshan, 243002, P. R. China

Алептеролична киселина је природни дитерпеноид изолован из папрати *Aleuritopteris argentea* (S.G. Gmél.) Fée, као једињење са потенцијалном медицинском применом, које се користи у кинеској народној медицини за регулацију менструалног циклуса и превенцију канцера. Ипак, постоји мало радова у којима су описане структурне моди-

фикације овог природног производа. Због широке примене 1,2,3-триазола у медицини, истраживању пестицида и материјала, постоји велико интересовање за синтезу деривата 1,2,3-триазола. У овом раду синтетисано је 23 деривата алептероличне киселине са 1,2,3-триазолским сегментом, применом реакција естерификације и "клик"-хемије, на брз, ефикасан и конвенционалан начин. Сви производи су добијени у добром приносу (од 72 до 97 %). Структуре једињења потврђене су ^{1}H-, ^{13}C-НМР и масеним спектрима. Употребом приступачних реагенаса под уобичајеним реакционим условима развијен је ефикасан поступак за синтезу деривата алептероличне киселине. Синтеза ових једињења ће омогућити даља биолошка испитивања у наредном периоду.

(Примљено 16. марта, ревидирано 30. маја, прихваћено 14. јуна 2021)

REFERENCES

1. H. Ageta, K. Awata, Y. Otake, *Proc. Symp. Nat. Org. Compd.* **6** (1962) 136 (https://doi.org/10.24496/tennenyuki.6.0_136)
2. E. Wollenweber, P. Rüedi, D. S. Seigler, *Z. Naturforsch., C* **37** (1982) 1283 (https://doi.org/10.1515/znc-1982-11-1231)
3. N. D. Idippily, Q. Zheng, C. Gan, A. Quamine, M. M. Ashcraft, B. Zhong, B. Su, *Bioorg. Med. Chem. Lett.* **27** (2017) 2292 (https://doi.org/10.1016/j.bmcl.2017.04.046)
4. Z. Xu, S.-j. Zhao, Y. Liu, *Eur. J. Med. Chem.* **183** (2019) 111700 (https://doi.org/10.1016/j.ejmech.2019.111700)
5. F. Reck, F. Zhou, M. Girardot, G. Kern, C. J. Eyermann, N. J. Hales, R. R. Ramsay, M. B. Gravestock, *J. Med. Chem.* **48** (2005) 499 (https://doi.org/10.1021/jm0400810)
6. R. Raj, P. Singh, P. Singh, J. Gut, P. J. Rosenthal, V. Kumar, *Eur. J. Med. Chem.* **62** (2013) 590 (https://doi.org/10.1016/j.ejmech.2013.01.032)
7. C. X. Tan, Y. X. Shi, J. Q. Weng, X. H. Liu, W. G. Zhao, B. J. Li, *J. Heterocycl. Chem.* **51** (2014) 690 (https://doi.org/10.1002/jhet.1656)
8. L.-h. Zhou, A. Amer, M. Korn, R. Burda, J. Balzarini, E. De Clercq, E. R. Kern, P. F. Torrence, *Antivir. Chem. Chemother.* **16** (2005) 375 (https://doi.org/10.1177/095632020501600604)
9. F. Mir, S. Shafi, M. Zaman, N. P. Kalia, V. S. Rajput, C. Mulakayala, N. Mulakayala, I. A. Khan, M. Alam, *Eur. J. Med. Chem.* **76** (2014) 274 (https://doi.org/10.1016/j.ejmech.2014.02.017)
10. L.-y. Ma, L.-p. Pang, B. Wang, M. Zhang, B. Hu, D.-q. Xue, K.-p. Shao, B.-l. Zhang, Y. Liu, E. Zhang, *Eur. J. Med. Chem.* **86** (2014) 368 (https://doi.org/10.1016/j.ejmech.2014.08.010)
11. D. Dheer, V. Singh, R. Shankar, *Bioorg. Chem.* **71** (2017) 30 (https://doi.org/10.1016/j.bioorg.2017.01.010)
12. K. Bozorov, J. Zhao, H. A. Aisa, *Bioorg. Med. Chem.* **27** (2019) 3511 (https://doi.org/10.1016/j.bmc.2019.07.005)
13. Y. W. He, C. Z. Dong, J. Y. Zhao, L. L. Ma, Y. H. Li, H. A. Aisa, *Eur. J. Med. Chem.* **76** (2014) 245 (https://doi.org10.1016/j.ejmech.2014.02.029)
14. M. W. Pertino, C. Theoduloz, E. Butassi, S. Zacchino, G. Schmeda-Hirschmann, *Molecules* **20** (2015) 8666 (https://doi.org/10.3390/molecules20058666)
15. T. Kasemsuk, N. Saehlim, P. Arsakhant, G. Sittithumcharee, S. Okada, R. Saeeng, *Bioorg. Med. Chem.* **29** (2021) 115886 (https://doi.org/10.1016/j.bmc.2020.115886)
16. G. Wei, W. Luan, S. Wang, S. Cui, F. Li, Y. Liu, Y. Liu, M. Cheng, *Org. Biomol. Chem.* **13** (2015) 1507 (https://doi.org/10.1039/C4OB01605J)

17. S. Zhang, N. Feng, J. Huang, M. Wang, L. Zhang, J. Yu, X. Dai, J. Cao, G. Huang, *Bioorg. Chem.* **98** (2020) 103756 (https://doi.org/10.1016/j.bioorg.2020.103756)
18. J. E. Moses, A. D. Moorhouse, *Chem. Soc. Rev.* **36** (2007) 1249 (https://doi.org/10.1039/B613014N)
19. C. Wang, L. Lu, H. Na, X. Li, Q. Wang, X. Jiang, X. Xu, F. Yu, T. Zhang, J. Li, Z. Zhang, B. Zheng, G. Liang, L. Cai, S. Jiang, K. Liu, *J. Med. Chem.* **57** (2014) 7342 (https://doi.org/10.1021/jm500763m)
20. J.-W. Zhao, J.-W. Guo, M.-J. Huang, Y.-Z. You, Z.-H. Wu, H.-M. Liu, L.-H. Huang, *Steroids* **150** (2019) 108431 (https://doi.org/10.1016/j.steroids.2019.108431)
21. P. Shanmugavelan, S. Nagarajan, M. Sathishkumar, A. Ponnuswamy, P. Yogeeswari, D. Sriram, *Bioorg. Med. Chem. Lett.* **21** (2011) 7273 (https://doi.org/10.1016/j.bmcl.2011.10.048)
22. X. Meng, X. Xu, T. Gao, B. Chen, *Eur. J. Org. Chem.* (2010) 5409 (https://doi.org/10.1002/ejoc.201000610).

Journal of the Serbian Chemical Society
JSCS@tmf.bg.ac.rs • www.shd.org.rs/JSCS
J. Serb. Chem. Soc. 86 (10) S186–S223 (2021) *Supplementary material*

SUPPLEMENTARY MATERIAL TO

Synthesis of new derivatives of alepterolic acid *via* click chemistry

XIN JIN[1,2], JIANGUO CAO[3], QINGJIE ZHAO[4], QI WANG[3], HONGMEI GUO[1,2], HAJI AKBER AISA[1]* and GUOZHENG HUANG[1,5]**

[1]*Key Laboratory of Plant Resources and Chemistry of Arid Zone, Xinjiang Technical Institute of Physics and Chemistry, Chinese Academy of Sciences, Urumqi, 830011, P.R. China,* [2]*University of Chinese Academy of Sciences, Beijing, 100049, P.R. China,* [3]*College of Life Sciences, Shanghai Normal University, Shanghai, 201418, P.R. China,* [4]*CAS Key Laboratory for Receptor Research, Shanghai Institute of Materia Medica, Chinese Academy of Sciences, Shanghai 201203, P. R. China and* [5]*College of Chemistry and Chemical Engineering, Anhui University of Technology, Ma'anshan, 243002, P. R. China*

J. Serb. Chem. Soc. 86 (10) (2021) 917–925

SPECTRUM DATA OF THE COMPOUNDS

*Prop-2-yn-1-yl (E)-5-((1R,4aS,6R,8aS)-6-hydroxy-5,5,8a-trimethyl-2-methylenedecahydro-naphthalen-1-yl)-3-methylpent-2-enoate (**3**)*

^{1}H NMR (400 MHz, $CDCl_3$) δ 5.68 (s, 1H, 14-H), 4.86 (s, 1H, 17-H), 4.69 (d, *J* = 2.4 Hz, 2H, a-CH_2), 4.49 (s, 1H, 17-H), 3.25 (dd, *J* = 11.7, 4.4 Hz, 1H, 3-H), 2.47 (t, *J* = 2.4 Hz, 1H, c-H), 2.40 (ddd, *J* = 12.8, 4.3, 2.4 Hz, 1H, 7-H), 2.35 – 2.27 (m, 12-H), 2.17 (d, *J* = 1.2 Hz, 3H, 16-CH_3), 2.01 – 1.90 (m, 2H), 1.81 – 1.52 (m, 7H), 1.37 (td, *J* = 12.9, 4.3 Hz, 1H, 6-H), 1.15 (td, *J* = 13.2, 3.8 Hz, 1H, 1-H), 1.07 (dd, *J* = 12.5, 2.8 Hz, 1H, 5-H), 0.99 (s, 3H, 18-CH_3), 0.77 (s, 3H, 19-CH_3), 0.68 (s, 3H, 20-CH_3). ^{13}C NMR (100 MHz, $CDCl_3$) δ 165.86 (C-15), 163.05 (C-13), 147.71 (C-8), 114.32 (C-14), 106.94 (C-17), 78.86 (C-3), 78.30 (b-C), 74.63 (c-C), 55.94 (C-9), 54.64 (C-5), 51.26 (a-C), 39.92 (C-10), 39.52 (C-4), 39.25 (C-7), 38.21 (C-12), 37.15 (C-1), 28.42 (C-18), 27.99 (C-2), 24.09 (C-6), 21.71 (C-11), 19.26 (C-16), 15.54 (C-19), 14.61 (C-20).

*(1-Phenyl-1H-1,2,3-triazol-4-yl)methyl (E)-5-((1R,4aS,6R,8aS)-6-hydroxy-5,5,8a-trimethyl-2--methylenedecahydronaphthalen-1-yl)-3-methylpent-2-enoate (**5a**)*

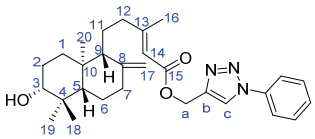

5a

Chemical Formula: $C_{29}H_{39}N_3O_3$
Exact Mass: 477.2991
Molecular Weight: 477.6490

*,** Corresponding authors. E-mail: (*)haji@ms.xjb.ac.cn; (**)guozheng.huang@ahut.edu.cn

35.6 mg, yield 90 %, white solid, m.p.= 50-52 °C; ^{1}H NMR (400 MHz, $CDCl_3$) δ 8.06 (s, 1H, c-H), 7.77 – 7.69 (m, 2H, 2×Ph-H), 7.58 – 7.40 (m, 3H, 3×Ph-H), 5.69 (q, J = 1.2 Hz, 1H, 14-H), 5.33 (s, 2H, a-CH_2), 4.85 (s, 1H, 17-H), 4.49 (s, 1H, 17-H), 3.24 (dd, J = 11.7, 4.4 Hz, 1H, 3-H), 2.39 (ddd, J = 12.8, 4.3, 2.4 Hz, 1H, 7-H), 2.34 – 2.25 (m, 1H, 12-H), 2.17 (d, J = 1.3 Hz, 3H, 16-CH_3), 2.01 – 1.88 (m, 2H, 7-H, 12-H), 1.80 – 1.46 (m, 7H, 1-H, 2-CH_2, 6-H, 9-H, 11-CH_2), 1.37 (qd, J = 12.9, 4.3 Hz, 1H, 6-H), 1.14 (td, J = 13.1, 3.6 Hz, 1H, 1-H), 1.07 (dd, J = 12.5, 2.7 Hz, 1H, 5-H), 0.98 (s, 3H, 18-CH_3), 0.76 (s, 3H, 19-CH_3), 0.67 (s, 3H, 20-CH_3). ^{13}C NMR (100 MHz, $CDCl_3$) δ 166.62 (C-15), 162.52 (C-13), 147.73 (C-8), 144.10 (b-C), 137.02 (Ph-C), 129.91 (2×Ph-C), 129.07 (Ph-C), 122.16 (c-C), 120.76 (2×Ph-C), 114.73 (C-14), 106.92 (C-17), 78.85 (C-3), 56.83 (a-CH_2), 55.99 (C-9), 54.63 (C-5), 39.94 (C-10), 39.52 (C-4), 39.24 (C-7), 38.20 (C-12), 37.14 (C-1), 28.41 (C-18), 27.98 (C-2), 24.08 (C-6), 21.75 (C-11), 19.27 (C-16), 15.54 (C-19), 14.60 (C-20). (+)ESI-HRMS *(m/z)*: calculated for [$C_{29}H_{39}N_3O_3$ + H^+] 478.3064, observed 478.3052.

*(1-(o-Tolyl)-1H-1,2,3-triazol-4-yl)methyl (E)-5-((1R,4aS,6R,8aS)-6-hydroxy-5,5,8a-trimethyl--2-methylenedecahydronaphthalen-1-yl)-3-methylpent-2-enoate (**5b**)*

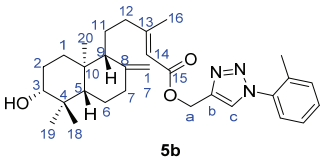

5b

Chemical Formula: $C_{30}H_{41}N_3O_3$
Exact Mass: 491.3148
Molecular Weight: 491.6760

29.8 mg, yield 73 %, white solid, m.p.= 46-48 °C; ^{1}H NMR (400 MHz, $CDCl_3$) δ 7.81 (s, 1H, c-H), 7.49 – 7.30 (m, 4H, 4×Ph-H), 5.70 (q, J = 1.3 Hz, 1H, 14-H), 5.34 (s, 2H, a-CH_2), 4.85 (s, 1H, 17-H), 4.49 (s, 1H, 17-H), 3.24 (dd, J = 11.7, 4.4 Hz, 1H, 3-H), 2.39 (ddd, J = 12.8, 4.3, 2.4 Hz, 1H, 7-H), 2.36 – 2.24 (m, 1H, 12-H), 2.22 (s, 3H, Ph-CH_3), 2.17 (d, J = 1.3 Hz, 3H, 16-CH_3), 2.03 – 1.86 (m, 2H, 7-H, 12-H), 1.81 – 1.47 (m, 7H, 1-H, 2-CH_2, 6-H, 9-H, 11-CH_2), 1.38 (qd, J = 12.9, 4.3 Hz, 1H, 6-H), 1.14 (td, J = 13.1, 3.7 Hz, 1H, 1-H), 1.07 (dd, J = 12.5, 2.7 Hz, 1H, 5-H), 0.98 (s, 3H, 18-CH_3), 0.76 (s, 3H, 19-CH_3), 0.67 (s, 3H, 20-CH_3). ^{13}C NMR (100 MHz, $CDCl_3$) δ 166.61 (C-15), 162.45 (C-13), 147.73 (C-8), 143.16 (b-C), 136.38 (Ph-C), 133.75 (Ph-C), 131.66 (Ph-C), 130.13 (Ph-C), 127.00 (Ph-C), 126.08 (c-C), 125.43 (Ph-C), 114.74 (C-14), 106.91 (C-17), 78.85 (C-3), 56.82 (a-CH_2), 55.99 (C-9), 54.63 (C-5), 39.93 (C-10), 39.51 (C-4), 39.24 (C-7), 38.20 (C-12), 37.14 (C-1), 28.41 (C-18), 27.97 (C-2), 24.07 (C-6), 21.74 (C-11), 19.25 (C-16), 18.05 (Ph-CH_3), 15.54 (C-19), 14.60 (C-20). (+)ESI-HRMS *(m/z)*: calculated for [$C_{30}H_{41}N_3O_3$ + H^+] 492.3221, observed 492.3208.

*(1-(m-Tolyl)-1H-1,2,3-triazol-4-yl)methyl (E)-5-((1R,4aS,6R,8aS)-6-hydroxy-5,5,8a-trimethyl--2-methylenedecahydronaphthalen-1-yl)-3-methylpent-2-enoate (**5c**)*

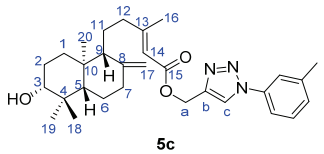

5c

Chemical Formula: $C_{30}H_{41}N_3O_3$
Exact Mass: 491.3148
Molecular Weight: 491.6760

37.5 mg, yield 92 %, white solid, m.p.= 50-53 °C; ^{1}H NMR (400 MHz, $CDCl_3$) δ 8.04 (s, 1H, c-H), 7.56 (s, 1H, Ph-H), 7.52 – 7.46 (m, 1H, Ph-H), 7.41 – 7.33 (m, 1H, Ph-H), 7.26 – 7.19 (m, 1H, Ph-H), 5.68 (q, J = 1.3 Hz, 1H, 14-H), 5.31 (s, 2H, a-CH_2), 4.84 (s, 1H, 17-H), 4.48 (s, 1H, 17-H), 3.24 (dd, J = 11.7, 4.4 Hz, 1H, 3-H), 2.44 (s, 3H, Ph-CH_3), 2.38 (ddd, J = 12.8, 4.3, 2.4 Hz, 1H, 7-H), 2.35 – 2.23 (m, 1H, 12-H), 2.17 (d, J = 1.2 Hz, 3H, 16-CH_3), 2.00 – 1.87 (m, 2H, 7-H, 12-H), 1.79 – 1.47 (m, 7H, 1-H, 2-CH_2, 6-H, 9-H, 11-CH_2), 1.37 (qd, J = 12.9, 4.2 Hz, 1H, 6-H), 1.14 (td, J = 13.0, 3.5 Hz, 1H, 1-H), 1.06 (dd, J = 12.5, 2.6 Hz, 1H, 5-H), 0.98 (s, 3H, 18-CH_3), 0.75 (s, 3H, 19-CH_3), 0.66 (s, 3H, 20-CH_3). ^{13}C NMR (100 MHz, $CDCl_3$) δ 166.60 (C-15), 162.47 (C-13), 147.70 (C-8), 143.92 (b-C), 140.15 (Ph-C), 136.91 (Ph-C), 129.80 (Ph-C), 129.66 (Ph-C), 122.21 (Ph-C), 121.38 (c-C), 117.78 (Ph-C), 114.72 (C-14), 106.89 (C-17), 78.81 (C-3), 56.81 (a-CH_2), 55.96 (C-9), 54.61 (C-5), 39.91 (C-10), 39.49 (C-4), 39.22 (C-7), 38.18 (C-12), 37.12 (C-1), 28.39 (C-18), 27.95 (C-2), 24.05 (C-6), 21.73 (C-11), 21.53 (Ph-CH_3) , 19.25 (C-16), 15.52 (C-19), 14.57 (C-20). (+)ESI--HRMS *(m/z)*: calculated for $C_{30}H_{41}N_3O_3$ [M+H+] 492.3221, observed 492.3208.

*(1-(p-Tolyl)-1H-1,2,3-triazol-4-yl)methyl (E)-5-((1R,4aS,6R,8aS)-6-hydroxy-5,5,8a-trimethyl--2-methylenedecahydronaphthalen-1-yl)-3-methylpent-2-enoate (**5d**)*

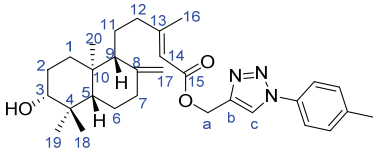

5d

Chemical Formula: $C_{30}H_{41}N_3O_3$
Exact Mass: 491.3148
Molecular Weight: 491.6760

38.8 mg, yield 95 %, white solid, m.p.= 48-49 °C; ^{1}H NMR (400 MHz, $CDCl_3$) δ 8.02 (s, 1H, c-H), 7.64 – 7.56 (m, 2H, 2×Ph-H), 7.37 – 7.28 (m, 2H, 2×Ph-H), 5.68 (q, J = 1.3 Hz, 1H, 14-H), 5.31 (s, 2H, a-CH_2), 4.84 (s, 1H, 17-H), 4.48 (s, 1H, 17-H), 3.86 (s, 3H, PhO-CH_3), 3.24 (dd, J = 11.7, 4.4 Hz, 1H, 3-H), 2.41 (s, 3H, Ph-CH_3) ,2.38 (ddd, J = 12.8, 4.3, 2.4 Hz, 1H, 7-H), 2.35 – 2.23 (m, 1H, 12-H), 2.17 (d, J = 1.2 Hz, 3H, 16-CH_3), 2.00 – 1.88 (m, 2H, 7-H, 12-H), 1.80 – 1.46 (m, 7H, 1-H, 2-CH_2, 6-H, 9-H, 11-CH_2), 1.37 (qd, J = 12.9, 4.2 Hz, 1H, 6-H), 1.14 (td, J = 13.2, 3.8 Hz, 1H, 1-H), 1.06 (dd, J = 12.5, 2.7 Hz, 1H, 5-H), 0.98 (s, 3H, 18-CH_3), 0.76 (s, 3H, 19-CH_3), 0.67 (s, 3H, 20-CH_3).^{13}C NMR (100 MHz, $CDCl_3$) δ 166.60 (C-15), 162.49 (C-13), 147.71 (C-8), 143.84 (b-C), 139.25 (Ph-C), 134.68 (Ph-C), 130.39 (2×Ph-C), 122.19 (c-C), 120.63 (2×Ph-C), 114.72 (C-14), 106.90 (C-17), 78.82 (C-3), 56.78 (a-CH_2), 55.97 (C-9), 54.61 (C-5), 39.92 (C-10), 39.50 (C-4), 39.23 (C-7), 38.18 (C-12), 37.13 (C-1), 28.39 (C-18), 27.96 (C-2), 24.06 (C-6), 21.73 (C-11), 21.25 (Ph-CH_3), 19.25 (C-16), 15.53 (C-19), 14.58 (C-20). (+)ESI-HRMS *(m/z)*: calculated for [$C_{30}H_{41}N_3O_4$ + H^+] 492.3221, observed 492.3207.

*(1-(4-Fluorophenyl)-1H-1,2,3-triazol-4-yl)methyl (E)-5-((1R,4aS,6R,8aS)-6-hydroxy-5,5,8a--trimethyl-2-methylenedecahydronaphthalen-1-yl)-3-methylpent-2-enoate (**5e**)*

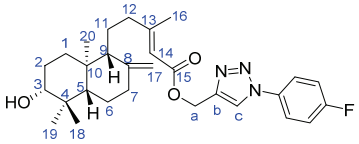

5e

Chemical Formula: $C_{29}H_{38}FN_3O_3$
Exact Mass: 495.2897
Molecular Weight: 495.6394

37.4 mg, yield 91 %, colorless oil, white solid, m.p.= 50-52 °C; ^{1}H NMR (400 MHz, $CDCl_3$) δ 8.02 (s, 1H, c-H), 7.78 – 7.62 (m, 2H, 2×Ph-H), 7.41 – 7.02 (m, 2H ,2×Ph-H), 5.68 (q, J = 1.3 Hz, 1H, 14-H), 5.31 (s, 2H, a-CH_2), 4.84 (s, 1H, 17-H), 4.48 (s, 1H, 17-H), 3.24 (dd, J = 11.7, 4.4 Hz, 1H, 3-H), 2.39 (ddd, J = 12.8, 4.3, 2.4 Hz, 1H, 7-H), 2.35 – 2.24 (m, 1H, 12-H), 2.17 (d, J = 1.2 Hz, 3H, 16-CH_3), 2.00 – 1.88 (m, 2H, 7-H, 12-H), 1.79 – 1.44 (m, 7H, 1-H, 2-CH_2, 6-H, 9-H, 11-CH_2), 1.37 (qd, J = 12.9, 4.3 Hz, 1H, 6-H), 1.14 (td, J = 13.1, 3.6 Hz, 1H, 1-H), 1.06 (dd, J = 12.5, 2.7 Hz, 1H, 5-H), 0.98 (s, 3H, 18-CH_3), 0.76 (s, 3H, 19-CH_3), 0.67 (s, 3H, 20-CH_3). ^{13}C NMR (100 MHz, $CDCl_3$) δ 166.59 (C-15), 162.64 (C-13), 162.61 (d, J = 249.3 Hz, Ph-C), 147.71 (C-8), 144.22 (b-C), 133.27 (d, J = 6.1 Hz, Ph-C), 122.74 (d, J = 8.6 Hz, 2×Ph-C), 122.35 (c-C), 116.89 (d, J = 23.4 Hz, 2×Ph-C), 114.65 (C-14), 106.89 (C-17), 78.83 (C-3), 56.75 (a-CH_2), 55.98 (C-9), 54.62 (C-5), 39.93 (C-10), 39.50 (C-4), 39.23 (C-7), 38.18 (C-12), 37.13 (C-1), 28.40 (C-18), 27.96 (C-2), 24.06 (C-6), 21.74 (C-11), 19.26 (C-16), 15.53 (C-19), 14.60 (C-20). (+)ESI-HRMS *(m/z)*: calculated for [$C_{29}H_{38}FN_3O_3$ + H^+] 496.2970, observed 496.2958.

*(1-(4-Chlorophenyl)-1H-1,2,3-triazol-4-yl)methyl (E)-5-((1R,4aS,6R,8aS)-6-hydroxy-5,5,8a--trimethyl-2-methylenedecahydronaphthalen-1-yl)-3-methylpent-2-enoate (**5f**)*

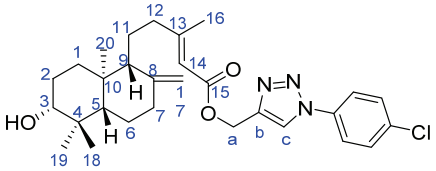

5f

Chemical Formula: $C_{29}H_{38}ClN_3O_3$
Exact Mass: 511.2602
Molecular Weight: 512.0910

38.3 mg, yield 90 %, colorless oil; ^{1}H NMR (400 MHz, $CDCl_3$) δ 8.04 (s, 1H, c-H), 7.72 – 7.65 (m, 2H, 2×Ph-H), 7.57 – 7.45 (m, 2H, 2×Ph-H), 5.67 (q, J = 1.3 Hz, 1H, 14-H), 5.31 (s, 2H, a-CH_2), 4.84 (s, 1H, 17-H), 4.48 (s, 1H, 17-H), 3.23 (dd, J = 11.7, 4.4 Hz, 1H, 3-H), 2.39 (ddd, J = 12.8, 4.3, 2.4 Hz, 1H, 7-H), 2.35 – 2.23 (m, 1H, 12-H), 2.16 (d, J = 1.2 Hz, 3H, 16-CH_3), 1.94 (m, 2H, 7-H, 12-H), 1.80 – 1.46 (m, 7H, 1-H, 2-CH_2, 6-H, 9-H, 11-CH_2), 1.37 (qd, J = 12.9, 4.2 Hz, 1H, 6-H), 1.14 (td, J = 13.1, 3.6 Hz, 1H, 1-H), 1.06 (dd, J = 12.5, 2.6 Hz, 1H, 5-H), 0.98 (s, 3H, 18-CH_3), 0.76 (s, 3H, 19-CH_3), 0.66 (s, 3H, 20-CH_3). ^{13}C NMR (100 MHz, $CDCl_3$) δ 166.58 (C-15), 162.64 (C-13), 147.72 (C-8), 144.41 (b-C), 135.50 (Ph-C), 134.80 (Ph-C), 130.08 (2×Ph-C), 122.02 (c-C), 121.86 (2×Ph-C), 114.65 (C-14), 106.90 (C-17), 78.83 (C-3), 56.77 (a-CH_2), 55.99 (C-9), 54.63 (C-5), 39.94 (C-10), 39.50 (C-4), 39.23 (C-7), 38.19 (C-12), 37.14 (C-1), 28.40 (C-18), 27.96 (C-2), 24.07 (C-6), 21.75

(C-11), 19.26 (C-16), 15.53 (C-19), 14.59 (C-20). (+)ESI-HRMS *(m/z)*: calculated for [$C_{29}H_{38}ClN_3O_3$ + H^+] 512.2674, observed 512.2668.

*(1-(4-Bromophenyl)-1H-1,2,3-triazol-4-yl)methyl (E)-5-((1R,4aS,6R,8aS)-6-hydroxy-5,5,8a--trimethyl-2-methylenedecahydronaphthalen-1-yl)-3-methylpent-2-enoate (**5g**)*

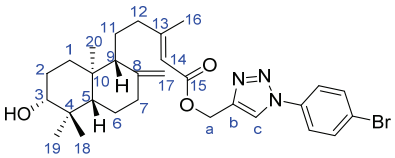

5g

Chemical Formula: $C_{29}H_{38}BrN_3O_3$
Exact Mass: 555.2097
Molecular Weight: 556.5450

41.6 mg, yield 90 %, white solid, m.p.= 66-68 °C; ^{1}H NMR (400 MHz, $CDCl_3$) δ 8.05 (s, 1H, c-H), 7.70 – 7.55 (m, 4H, 4×Ph-H), 5.67 (q, J = 1.2 Hz, 1H, 14-H), 5.31 (s, 2H, a-CH_2), 4.84 (s, 1H, 17-H), 4.47 (s, 1H, 17-H), 3.23 (dd, J = 11.7, 4.4 Hz, 1H, 3-H), 2.38 (ddd, J = 12.8, 4.3, 2.4 Hz, 1H, 7-H), 2.29 (ddt, J = 13.0, 8.7, 1.5 Hz, 1H, 12-H), 2.16 (d, J = 1.2 Hz, 3H, 16-CH_3), 1.93 (m, 2H, 7-H, 12-H), 1.80 – 1.43 (m, 7H, 1-H, 2-CH_2, 6-H, 9-H, 11-CH_2), 1.37 (qd, J = 12.9, 4.3 Hz, 1H, 6-H), 1.13 (td, J = 13.0, 3.6 Hz, 1H, 1-H), 1.06 (dd, J = 12.5, 2.7 Hz, 1H, 5-H), 0.97 (s, 3H, 18-CH_3), 0.75 (s, 3H, 19-CH_3), 0.66 (s, 3H, 20-CH_3). ^{13}C NMR (100 MHz, $CDCl_3$) δ 166.57 (C-15), 162.64 (C-13), 147.71 (C-8), 144.42 (b-C), 135.97 (Ph-C), 133.02 (2×Ph-C), 122.66 (2×Ph-C), 122.07 (2×Ph-C), 121.95 (c-C), 114.64 (C-14), 106.89 (C-17), 78.81 (C-3), 56.76 (a-CH_2), 55.99 (C-9), 54.62 (C-5), 39.93 (C-10), 39.50 (C-4), 39.23 (C-7), 38.18 (C-12), 37.14 (C-1), 28.40 (C-18), 27.96 (C-2), 24.06 (C-6), 21.74 (C-11), 19.26 16(C-16), 15.53 (C-19), 14.58 (C-20). (+)ESI-HRMS *(m/z)*: calculated for [$C_{29}H_{38}BrN_3O_3$ + H^+] 556.2169, observed 556.2183.

*(1-(4-Methoxyphenyl)-1H-1,2,3-triazol-4-yl)methyl (E)-5-((1R,4aS,6R,8aS)-6-hydroxy-5,5,8a--trimethyl-2-methylenedecahydronaphthalen-1-yl)-3-methylpent-2-enoate (**5h**)*

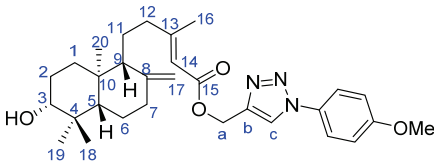

5h

Chemical Formula: $C_{30}H_{41}N_3O_4$
Exact Mass: 507.3097
Molecular Weight: 507.6750

34.1 mg, yield 81 %, white solid, m.p.= 48-49 °C; ^{1}H NMR (400 MHz, $CDCl_3$) δ 7.98 (s, 1H, c-H), 7.66 – 7.57 (m, 2H, 2×Ph-H), 7.06 – 6.97 (m, 2H, 2×Ph-H), 5.68 (q, J = 1.3 Hz, 1H, 14-H), 5.32 (s, 2H, a-CH_2), 4.85 (s, 1H, 17-H), 4.48 (s, 1H, 17-H), 3.86 (s, 3H, PhO-CH_3), 3.24 (dd, J = 11.7, 4.4 Hz, 1H, 3-H), 2.39 (ddd, J = 12.8, 4.3, 2.4 Hz, 1H, 7-H), 2.34 – 2.25 (m, 1H, 12-H), 2.17 (d, J = 1.2 Hz, 3H, 16-CH_3), 2.00 – 1.89 (m, 2H, 7-H, 12-H), 1.81 – 1.45 (m, 7H, 1-H, 2-CH_2, 6-H, 9-H, 11-CH_2), 1.37 (qd, J = 12.9, 4.2 Hz, 1H, 6-H), 1.14 (td, J = 13.1, 3.6 Hz, 1H, 1-H), 1.07 (dd, J = 12.5, 2.7 Hz, 1H, 5-H), 0.98 (s, 3H, 18-CH_3), 0.76 (s, 3H, 19-CH_3), 0.67 (s, 3H, 20-CH_3).^{13}C NMR (100 MHz, $CDCl_3$) δ 166.62 (C-15), 162.50 (C-13), 160.09 (Ph-C), 147.72 (C-8), 143.77 (b-C), 130.40 (Ph-C), 122.41 (2×Ph-C), 122.36

(c-C), 114.92 (2×Ph-C), 114.74 (C-14), 106.92 (C-17), 78.84 (C-3), 56.78 (a-CH_2), 55.98 (C-9), 55.78 (Ph-OCH_3), 54.63 (C-5), 39.93 (C-10), 39.51 (C-4), 39.24 (C-7), 38.20 (C-12), 37.14 (C-1), 28.41 (C-18), 27.98 (C-2), 24.08 (C-6), 21.75 (C-11), 19.27 (C-16), 15.54 (C-19), 14.60 (C-20). (+)ESI-HRMS *(m/z)*: calculated for [$C_{30}H_{41}N_3O_4$ + H^+] 508.3170, observed 508.3158.

*(1-(4-Cyanophenyl)-1H-1,2,3-triazol-4-yl)methyl (E)-5-((1R,4aS,6R,8aS)-6-hydroxy-5,5,8a--trimethyl-2-methylenedecahydronaphthalen-1-yl)-3-methylpent-2-enoate (**5i**)*

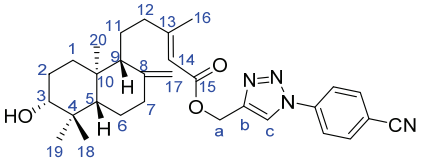

5i

Chemical Formula: $C_{30}H_{38}N_4O_3$
Exact Mass: 502.2944
Molecular Weight: 502.6590

38.4 mg, yield 92 %, white solid, m.p.= 65-68°C; ^{1}H NMR (400 MHz, $CDCl_3$) δ 8.13 (s, 1H, c-H), 7.95 – 7.89 (m, 2H, 2×Ph-H), 7.88 – 7.81 (m, 2H, 2×Ph-H), 5.68 (q, J = 1.4 Hz, 1H, 14-H), 5.33 (s, 2H, a-CH_2), 4.85 (s, 1H, 17-H), 4.48 (s, 1H, 17-H), 3.24 (dd, J = 11.7, 4.4 Hz, 1H, 3-H), 2.40 (ddd, J = 13.0, 4.1, 2.4 Hz, 1H, 7-H), 2.35 – 2.25 (m, 1H, 12-H), 2.17 (d, J = 1.2 Hz, 3H, 16-CH_3), 2.01 – 1.88 (m, 2H, 7-H, 12-H), 1.80 – 1.45 (m, 7H, 1-H, 2-CH_2, 6-H, 9-H, 11-CH_2), 1.38 (qd, J = 97.0, 12.9, 4.3 Hz, 1H, 6-H), 1.15 (td, J = 13.0, 12.3, 3.7 Hz, 1H, 1-H), 1.07 (dd, J = 12.6, 2.6 Hz, 1H, 5-H), 0.99 (s, 3H, 18-CH_3), 0.76 (s, 3H, 19-CH_3), 0.67 (s, 3H, 20-CH_3). ^{13}C NMR (100 MHz, $CDCl_3$) δ 166.58 (C-15), 162.98 (C-13), 147.74 (C-8), 145.02 (b-C), 139.82 (Ph-C), 134.10 (2×Ph-C), 121.85 (c-C), 120.76 (2×Ph-C), 117.80 (Ph-CN), 114.54 (C-14), 112.71 (Ph-C), 106.92 (C-17), 78.87 (C-3), 56.67 (a-CH_2), 56.02 (C-9), 54.65 (C-5), 39.98 (C-10), 39.54 (C-4), 39.26 (C-7), 38.21 (C-12), 37.17 (C-1), 28.42 (C 18), 27.98 (C-2), 24.08 (C-6), 21.77 (C-11), 19.31 (C-16), 15.54 (C-19), 14.61 (C-20). (+)ESI-HRMS *(m/z)*: calculated for [$C_{30}H_{38}N_3O_3$ + H^+] 503.3017, observed 503.3011.

*(1-(4-(Trifluoromethyl)phenyl)-1H-1,2,3-triazol-4-yl)methyl (E)-5-((1R,4aS,6R,8aS)-6-hydroxy-5,5,8a-trimethyl-2-methylenedecahydronaphthalen-1-yl)-3-methylpent-2-enoate (**5j**)*

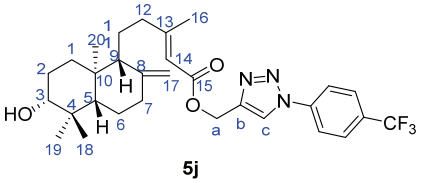

5j

Chemical Formula: $C_{30}H_{38}F_3N_3O_3$
Exact Mass: 545.2865
Molecular Weight: 545.6472

40.3 mg, yield 89 %, white solid, m.p.= 56-58 °C; ^{1}H NMR (400 MHz, $CDCl_3$) δ 8.13 (s, 1H, c-H), 7.97 – 7.85 (m, 2H, 2×Ph-H), 7.84 – 7.77 (m, 2H, 2×Ph-H), 5.69 (q, J = 1.2 Hz, 1H, 14-H), 5.33 (s, 2H, a-CH_2), 4.85 (s, 1H, 17-H), 4.48 (s, 1H, 17-H), 3.24 (dd, J = 11.7, 4.4 Hz, 1H, 3-H), 2.39 (ddd, J = 12.8, 4.3, 2.4 Hz, 1H, 7-H), 2.36 – 2.24 (m, 1H, 12-H), 2.17 (d, J = 1.2 Hz, 3H, 16-CH_3), 1.95 (m, 2H, 7-H, 12-H), 1.81 – 1.44 (m, 7H, 1-H, 2-CH_2, 6-H, 9-H, 11-CH_2), 1.38 (qd, J = 13.0, 4.3 Hz, 1H, 6-H), 1.14 (td, J = 13.0, 3.7 Hz, 1H, 1-H), 1.07 (dd,

J = 12.5, 2.6 Hz, 1H, 5-H), 0.98 (s, 3H, 18-CH_3), 0.76 (s, 3H, 19-CH_3), 0.67 (s, 3H, 20-CH_3). ^{13}C NMR (100 MHz, $CDCl_3$) δ 166.60 (C-15), 162.82 (C-13), 147.73 (C-8), 144.72 (b-C), 139.41 (Ph-C), 130.98 (q, J = 33.1 Hz, Ph-C), 127.27 (q, J = 3.6 Hz, 2×Ph-C), 123.62 (q, J = 272.2 Hz, Ph-CF_3), 121.99 (c-C), 120.63 (2×Ph-C), 114.60 (C-14), 106.91 (C-17), 78.85 (C-3), 56.73 (a-CH_2), 56.00 (C-9), 54.64 (C-5), 39.96 (C-10), 39.52 (C-4), 39.24 (C-7), 38.20 (C-12), 37.15 (C-1), 28.41 (C-18), 27.97 (C-2), 24.07 (C-6), 21.76 (C-11), 19.29 (C-16), 15.53 (C-19), 14.60 (C-20). (+)ESI-HRMS *(m/z)*: calculated for [$C_{30}H_{38}F_3N_3O_3$ + H^+] 546.2938, observed 546.2941.

*(1-(4-Nitrophenyl)-1H-1,2,3-triazol-4-yl)methyl (E)-5-((1R,4aS,6R,8aS)-6-hydroxy-5,5,8a--trimethyl-2-methylenedecahydronaphthalen-1-yl)-3-methylpent-2-enoate (**5k**)*

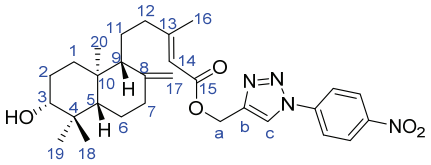

5k

Chemical Formula: $C_{29}H_{38}N_4O_5$
Exact Mass: 522.2842
Molecular Weight: 522.6460

37.3 mg, yield 86 %, colorless oil; ^{1}H NMR (400 MHz, $CDCl_3$) δ 8.45 – 8.36 (m, 2H, 2×Ph-H), 8.19 (s, 1H, c-H), 8.02 – 7.94 (m, 2H, 2×Ph-H), 5.68 (q, J = 1.3 Hz, 1H, 14-H), 5.33 (s, 2H, a-CH_2), 4.84 (s, 1H, 17-H), 4.48 (s, 1H, 17-H), 3.24 (dd, J = 11.7, 4.4 Hz, 1H, 3-H), 2.39 (ddd, J = 12.8, 4.3, 2.4 Hz, 1H, 7-H), 2.36 – 2.24 (m, 1H, 12-H), 2.17 (d, J = 1.2 Hz, 3H, 16-CH_3), 2.01 – 1.87 (m, 2H, 7-H, 12-H), 1.80 – 1.44 (m, 7H, 1-H, 2-CH_2, 6-H, 9-H, 11-CH_2), 1.37 (qd, J = 12.9, 4.3 Hz, 1H, 6-H), 1.14 (td, J = 13.0, 3.6 Hz, 1H, 1-H), 1.06 (dd, J = 12.5, 2.7 Hz, 1H, 5-H), 0.98 (s, 3H, 18-CH_3), 0.75 (s, 3H, 19-CH_3), 0.66 (s, 3H, 20-CH_3). ^{13}C NMR (100 MHz, $CDCl_3$) δ 166.55 (C-15), 163.03 (C-13), 147.70 (C-8), 147.39 (Ph-C), 145.10 (b C), 141.13 (Ph-C), 125.68 (2×Ph-C), 122.04 (c-C), 120.67 (2×Ph-C), 114.48 (C-14), 106.89 (C-17), 78.84 (C-3), 56.61 (a-CH_2), 55.99 (C-9), 54.62 (C-5), 39.96 (C-10), 39.50 (C-4), 39.22 (C-7), 38.18 (C-12), 37.14 18(1-C), 28.40 (C-18), 27.94 (C-2), 24.05 (C-6), 21.75 (C-11), 19.29 (C-16), 15.53 (C-19), 14.58 (C-20). (+)ESI-HRMS *(m/z)*: calculated for [$C_{29}H_{38}N_4O_5$ + H^+] 523.2909, observed 523.2914.

*(1-(2,4-Dichlorophenyl)-1H-1,2,3-triazol-4-yl)methyl (E)-5-((1R,4aS,6R,8aS)-6-hydroxy--5,5,8a-trimethyl-2-methylenedecahydronaphthalen-1-yl)-3-methylpent-2-enoate (**5l**)*

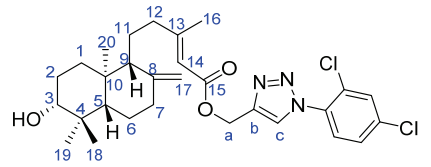

5l

Chemical Formula: $C_{29}H_{37}Cl_2N_3O_3$
Exact Mass: 545.2212
Molecular Weight: 546.5330

32.7 mg, yield 72 %, white solid, m.p.= 49-52 °C; ^{1}H NMR (400 MHz, $CDCl_3$) δ 8.05 (s, 1H, c-H), 7.63 – 7.52 (m, 2H, 2×Ph-H), 7.47 – 7.39 (m, 1H, Ph-H), 5.68 (q, J = 1.2 Hz, 1H, 14-H), 5.33 (s, 2H, a-CH_2), 4.84 (s, 1H, 17-H), 4.48 (s, 1H, 17-H), 3.24 (dd, J = 11.7, 4.4 Hz,

1H, 3-H), 2.39 (ddd, *J* = 12.8, 4.4, 2.5 Hz, 1H, 7-H), 2.35 – 2.24 (m, 1H, 12-H), 2.16 (d, *J* = 1.2 Hz, 3H, 16-CH_3), 2.01 – 1.88 (m, 2H, 7-H, 12-H), 1.81 – 1.44 (m, 7H, 1-H, 2-CH_2, 6-H, 9-H, 11-CH_2), 1.37 (qd, *J* = 12.9, 4.3 Hz, 1H, 6-H), 1.14 (td, *J* = 13.1, 3.5 Hz, 1H, 1-H), 1.06 (dd, *J* = 12.5, 2.6 Hz, 1H, 5-H), 0.98 (s, 3H, 18-CH_3), 0.76 (s, 3H, 19-CH_3), 0.67 (s, 3H, 20-CH_3). ^{13}C NMR (100 MHz, $CDCl_3$) δ 166.53, 166.51 (C-15), 162.54 (C-13), 147.71 (C-8), 143.47 (b-C), 136.46 (Ph-C), 133.50 (Ph-C), 130.74 (Ph-C), 129.4 (Ph-C), 128.62 (Ph-C), 128.44 (Ph-C), 125.81 (c-C), 114.68 (C-14), 106.91 (C-17), 78.83 (C-3), 56.74 (a-CH_2), 55.97 (C-9), 54.63 (C-5), 39.92 (C-10), 39.50 (C-4), 39.23 (C-7), 38.19 (C-12), 37.14 (C-1), 28.40 (C-18), 27.96 (C-2), 24.07 (C-6), 21.72 (C-11), 19.25 (C-16), 15.53 (C-19), 14.59 (C-20). (+)ESI-HRMS *(m/z)*: calculated for [$C_{29}H_{37}Cl_2N_3O_3$ + H^+] 546.2285, observed 546.2291.

*(1-(3,4-Dichlorophenyl)-1H-1,2,3-triazol-4-yl)methyl (E)-5-((1R,4aS,6R,8aS)-6-hydroxy--5,5,8a-trimethyl-2-methylenedecahydronaphthalen-1-yl)-3-methylpent-2-enoate (**5m**)*

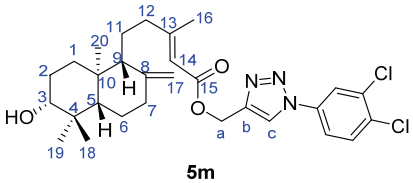

5m

Chemical Formula: $C_{29}H_{37}Cl_2N_3O_3$
Exact Mass: 545.2212
Molecular Weight: 546.5330

41.7 mg, yield 92 %, colorless oil; ^{1}H NMR (400 MHz, $CDCl_3$) δ 8.06 (s, 1H, c-H), 7.94 – 7.84 (m, 1H, Ph-H), 7.66 – 7.55 (m, 2H, 2×Ph-H), 5.67 (q, *J* = 1.3 Hz, 1H, 14-H), 5.30 (s, 2H, a-CH_2), 4.84 (s, 1H, 17-H), 4.47 (s, 1H, 17-H), 3.23 (dd, *J* = 11.7, 4.3 Hz, 1H, 3-H), 2.38 (ddd, *J* = 12.8, 4.3, 2.4 Hz, 1H, 7-H), 2.35 – 2.23 (m, 1H, 12-H), 2.16 (d, *J* = 1.3 Hz, 3H, 16-CH_3), 1.93 (m, 2H, 7-H, 12-H), 1.80 – 1.43 (m, 7H, 1-H, 2-CH_2, 6-H, 9-H, 11-CH_2), 1.36 (qd, *J* = 12.9, 4.3 Hz, 1H, 6-H), 1.13 (td, *J* = 13.0, 3.4 Hz, 1H, 1-H), 1.06 (dd, *J* = 12.5, 2.6 Hz, 1H, 5-H), 0.97 (s, 3H, 18-CH_3), 0.75 (s, 3H, 19-CH_3), 0.66 (s, 3H, 20-CH_3). ^{13}C NMR (100 MHz, $CDCl_3$) δ 166.55 (C-15), 162.80 (C-13), 147.69 (C-8), 144.65 (b-C), 135.98 (Ph-C), 134.10 (Ph-C), 133.09 (Ph-C), 131.59 (Ph-C), 122.37 (Ph-C), 121.97 (c-C), 119.56 (Ph-C), 114.55 (C-14), 106.88 (C-17), 78.78 (C-3), 56.68 (a-CH_2), 55.97 (C-9), 54.60 (C-5), 39.93 (C-10), 39.48 (C-4), 39.21 (C-7), 38.17 (C-12), 37.12 (C-1), 28.39 (C-18), 27.93 (C-2), 24.04 (C-6), 21.73 (C-11), 19.26 (C-16), 15.52 (C-19), 14.57 (C-20). (+)ESI-HRMS *(m/z)*: calculated for [$C_{29}H_{37}Cl_2N_3O_3$ + H^+] 546.2285, observed 546.2298.

*(1-(Naphthalen-1-yl)-1H-1,2,3-triazol-4-yl)methyl (E)-5-((1R,4aS,6R,8aS)-6-hydroxy-5,5,8a--trimethyl-2-methylenedecahydronaphthalen-1-yl)-3-methylpent-2-enoate (**5n**)*

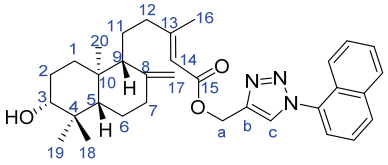

5n

Chemical Formula: $C_{33}H_{41}N_3O_3$
Exact Mass: 527.3148
Molecular Weight: 527.7090

36.8 mg, yield 84 %, colorless oil; ^{1}H NMR (400 MHz, $CDCl_3$) δ 8.07 – 7.93 (m, 3H, c-H, 2×Ph-H), 7.66 – 7.47 (m, 5H, 5×Ph-H), 5.72 (q, J = 1.2 Hz, 1H, 14-H), 5.41 (s, 2H, a-CH_2), 4.85 (s, 1H, 17-H), 4.49 (s, 1H, 17-H), 3.23 (dd, J = 11.7, 4.4 Hz, 1H, 3-H), 2.39 (ddd, J = 12.8, 4.3, 2.4 Hz, 1H, 7-H), 2.37 – 2.24 (m, 1H, 12-H), 2.18 (d, J = 1.2 Hz, 3H, 16-CH_3), 2.01 – 1.90 (m, 2H, 7-H, 12-H), 1.81 – 1.45 (m, 7H, 1-H, 2-CH_2, 6-H, 9-H, 11-CH_2), 1.37 (qd, J = 12.9, 4.2 Hz, 1H, 6-H), 1.14 (td, J = 13.1, 3.6 Hz, 1H, 1-H), 1.06 (dd, J = 12.5, 2.7 Hz, 1H, 5-H), 0.98 (s, 3H, 18-CH_3), 0.75 (s, 3H, 19-CH_3), 0.67 (s, 3H, 20-CH_3). ^{13}C NMR (100 MHz, $CDCl_3$) δ 166.59 (C-15), 162.49 (C-13), 147.71 (C-8), 143.38 (b-C), 134.23 (Ph-C), 133.61 (Ph-C), 130.63 (Ph-C), 128.50 (Ph-C), 128.41 (Ph-C), 128.05 (Ph-C), 127.22 (Ph-C), 126.44 (Ph-C), 125.07 (Ph-C), 123.69 (Ph-C), 122.36 (c-C), 114.72 (C-14), 106.89 (C-17), 78.79 (C-3), 56.92 (a-CH_2), 55.96 (C-9), 54.60 (C-5), 39.92 (C-10), 39.49 (C-4), 39.21 (C-7), 38.18 (C-12), 37.12 (C-1), 28.38 (C-18), 27.94 (C-2), 24.05 (C-6), 21.72 (C-11), 19.25 (C-16), 15.52 (C-19), 14.57 (C-20). (+)ESI-HRMS *(m/z)*: calculated for [$C_{33}H_{41}N_3O_3$ + H^+] 528.3221, observed 528.3213.

*(1-Benzyl-1H-1,2,3-triazol-4-yl)methyl (E)-5-((1R,4aS,6R,8aS)-6-hydroxy-5,5,8a-trimethyl-2--methylenedecahydronaphthalen-1-yl)-3-methylpent-2-enoate (**5o**)*

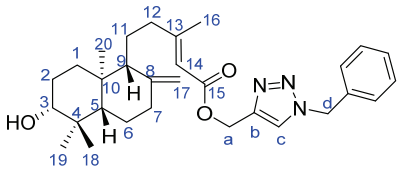

5o

Chemical Formula: $C_{30}H_{41}N_3O_3$
Exact Mass: 491.3148
Molecular Weight: 491.6760

35.5 mg, yield 87 %, colorless oil; ^{1}H NMR (400 MHz, $CDCl_3$) δ 7.54 (s, 1H, c-H), 7.42 – 7.32 (m, 3H, 3×Ph-H), 7.30 – 7.24 (m, 2H, 2×Ph-H), 5.63 (q, J = 1.3 Hz, 1H, 14-H), 5.52 (s, 2H, d-CH_2), 5.24 – 5.16 (s, 2H, a-CH_2), 4.84 (s, 1H, 17-H), 4.47 (s, 1H, 17-H), 3.24 (dd, J = 11.7, 4.3 Hz, 1H, 3-H), 2.38 (ddd, J = 12.8, 4.3, 2.4 Hz, 1H, 7-H), 2.33 – 2.21 (m, 1H, 12-H), 2.13 (d, J = 1.3 Hz, 3H, 16-CH_3), 2.00 – 1.86 (m, 2H, 7-H, 12-H), 1.79 – 1.45 (m, 7H, 1-H, 2-CH_2, 6-H, 9-H, 11-CH_2), 1.37 (qd, J = 12.9, 4.2 Hz, 1H, 6-H), 1.13 (td, J = 13.0, 3.5 Hz, 1H, 1-H), 1.06 (dd, J = 12.5, 2.7 Hz, 1H, 5-H), 0.98 (s, 3H, 18-CH_3), 0.76 (s, 3H, 19-CH_3), 0.66 (s, 3H, 20-CH_3). ^{13}C NMR (100 MHz, $CDCl_3$) δ 166.51 (C-15), 162.36 (C-13), 147.71 (C-8), 143.55 (b-C), 134.29 (Ph-C), 129.30 (2×Ph-C), 129.03 (c-C), 128.30 (2×Ph-C), 123.82 (Ph-C), 114.70 (C-14), 106.89 (C-17), 78.81 (C-3), 56.66 (a-CH_2), 55.96 (C-9), 54.61 (C-5), 54.53 (d-CH_2), 39.89 (C-10), 39.49 (C-4), 39.23 (C-7), 38.18 (C-12), 37.12 (C-1), 28.40 (C-18), 27.96 (C-2), 24.06 (C-6), 21.71 (C-11), 19.20 (C-16), 15.53 (C-19), 14.58 (C-20). (+)ESI-HRMS *(m/z)*: calculated for [$C_{30}H_{41}N_3O_3$ + H^+] 492.3221, observed 492.3210.

*(1-(4-Methylbenzyl)-1H-1,2,3-triazol-4-yl)methyl (E)-5-((1R,4aS,6R,8aS)-6-hydroxy-5,5,8a--trimethyl-2-methylenedecahydronaphthalen-1-yl)-3-methylpent-2-enoate (**5p**)*

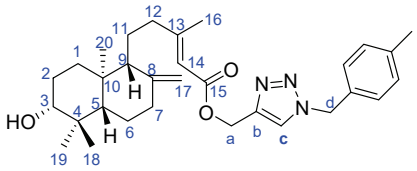

5p

Chemical Formula: $C_{31}H_{43}N_3O_3$
Exact Mass: 505.3304
Molecular Weight: 505.7030

40.3 mg, yield 96 %, colorless oil; ^{1}H NMR (400 MHz, $CDCl_3$) δ 7.51 (s, 1H, c-H), 7.17 (s, 4H, 4×Ph-H), 5.63 (q, J = 1.2 Hz, 1H, 14-H), 5.47 (s, 2H, d-CH_2), 5.20 (s, 2H, a-CH_2), 4.84 (s, 1H, 17-H), 4.47 (d, J = 1.6 Hz, 1H, 17-H), 3.24 (dd, J = 11.7, 4.3 Hz, 1H, 3-H), 2.38 (ddd, J = 13.0, 4.3, 2.5 Hz, 1H, 7-H), 2.34 (s, 3H, Ph-CH_3), 2.32 – 2.21 (m, 1H, 12-H), 2.13 (d, J = 1.2 Hz, 3H, 16-CH_3), 2.00 – 1.87 (m, 2H, 7-H, 12-H), 1.80 – 1.46 (m, 7H, 1-H, 2-CH_2, 6-H, 9-H, 11-CH_2), 1.37 (qd, J = 12.9, 4.2 Hz, 1H, 6-H), 1.13 (td, J = 13.0, 3.4 Hz, 1H, 1-H), 1.06 (dd, J = 12.5, 2.6 Hz, 1H, 5-H), 0.98 (s, 3H, 18-CH_3), 0.76 (s, 3H, 19-CH_3), 0.66 (s, 3H, 20-CH_3). ^{13}C NMR (100 MHz, cdcl$_3$) δ 166.50 (C-15), 162.25 (C-13), 147.71 (C-8), 143.49 (b-C), 138.97 (Ph-C), 131.31 (Ph-C), 129.92 (2×Ph-C), 128.34 (2×Ph-C), 123.63 (c-C), 114.73 (C-14), 106.88 (C-17), 78.80 (C-3), 56.72 (a-CH_2), 55.95 (C-9), 54.60 (C-5), 54.27 (d-CH_2), 39.88 (C-10), 39.48 (C-4), 39.22 (C-7), 38.17 (C-12), 37.12 (C-1), 28.39 (C-18), 27.95 (C-2), 24.05 (C-6), 21.70 (C-11), 21.30 (Ph-CH_3), 19.19 (C-16), 15.53 (C-19), 14.57 (C-20). (+)ESI-HRMS *(m/z)*: calculated for [$C_{31}H_{43}N_3O_3$ + H^+] 506.3377, observed 506.3370.

*(1-(4-Fluorobenzyl)-1H-1,2,3-triazol-4-yl)methyl (E)-5-((1R,4aS,6R,8aS)-6-hydroxy-5,5,8a-trimethyl-2-methylenedecahydronaphthalen-1-yl)-3-methylpent-2-enoate (**5q**)*

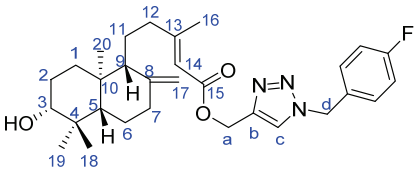

5q

Chemical Formula: $C_{30}H_{40}FN_3O_3$
Exact Mass: 509.3054
Molecular Weight: 509.6664

33.4 mg, yield 79 %, colorless oil; ^{1}H NMR (400 MHz, $CDCl_3$) δ 7.53 (s, 1H, c-H), 7.34 – 7.23 (m, 2H, 2×Ph-H), 7.13 – 6.97 (m, 2H, 2×Ph-H), 5.63 (q, J = 1.2 Hz, 1H, 14-H), 5.48 (s, 2H, d-CH_2), 5.21 (s, 2H, a-CH_2), 4.84 (s, 1H, 17-H), 4.47 (s, 1H, 17-H), 3.23 (dd, J = 11.7, 4.3 Hz, 1H, 3-H), 2.38 (ddd, J = 12.8, 4.3, 2.4 Hz, 1H, 7-H), 2.33 – 2.21 (m, 1H, 12-H), 2.13 (d, J = 1.3 Hz, 3H, 16-CH_3), 1.98 – 1.86 (m, 2H, 7-H, 12-H), 1.79 – 1.42 (m, 7H, 1-H, 2-CH_2, 6-H, 9-H, 11-CH_2), 1.37 (qd, J = 12.9, 4.3 Hz, 1H, 6-H), 1.13 (td, J = 12.9, 3.7 Hz, 1H, 1-H), 1.06 (dd, J = 12.5, 2.8 Hz, 1H, 5-H), 0.98 (s, 3H, 18-CH_3), 0.76 (s, 3H, 19-CH_3), 0.66 (s, 3H, 20-CH_3). ^{13}C NMR (100 MHz, $CDCl_3$) δ 166.52 (C-15), 163.01 (d, J = 248.1 Hz, Ph-C), 162.35 (C-13), 147.72 (C-8), 143.79 (b-C), 130.29 (d, J = 3.2 Hz, Ph-C), 130.17 (d, J = 8.4 Hz, 2×Ph-C), 123.65 (c-C), 116.29 (d, J = 21.7 Hz, 2×Ph-C), 114.70 (C-14), 106.88 (C-17),

78.81 (C-3), 56.74 (a-CH_2), 55.98 (C-9), 54.62 (C-5), 53.67 (d-CH_2), 39.90 (C-10), 39.49 (C-4), 39.23 (C-7), 38.18 (C-12), 37.14 (C-1), 28.40 (C-18), 27.96 (C-2), 24.06 (C-6), 21.72 (C-11), 19.19 (C-16), 15.53 (C-19), 14.58 (C-20). (+)ESI-HRMS *(m/z)*: calculated for [$C_{30}H_{40}FN_3O_3$ + H^+] 510.3126, observed 510.3115.

*(1-(4-Chlorobenzyl)-1H-1,2,3-triazol-4-yl)methyl (E)-5-((1R,4aS,6R,8aS)-6-hydroxy-5,5,8a--trimethyl-2-methylenedecahydronaphthalen-1-yl)-3-methylpent-2-enoate (**5r**)*

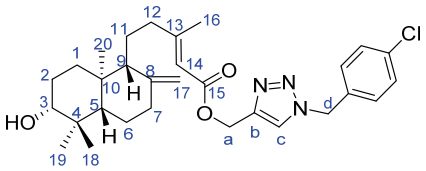

5r

Chemical Formula: $C_{30}H_{40}ClN_3O_3$
Exact Mass: 525.2758
Molecular Weight: 526.1180

34.9 mg, yield 80 %, colorless oil; ^{1}H NMR (400 MHz, $CDCl_3$) δ 7.54 (s, 1H, c-H), 7.40 – 7.31 (m, 2H, 2×Ph-H), 7.24 – 7.18 (m, 2H, 2×Ph-H), 5.63 (q, J = 1.2 Hz, 1H, 14-H), 5.48 (s, 2H, d-CH_2), 5.20 (s, 2H, a-CH_2), 4.84 (s, 1H, 17-H), 4.47 (s, 1H, 17-H), 3.23 (dd, J = 11.7, 4.3 Hz, 1H, 3-H), 2.38 (ddd, J = 12.8, 4.3, 2.4 Hz, 1H, 7-H), 2.33 – 2.21 (m, 1H, 12-H), 2.13 (d, J = 1.2 Hz, 3H, 16-CH_3), 1.99 – 1.86 (m, 2H, 7-H, 12-H), 1.79 – 1.45 (m, 7H, 1-H, 2-CH_2, 6-H, 9-H, 11-CH_2), 1.37 (qd, J = 13.0, 4.3 Hz, 1H, 6-H), 1.13 (td, J = 13.0, 3.7 Hz, 1H, 1-H), 1.06 (dd, J = 12.5, 2.8 Hz, 1H, 5-H), 0.98 (s, 3H, 18-CH_3), 0.76 (s, 3H, 19-CH_3), 0.66 (s, 3H, 20-CH_3). ^{13}C NMR (100 MHz, $CDCl_3$) δ 166.51 (C-15), 162.34 (C-13), 147.71 (C-8), 143.90 (b-C), 135.02 (Ph-C), 132.96 (Ph-C), 129.57 (2×Ph-C), 129.46 (2×Ph-C), 123.68 (c-C), 114.70 (C-14), 106.87 (C-17), 78.80 (C-3), 56.77 (a-CH_2), 55.97 (C-9), 54.62 (C-5), 53.62 (d-CH_2), 39.89 (C-10), 39.49 (C-4), 39.22 (C-7), 38.18 (C-12), 37.13 (C-1), 28.39 (C-18), 27.96 (C-2), 24.06 (C-6), 21.72 (C-11), 19.19 (C-16), 15.52 (C-19), 14.58 (C-20). (+)ESI--HRMS *(m/z)*: calculated for [$C_{30}H_{40}ClN_3O_3$ + H^+] 526.2831, observed 526.2831.

*(1-(4-Bromobenzyl)-1H-1,2,3-triazol-4-yl)methyl (E)-5-((1R,4aS,6R,8aS)-6-hydroxy-5,5,8a--trimethyl-2-methylenedecahydronaphthalen-1-yl)-3-methylpent-2-enoate (**5s**)*

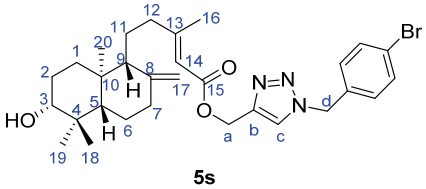

5s

Chemical Formula: $C_{30}H_{40}BrN_3O_3$
Exact Mass: 569.2253
Molecular Weight: 570.5720

37.9 mg, yield 80 %, colorless oil; ^{1}H NMR (400 MHz, $CDCl_3$) δ 7.54 (s, 1H, c-H), 7.52 – 7.47 (m, 2H, 2×Ph-H), 7.21 – 7.10 (m, 2H, 2×Ph-H), 5.64 (q, J = 1.3 Hz, 1H, 14-H), 5.47 (s, 2H, d-CH_2), 5.21 (s, 2H, a-CH_2), 4.84 (s, 1H, 17-H), 4.47 (s, 1H, 17-H), 3.24 (dd, J = 11.7, 4.3 Hz, 1H, 3-H), 2.39 (ddd, J = 12.8, 4.3, 2.4 Hz, 1H, 7-H), 2.34 – 2.22 (m, 1H, 12-H), 2.14 (d, J = 1.2 Hz, 3H, 16-CH_3), 2.00 – 1.88 (m, 2H, 7-H, 12-H), 1.79 – 1.46 (m, 7H, 1-H, 2-CH_2, 6-H, 9-H, 11-CH_2), 1.37 (qd, J = 13.0, 4.4 Hz, 1H, 6-H), 1.14 (td, J = 13.0, 3.7 Hz, 1H, 1-H),

1.06 (dd, J = 12.5, 2.8 Hz, 1H, 5-H), 0.99 (s, 3H, 18-CH_3), 0.76 (s, 3H, 19-CH_3), 0.67 (s, 3H, 20-CH_3). ^{13}C NMR (100 MHz, $CDCl_3$) δ 166.53 (C-15), 162.41 (C-13), 147.73 (C-8), 143.90 (b-C), 133.43 (Ph-C), 132.47 (2×Ph-C), 129.87 (2×Ph-C), 123.74 (c-C), 123.21 (Ph-C), 114.70 (C-14), 106.90 (C-17), 78.84 (C-3), 56.73 (a-CH_2), 56.00 (C-9), 54.64 (C-5), 53.75 (d-CH_2), 39.92 (C-10), 39.51 (C-4), 39.24 (C-7), 38.20 (C-12), 37.15 (C-1), 28.41 (C-18), 27.99 (C-2), 24.08 (C-6), 21.74 (C-11), 19.22 (C-16), 15.53 (C-19), 14.60 (C-20). (+)ESI--HRMS *(m/z)*: calculated for [$C_{30}H_{40}BrN_3O_3$ + H^+] 570.2326, observed 570.2346.

*(1-(4-Methoxybenzyl)-1H-1,2,3-triazol-4-yl)methyl (E)-5-((1R,4aS,6R,8aS)-6-hydroxy-5,5,8a--trimethyl-2-methylenedecahydronaphthalen-1-yl)-3-methylpent-2-enoate (**5t**)*

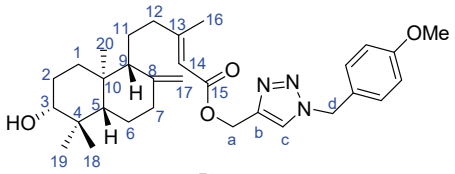

5t

Chemical Formula: $C_{31}H_{43}N_3O_4$
Exact Mass: 521.3254
Molecular Weight: 521.7020

35.1 mg, yield 81 %, colorless oil; ^{1}H NMR (400 MHz, $CDCl_3$) δ 7.51 (s, 1H, c-H), 7.25 – 7.16 (m, 2H, 2×Ph-H), 6.94 – 6.81 (m, 2H, 2×Ph-H), 5.63 (q, J = 1.3 Hz, 1H, 14-H), 5.44 (s, 2H, d-CH_2), 5.20 (s, 2H, a-CH_2), 4.83 (s, 1H, 17-H), 4.47 (s, 1H, 17-H), 3.80 (s, 3H, Ph-OCH_3), 3.23 (dd, J = 11.7, 4.3 Hz, 1H, 3-H), 2.38 (ddd, J = 12.2, 4.3, 2.4 Hz, 1H, 7-H), 2.33 – 2.21 (m, 1H, 12-H), 2.12 (d, J = 1.2 Hz, 3H, 16-CH_3), 1.98 – 1.87 (m, 2H, 7-H, 12-H), 1.79 – 1.44 (m, 7H, 1-H, 2-CH_2, 6-H, 9-H, 11-CH_2), 1.37 (qd, J = 12.9, 4.1 Hz, 1H, 6-H), 1.13 (td, J = 13.0, 3.5 Hz, 1H, 1-H), 1.06 (dd, J = 12.5, 2.7 Hz, 1H, 5-H), 0.98 (s, 3H, 18-CH_3), 0.75 (s, 3H, 19-CH_3), 0.66 (s, 3H, 20-CH_3). ^{13}C NMR (100 MHz, $CDCl_3$) δ 166.50 (C-15), 162.32 (C-13), 160.11 (Ph-C), 147.71 (C-8), 143.38 (b-C), 129.91 (2×Ph-C), 126.22 (Ph-C), 123.59 (c-C), 114.70 (C-14), 114.62 (2×Ph-C), 106.87 (C-17), 78.79 (C-3), 56.63 (a-CH_2), 55.94 (C-9), 55.46 (C-5), 54.60 (Ph-OCH_3), 54.09 (d-CH_2), 39.87 (C-10), 39.48 (C-4), 39.22 (C-7), 38.17 (C-12), 37.11 (C-1), 28.39 (C-18), 27.95 (C-2), 24.05 (C-6), 21.69 (C-11), 19.20 (C--16), 15.53 (C-19), 14.57 (C-20). (+)ESI-HRMS *(m/z)*: calculated for [$C_{31}H_{43}N_3O_4$ + H^+] 522.3326, observed 522.3320.

*(1-(4-Cyanidebenzyl)-1H-1,2,3-triazol-4-yl)methyl (E)-5-((1R,4aS,6R,8aS)-6-hydroxy-5,5,8a-trimethyl-2-methylenedecahydronaphthalen-1-yl)-3-methylpent-2-enoate (**5u**)*

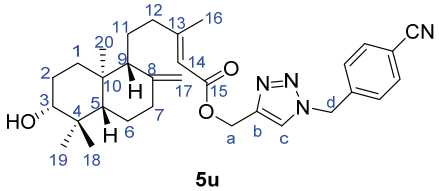

5u

Chemical Formula: $C_{31}H_{40}N_4O_3$
Exact Mass: 516.3100
Molecular Weight: 516.6860

40.3 mg, yield 94 %, colorless oil; ^{1}H NMR (400 MHz, $CDCl_3$) δ 7.72 – 7.63 (m, 2H, 2×Ph-H), 7.60 (s, 1H, c-H), 7.38 – 7.32 (m, 2H, 2×Ph-H), 5.64 (q, J = 1.3 Hz, 1H, 14-H), 5.58 (s, 2H, d-CH_2), 5.23 (s, 2H, a-CH_2), 4.84 (s, 1H, 17-H), 4.47 (s, 1H, 17-H), 3.24 (dd, J = 11.7, 4.3 Hz, 1H, 3-H), 2.39 (ddd, J = 12.8, 4.3, 2.5 Hz, 1H, 7-H), 2.34 – 2.22 (m, 1H, 12-H), 2.14 (d, J = 1.2 Hz, 3H, 16-CH_3), 2.02 – 1.84 (m, 2H, 7-H, 12-H), 1.80 – 1.45 (m, 7H, 1-H, 2-CH_2, 6-H, 9-H, 11-CH_2), 1.37 (qd, J = 12.9, 4.3 Hz, 1H, 6-H), 1.13 (td, J = 13.1, 3.6 Hz, 1H, 1-H), 1.06 (dd, J = 12.5, 2.7 Hz, 1H, 5-H), 0.98 (s, 3H, 18-CH_3), 0.76 (s, 3H, 19-CH_3), 0.67 (s, 3H, 20-CH_3). ^{13}C NMR (100 MHz, $CDCl_3$) δ 166.53 (C-15), 162.58 (C-13), 147.73 (C-8), 144.25 (b-C), 139.64 (Ph-C), 133.04 (2×Ph-C), 128.59 (2×Ph-C), 124.03 (c-C), 118.21 (Ph-CN), 114.63 (C-14), 113.02 (Ph-C), 106.89 (C-17), 78.84 (C-3), 56.73 (a-CH_2), 55.99 (C-9), 54.65 (C-5), 53.62 (d-CH_2), 39.93 (C-10), 39.51 (C-4), 39.24 (C-7), 38.19 (C-12), 37.16 (C-1), 28.41 (C-18), 27.98 (C-2), 24.07 (C-6), 21.74 (C-11), 19.22 (C-16), 15.53 (C-19), 14.60 (C-20). (+)ESI-HRMS *(m/z)*: calculated for [$C_{31}H_{40}N_4O_3$ + H^+] 517.3173, observed 517.3163.

*(1-(4-Trifluorobenzyl)-1H-1,2,3-triazol-4-yl)methyl (E)-5-((1R,4aS,6R,8aS)-6-hydroxy-5,5,8a-trimethyl-2-methylenedecahydronaphthalen-1-yl)-3-methylpent-2-enoate (**5v**)*

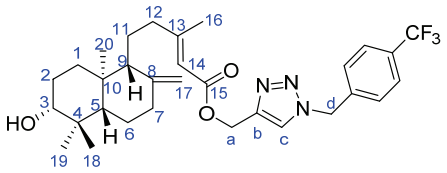

5v

Chemical Formula: $C_{31}H_{40}F_3N_3O_3$
Exact Mass: 559.3022
Molecular Weight: 559.6742

40.1 mg, yield 88 %, colorless oil; ^{1}H NMR (400 MHz, $CDCl_3$) δ 7.66 – 7.60 (m, 2H, 2×Ph-H), 7.59 (s, 1H, c-H), 7.40 – 7.35 (m, 2H, 2×Ph-H), 5.64 (q, J = 1.2 Hz, 1H, 14-H), 5.58 (s, 2H, d-CH_2), 5.22 (s, 2H, a-CH_2), 4.84 (s, 1H, 17-H), 4.47 (s, 1H, 17-H), 3.24 (dd, J = 11.7, 4.3 Hz, 1H, 3-H), 2.38 (ddd, J = 12.8, 4.3, 2.4 Hz, 1H, 7-H), 2.34 – 2.21 (m, 1H, 12-H), 2.13 (d, J = 1.3 Hz, 3H, 16-CH_3), 2.01 – 1.88 (m, 2H. 7-H, 12-H), 1.80 – 1.45 (m, 7H, 1-H, 2-CH_2, 6-H, 9-H, 11-CH_2), 1.37 (qd, J = 12.9, 4.3 Hz, 1H, 6-H), 1.13 (td, J = 13.0, 3.4 Hz, 1H, 1-H), 1.06 (dd, J = 12.5, 2.7 Hz, 1H, 5-H), 0.98 (s, 3H, 18-CH_3), 0.76 (s, 3H, 19-CH_3), 0.66 (s, 3H, 20-CH_3). ^{13}C NMR (100 MHz, $CDCl_3$) δ 166.52 (C-15), 162.55 (C-13), 147.72 (C-8), 143.99 (b-C), 138.32 (Ph-C), 131.26 (q, J = 32.3Hz, Ph-C), 128.42 (c-C), 126.28 (q, J = 3.7 Hz, 2×Ph-C), 123.99 (2×Ph-C), 123.83 (q, J = 273.7 Hz, Ph-CF_3), 114.63 (C-14), 106.88 (C-17), 78.83 (C-3), 56.65 (a-CH_2), 55.98 (C-9), 54.62 (C-5), 53.76 (d-CH_2), 39.91 (C-10), 39.50 (C-4), 39.23 (C-7), 38.18 (C-12), 37.13 (C-1), 28.40 (C-18), 27.96 (C-2), 24.06 (C-6), 21.72 (C-11), 19.20 (C-16), 15.53 (C-19), 14.58 (C-20). (+)ESI-HRMS *(m/z)*: calculated for [$C_{31}H_{40}F_3N_3O_3$ + H^+] 560.3095, observed 560.3058.

*(1-(4-Nitrobenzyl)-1H-1,2,3-triazol-4-yl)methyl (E)-5-((1R,4aS,6R,8aS)-6-hydroxy-5,5,8a-trimethyl-2-methylenedecahydronaphthalen-1-yl)-3-methylpent-2-enoate (**5w**)*

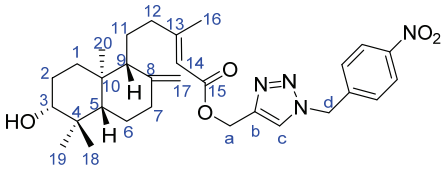

5w

Chemical Formula: $C_{30}H_{40}N_4O_5$
Exact Mass: 536.2999
Molecular Weight: 536.6730

43.2 mg, yield 97 %, colorless oil; ^{1}H NMR (400 MHz, $CDCl_3$) δ 8.28 – 8.16 (m, 2H, 2×Ph-H), 7.63 (s, 1H, c-H), 7.53 – 7.37 (m, 2H, 2×Ph-H), 5.64 (s, 3H, 14-H, d-CH_2), 5.23 (s, 2H, a-CH_2), 4.84 (s, 1H, 17-H), 4.46 (s, 1H, 17-H), 3.23 (dd, J = 11.7, 4.3 Hz, 1H, 3-H), 2.38 (ddd, J = 12.8, 4.3, 2.4 Hz, 1H, 7-H), 2.34 – 2.22 (m, 1H, 12-H), 2.13 (d, J = 1.0 Hz, 3H, 16-CH_3), 2.00 – 1.86 (m, 2H, 7-H, 12-H), 1.79 – 1.45 (m, 7H, 1-H, 2-CH_2, 6-H, 9-H, 11-CH_2), 1.37 (qd, J = 12.9, 4.3 Hz, 1H, 6-H), 1.13 (td, J = 13.0, 3.5 Hz, 1H, 1-H), 1.06 (dd, J = 12.5, 2.7 Hz, 1H, 5-H), 0.98 (s, 3H, 18-CH_3), 0.76 (s, 3H, 19-CH_3), 0.66 (s, 3H, 20-CH_3). ^{13}C NMR (100 MHz, $CDCl_3$) δ 166.52 (C-15), 162.63 (C-13), 148.23 (Ph-C), 147.72 (C-8), 144.27 (b-C), 141.46 (Ph-C), 128.80 (2×Ph-C), 124.46 (2×Ph-C), 124.11 (c-C), 114.60 (C-14), 106.88 (C-17), 78.83 (C-3), 56.68 (a-CH_2), 55.98 (C-9), 54.63 (C-5), 53.34 (d-CH_2), 39.92 (C-10), 39.50 (C-4), 39.23 (C-7), 38.18 (C-12), 37.14 (C-1), 28.40 (C-18), 27.96 (C-2), 24.06 (C-6), 21.73 (C-11), 19.21 (C-16), 15.52 (C-19), 14.59 (C-20). (+)ESI-HRMS *(m/z)*: calculated for [$C_{30}H_{40}N_4O_5$ + H^+] 537.3071, observed 537.3060.

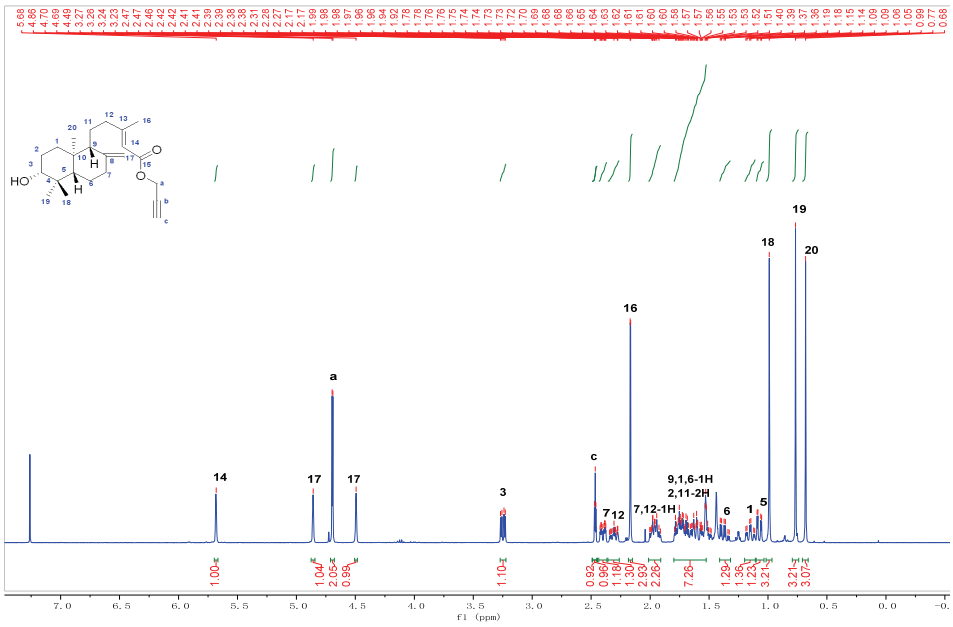

Fig. S-1. ^{1}H NMR spectrum of compound 3 ($CDCl_3$, 400 MHz).

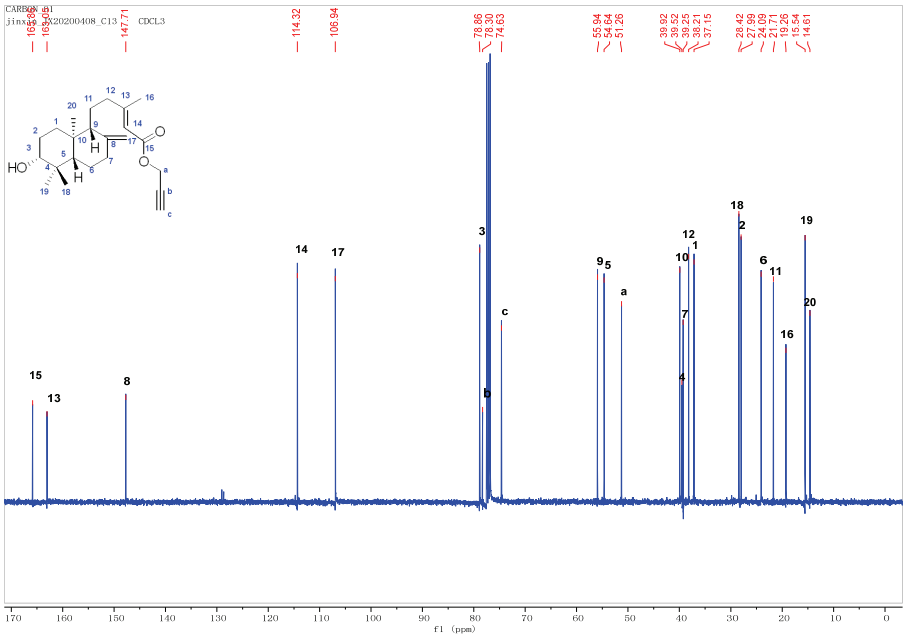

Fig. S-2. ^{13}C NMR spectrum of compound 3 ($CDCl_3$, 100 MHz)

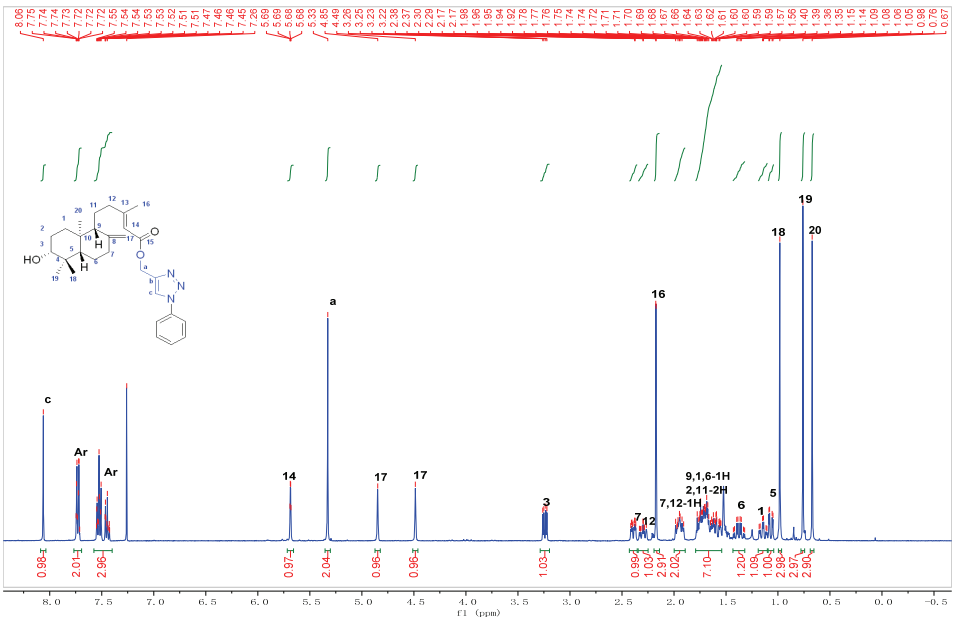

Fig. S-3. ^{1}H NMR spectrum of compound 5a ($CDCl_3$, 400 MHz)

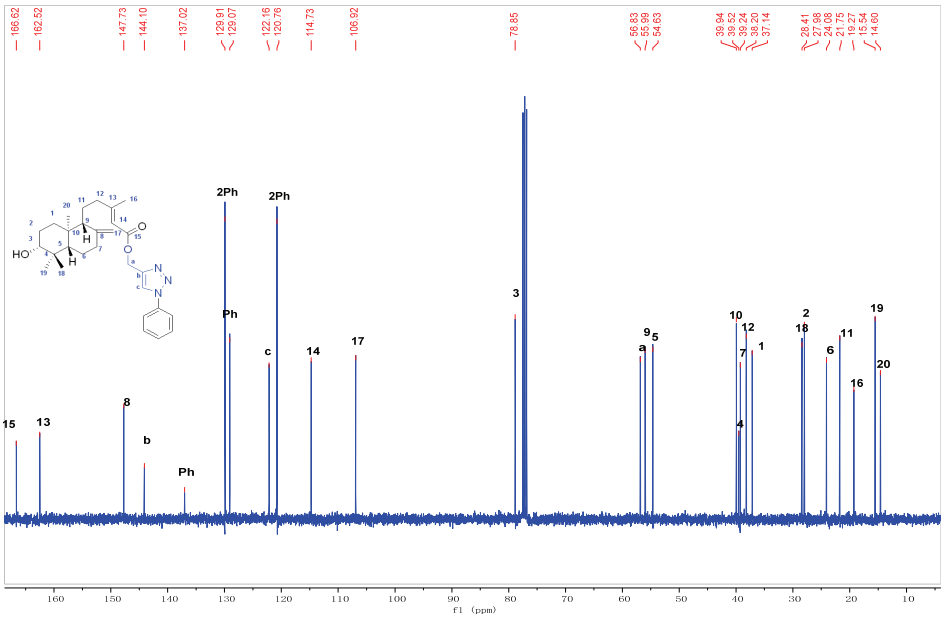

Fig. S-4. ^{13}C NMR spectrum of compound 5a ($CDCl_3$, 100 MHz)

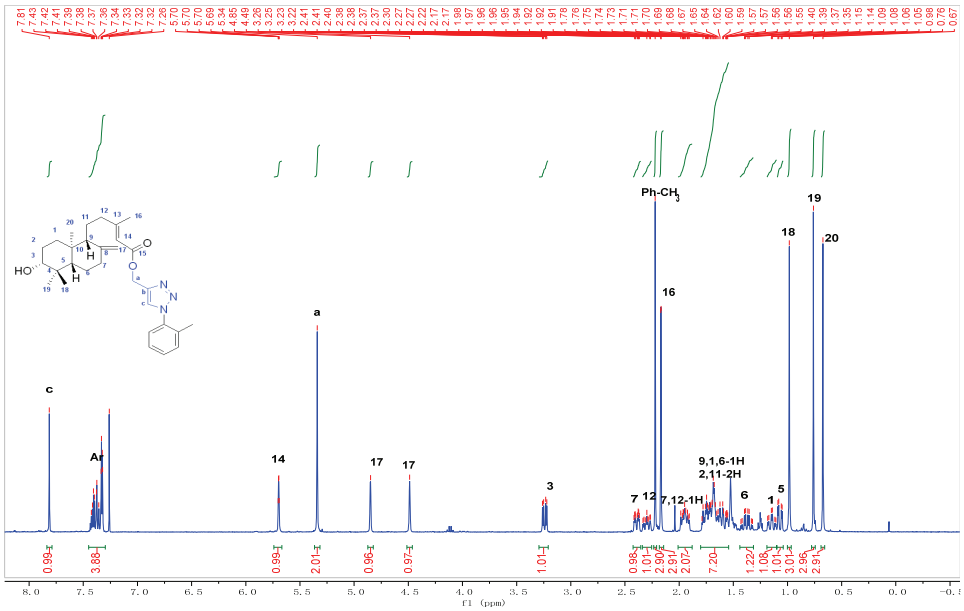

Fig. S-5. ^{1}H NMR spectrum of compound 5b ($CDCl_3$, 400 MHz)

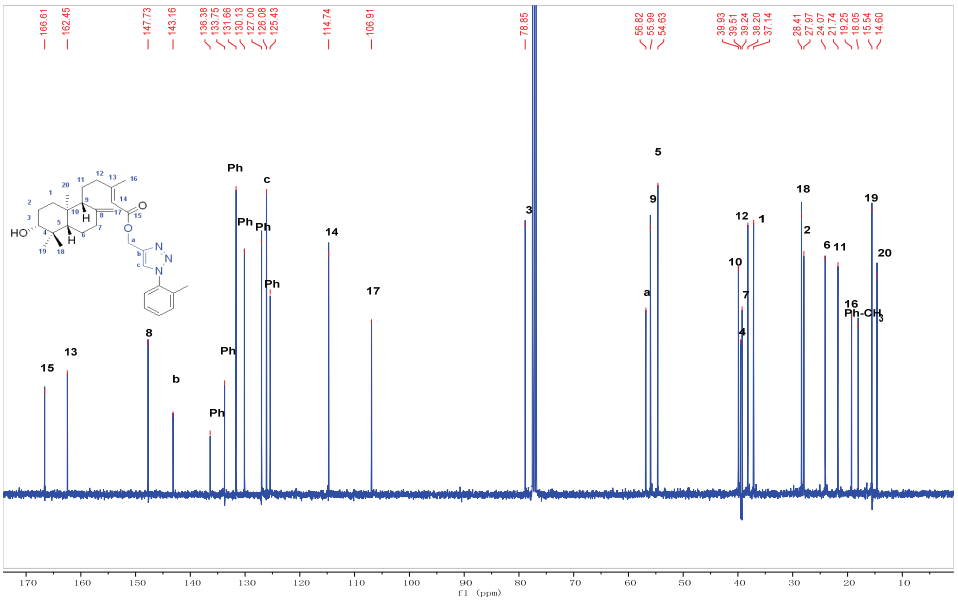

Fig. S-6. ^{13}C NMR spectrum of compound 5b ($CDCl_3$, 100 MHz)

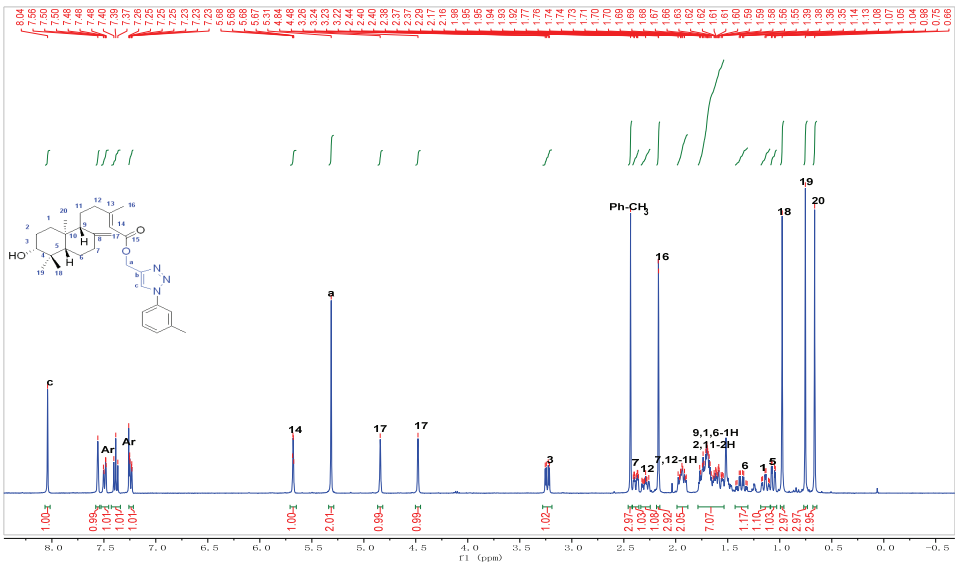

Fig. S-7. ^{1}H NMR spectrum of compound 5c ($CDCl_3$, 400 MHz)

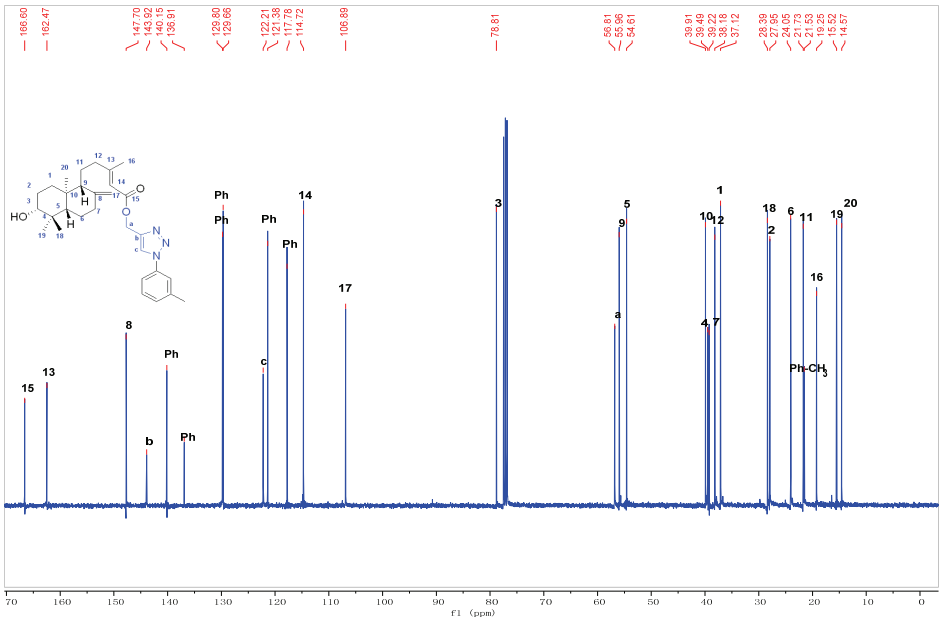

Fig. S-8. ^{13}C NMR spectrum of compound 5c ($CDCl_3$, 100 MHz)

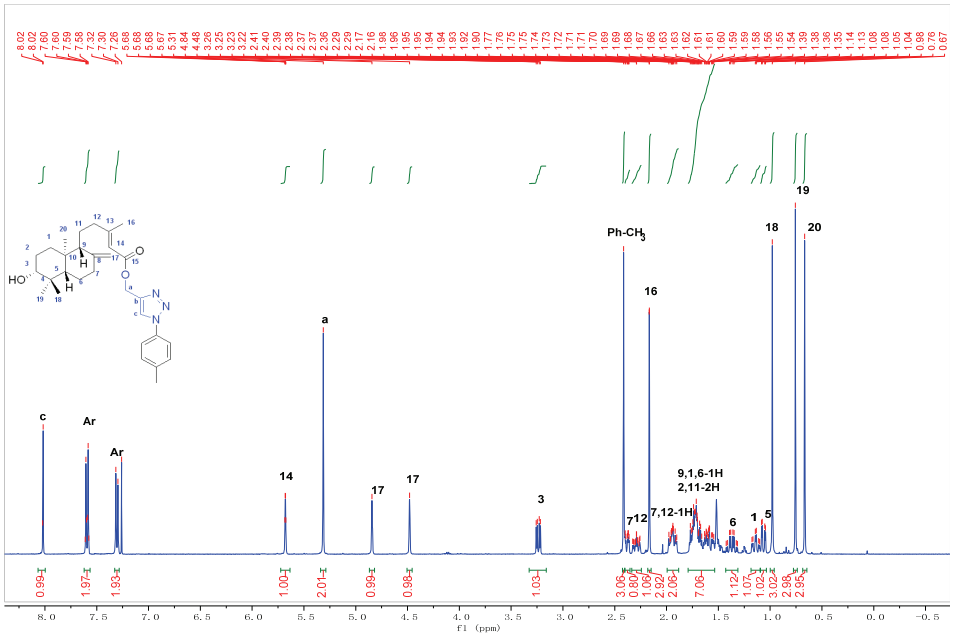

Fig. S-9. ^{1}H NMR spectrum of compound 5d ($CDCl_3$, 400 MHz)

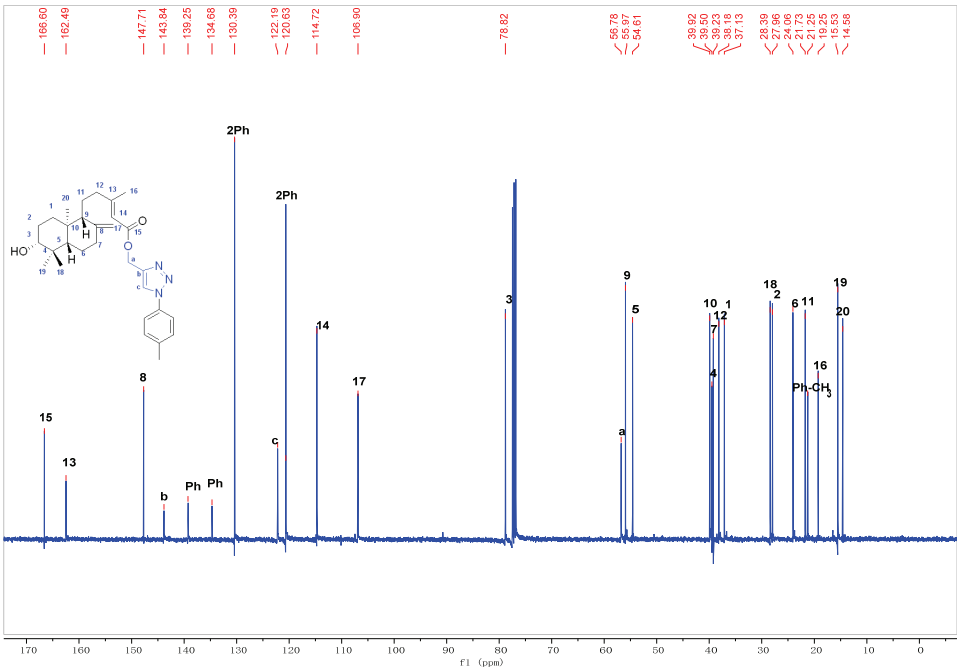

Fig. S-10. ^{13}C NMR spectrum of compound 5d ($CDCl_3$, 100 MHz)

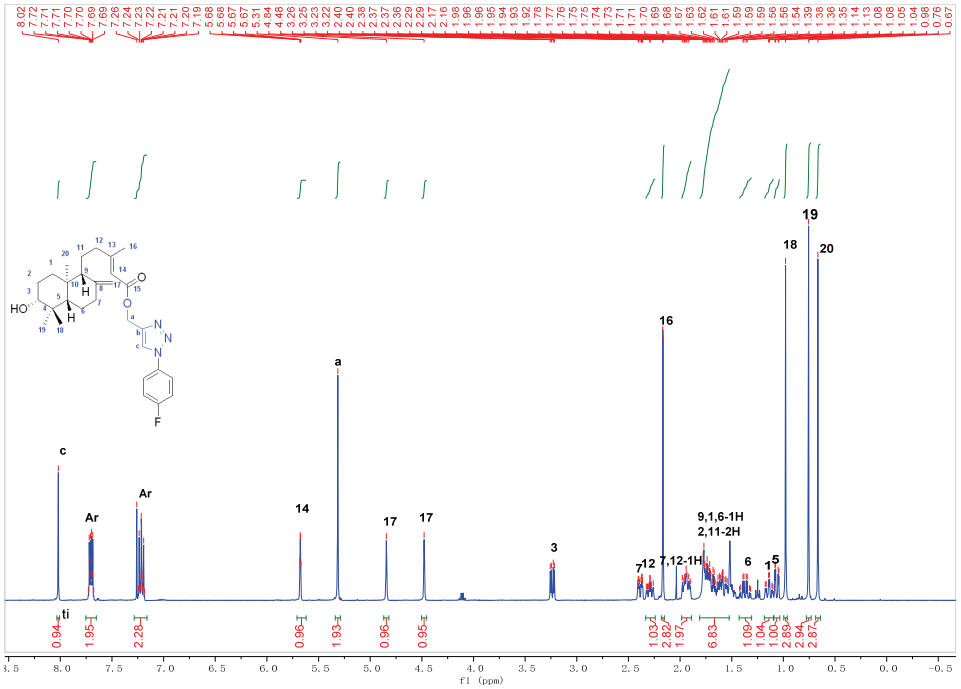

Fig. S-11. ^{1}H NMR spectrum of compound 5e ($CDCl_3$, 400 MHz)

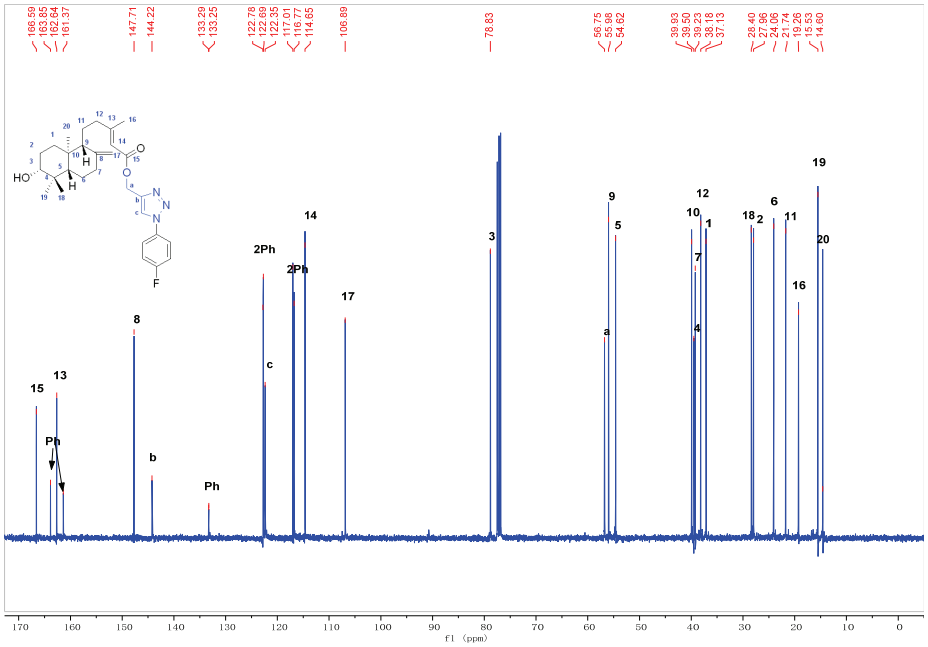

Fig. S-12. ^{13}C NMR spectrum of compound 5e ($CDCl_3$, 100 MHz)

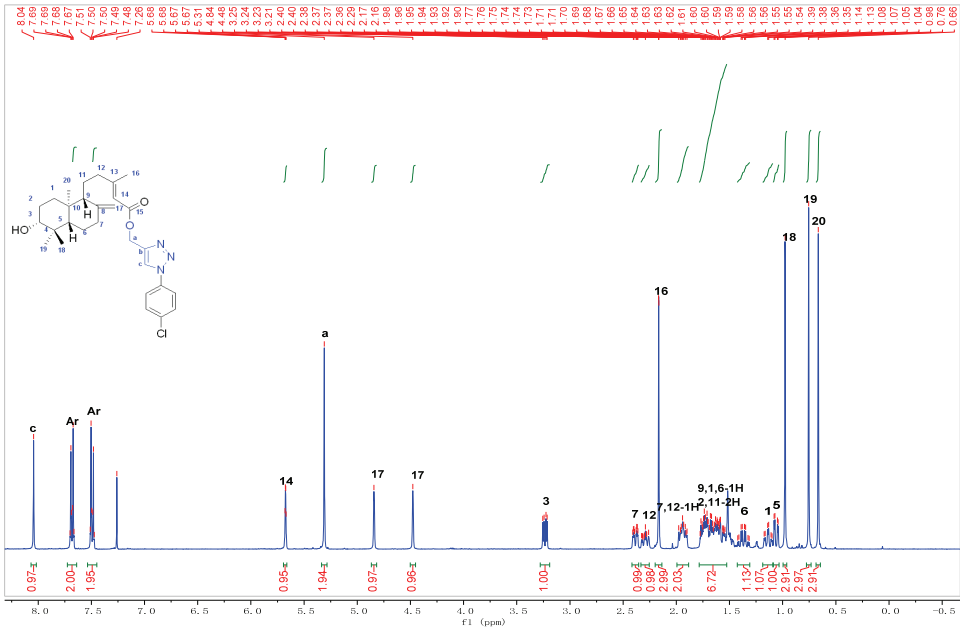

Fig. S-13. ^{1}H NMR spectrum of compound 5f ($CDCl_3$, 400 MHz)

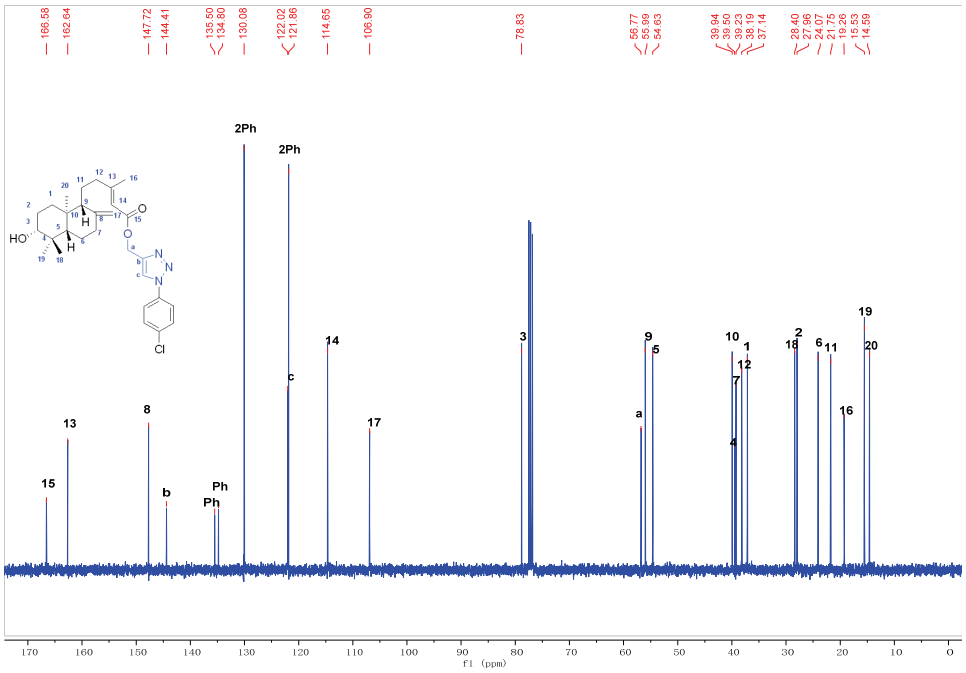

Fig. S-14. ^{13}C NMR spectrum of compound 5f ($CDCl_3$, 100 MHz)

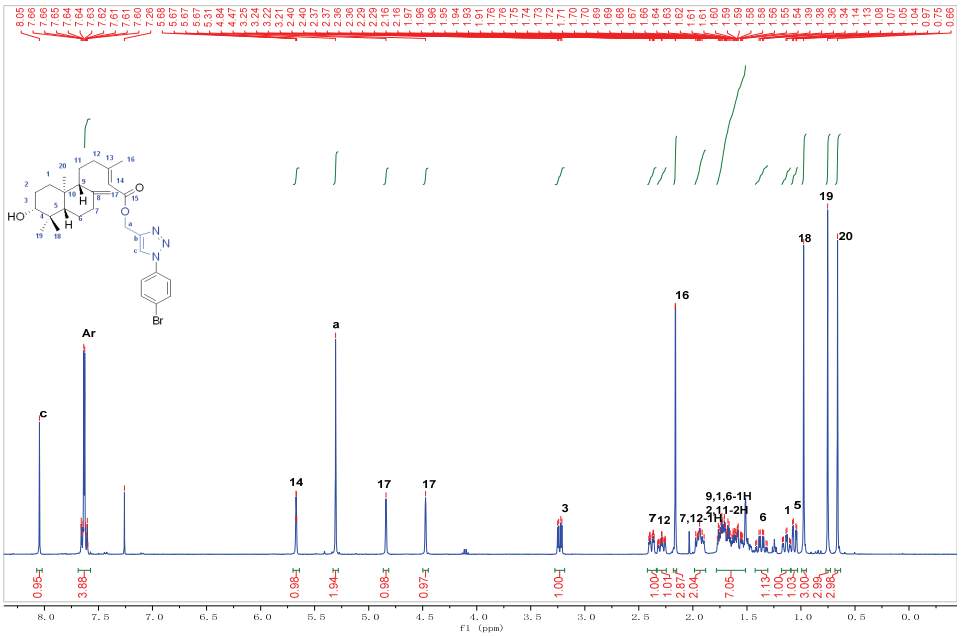

Fig. S-15. ^{1}H NMR spectrum of compound 5g ($CDCl_3$, 400 MHz)

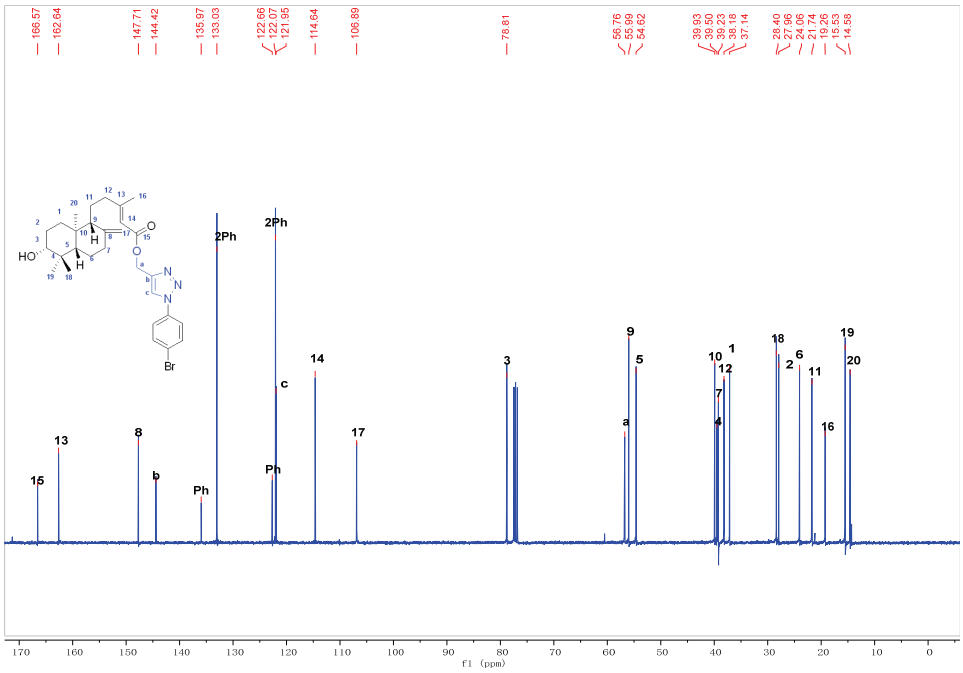

Fig. S-16. ^{13}C NMR spectrum of compound 5g ($CDCl_3$, 100 MHz)

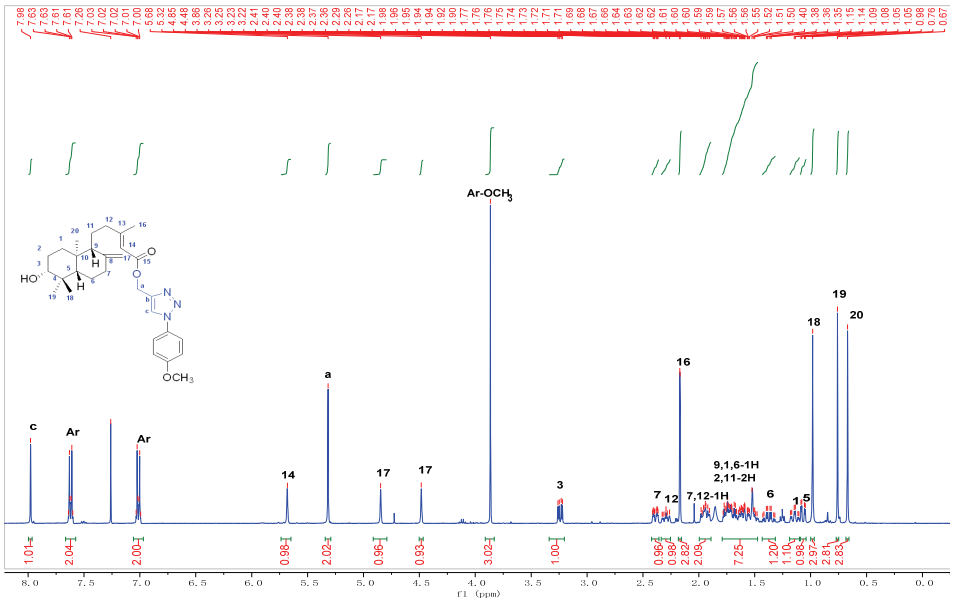

Fig. S-17. ^{1}H NMR spectrum of compound 5h ($CDCl_3$, 400 MHz)

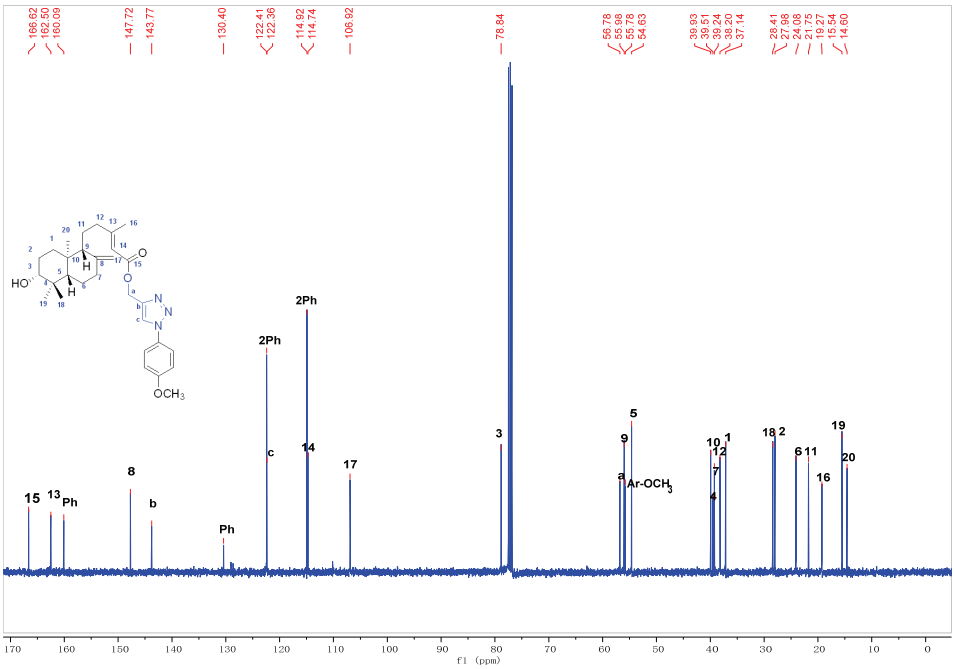

Fig. S-18. ^{13}C NMR spectrum of compound 5h ($CDCl_3$, 100 MHz)

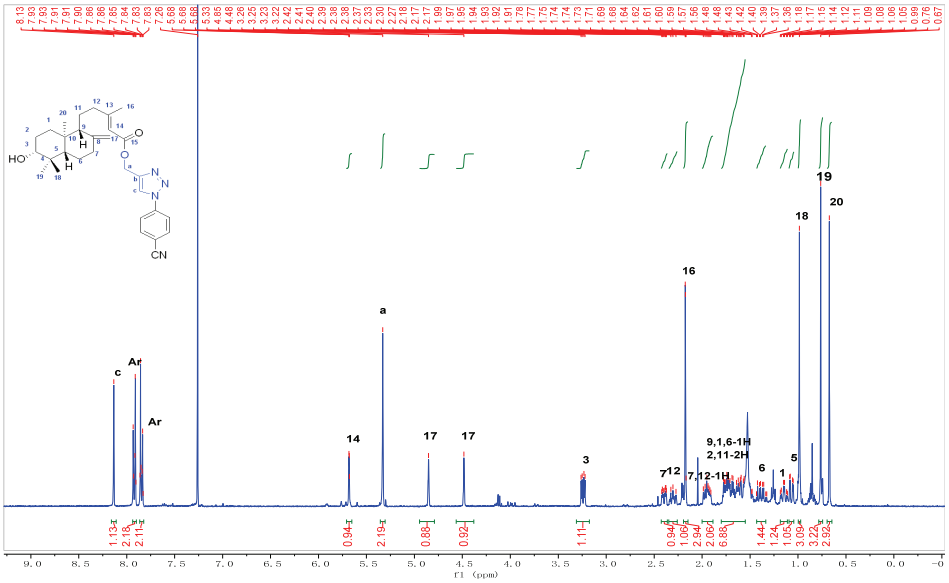

Fig. S-19. ^{1}H NMR spectrum of compound 5i ($CDCl_3$, 400 MHz)

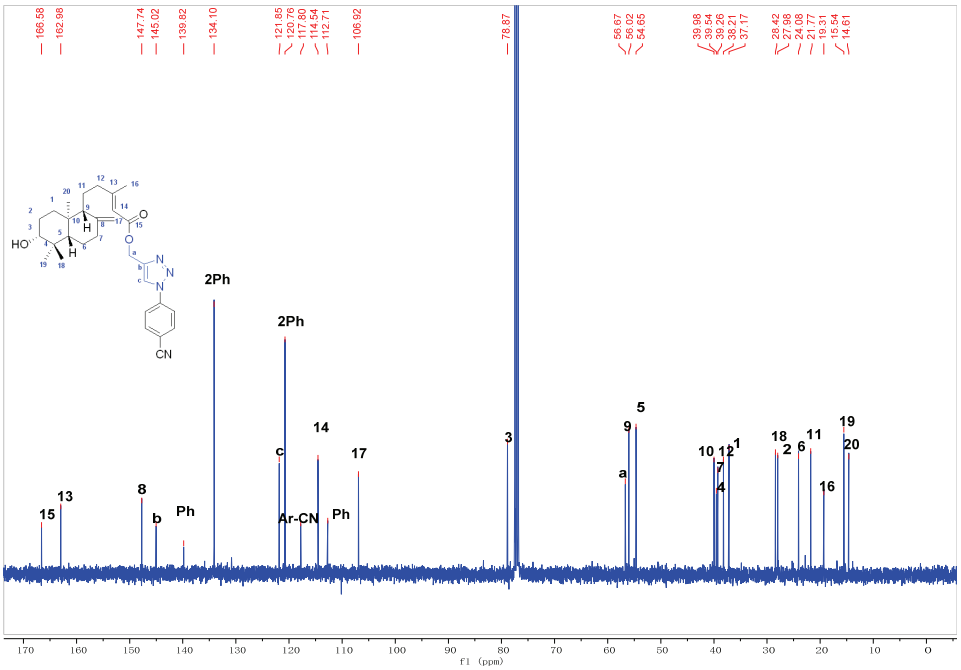

Fig. S-20. ^{13}C NMR spectrum of compound 5i ($CDCl_3$, 100 MHz)

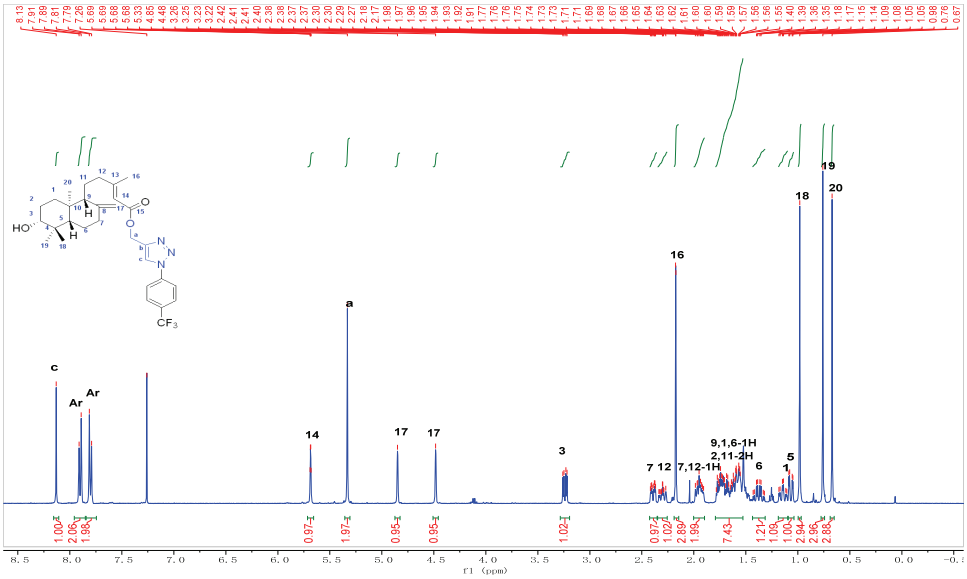

Fig. S-21. ^{1}H NMR spectrum of compound 5j ($CDCl_3$, 400 MHz)

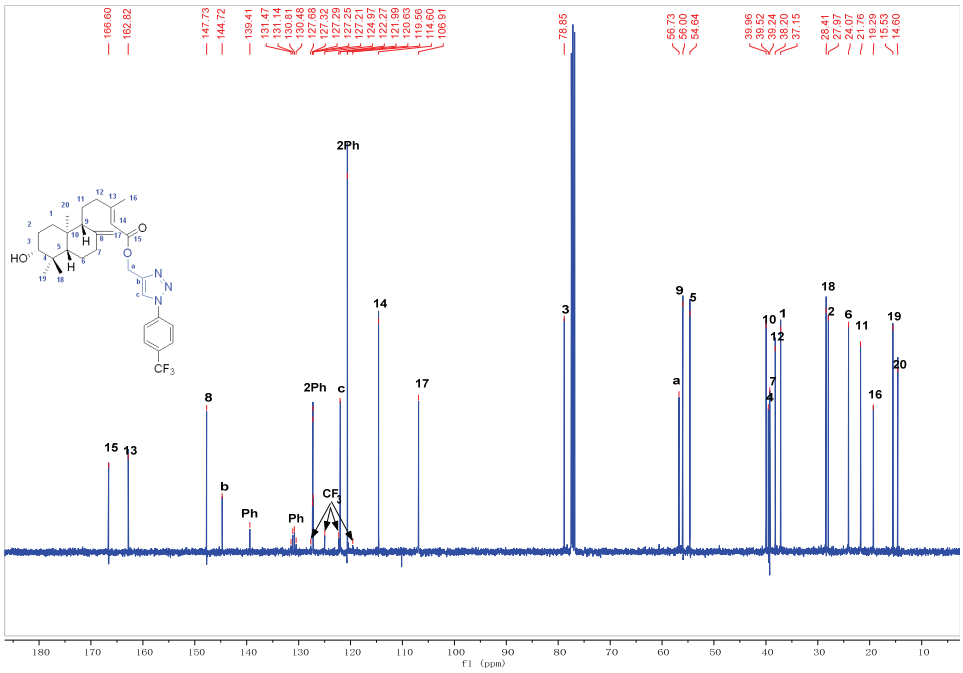

Fig. S-22. ^{13}C NMR spectrum of compound 5j ($CDCl_3$, 100 MHz)

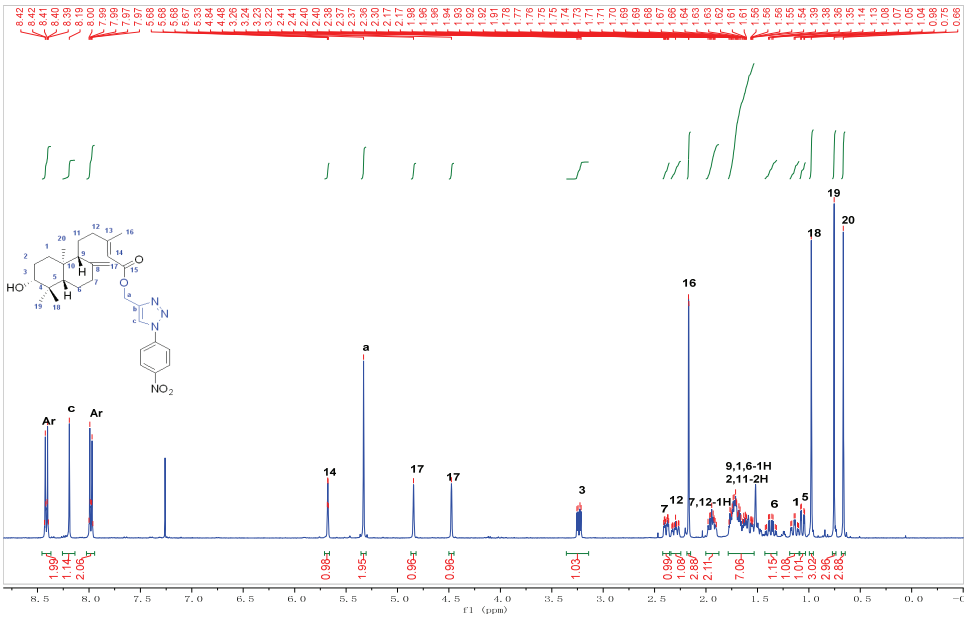

Fig. S-23. ^{1}H NMR spectrum of compound 5k ($CDCl_3$, 400 MHz)

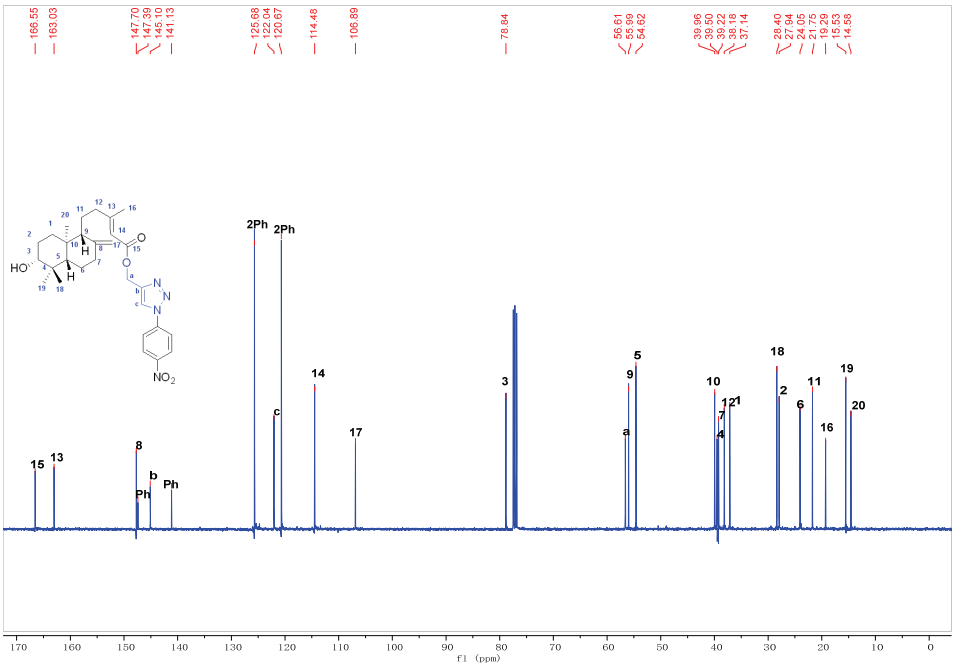

Fig. S-24. ^{13}C NMR spectrum of compound 5k ($CDCl_3$, 100 MHz)

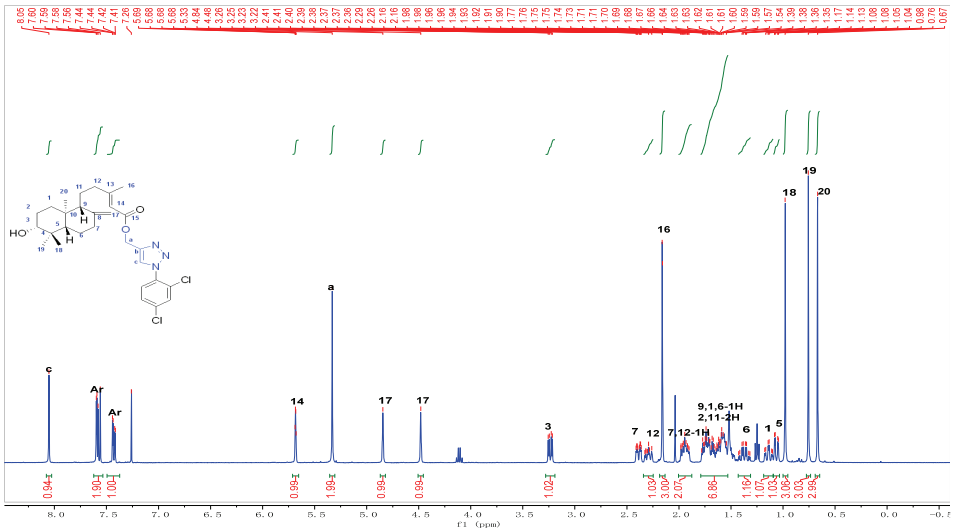

Fig. S-25. ^{1}H NMR spectrum of compound 5l ($CDCl_3$, 400 MHz)

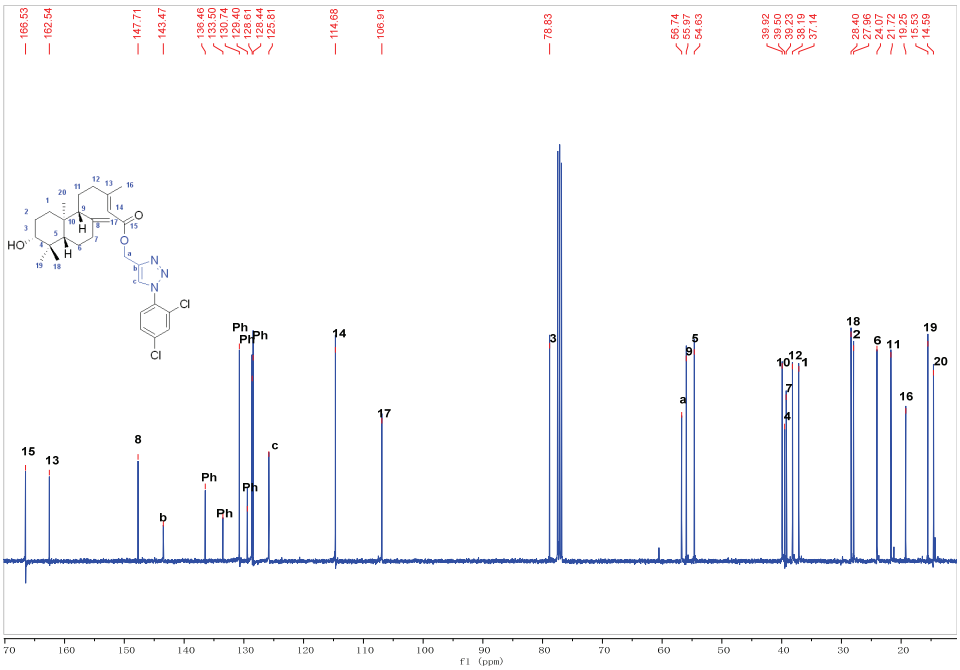

Fig. S-26. ^{13}C NMR spectrum of compound 5l ($CDCl_3$, 100 MHz)

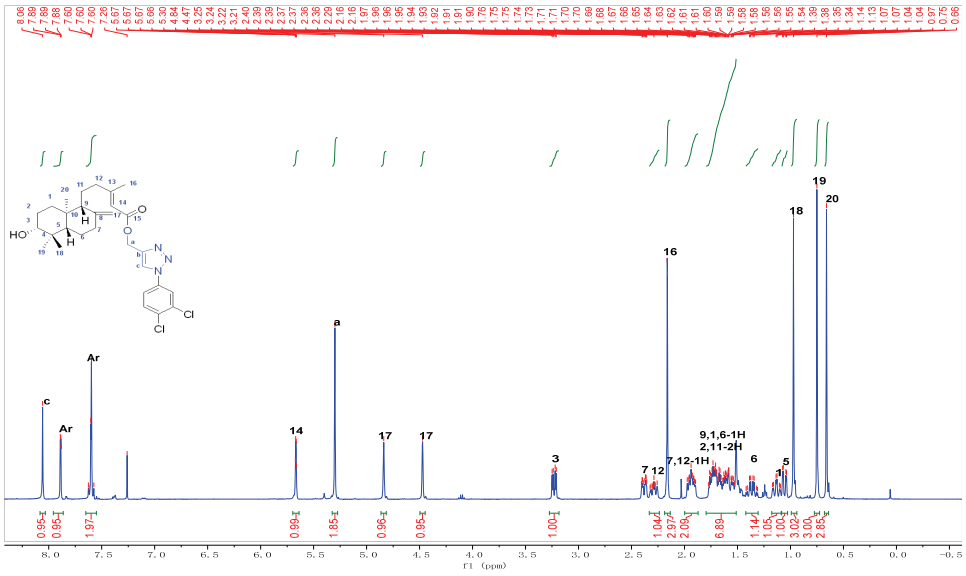

Fig. S-27. ^{1}H NMR spectrum of compound 5m ($CDCl_3$, 400 MHz)

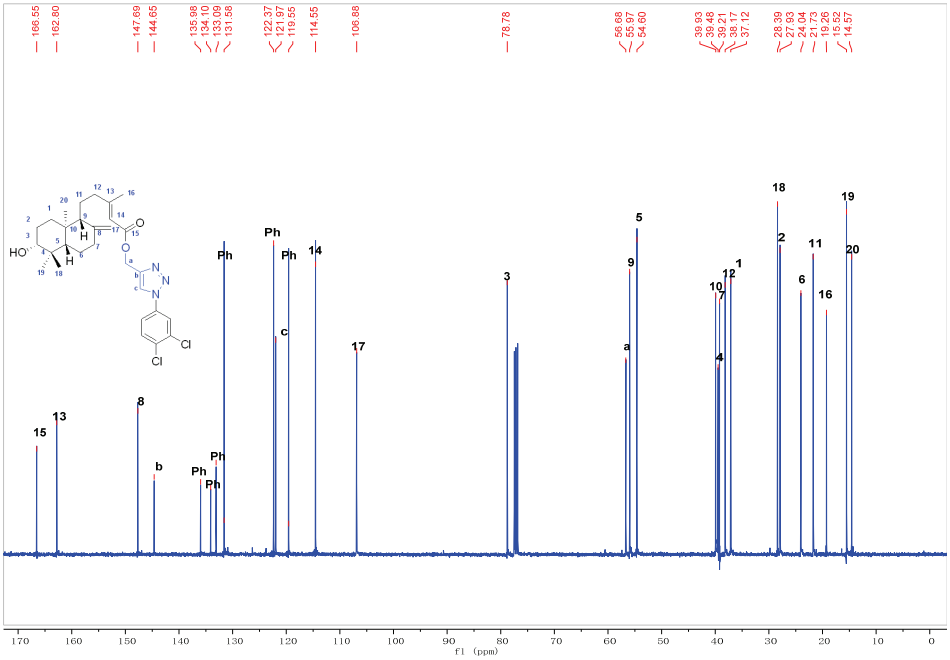

Fig. S-28. ^{13}C NMR spectrum of compound 5m ($CDCl_3$, 100 MHz)

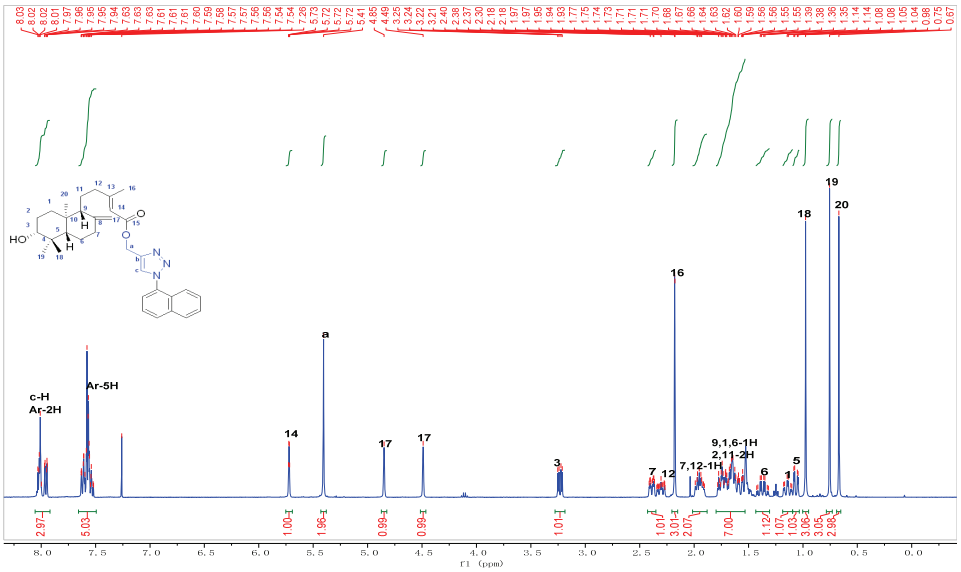

Fig. S-29. ^{1}H NMR spectrum of compound 5n ($CDCl_3$, 400 MHz)

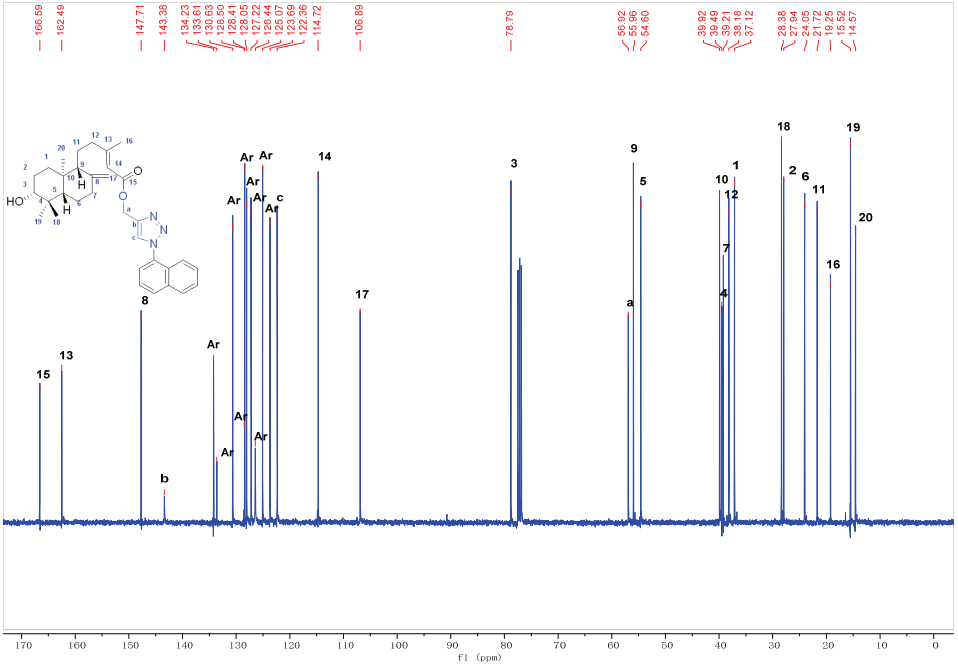

Fig. S-30. ^{13}C NMR spectrum of compound 5n ($CDCl_3$, 100 MHz)

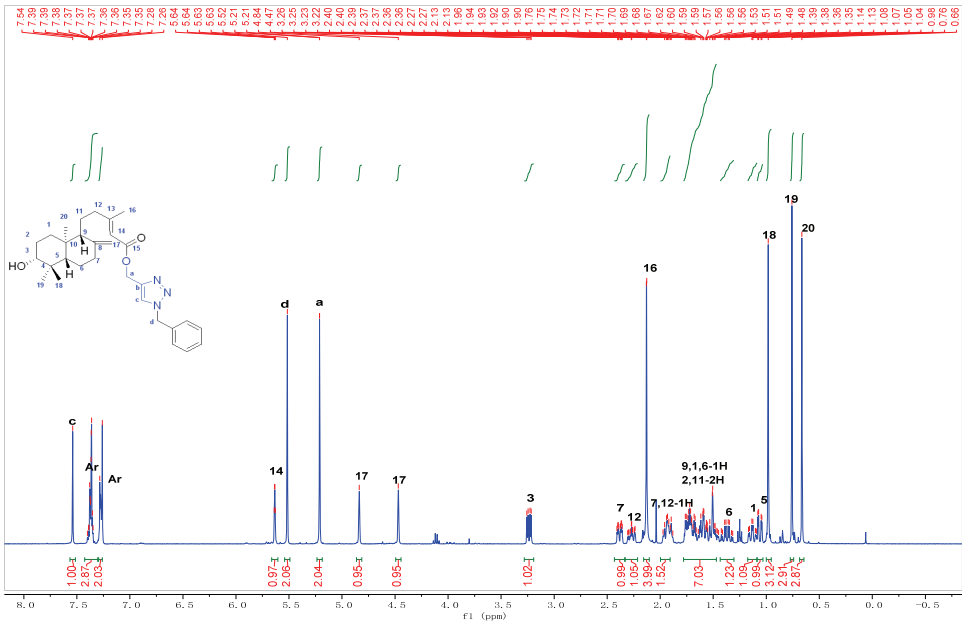

Fig. S-31. ^{1}H NMR spectrum of compound 5o ($CDCl_3$, 400 MHz)

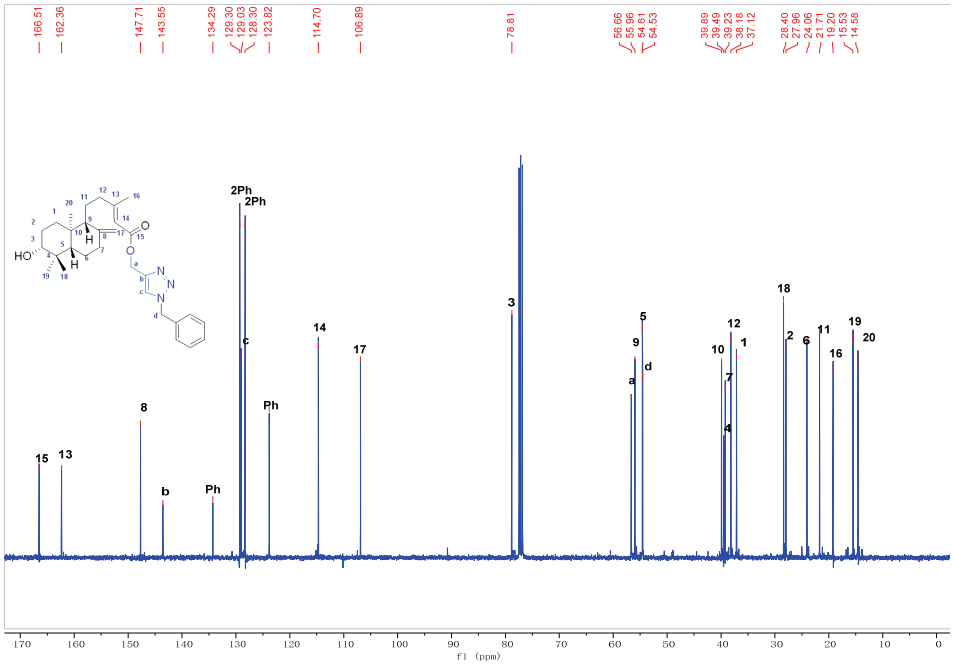

Fig. S-32. ^{13}C NMR spectrum of compound 5o ($CDCl_3$, 100 MHz)

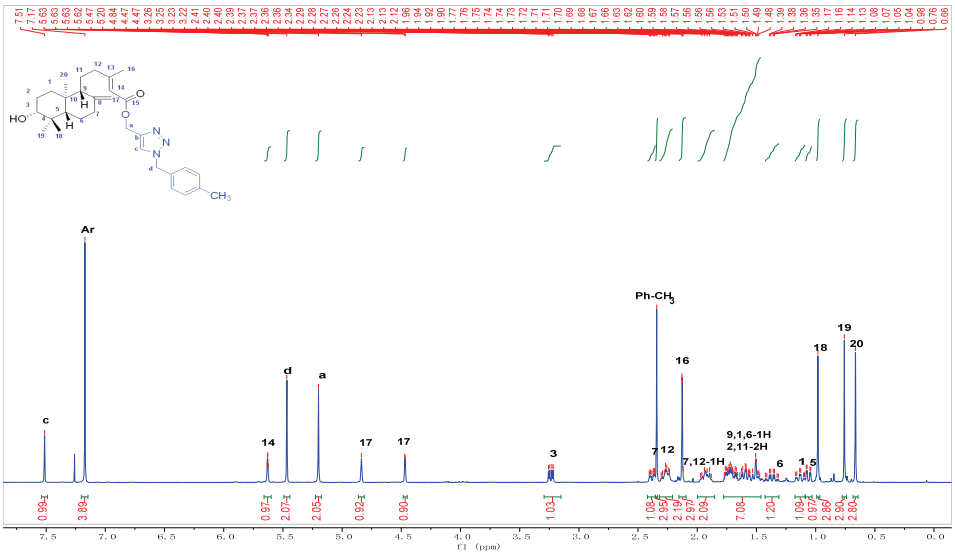

Fig. S-33. ^{1}H NMR spectrum of compound 5p ($CDCl_3$, 400 MHz)

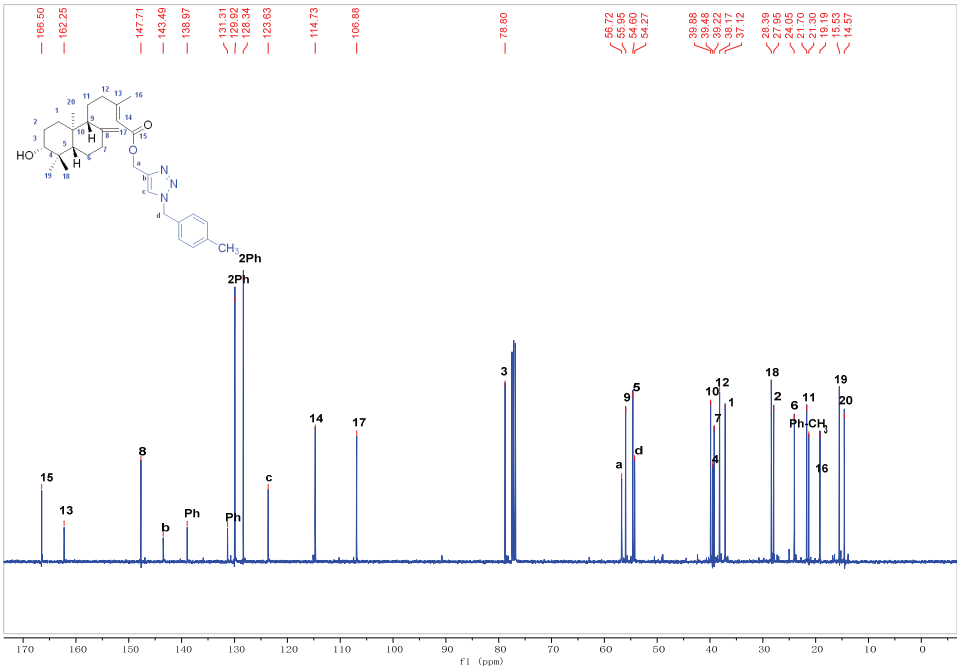

Fig. S-34. ^{13}C NMR spectrum of compound 5p ($CDCl_3$, 100 MHz)

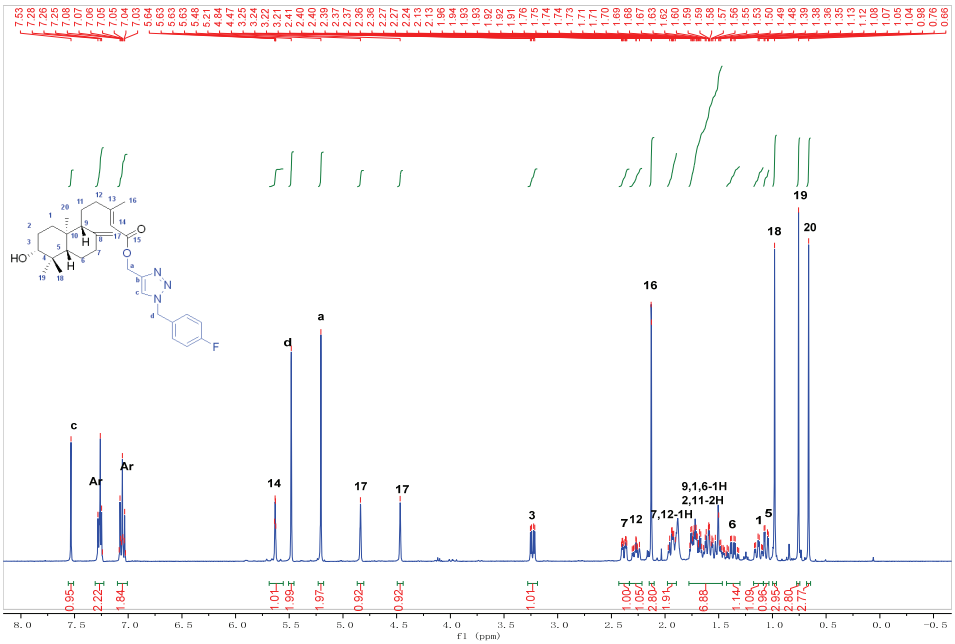

Fig. S-35. ^{1}H NMR spectrum of compound 5q ($CDCl_3$, 400 MHz)

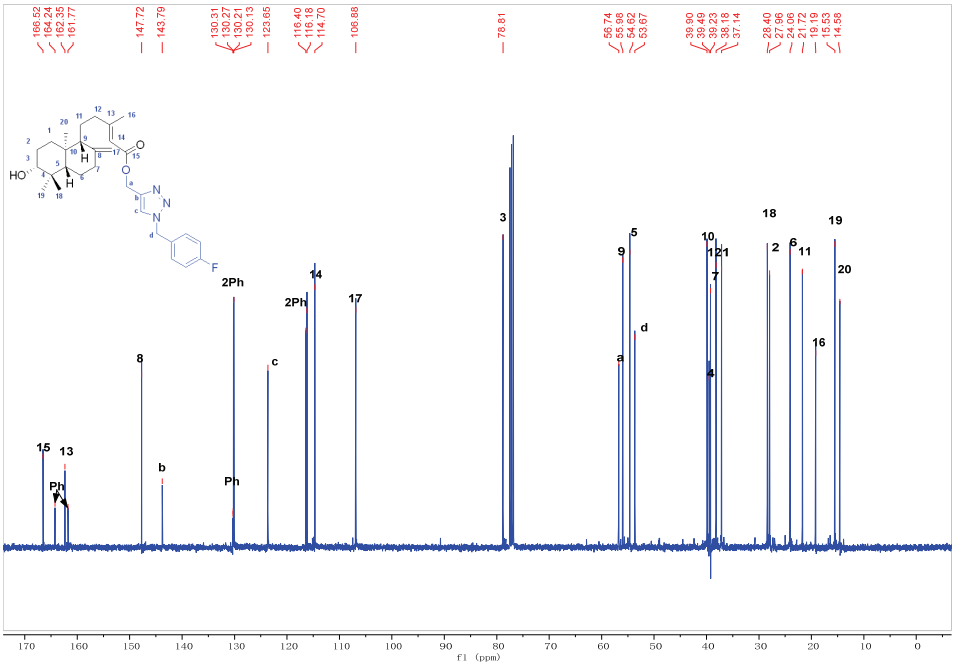

Fig. S-36. ^{13}C NMR spectrum of compound 5q ($CDCl_3$, 100 MHz)

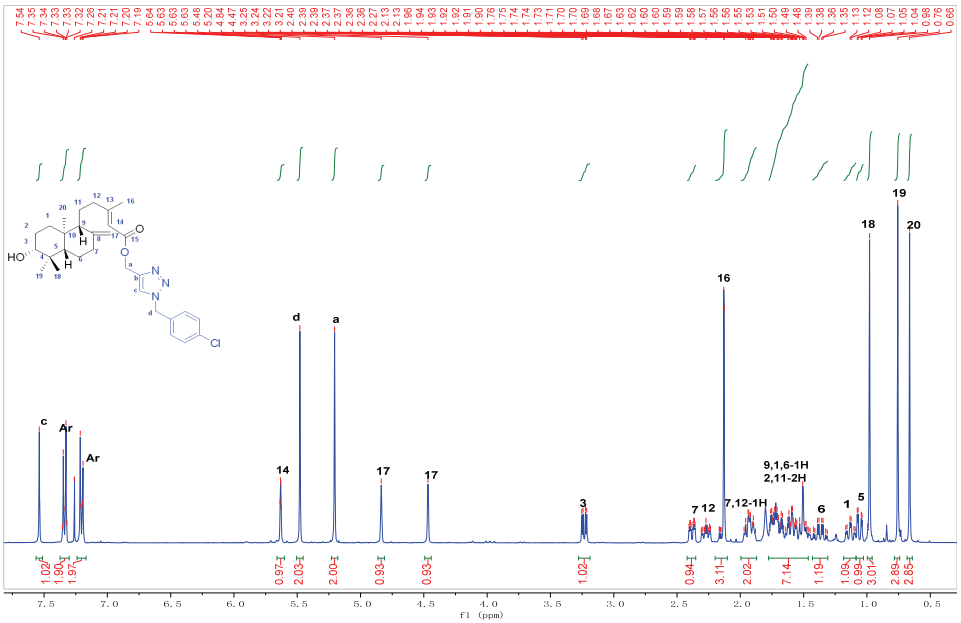

Fig. S-37. ^{1}H NMR spectrum of compound 5r ($CDCl_3$, 400 MHz)

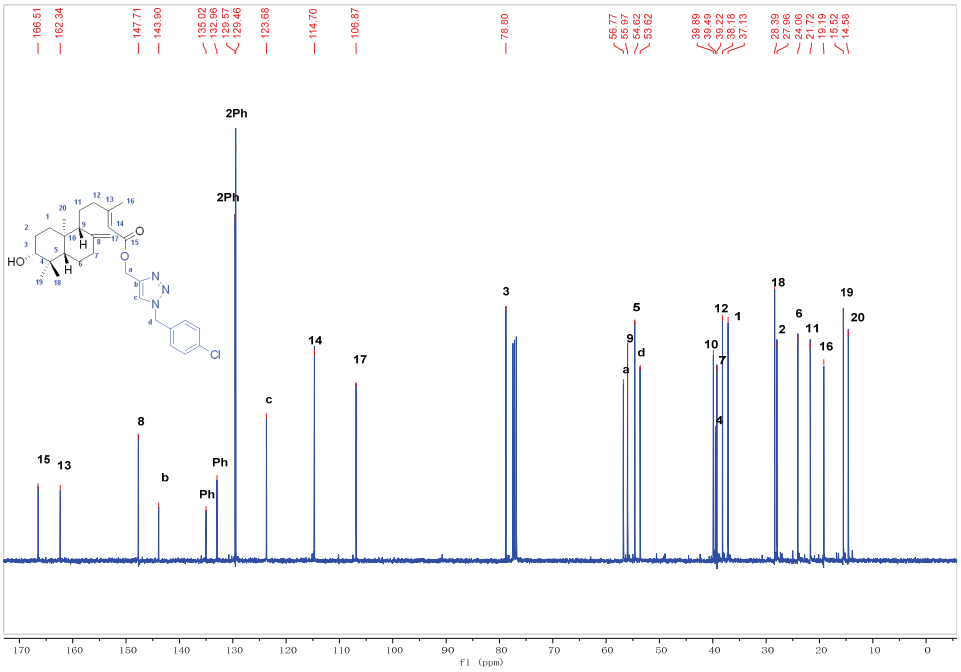

Fig. S-38. ^{13}C NMR spectrum of compound 5r ($CDCl_3$, 100 MHz)

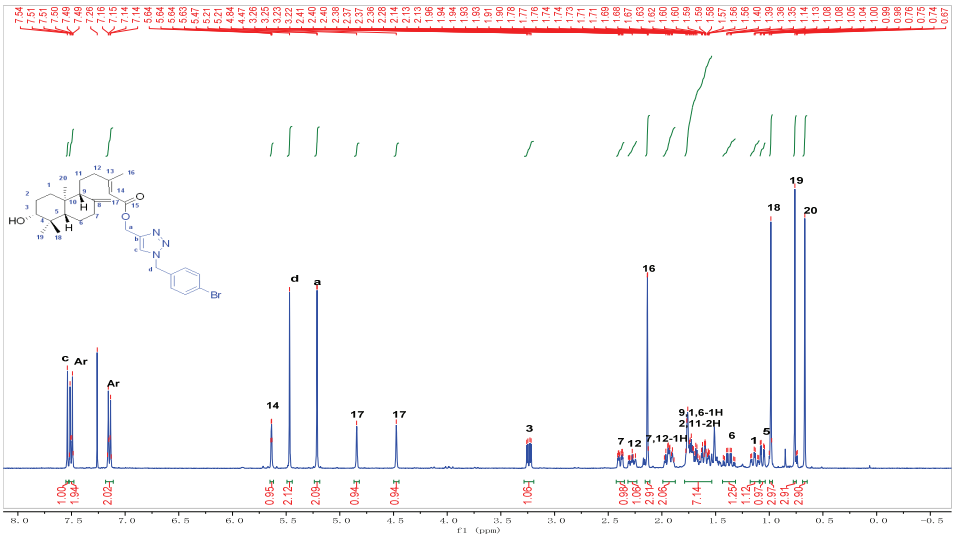

Fig. S-39. ^{1}H NMR spectrum of compound 5s ($CDCl_3$, 400 MHz)

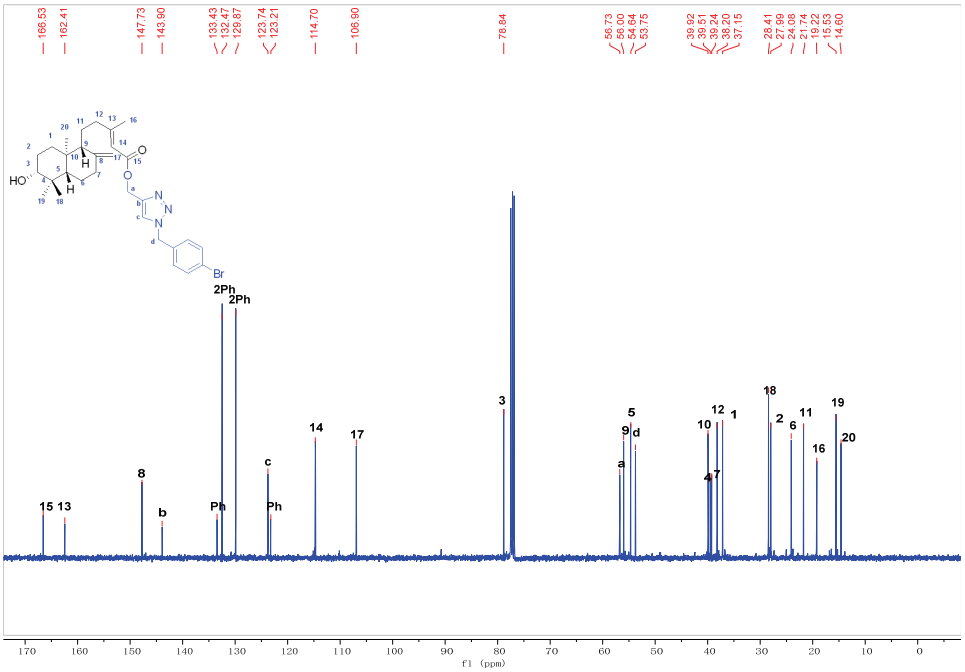

Fig. S-40. ^{13}C NMR spectrum of compound 5s ($CDCl_3$, 100 MHz)

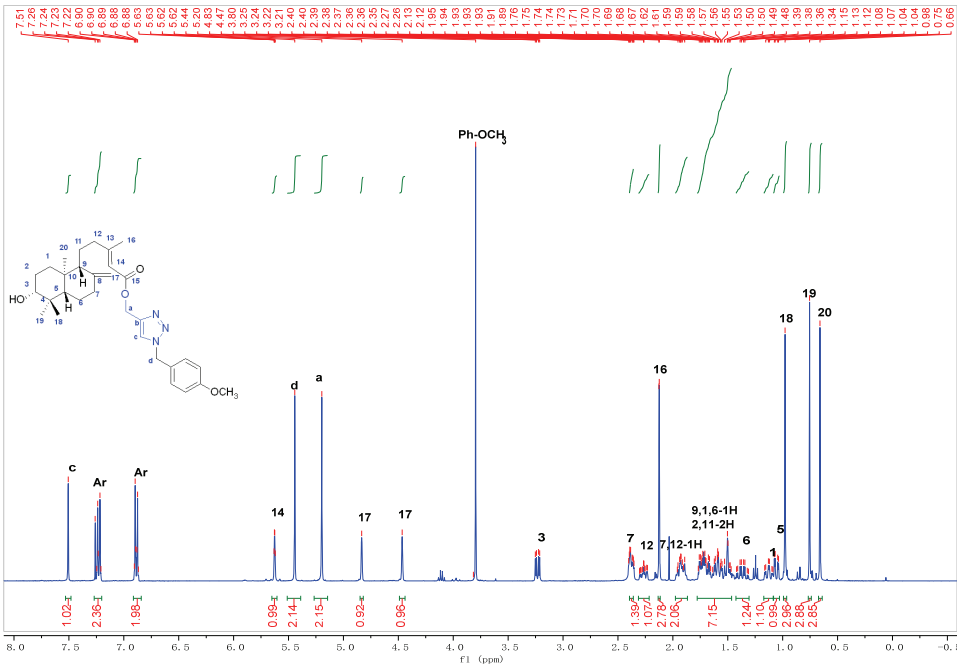

Fig. S-41. ^{1}H NMR spectrum of compound 5t ($CDCl_3$, 400 MHz)

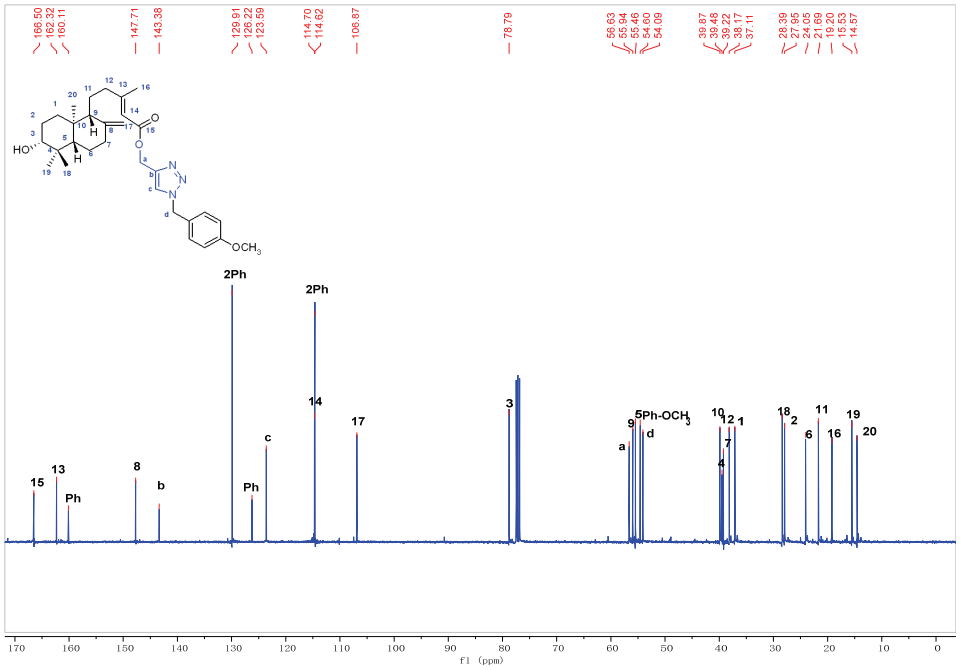

Fig. S-42. ^{13}C NMR spectrum of compound 5t ($CDCl_3$, 100 MHz)

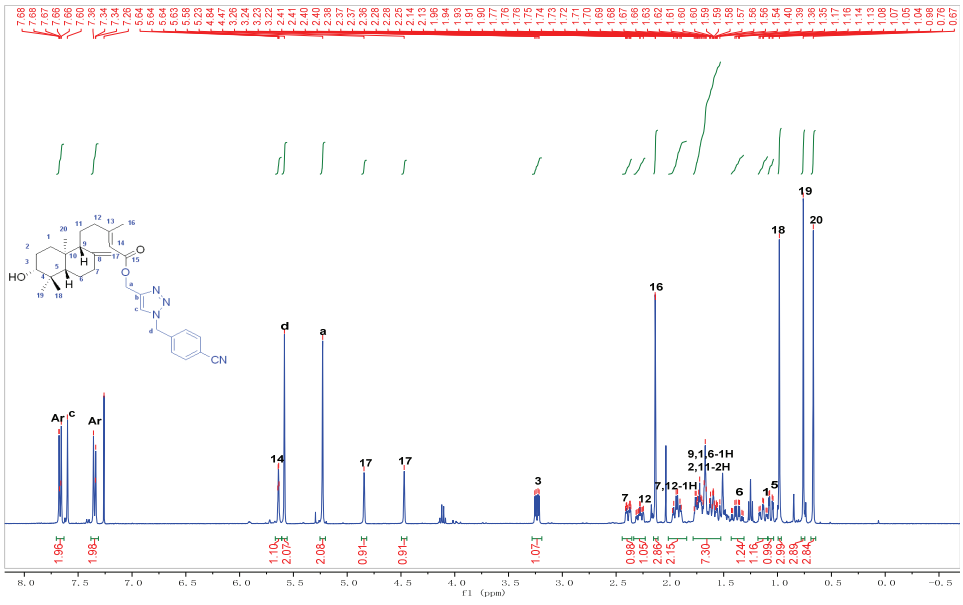

Fig. S-43. ^{1}H NMR spectrum of compound 5u ($CDCl_3$, 400 MHz)

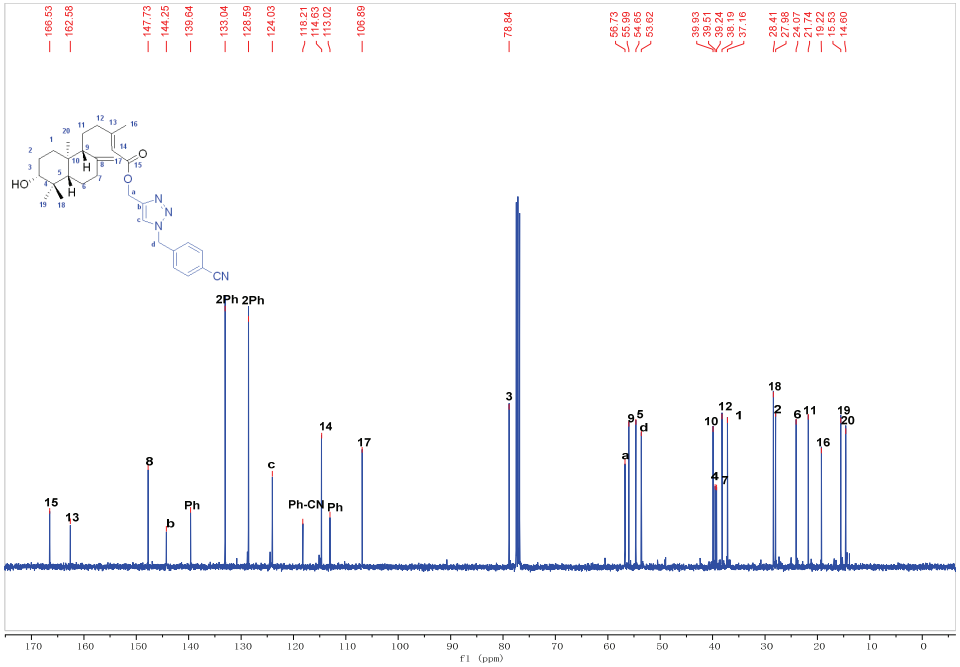

Fig. S-44. ^{13}C NMR spectrum of compound 5u ($CDCl_3$, 100 MHz)

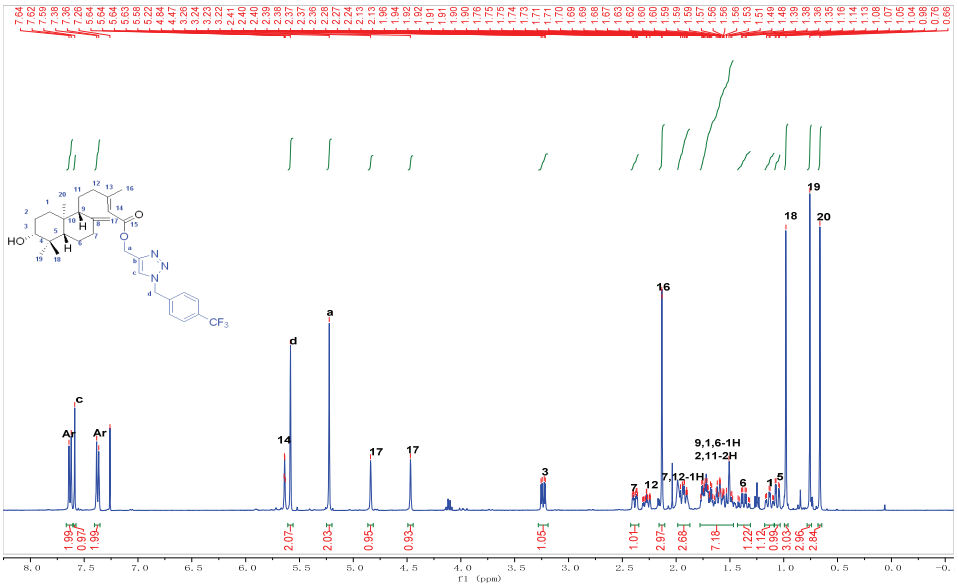

Fig. S-45. ^{1}H NMR spectrum of compound 5v ($CDCl_3$, 400 MHz)

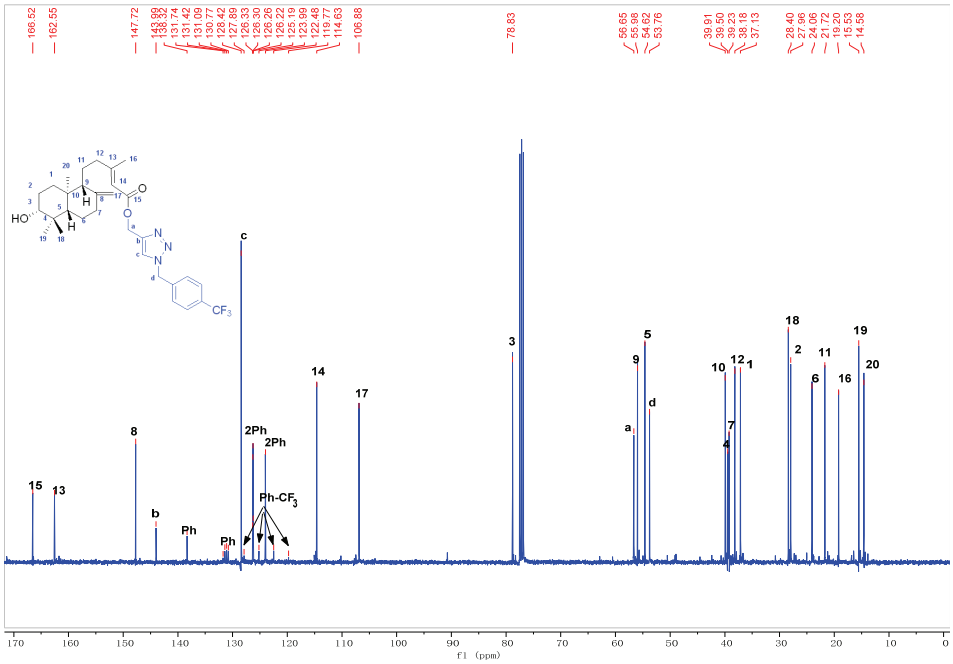

Fig. S-46. ^{13}C NMR spectrum of compound 5v ($CDCl_3$, 100 MHz)

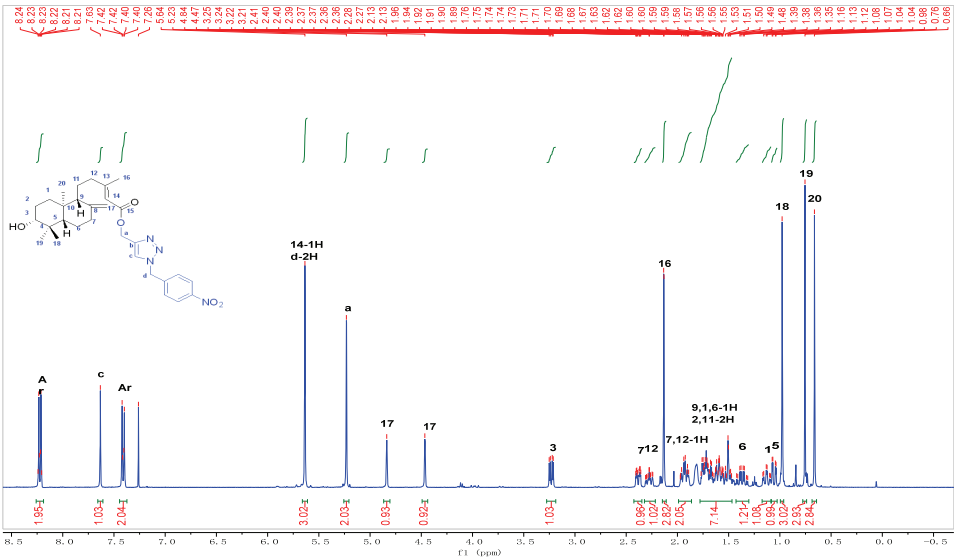

Fig. S-47. ^{1}H NMR spectrum of compound 5w ($CDCl_3$, 400 MHz)

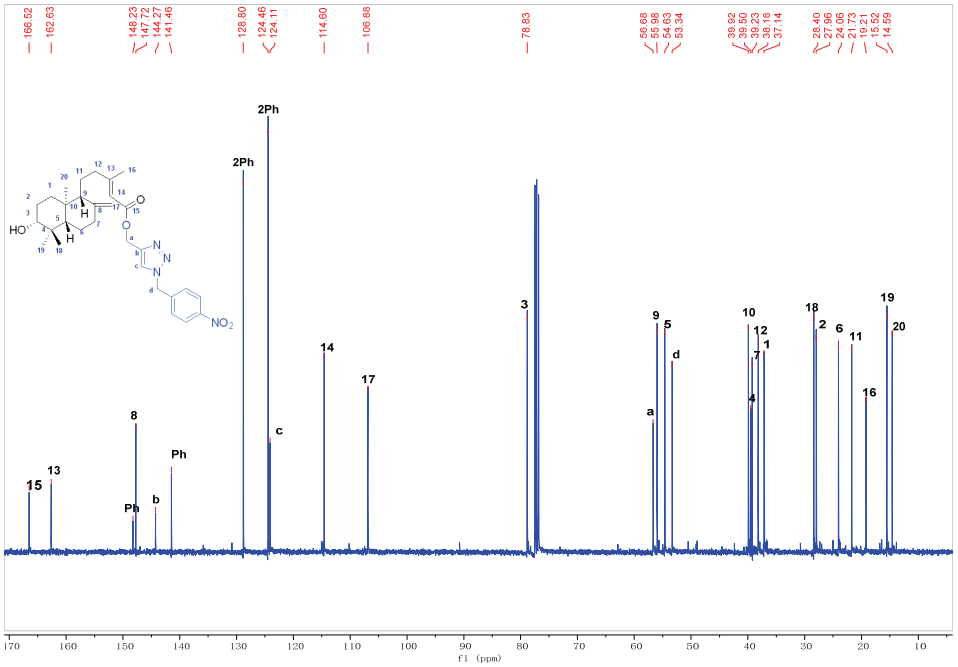

Fig. S-48. ^{13}C NMR spectrum of compound 5w ($CDCl_3$, 100 MHz).

Journal of the Serbian Chemical Society
JSCS-info@shd.org.rs • www.shd.org.rs/JSCS
J. Serb. Chem. Soc. *86* (10) 927–940 (2021)
JSCS–5473
Original scientific paper
Published 10 September 2021

Macroelements *versus* toxic elements in selected wild edible mushrooms of the Russulacea family from Serbia

MARIJA DIMITRIJEVIĆ[1]*, VIOLETA MITIĆ[2], DRAGAN ĐORĐEVIĆ[2], GORDANA POPOVIĆ[3], NENAD KRSTIĆ[2#], JELENA NIKOLIĆ[2] and VESNA STANKOV JOVANOVIĆ[2]

[1]*University of Niš, Faculty of Medicine, Boulevard of dr Zorana Đinđića 81, 18000 Niš, Serbia,* [2]*University of Niš, Faculty of Science and Mathematics, Department of Chemistry, Višegradska 33, 18000 Niš, Serbia and* [3]*University of Belgrade, Faculty of Pharmacy, Department of General and Inorganic Chemistry, Vojvode Stepe 450, 11000 Belgrade, Serbia*

(Received 10 April, revised 19 May, accepted 24 May 2021)

Abstract: Three edible mushrooms of the Russulacea family (*Lactarius deliciosus*, *Lactarius sanguifluus* and *Lactarius semisanguifluus*), most frequently consumed in Serbia, were analyzed using the ICP-OES technique to evaluate the content of K, P, Ca, Mg, Na, Al, As, Cd and Pb, both in cap and stipe. Corresponding soils were analyzed, too. Based on the obtained values for the elemental composition of the mushrooms and the soil, bioaccumulation and translocation factors were calculated. All the examined mushrooms species were recognized as bioexclusors of analyzed toxic elements, but bioaccumulators of K, P and Ca. The studied mushrooms are good sources of macroelements. One portion of 300 g of fresh mushrooms had a significant contribution of K and P, exceeding 15 % of the recommended daily intake for the elements. On the contrary, mushrooms had a low potential to bioaccumulate toxic elements, and presented results indicated the regular consumption of wild edible mushrooms is safe for human health. Correlation analysis was applied to determine phosphorus's influence on the elements' content in the mushrooms and corresponding soils, demonstrating the most remarkable mushrooms' tendency to accumulate phosphorus.

Keywords: element composition; correlation analysis; bioaccumulation factor; translocation factor.

* Corresponding author. E-mail: marija.dimitrijevic@pmf.edu.rs
# Serbian Chemical Society member.
https://doi.org/10.2298/JSC210410038D

INTRODUCTION

Nowadays, food is not just an energy source for human beings. It is required to be functional, to have medical properties, and thus to contribute to the well-being of the organism. The mushrooms are appreciated in diet due to their chemical and nutritional properties and their therapeutic and disease-preventing characteristics.[1] Although commercial mushroom species are used in the diet on a massive scale, the consumption of wild edible mushrooms is becoming increasingly popular in Serbia.

The elemental composition of mushroom represents a spectrum of macro and microelements. The abundance of macroelements such as P, K, Ca, Mg and Na is desired in the human diet, and their determination in edible wild-grown mushrooms is of great importance. Mushrooms can uptake large amounts of water and elements (*e.g.*, phosphorus, iron, potassium, cadmium, magnesium, copper and zinc) due to mycelium's extensive surface contact with the top layer of soil.[2] Mycelium is perfectly adopted to penetrate and access soil pore spaces. The fungal hyphae's vast surface area and physiology enable an effective absorption and bioconcentration of various metals, metalloids, and nonmetals.[3] Despite many positive aspects of mushroom consumption, there are risks associated with their ingestion, such as poisoning with harmful elements, *e.g.*, mercury, lead, cadmium and arsenic, which might accumulate in mushrooms.[4] These elements are considered hazardous because, with greater exposure, they can lead to increased health risks. A particular problem is the accumulation and deposition of certain elements in the human tissues, from which they are difficult to eliminate. The ability to accumulate heavy metals differs in certain types of mushrooms. Usually, element concentration in caps is higher than in other parts of fruiting bodies of mushrooms.[5]

A detailed review of the literature points to the lack of publication of the elements' content in the Russulacea family's mushrooms from Serbia. The aim of this paper was to identify the inorganic composition of three wild edible mushrooms: *L. deliciosus, L. sanguifluus* and *L. semisanguifluus*. Content of toxic elements (Al, As, Cd and Pb) and macroelemnts (K, P, Ca, Mg and Na) was determined in caps and stipes, as well as in corresponding soil substrates. The obtained values enabled a better understanding of the accumulation potential of the mentioned mushrooms because it was possible to calculate the translocation factor (TF) and bioaccumulation factor (BAF) for each element. Also, the nutritional value and possible risk of consuming wild edible mushrooms were determined.

EXPERIMENTAL

Chemicals and instrumentation for inorganic characterization

All reagents were analytical-reagent grade, purchased from Merck (Darmstadt, Germany). Multielement standard solutions for ICP analysis were purchased from Ultra Scientific (North Kingstown, RI, USA). Inorganic characterization (K, P, Ca, Mg, Na, Al, As, Cd and

Pb) of mushrooms and corresponding soil substrates were carried by an ICP-OES iCAP 6000, Thermo Scientific. In Table I are presented analytical parameters for ICP-OES that were used for all measurements.

TABLE I. ICP-OES instrumental parameters

Flush pump rate	100 rev. min^{-1}
Analysis pump rate	50 rev. min^{-1}
Nebulizer gas	0.7 L min^{-1}
Coolant gas flow	12 L min^{-1}
Auxiliary gas flow	0.5 L min^{-1}
Plasma view	Axial
Flush time	30 s

The accuracy of method was determined using the European Reference Materials "ERM-CD281: K, Ca, Na, As, Cd and Pb." The referenced value is reported in Table II.

TABLE II. Comparison of found element concentrations and certified values, and obtained recoveries (concentration±*SD*)

Element	Certified concentration, mg kg^{-1}	Found concentration, mg kg^{-1}	Recovery, %
K	34000	33000	97.0
P	2800	2700	96.4
Ca	6300	6000	95.2
Mg	1600	1550	96.9
Na	4000	3900	97.5
As	0.04±0.01	0.04±0.01	95.2
Cd	0.120±0.007	0.11±0.03	96.7
Pb	1.7±0.1	1.6±0.1	96.4

Quantification of wavelengths for each element, the detection limits (*LOD*), the limits of quantification (*LOQ*), and the correlation coefficients (r^2) are represented in Table III.

TABLE III. Emission wavelengths, correlation coefficient of calibration curves, limit of detection (*LOD*) and limit of quantification (*LOQ*) for each element analyzed

Element	λ / nm	r^2	*LOD* / µg L^{-1}	*LOQ* / µg L^{-1}
K	766.5	0.9914	39.43	131.44
P	213.6	0.9995	6.93	23.10
Ca	393.4	0.9999	0.09	0.32
Mg	279.6	0.9999	0.12	0.41
Na	588.9	1	0.46	1.53
Al	308.2	0.9998	4.52	15.07
As	189.0	0.9995	2.76	9.19
Cd	226.5	0.9994	0.19	0.63
Pb	220.353	0.99966	2.42	8.05

All the experimental results were the mean ± standard deviation of three parallel measurements.

Sample collection

The mushroom samples (*Lactarius deliciosus*, *Lactarius sanguifluus* and *Lactarius semisanguifluus*) were identified as edible mushrooms belonging to the family Russulaceae. The samples of the species mentioned above were collected during 2020, in the rural, unpolluted part of the Sićevo gorge, in the forests dominated by pine, away from the road. The specimen vouchers were deposited in the Herbarium Moesiacum Nis (HMN), Department of Biology and Ecology, Faculty of Science and Mathematics, University of Niš, under the acquisition numbers 17, 18 and 19. The mushrooms were collected at three experimental points to overcome variability, taking approximately 200 g of each examined mushroom species. Mushroom samples were cleaned, cut, and separated into two parts: cap and stipe; for each mushroom species sampled, the soil, down to the depth of 10 cm, after removing the superficial organic layer.

Digestion of mushroom samples

The element content of mushrooms was determined by the wet mineralization using a modified procedure of Tüzen.[6] One gram of each mushroom species was mixed with 15 mL oxi-acidic mixture consisting of HNO_3:H_2SO_4:H_2O_2 (4:1:1), heated up to 150 °C for 4 h, and diluted to 25 mL with deionized water. A blank sample was prepared in the same way.

Digestion of soil samples

According to Method 3050B,[7] the pseudo total element contents of soils were determined. Weighted soil sample mass (1 g) was placed into an Erlenmeyer and treated with 10 mL of concentrated HNO_3 for 24 h and then heated to a small volume. A mixture of 30 % H_2O_2 and H_2O (3:2, volume ratio) was added and evaporated to a small volume. After cooling, 3 mL of 30 % H_2O_2 was added and evaporated. Then added 10 mL of concentrated HCl and samples were left overnight. Obtained digestates were filtered and diluted with distilled water to 25 mL.

RESULTS AND DISCUSSION

The element composition of fruiting bodies of three wild edible mushrooms in the caps, stipes, and surrounding soils are presented in Table IV. All element concentrations were determined on a dry weight (DW) basis. Still, for intake calculations, 300 g of fresh weight (FW) mushroom samples (containing 30 g of dry matter)[8] were presented, assuming the average portion per person (average body weight 65–70 kg).[9] The intake calculations were done on the average element content in mushrooms. The intake of each element was calculated by consuming a portion of 300 g. The results are presented in Table V.

Worth mentioning is that elements are accumulated in different quantities comparing the cap and the stipe, depending on the species and the element concentrations in the substrate that the mushroom grew on.

Daily, the human body requires specific amounts of elements for the organism's proper functioning and development. Elements which in large quantities can be found in the body, such as K, Na, Mg, Ca and P, are required for many essential processes in human metabolism, such as fluid balance, proper formation of bones and teeth, muscle contraction, and the functioning of the nervous system. Mushrooms can be considered an essential source of biologically important

elements, suggesting the existence of a very effective mechanism enabling them to take up elements from the substrate more readily.[10]

TABLE IV. Element composition in studied mushroom species of the Russulaceae family in caps, stipes and in corresponding soil substrates, and the bioaccumulation (BAF) and translocation factor (TF) for the analyzed samples

Element/Content		Origin	*L. deliciosus*	*L. sanguifluus*	*L. semisamguiufulus*
K	Content ± *SD*	Cap	14143±498	13337±450	134923±452
	mg kg^{-1} DW	Stipe	11074±430	116556±441	12387±451
		Soil	84412±801	10552±512	9242±501
	BAF		3	2.4	2.8
	TF		1.3	1.1	1.1
P	Content ± *SD*	Cap	8212±199	6510±193	6386±193
	mg kg^{-1} DW	Stipe	5117±181	4778±180	4939±182
		Soil	1094±112	1045±109	927±99
	BAF		12.2	10.8	12.2
	TF		1.6	1.4	1.3
Ca	Content ± *SD*	Cap	261±13	266±12	332±22
	mg kg^{-1} DW	Stipe	232±13	245±12	340±22
		Soil	311±21	520±32	379±25
	BAF		1.6	1	1.8
	TF		1.1	1.1	1
Mg	Content ± *SD*	Cap	718±52	630±50	697±45
	mg kg^{-1} DW	Stipe	519±21	517±31	578±32
		Soil	4791±180	5104±191	5144±190
	BAF		0.3	0.2	0.2
	TF		1.4	1.2	1.2
Na	Content ± *SD*	Cap	2.3±0.1	8.4±0.8	7.1±0.6
	mg kg^{-1} DW	Stipe	12±1	10±1	8±1
		Soil	17±1	18±1	19±1
	BAF		0.8	1	0.8
	TF		0.2	0.8	0.8
Al	Content ± *SD*	Cap	73±6	98±8	87±7
	mg kg^{-1} DW	Stipe	82±7	105±9	159±9
		Soil	57871±600	64563±655	64436±654
	BAF		0.003	0.003	0.004
	TF		0.886	0.93	0.548
As	Content ± *SD*	Cap	0.55±0.05	0.58±0.05	0.44±0.05
	mg kg^{-1} DW	Stipe	0.40±0.04	0.49±0.05	0.48±0.05
		Soil	22±2	24±2	24±2
	BAF		0.044	0.045	0.039
	TF		1.345	1.191	0.928
Cd	Content ± *SD*	Cap	1.1±0.1	0.58±0.05	0.45±0.05
	mg kg^{-1} DW	Stipe	0.53±0.04	0.36±0.04	0.34±0.04
		Soil	8.13	8.78	9.98
	BAF		0.196	0.004	0.09
	TF		2.028	1.604	1.306

TABLE IV. Continued

Element/Content		Origin	*L. deliciosus*	*L. sanguifluus*	*L. semisamguiufulus*
Pb	Content ± S*D*	Cap	0.75±0.09	1.3±0.1	1.0±0.1
	mg kg^{-1} DW	Stipe	0.67±0.05	1.1±0.1	0.56±0.06
		Soil	45±3	49±3	48±3
	BAF		0.031	0	0.032
	TF		1.126	1.24	1.82

TABLE V. Content of nutritionally important macroelements and toxic elements in selected mushroom species calculated on 300 g of fresh mushrooms; daily intake of element relative to *RDI*; *DIE* – daily intake of element relative to *RDI*

Species	K		P		Ca		Mg		Na	
	Content mg/300 g FW	*DIE* %	Content mg/300 g FW	*DIE* %	Content mg/300 g FW	*DIE* %	Content mg/300 g FW	*DIE* %	Content mg/300 g FW	*DIE* %
L. deliciosus	378.3	18.9	199.9	36.4	7.4	0.9	18.6	5.8	0.22	0.014
L. sanguifluus	374.9	18.7	169.3	30.8	7.7	1.0	17.2	5.4	0.28	0.018
L. semisamguiufulus	388.2	19.4	169.9	30.9	10.1	1.3	19.1	6.0	0.23	0.016

	Al	As	Cd	Pb
	Content, mg/300 g FW			
L. deliciosus	2.3	0.014	0.024	0.021
L. sanguifluus	3.1	0.016	0.014	0.036
L. semisamguiufulus	3.7	0.014	0.012	0.024

A portion of mushrooms' contribution is considered to be significant if it provides 15 % of the recommended daily intake (RDI) of nutritionally valuable elements.[11]

Macroelements, namely potassium and phosphorus, can be found in the most considerable quantities in mushrooms. Potassium levels are between 20- and 40--fold higher in fruiting bodies than in underlying substrates.[12] Among the analyzed mushroom species, the content of K is higher in the caps than in the stipes, and mushroom *L. deliciosus* stood out with the highest potassium content, 14143 mg kg^{-1}. Seeger reported that the potassium content in 410 wild fungi species ranges from 1.5–117 g kg^{-1}.[13] Therefore, mushrooms can be used in the diet of patients with chronic potassium deficiency, but care must be taken in people with renal insufficiency. The *RDI* of potassium for adults is 2000 mg.[14] From Table V, it can be seen that all analyzed mushroom samples have a significant contribution of potassium, from a portion of 300g of fresh mushrooms, because it exceeds 15 %.

Phosphorus is the second most abundant element in edible and wild mushrooms that can bioaccumulate in large quantities from the substrate. The concentration of P in the analyzed mushrooms ranges from 4778 mg kg^{-1} (stipe of *L. sanguifluus*) to 8212 mg kg^{-1} (cap of *L. deliciosus*). Also, it can be observed that the bioaccumulation of phosphorus in the caps is higher than in the stipes. The *RDI* for phosphorus is 550 mg.[15] Based on the results, it can be noticed that all analyzed samples of mushrooms have a significant contribution to the daily intake of phosphorus (> 15 %), and the species *L. deliciosus* has the highest value, 36.4 %.

Calcium and magnesium are determined in mushrooms in lower amounts than phosphorus and potassium. Calcium occurs in very similar concentrations in caps and stipes in all the analyzed mushrooms. The species *L. semisanguifluus* was separated with a slightly higher calcium content, 332 mg kg^{-1} in cap and 340 mg kg^{-1} in stipe. The *RDI* for calcium is 800 mg,[14] and the highest Ca concentration found in this study is 10.07 mg/300 g of fresh mushrooms, which is 1.3 % of the average daily intake. It can be concluded that mushrooms represent a small source of Ca in the diet. However, as calcium is generally not classified as an element deficient in the human diet, this deficiency can be ignored.

Magnesium content in fruiting bodies were even lower than those in substrates.[12] It seems either evenly distributed in caps and stipes, or somewhat higher levels are observed in caps than in stipes,[16] which is the case with these mushroom samples. Among the tested mushroom samples, *L. deliciosus* has the highest content of magnesium, 718 mg kg^{-1}, and consuming a portion of 300 g of fresh mushrooms can provide a maximum of 6 % of magnesium daily intake.

Sodium is a macroelement found in small amounts in mushrooms, which is very important because sodium excess in nutrition can lead to high blood pressure. This element differs from other macroelements due to its more significant presence in stipe than in the caps. All analyzed mushrooms showed lower sodium levels than average, ranging from 50-750 mg kg^{-1}.[16] Mushrooms *L. deliciosus* is different in terms of the highest sodium content in the stipe (12 mg kg^{-1}) and the lowest in the cap (2.3 mg kg^{-1}). The *RDI* for sodium is 1500 mg.[17] Consuming a portion of 300 g of fresh mushrooms provides about 0.018 % of sodium per day, which qualifies mushrooms as food recommended for consumption without the risk of hypertension.

Since mushrooms have been viewed from a nutritional point of view and have been found to accumulate macronutrients in appropriate amounts, toxicological testing is necessary to determine that they are safe to consume.

Previous research showed a wide range of aluminium content in wild-growing species (<25 to 500 mg kg^{-1} DW).[16] The Al concentration in the mushroom caps is 73 to 98 mg kg^{-1}, and these concentrations are lower than in the stipe in all analyzed species. This metal concentration in the stipe was the highest in *L.*

semisanguifluus, 159 mg kg^{-1}, while *L. deliciosus* had the lowest, 82 mg kg^{-1}. Zsigmond *et al.*[18] obtained similar results examining the inorganic composition of many mushrooms, among which the species *L. deliciosus*, and the obtained results are similar to the results of this study, except that the concentration of aluminum in the cap (52.4 mg kg^{-1}) is higher than in the stipe (31.3 mg kg^{-1}). Sarikurkcu *et al.*[20] reported lower concentrations of Al in *L. sanguifluus* (63 mg kg^{-1} DW).[19]

According to the literature analysis, provisional tolerable weekly intake (*PTWI*) was determined most frequently, but the Joint FAO/WHO Expert Committee on Food Additives (JECFA) gives tolerable intake levels for contaminants, expressed on either a daily or a weekly basis.[20] In view of the cumulative nature of aluminium in the organism after dietary exposure, the Panel considered it more appropriate to establish a tolerable weekly intake (*TWI*) for aluminium rather than a tolerable daily intake (*TDI*) and based on the combined evidence from the abovementioned studies, the Panel established a *TWI* of 1 (mg Al/kg bw)/ /week.[21] If 70 kg is taken as the consumer's average weight, the *TWI* for Al is 70 mg per week. By consumption 300 g portions of fresh studied mushrooms weekly, percentage of entered quantity Al ranges between 3.3 and 5.3 %.

Arsenic in mushrooms can be present in organic and inorganic forms.[16] The average content of arsenic in wild mushrooms are usually less than 1 mg kg^{-1} DW.[12] In the present study, arsenic concentrations are similar in caps and stipes for all analyzed mushroom species and ranged from 0.4 to 0.58 mg kg^{-1}. There are no significant differences observed between species. However, the *L. sanguifluus* possessed a slightly more elevated mean concentration, 0.58 mg kg^{-1} in cap and 0.49 mg kg^{-1} in the stipe, than the other species. Xu *et al.*[22] reported that *L. deliciosus* had average arsenic concentration of 0.75 mg kg^{-1}, which is slightly higher than the result in this paper. Genetic and environmental factors determine the concentration of arsenic in mushrooms. The role of genetic factors in As regulation can be stated based on the remarkably high arsenic contents of the same genus' mushroom species (Agaricus, Clitocybe, Lepista, Macrolepiota).[23] JEFCA noted that the previously established *PTWI* of 15 μg/kg body weight (equivalent to 2.1 μg kg^{-1} body weight per day) for inorganic arsenic was in the region of the benchmark dose lower confidence limit ($BMDL_{0.5}$) and therefore was no longer appropriate. This *PTWI* was therefore withdrawn by the Committee.[24] The CONTAM panel found $BMDL_{01}$ values between 0.3 and 8.0 (μg/kg bw)/day for an increased risk of lung, skin, and bladder cancer, as well as skin lesions.[24] Calculated at 70 kg body weight, it amounts to 0.021 to 0.56 mg arsenic per day. A portion of 300 g of fresh mushrooms maximum contains 16 μg of arsenic, which does not exceed the regulations' acceptable daily intake.

Cadmium is one of the most frequently determined elements in mushrooms due to its harmful effects on human health.[16] Cd is often found in soil and enters

the food chain through plants.[25] Most significant concentrations of Cd were obtained among analyzed species *in L. deliciosus* (1.1 mg kg^{-1} in cap and 0.53 mg kg^{-1} in stipe). Literature data reveal normal cadmium levels between <1–5 mg kg^{-1} DW in wild-growing species, whereas contents >1 mg kg^{-1} DW are sparse within cultivated mushrooms.[16] Commonly, cadmium contents are higher in caps than in stipes,[16] as is the case with results presented in this research. In previous studies, content of Cd in *L. deliciosus* was 0.54 mg kg^{-1},[26] 1.91 mg kg^{-1},[22] and in *L. sanguifluus* was 0.43 mg kg^{-1}.[19] Aloupi *et al.*[27] reported Cd concentrations at 0.06–0.25 mg kg^{-1} in *L. deliciosus*, 0.08–0.59 mg kg^{-1} in *L. sanguifluus*, and 0.06–0.61 mg kg^{-1} in *L. semisanguifluus*, which is similar to results for the same mushrooms presented in this research.

The CONTAM Panel established *TWI* for cadmium of 2.5 μg/kg bw, which for a 70 kg consumer is 0.175 mg per week and 0.025 mg per day.[28] So, consuming a portion of 300 g *L. deliciosus*, 95.6 % of the cadmium could be ingested daily.

Like most toxic elements, lead can be accumulated in the body for a long time, and it is necessary to monitor its even low concentration in potential sources.[29] Obtained results (Table IV) point to lead evenly distribution in caps and stipes. *L. sanguifluus* showed a slightly higher lead content compared to the other two species, 1.3 (cap) and 1.1 mg kg^{-1} (stipe). The analysis of the lead concentration in species *L. deliciosus* and *L. sanguifluus* was previously reported from other researchers which indicated a lower content of this element in the mentioned species.[26] Regarding lead, the CONTAM panel concluded that the provisional *PTWI* of 25 μg/kg body weight, set by JECFA and adopted by the Scientific Committee on Food (SCF) is no longer appropriate.[30,31] The respective *BMDL*s derived from blood lead levels in μg L^{-1} (corresponding dietary intake values in μg/kg bw per day) were: developmental neurotoxicity $BMDL_{01}$, 12 (0.50, corresponding to 35 μg per day for the average consumer); effects on systolic blood pressure $BMDL_{01}$, 36 (1.50, corresponding to 105 μg per day for the average consumer); effects on prevalence of chronic kidney disease $BMDL_{10}$, 15 (0.63, corresponding to 44.1 μg per day for the average consumer).[30] A portion of 300 g of fresh *L. sanguifluus* may pose a risk to the health of consumers because it contains 0.036 mg arsenic.

The logs of woods decomposed agro- and animal-wastes and soil are the mushrooms' natural substrates. Nutrients from the soil are available through external digestion and absorption by the mycelium. The concentration of elements in the mushrooms and corresponding soils, served for each element's bioaccumulation factor calculation (*BAF*). The *BAF* is precious tool for estimation of the accumulation efficiency of elements in mushrooms from growing media. For a plant or mushroom to be an efficient for the polluted soil bioremediation, the bioaccumulation factor has to be higher than 1.[32]

The *BAF* values for most macroelements are higher than 1, meaning these mushrooms can be considered as accumulators of these elements. Of all the analyzed elements, phosphorus showed the highest value of *BAF* in all three species of mushrooms, which means that mushrooms can be considered accumulators and hyperaccumulators of this element. The determined content of toxic elements in all mushroom species was very low (*BAF* < 1). The extremely low *BAF* values for analyzed toxic elements in all the mushrooms suggest that none of the species act as an accumulator of hazardous elements to human health. Based on the bioaccumulation factor, all the analyzed species were found to be bioexclusors of toxic elements. Due to the low content of toxic elements, their intensive consumption cannot lead to exceeding the tolerable levels of toxic elements intake.

The ratio cap/stipe expresses the translocation factor (*TF*) in the fruiting body of mushrooms.[33] For all macroelements, except Na, the *TF* value is greater than 1, which means that the macroelements' concentration is higher in cap than in stipe for all of these species.

The translocation factor of toxic elements had high values, which means that the concentration level for these elements was more elevated in the cap than the stipe of mushroom.

Correlation analysis

The obtained results show that mushrooms contain the highest potassium concentration, but based on the bioaccumulation factor, they offer the most increased tendency to accumulate phosphorus. Consequently, P influences, or is influenced by, the availability or utilization of many other elements, both essential and nonessential.[34] For that reason, the impact of the concentration of phosphorus in soil on the concentration of other elements in soil and parts of mushrooms was monitored.

Correlation coefficients among elements of the fruiting body (caps and stipes) and corresponding soil substrates are presented in Fig. 1. Regarding correlation coefficients, it can be noticed that the concentration of macro and toxic elements in the soil depends on the concentration of phosphorus in the soil. The concentration of phosphorus is negatively correlated with all determined elements in the soil, which suggests that the concentration of macro and toxic elements decreases with this element's increase. This fact is significant from the toxicology point of view because it indicates that soil rich in phosphorus results in a lower concentration of toxic elements in mushrooms. The concentration of phosphorus in soil has the greatest influence on cadmium and sodium concentration, according to the high correlation coefficient ($r = -1$ and 0.97, respectively, $p < 0.05$).

The other elements concentration (in the stipe and cap) was strongly affected by phosphorus concentration.

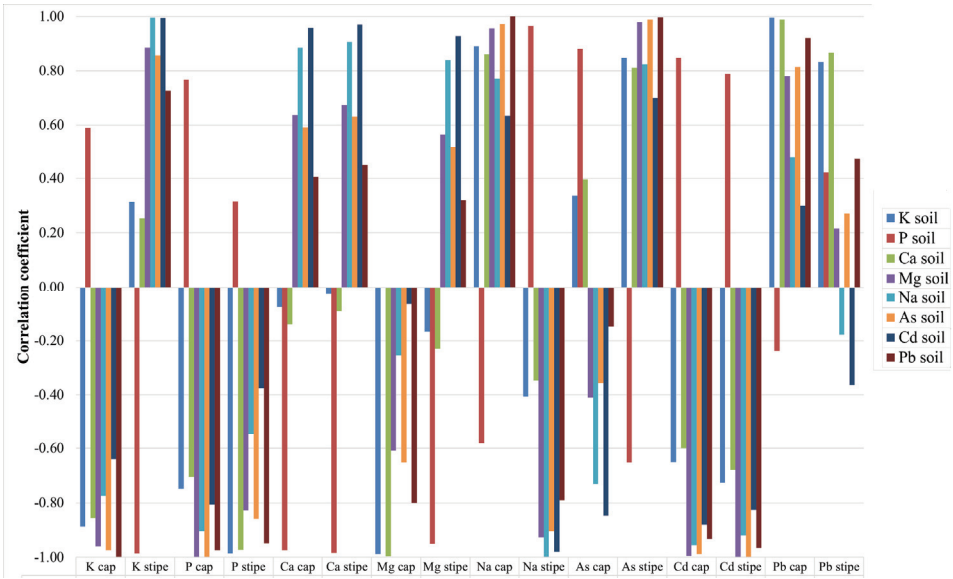

Fig. 1. Correlation of content of elements in soil and different parts of mushrooms.

The highest positive correlation was recorded between P in soil and Na in the stipe, $r = 0.95$ ($p < 0.05$), which indicates that mushrooms grown on P-rich soil accumulate more Na in the stipe than in the cap. This is confirmed by the translocation factor, which is the lowest for sodium, $TF = 0.2$. The strongest negative correlations were between phosphorus in the soil and potassium in the stipe, $r = –0.99$ ($p < 0.05$).

CONCLUSION

Results of this study confirm that mushrooms are a good source of macro-elements, providing a balanced diet. The study results pointed to high K and P contents surpassing more than 15 % of the recommended daily intake elements. It was found that the consumption of these mushrooms does not represent a toxicological risk. Regarding the content of toxic elements, the studied mushrooms are safe to consume and do not pose a risk to human health if consumed in the prescribed portions.

Depending on mushroom species, *BAF* values varied highly depending on the chemical element and were >1 for K, P, and Ca, while they were <1 for Mg, Na, Al, As, Cd and Pb. The translocation factor depends on the studied elements and their mobility in the mushroom's fruiting body and the mushroom species. The highest mobility in the fruiting body was shown by cadmium, $TF = 2$ for *L. deliciosus* species.

Correlation analysis showed that phosphorus concentration in the soil affects other elements' concentration in the soil and mushrooms.

Acknowledgement. Financial support of the Ministry of Education, Science and Technological Development of Serbia (Grant Nos. 451-03-68/2020-14/200124 and 451-03-68/2020--14/200113) is gratefully acknowledged.

И З В О Д

ПОРЕЂЕЊЕ САДРЖАЈА МАКРО- И ТОКСИЧНИХ ЕЛЕМЕНАТА У ОДАБРАНИМ САМОНИКЛИМ ПЕЧУРКАМА КОЈЕ ПРИПАДАЈУ ПОРОДИЦИ RUSSULACEA

МАРИЈА ДИМИТРИЈЕВИЋ[1], ВИОЛЕТА МИТИЋ[2], ДРАГАН ЂОРЂЕВИЋ[2], ГОРДАНА ПОПОВИЋ[3], НЕНАД КРСТИЋ[2], ЈЕЛЕНА НИКОЛИЋ[2] и ВЕСНА СТАНКОВ ЈОВАНОВИЋ[2]

[1]Универзитет у Нишу, Медицински факултет, Булевар др Зорана Ђинђића 81, 18000 Ниш, [2]Универзитет у Нишу, Природно–математички факултет, Департман за хемију, Вишеградска 33, 18000 Ниш и [3]Универзитет у Београду, Фармацеутски факултет, Департман за општу и неорганску хемију, Војводе Степе 450, 11000 Београд

Циљ овог рада било је одређивање садржаја K, P, Ca, Mg, Na, Al, As, Cd и Pb у три јестиве, самоникле печурке (*Lactarius deliciosus*, *Lactarius sanguifluus* и *Lactarius semisanguifluus*) које припадају породици Russulacea. Такође, одређен је и садржај поменутих елемената у земљишту на коме су расле анализиране печурке. На основу добијених резултата, за сваки елемент је израчунат биоакумулациони и транслокациони фактор. Будући да је утврђено да печурке акумулирају одговарајуће макроелементе, резултати су приказани и као унос (%) одговарајућих елемената на основу препоручене дневне дозе, прерачунато на порцију од 300 g свежих печурака. За токсичне елементе израчунат је садржај уноса елемената на основу прихватљивог недељног уноса. Корелациона анализа је коришћена како би се утврдио утицај фосфора на садржај елемената у печуркама и одговарајућим земљиштима, обзиром да је фосфор показао најзначајнију тенденцију акумулације.

(Примљено 10. априла, ревидирано 19. маја, прихваћено 24.маја 2021)

REFERENCES

1. D. Agrahar-Murugkar, G. Subbuakshmi, *Food Chem*. **89** (2005) 599 (https://doi.org/10.1016/j.foodchem.2004.03.042)
2. X. M. Wang, J. Zhang, T. Li, Y.Z. Wang, H.G. Liu, J. *Anal. Methods Chem*. **2015** (2015) 1 (https://doi.org/10.1155/2015/165412)
3. J. Falandysz, M. Drewnowska, M. Chudzinska, D. Barałkiewicz, *Ecotoxicol. Environ. Saf.* **137** (2017) 265 (https://doi.org/10.1016/j.ecoenv.2016.12.014)
4. I. Širić, A. Kasap, D. Bedeković, J. Falandysz, *J. Environ. Sci. Health., B* **52** (2017) 156 (https://doi.org/10.1080/03601234.2017.1261538)
5. W. Reczyński, B. Muszyńska, W. Opoka, A. Smalec, K. Sułkowska-Ziaja, M. Malec, *Biol. Trace Elem. Res.* **153** (2013) 355 (https://doi.org/10.1007/s12011-013-9670-3)
6. M. Tüzen, *Microchem. J.* **74** (2003) 289 (https://doi.org/10.1016/S0026-265X(03)00035-3)
7. *US EPA: Method 3050B: acid digestion of sediments, sludges, and soils*, 1996
8. P. Kalač, L. Svoboda, *Food Chem.* **69** (2000) 273 (https://doi.org/10.1016/S0308-8146(99)00264-2)
9. EFSA Scientific Committee, *EFSA J.* **10** (2012) 2579 (https://efsa.onlinelibrary.wiley.com/doi/epdf/10.2903/j.efsa.2012.2579)
10. E. Sesli, M. Tüzen, *Food Chem.* **65** (1999) 453 (https://doi.org/10.1016/S0308-8146(98)00194-0)

11. V. Stefanović, *Determination of the contents of macroelements and microelements in samples of* Macrolepiota procera *mushrooms and soil substrates from Rasina district*, University of Belgrade, 2016 (in Serbian)
12. P. Kalač, *Food Chem.* **113** (2009) 9 (https://doi.org/10.1016/j.foodchem.2008.07.077)
13. R. Seeger, *Z. Lebensm. Unters. Forsch.* **167** (1978) 23 (https://doi.org/10.1007/BF01122881)
14. *EEC, Amending Council Directive 90/496/EEC on nutrition labelling for foodstuffs as regards recommended daily allowances, energy conversion factors and definitions. Official Journal of the European Union, Commission Directive 2008/100/EC*, 2008
15. EFSA Scientific Committee*, EFSA J.* 2017 e15121 (https://efsa.onlinelibrary.wiley.com/doi/epdf/10.2903/sp.efsa.2017.e15121)
16. P. Kalač, *Mineral Composition and Radioactivity of Edible Mushrooms*, Academic Press is an imprint of Elsevier, Amsterdam, 2019 (https://doi.org/10.1016/C2018-0-02278-1)
17. EFSA Scientific Committee, *EFSA J.***17** (2019) 57782019 (https://efsa.onlinelibrary.wiley.com/doi/epdf/10.2903/j.efsa.2019.5778)
18. R. Zsigmond, K. Varga, S. Harangi, E. Baranyai, I. Urák, *Acta Univ. Sapient. Agric. Environ.* **7** (2015) 98 (https://doi.org/10.1515/ausae-2015-0009)
19. C. Sarikurkcu. J. Popović-Djordjević, M. H. Solak, *Ecotoxicol. Environ. Saf.* **190** (2020) 110058 (https://doi.org/10.1016/j.ecoenv.2019.110058)
20. P. Świsłowski, A. Dołhańczuk-Śródka, M. Rajfur, *Environ. Sci. Pollut. Res.* **27** (2020) 22235 (https://doi.org/10.1007/s11356-020-08693-5)
21. EFSA Scientific Committee, *EFSA J.* **754** (2008) 1 (https://doi.org/10.2903/j.efsa.2008.754)
22. Z. Xu, L. Fu, S. Feng, M. Yuan, Y. Huang, J. Liao, L. Zhou, H. Yang, C. Ding, *Molecules* **24** (2019) 1357 (https://doi.org/10.3390/molecules24071357)
23. M. J. Melgar, J. Alonso, M. A. García, *Food Chem. Toxicol*. **73** (2014) 44 (https://doi.org/10.1016/j.fct.2014.08.003)
24. *FAO and WHO, Safety evaluation of certain contaminants in food. WHO Food Additive Series 63/FAO JECFA Monographs 8*, WHO Press, Geneva, 2011
25. H. Karami, N. Shariatifar, S. Nazmara, M. Moazzen, B. Mahmoodi, A. M. Khaneghah, *Biol. Trace Elem. Res.* **99** (2021) 389 (https://doi.org/10.1007/s12011-020-02130-x)
26. M. Kosanić, B. Ranković, A. Rančić, T. Stanojković, *J. Food Drug Anal*. **24** (2016) 477 (https://doi.org/10.1016/j.jfda.2016.01.008)
27. M. Aloupi, G. Koutrotsios, M. Koulousaris, N. Kalogeropoulos, *Ecotoxicol. Environ. Saf.* **78** (2012) 184 (https://doi.org/10.1016/j.ecoenv.2011.11.018)
28. EFSA Scientific Committee*, EFSA J.* **980** (2009) 1 (https://doi.org/10.2903/j.efsa.2009.980)
29. M. V. Dimitrijevic, V. D. Mitic, J. S. Cvetkovic, V. P. Stankov Jovanovic, J. J. Mutic, S. D. Nikolic Mandic, *Eur. Food Res. Technol*. **242** (2016) 1 (https://doi.org/10.1007/s00217-015-2512-0)
30. EFSA Scientific Committee*, EFSA J.* **8** (2010) 1570 (https://doi.org/10.2903/j.efsa.2010.1570)
31. EFSA Scientific Committee, *EFSA J.* **10** (2012) 2831 (https://doi.org/10.2903/j.efsa.2012.2831)
32. A. Scragg, *Environmental Biotechnology*, Oxford University Press, New York, 2005

33. C. C. Elekes, G. Busuioc, I. Dumitriu, *Adv. Biomed. Res*. 464 (http://www.wseas.us/e-library/conferences/2010/Cambridge/MABIPH/MABIPH-61.pdf)
34. F. Adams, *The Role of Phosphorus in Agriculture*, American Society of Agronomy, Madison, WI, 1980 (https://doi.org/10.2134/1980.roleofphosphorus).

Journal of the Serbian Chemical Society
JSCS@tmf.bg.ac.rs • www.shd.org.rs/JSCS
J. Serb. Chem. Soc. *86* (10) 941–954 (2021)
JSCS–5474
Original scientific paper
Published 10 September 2021

Synthesis, spectroscopic characterization, DFT, oxygen binding and antioxidant activity of Fe(III), Co(II) and Ni(II) complexes with a tetradentate ONNO donor Schiff base ligand

SATYENDRA N. SHUKLA*, PRATIKSHA GAUR, MOHAN L. RAIDAS and SANJAY S. BAGRI

Coordination Chemistry Research Lab, Department of Chemistry, Govt. Science College, Jabalpur (M.P.), India

(Received 30 December 2020, revised 14 March, accepted 7 April 2021)

Abstract: The Schiff base ligand, namely (7*E*)-*N*-benzylidene-2-styrylbenzenamine-1,2-diamine-2,4-dihydroxy-phenol (**L**), was synthesized by condensation of 2,4-dihydroxybenzaldehyde with *o*-phenylenediamine. The reaction of the ligand with Fe(III), Co(II) and Ni(II) salts in an 1:1 ratio yielded three complexes (**1**–**3**). Different analytical tools, like elemental analysis, ESI-MS, UV–Vis, FT-IR, NMR and EPR spectroscopy, then molar conductivity and magnetic susceptibility spectra, were used to elucidate the structure of the ligand and complexes. Density functional theory calculation at the B3LYP/3--211G++/LANL2DZ level of the theory has been carried out to optimize the geometry of the ligand and complexes. The tetradentate ligand has coordinated to metals through ONNO donors affording octahedral geometry. Complexes were studied for their oxygen-binding activity and free radical scavenging activities. Complexes **1** and **2**, which contain Fe(III) and Co(II), displayed reversible oxygen binding activity. On the other hand, complex **3** fails to show oxygen binding. The order of antioxidant activity is: **3** > **1** > **2** > **L**.

Keywords: oxygen binding study; thermodynamic parameters; FT-IR spectra; UV–Vis spectra.

INTRODUCTION

The discovery of reversible oxygenation of salicylaldimine cobalt complex by Tsumaki in 1938[1] has given considerable impetus to this objective. Since then, it has been inspiring synthetic chemists to prepare artificial respiratory pigment systems to imitate the natural ones in their activity. The proteins responsible for oxygen transportation and storage in mammalian cells, haemoglobin (Hb) and myoglobin (Mb), have often been used as examples of protein conform-

* Corresponding author. E-mail: sns1963_1@rediffmail.com; ccrl_2004@rediffmail.com
https://doi.org/10.2298/JSC201230037S

ation, dynamics and function.[2] The compounds called natural respiratory pigments can reversibly absorb molecular oxygen.[3] Naturally occurring oxygen carriers and storage proteins contain a transition metal ion to which O_2 can reversibly bind, typically iron (in the form of ferrous heme in proteins such as myoglobin and haemoglobin) or copper (hemocyanin). Many complexes of this type have been used as models to aid in understanding protein's function. Cobalt-substituted oxymyoglobin ($CoMbO_2$) was also characterized, as well as synthetic analogues.[4] Cobalt(II) complexes of Schiff bases, porphyrins or phthalocyanines have been widely studied as models of oxygen carriers.[5]

Interestingly, four-coordinated Schiff base derivative and macrocyclic complexes of cobalt(II) are poor oxygen binders. In contrast, their corresponding five-coordinate cobalt complexes with heterocyclic as the cobalt(II) ligand readily bind oxygen reversibly under an ambient pressure of oxygen.[6] The reversible O_2 binding can also occur for dicobalt(II) systems based on alkoxido and phenolato-hinged dinucleating ligands. In these, both cobalt atoms are oxidized from Co(II) to Co(III) by the oxidative addition of dioxygen, thus facilitating the reduction of O_2 to peroxide rather than the highly reactive superoxide as is the case for the mononuclear systems and which are prone to irreversible self-annihilation reaction.[7] With the experience of Co(salen) and other complexes and their O_2 binding activity many complexes incorporating Co(II), Fe(III) and Ni(II) have been prepared with different tetradentate Schiff base in search of good oxygen-binding activity.[8] Presence of oxygen in the living system is an essential condition for the survival of the organism. Still, it is also associated with the generation of different free radicals in the system. The living systems have the inherent protective mechanism to disseminate and neutralize these radicals. However, sometimes due to a higher concentration of the free radicals in the body system, a life-threatening situation may occur. In this situation role of free radical scavenger known as antioxidants become more important.[9]

Therefore, in anticipation of good reactivity, oxygen-binding activity and effective antioxidant activity of the resulting complexes, we have prepared a tetradentate Schiff base by condensation of 2,4-dihydroxybenzaldehyde with *o*-phenylenediamine. The reaction of the ligand with Fe(III), Co(II) and Ni(II) leads to the synthesis of three novel complexes. Synthesized compounds were characterized by spectroscopy. In the absence of a single crystal, density functional theory (DFT) studies have been performed to optimize ligand and complexes' structure. A general scheme for the synthesis of ligand and complexes is given in Fig. 1.

EXPERIMENTAL

o-Phenylenediamine (Research Lab), 2,4-dihydroxybenzaldehyde (Sigma–Aldrich), anhydrous $FeCl_3$, $CoCl_2{\cdot}6H_2O$, $NiCl_2{\cdot}6H_2O$ were purchased from E. Merck. Analytical reagent grade solvents were used. Conductivity measurements were carried out at 25 °C on an EI-

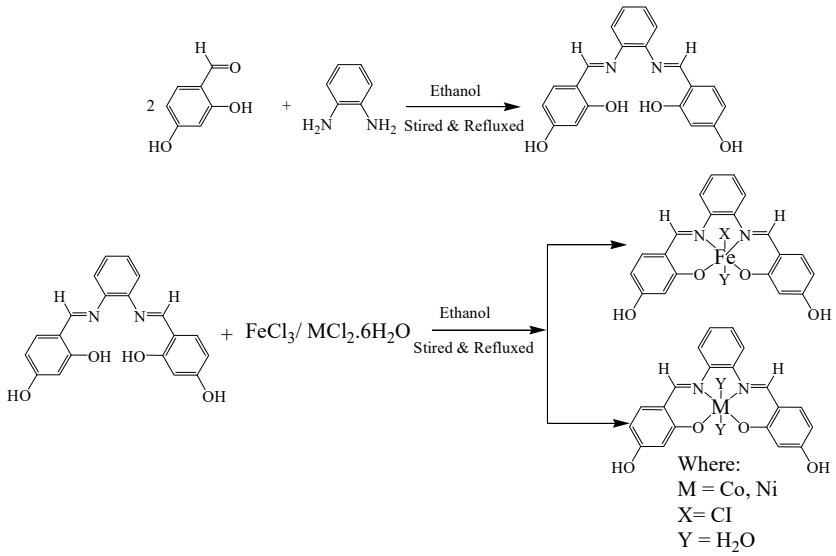

Fig. 1. General scheme for the synthesis of ligand **L** and complexes.

-181 conductivity bridge with a dipping type cell. ESI-MS spectra were recorded on Agilent-6520(QTOF) mass spectrometer. FT-IR spectra were recorded in KBr pellets on Shimadzu-8400 PC. Electronic absorption spectra were recorded with EI-2305, double beam spectrophotometer equipped with a PC. ^{1}H-NMR and ^{13}C-NMR spectra were recorded in DMSO-d_6 on Agilent-700-vnmrs 700. The metal contents were analyzed gravimetrically by the literature procedure. EPR spectra of the complexes were recorded at X-band (9.439 GHz) frequency in the EPR JEOL spectrometer.

*Synthesis of Schiff base ligand (7*E*)-*N*-benzylidene-2-styrylbenzenamine-1,2-diamine-2,4-dihydroxy-phenol (**L**)*

2,4-dihydroxybenzaldehyde (2.76 g, 0.010 mol) dissolved in 25 mL of ethanol was mixed with a solution of *o*-phenylenediamine (1.08 mL, 0.010 mol) in 25 mL of ethanol in a flat bottom flask, and the resulting mixture was stirred for 1 h. After that, the reaction mixture was kept under reflux for 8 h in an inert atmosphere. A pale yellow solid was obtained after cooling the mixture, which was filtered off, washed several times with methanol. The solid obtained was recrystallized from hot methanol to yield yellow crystals, dried over anhydrous calcium chloride in a desiccator under vacuum.

Synthesis of complexes

Ligand (**L**, 0.348 g, 0.0010 mol) was dissolved in 25 mL ethanol in a two neck flat bottom flask. $FeCl_3$ (0.161 g, 0.001 mol)/$CoCl_2{\cdot}6H_2O$ (0.237 g, 0.0010 mol)/$NiCl_2{\cdot}6H_2O$ (0.237 g, 0.0010 mol) dissolved in 25 mL ethanol was added to the above reaction mixture dropwise and stirred for 2 h. After that, the reaction mixture was refluxed for 9 h in an inert atmosphere. A red precipitate was obtained, filtered, recrystallized by 2:2:1 volume ratio of ethanol:methanol:acetone solvent mixture, and dried in a vacuum. Unfortunately, after several attempts, we did not find any crystal suitable for single-crystal XRD.

DFT Study

Density functional theory (DFT) was employed to achieve more insight into the molecular structure. It was carried out using the method of B3LYP with 6-311++G(d,p) basis set for all nonmetallic atoms and Los Alamos National Laboratory 2 double zeta (LANL2DZ) basic set for the central metal atoms in the gas phase.[11] Gaussian-09 software package was employed to carry out all the quantum chemical calculations.[12] Optimized structural parameter of the compounds, such as bond lengths and bond angles, were calculated with the molecule's atom numbering scheme. Several quantum chemical parameters have been calculated.[13] The FT-IR, ^{1}H-NMR and ^{13}C-NMR Chemical Shifts of the molecule were calculated by the gauge-independent atomic orbital (GIAO) method and compared with experimental results.

Oxygen binding study

A reversible oxygen-binding study of the synthesized complexes was done in the experimental setup described earlier.[14] In the second experiment, the most effective iron and cobalt complexes were studied further, and oxygen-binding ability was observed at different temperatures (273–303 K) in DMF.[15] The thermodynamics parameter such as ΔH^{o} and ΔS^{o} were calculated using Van't Hoff equation.[16,17]

Antioxidant activity

The free radical scavenging activity of the compounds was determined with the 2,2-diphenyl-1-picrylhydrazyl (DPPH) method. Four solutions of different micromolar concentrations of the compounds (0.002, 0.004, 0.006 and 0.008 μM) and standard ascorbic acid were prepared in ethanol. The volume of each test tube was adjusted to 1.0 mL by adding ethanol. DPPH was used as a control. After that, a 5 mL ethanolic solution of DPPH (0.1 μM) was added. The tubes were kept at ambient temperature for 30 min. The absorbance of test solutions and a blank solution of DPPH (2 mL) was measured at 517 nm. The decrease in the absorbance of DPPH was calculated comparative to the measured absorbance of the control.[18] Radical scavenging activity was calculated as:

$$\text{Radical scavenging activity, \%} = 100\frac{A_{\text{control}} - A_{\text{test}}}{A_{\text{control}}} \quad (1)$$

where A_{control} is absorbance of the control and A_{test} is absorbance of the test.

RESULTS AND DISCUSSION

Spectral characterization of complexes

Stoichiometries of the complexes conformed with elemental analyses data. Molar conductance (Λ_m) for complexes in 10^{-3} M concentration in DMSO was in the range 1–4 Ω^{-1} cm^2 mol^{-1}, indicative of their 1:1 electrolytic nature.[19] ESI--MS spectra of complexes exhibit several peaks. However, a pseudomolecular ion peak for [M+H$^+$] was present consistently in each case, which indicated the molecular mass. ESI-MS spectra of ligand **L** and complexes are shown in Figs. S-1 and S-2a–c of the Supplementary material to this paper, respectively.

In the FT-IR spectrum of complexes, the band observed at ~3207 cm^{-1}, assigned for –OH vibration in ligand completely vanished, and a new peak at lower frequency appeared at ~512 cm^{-1}, which was assigned to M–O.[20] The appearance of this peak indicates the bonding of metal with phenolic oxygen.

The band due to azomethine HC=N groups was shifted downwards by 1598 cm^{-1} in complexes, which confirms the coordination of azomethine nitrogen with metal. The coordination of azomethine nitrogen with metal was further ascertained by the appearance of a peak at a lower frequency at ~433 cm^{-1}, assigned to M–N vibration stretching.[21] Complexes also exhibit a band observed at ~2871 cm^{-1} attributed to the aromatic ring's C–H vibration. The vibrational band for C–O stretching was observed at ~1180 cm^{-1}.[22] The experimental (solid phase) and theoretical (gas phase) FT-IR spectra data of **L** and complex **2** is correlated in TABLE S-I of the Supplementary material.

The calculated IR vibrations were slightly shifted from experimental values. DFT calculations generally overestimate the frequencies and neglect the crystal packing effects. However, anharmonicity and incompleteness of the basis set and dynamic electronic correlation were also responsible for the above-stated deviations.[23] Therefore, we have derived scaling factors and applied them to get a satisfactory value. The scaling factor for **L** was determined as 1.012 (R^2 = 0.999) over a complete range of spectrum and that in complex **2,** it is 1.005 (R^2 = = 0.998). In comparison, it was observed that in the theoretical spectra after scaling, the peaks for ν(C–H), ν(HC=N), $\nu(C–O)_{sym}$, ν(C–C), ν(C–H), ν(O–H), ν(M–O) and ν(M–N) were observed with a very small deviation of 0.1 %. The experimental and theoretical FT-IR spectra of ligand **L** are shown in Figs. S-3 and S-4 of the Supplementary material. Similarly, the experimental and theoretical FT-IR spectrum of complex **2** is shown in Figs. S-5 and S-6. The FT-IR correlation curve for ligand **L** and complex **2** is shown in Fig. S-7. The experimental spectra of complexes **1** and **3** are shown in Figs. S-8 and S-9.

In the UV–Vis spectra of ligand **L**, an absorption band at 280 nm was assigned to the intra-ligand π→π* transition, and a strong absorption band at 340 nm was ascribed to n→π*transition associated with imine moiety. Fe(III) complexes exhibit a magnetic moment of ~5.54 BM as expected for the high spin case. The ground state of high spin octahedral Fe(III) complexes is $^6A_{1g}$. The electronic spectrum of this complex exhibits bands at 660, 540 and 340 nm assigned for the following transitions: $^6A_{1g}\rightarrow{}^4T_{1g}$, $^6A_{1g}\rightarrow{}^4T_{2g}$ and $^6A_{1g}\rightarrow{}^4T_{1g}$, ^4E_g, respectively, as expected for the iron(III) octahedral complexes. Co(II) complexes exhibit magnetic moments of ~4.59 BM due to the presence of three unpaired electron. The electronic spectrum of complexes exhibits bands at ~630, ~560 and ~390 nm assigned for the following transitions: $^4T_{1g}$ (F)→$^4T_{2g}$ (P) (ν_1), $^4T_{1g}$ (F)→$^4A_{2g}$ (F) (ν_2) and $^4T_{1g}$ (F)→$^4T_{2g}$ (F) (ν_3), respectively. This transitions suggest an octahedral environment around the cobalt(II) ion.[24] Ni(II) complexes exhibit ~3.02 BM, indicating two unpaired electrons in Ni(II) ion consistent with octahedral geometry. A spectrum of the nickel(II) complex exhibits three bands at ~610, ~520 and ~360 nm corresponding to $^3A_{2g}\rightarrow{}^3T_{2g}$, $^3A_{2g}\rightarrow{}^3T_{1g}$ and $^3A_{2g}\rightarrow{}^3T_{1g}$(P) transitions, respectively, which indicate an octa-

hedral geometry around nickel atom.[25] UV–Vis spectra of **L** and complexes are given in Figs. S-10 and S-11a–c of the Supplementary material.

^{1}H-NMR of **L** exhibits a signal at δ 8.81 ppm for two protons (numbered as 3 and 16) were attributed to two azomethine group present in the ligand. It is positive evidence for the Schiff base formation.[26] Two deshielded signals appeared at δ 13.18 and ~9.91 ppm for two protons each, were assigned for the phenolic-OH present at ortho (numbered as 40 and 41) and para-position (numbered as 39 and 42) to azomethine. A multiplet centred at δ 6.87 ppm for four protons were due to four phenylene proton atoms (numbered as 10, 11, 12 and 13). A double doublet centred at δ 7.56 ppm for two protons were assigned to the phenolic ring proton atoms present ortho to azomethine (numbered as 3 and 24). A multiplet centred at δ 7.37 ppm for two protons was attributed to phenolic ring proton atoms present meta to azomethine (numbered as 25 and 33). A singlet for two protons at δ 6.36 ppm was attributed to phenolic ring proton atoms present between two hydroxyl groups (numbered as 23 and 32). The ^{1}H-NMR spectrum of ligand **L** is shown in Fig. S-12. The GIAO method calculated the theoretical chemical shift values using TMS HF/6-31G(d) GIAO and TMS B3LYP/6--311+G(2d,p) GIAO level theory. The correlation coefficients of ^{1}H-NMR were determined as 0.978, as shown in Fig. S-13. For ligand **L** ^{1}H-NMR δ_{cal} 0.934, δ_{exp} + 0.327 (R^2 = 0.978). It was evident from the correlation graph that good correlation exists in theoretical and experimental δ values.

In the ^{13}C-NMR of ligand **L**, a strong signal at δ ~173.0 ppm was assigned for the presence of imine (>C=N–) carbon. The signal that appeared at δ ~166.0 ppm was attributed to the carbon linked with a hydroxyl group. All aromatic carbon of phenylene and phenolic moiety display signals between δ 116.00 and 162.00 ppm.[27] The ^{13}C-NMR spectrum of **L** is shown in Fig. S-14. The correlation coefficients of ^{13}C-NMR for **L** was determined as 0.942, as shown in Fig. S-15. For **L,** ^{13}C-NMR δ_{cal} 0.856, δ_{exp} + 22.68 (R^2 = 0.942). It was evident from the correlation graph that a good correlation exists in theoretical and experimental δ values. The DFT and ^{1}H-NMR and ^{13}C-NMR were correlated with the experimental and theoretical δ values. Data of **L** are displayed in TABLE S-II.

The EPR analysis of complexes **1**–**3** was performed at solid-state at room temperature (RT).[28] Spin-Hamiltonian parameters calculated for complex **1** at RT shows g values: $g_\perp \approx 2.408$, $g_\| \approx 2.086$ and $g_e \approx 2.009$. Spin-Hamiltonian parameters calculated for complex **2** at RT shows g values: $g_\perp \approx 2.554$, $g_\| \approx$ ≈ 2.148 and $g_e \approx 2.013$. Spin-Hamiltonian parameters calculated for complex **3** at RT shows g value: $g_\perp \approx 2.354$, $g_\| \approx 2.048$ and $g_e \approx 2.011$, suggesting that the unpaired electron resides in $d_{x^2-y^2}$ orbital and slightly distorted octahedral geometry of the complexes. The EPR spectra of complexes **1**–**3** are shown in Fig. S-16a–c.

Quantum chemical calculations

The Mulliken population analysis obtained the net atomic charges of ligand, **L** and complex **2**.[29] The Mulliken charge shows that in **L** maximum charge of +0.28944 is observed on C27 because C27 is flanked between three highly electronegative atoms. Electronegative atoms such as O, N, N and O exhibit highly negative charge due to the +I effect. O38 atoms from the hydroxyl group being highly shielded have a maximum negative Mulliken charge value of -0.62650, and azomethine-N have a charge of -0.27821. In complex **2,** maximum *+ve* charges of +0.326542 are observed on C27 since C27 is flanked between three highly electronegative atoms. Electronegative atoms such as O, N, N and O exhibit highly negative charge due to the +I effect. O41 atoms from the hydroxyl group being highly shielded have a maximum *–ve* Mulliken charge of -0.580976, and azomethine-N have a charge of -0.319319. The Mulliken charges of all complexes are listed in TABLE S-III.

The atomic charge distributions for the complex was calculated with the B3LYP/LanL2DZ//6–311++G* basis set. The highest and lowest negative charge to be found on complex **2** at N(2) (–0.47669 e) and O(37) (–0.74449 e). Thus the observed bond length of Co–N(14), 1.87956 Å and Co–O(35) 1.82787 Å are different. According to the NPA, the natural electron configuration of Co is: [core] 4s(0.26)3d(7.65)4p(0.51)4d(0.02). Thus, (17.99025) core electrons, (8.41330) valence electrons (on 4s, 3d and 4p atomic orbitals) and (0.02571) Rydberg electrons (mainly on 4p, 4d and 5p orbitals) give 26.42926 electrons. This value is consistent with the calculated natural charge on Co atom +0.57074 in complex **2**, which corresponds to the difference between 26.42926 e and the total number of electrons in the isolated cobalt atom 27 e. In addition, the atoms O(35), O(36), N(2) and N(14), have negative charge –0.63188, –0.61051, –0.47669 and –0.54181 e, respectively. The charges of the atoms in the ligand **L** and complex **2** are listed in TABLE S-IV.

The natural bond orbital (NBO) analysis of a representative complex **2** was carried out by the B3LYP/LANL2DZ level basis set.[30] As expected, the strongest donation occurs in the ligand **L**, which from the π(N2–C2) to π*(C6) antibonding orbital and has the energy of 157.60 kJ/mol. The interaction between the σ(C2–C5) and σ*(N2–C5) has the second-highest value of around 105.65 kJ/mol. These transitions give greater stabilization to the molecule. The hyper conjugative interactions of the σ and π electrons of selected C–C to anti– C–C bonds in the complex **2** are listed in TABLE S-V. The values of stabilization energies are in the range of 0.29–1.10 kJ/mol for σ→σ* transitions, 0.58-44.80 kJ/mol for π→π* transitions. The π→π* transitions have high resonance energies, such as C28-C29→C26-C27, C26-C27→C30-C31, C30-C31→C28-C29, C17 C18→ →C21-C22, C21-C22→C15-C20 and C15-C20→C21-C22, with the resonance energies 10.52, 10.50, 11.02, 11.10, 13.69 and 44.80 kJ/mol, respectively, that

lead to the stability of the complex. According to the n→σ* and n→π* interactions, the strongest interactions are due to LP(1)C1→σ*(C30–C31) 17.52, LP(1)N→σ*(O36–Co44) 28.00, LP (1)C19→σ*(C15–C20) 98.94, LP (1)C19→ →π*(C17–C18) 37.97, LP*(6)Co44→π*(N2–C5) 84.91, LP*(6)Co44→ →π*(C4–C5) 16.57, π(N2–C5)→LP*(4)Co(44) 21.22 kJ/mol.

The molecule's MEP surface was calculated by the B3LYP/LANL2DZ method with the 6-311++G(d,p) basis set. As it can be easily observed from the ligand **L** MEP map**,** the negative regions in MEP are related to the electronegative or electrophilic site. In contrast, the positive regions are related to the electropositive or nucleophilic site. This molecule has several possible sites for coordination. The negative regions are mainly over the oxygen atoms (deep red/yellow) on each of the O–H groups and nitrogen atoms of imine groups. The oxygen and carbon atoms bear the maximum region of positive charge, and the most positive regions (blue/green) are observed around the O–H groups as well as carbon atoms of imine groups. The colour codes of this map are in the ranges between –0.122 (deep red) and +0.122 a.u. (deep blue) in the ligand **L**. Similarly, in the complexes, the MEP map is between –0.113 and +0.113 a.u. for complex **1**, –8.512 and +8.512 a.u. for complex **2** and –9.163 and + 9.163 a.u. for complex **3**, respectively. The potential increases in the order: red < orange < yellow < < green < blue.[31] The MEP map of ligand **L** and comple**xes** are shown in Fig. S-17a–d.

FMOs analysis

The HOMO is the orbital that primarily acts as an electron donor, and the LUMO largely acts as the electron acceptor. The energy gap between HOMO and LUMO set apart the chemical stability of the molecule.[32] The FMOs of the energies of compounds are shown in TABLE S-VI. The energy differences between HOMO and LUMO for ligand **L** is 4.13035 eV while in complexes 3.04545, 3.54941 and 2.97987 eV, respectively. The HOMO and LUMO energy level diagrams of ligand **L** and complex**es** are shown in Fig. S-18a–d. The calculated energies of the HOMO and LUMO show that there is a very small energy gap (ΔE) in complex **3,** which may be responsible for its low kinetic stability, reflecting efficient electronic charge transfer interaction and high chemical reactivity, making the ligand strongly polarizable. It may lead to high free radical scavenging activity.

Bond parameters

The optimized bond lengths and bond angles of investigated compounds calculated by B3LYP/LANL2DZ methods with 6-311++G (d,p) basis set were listed in TABLEs S-VII and S-VIII following the atom numbering scheme as shown in Fig. 2a–d. The optimized geometrical parameters of ligand were compared with complexes. The optimized O–H bond length in ligand was 0.962 Å

which was diminished in complexes, and a new M–O bond is formed with a bond length of 1.800–1.828 Å. The calculated >C=N– bond distance in ligand was observed as ~1.293 Å, which shows an increase of 0.005–0.006 Å in the case of complexes. This increase in the bond distance is due to the transfer of double bond electron density towards metal and the decrease in the double bond character of C=N, which confirms the coordination of metal with azomethine-N. This elongation in M–N bond lengths caused a slight distortion from the regular octahedral geometry.

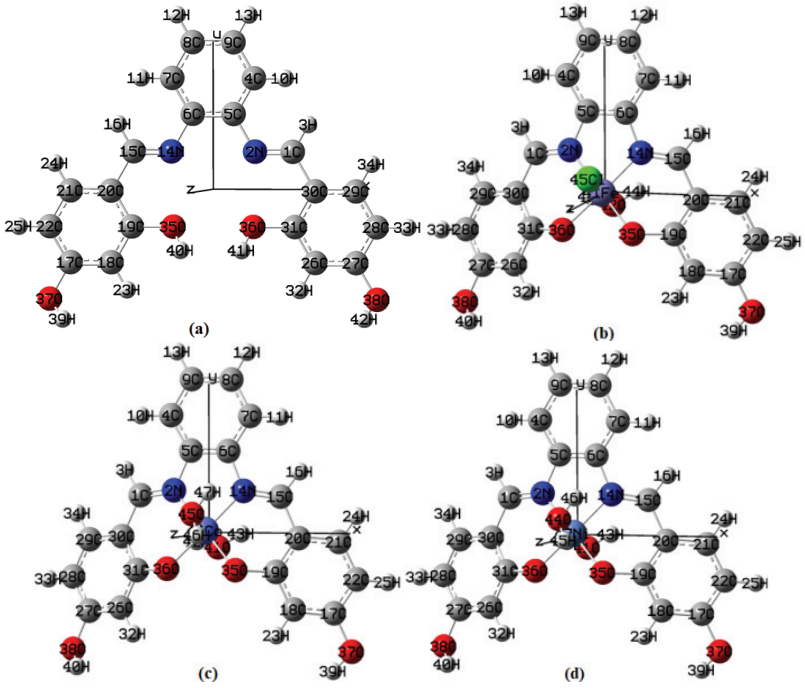

Fig. 2. DFT optimized structure of: a) ligand **L** and complexes: b) **1**, c) **2** and d) **3**.

Based on elemental analysis, electronic spectra, ESI-MS, FT-IR, ^{1}H-NMR, ^{13}C-NMR and DFT studies, optimized structures of the ligand **L** is suggested in Fig. 2a. Similarly, based on elemental analysis, molar conductance, electronic spectra, ESI-MS, FT-IR, EPR and DFT studies, optimized structures of the complexes are given in Fig. 2b–d.

Oxygen binding study

Complexes dissolved in DMF were explored for Oxygen binding study, and results are shown as spectra in Fig. 3. Absorbance change was noticed only in complexes **1** and **2** containing Fe (III) and Co (II) as a central metal ion. However, complex **3** exhibited no change in the absorbance; Ni (II) as a central metal.

It could be explained based on DFT optimization. It was observed in DFT optimized structure that Ni–O(H_2O) bonds are slightly smaller than other M–O(H_2O) bonds and probably more stable, which may be the reason for the non-participation of these complexes in oxygen binding activity. From the graph, it was observed that the prominent absorption at 360 nm in complex **1**, 390 nm in complex **2** diminished with time and seems to disappear in the presence of oxygen. Interestingly, at the same time, the absorption of broad bands between 440–650 nm attributable to d–d transitions becomes more pronounced. In cobalt complexes, the reaction that most probably occurs in the presence of O_2 is:

$$[CoL(H_2O)_2] + 2DMF \leftrightarrow [CoL(DMF)_2] + 2H_2O \quad (2)$$

$$[CoL(DMF)_2] + O_2 \leftrightarrow [CoL(DMF)(O_2)] + DMF \quad (3)$$

However, in the case of Fe (III) complex reaction appears to proceed in the following manner:

$$[FeL(H_2O)Cl] + DMF \leftrightarrow [FeL(DMF)Cl] + H_2O \quad (4)$$

$$[FeL(DMF)Cl] + O_2 \leftrightarrow [FeL(O_2)Cl] + DMF \quad (5)$$

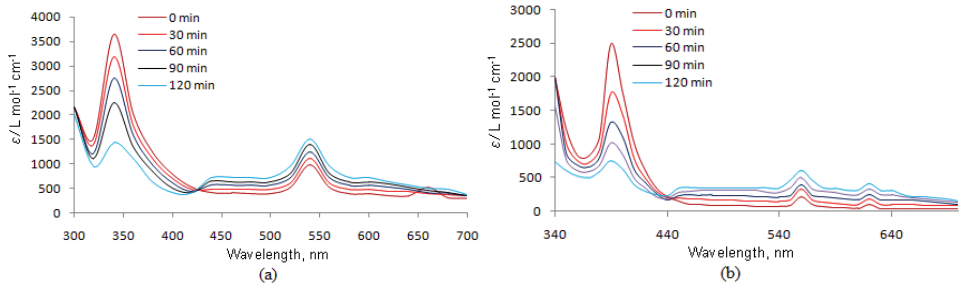

Fig. 3. UV–Vis spectra of oxygen binding study of complexes **1** (a) and **2** (b).

To understand the thermodynamics of oxygen binding reaction of complexes, the reaction was carried out at various temperatures and the oxygenation constant (K_{O_2}), which is calculated according to the relation below:

$$K_{O_2} = (C\text{ML(DMF)}_{O_2}/C\text{ML(DMF)})P_{O_2} \quad (6)$$

The data clearly show that the oxygenation constant decreases with an increase in temperature, which indicates that the oxygen-binding ability of complexes decreases with rising temperature.[33] The oxygenation constants at different working temperatures are given in TABLE S-IX. The experimental values of K_{O_2}, at different temperatures, obey the Van't Hoff equation.[34] To determine the thermodynamic parameters, such as $\Delta H°$ and $\Delta S°$, the plot of ln K_{O_2} *vs.* 1000/T was drawn Fig. S-19:

$$\ln K_{O_2} = f(1/T) \quad (7)$$

$$\ln K_{O_2} = -(\Delta H°/RT) + (\Delta S°/R) \quad (8)$$

It was observed from TABLE S-IX that the enthalpy change of complex **1** is maximum negative. Negative enthalpy change is also an indicator of exothermic oxygenation reaction. The negative value of $\Delta H°$ and $\Delta S°$ for complexes **1** and **2** demonstrate that these complexes consist of a good oxygen-binding capacity.[35]

In vitro *antioxidant activity*

The results of the free radical scavenging activity of the compounds at different micromolar concentrations (0.002–0.008 μM) are shown in TABLE S-X. Ascorbic acid was used as a control to estimate the effectiveness of the tested compounds under the same conditions. The measured compounds have exhibited significant scavenging activity but lower than ascorbic acid. It has been observed that complex **3** exhibited higher antioxidant activity of 46.33–76.33 % in the given concentration range. It could be explained based on DFT, which calculates the lower energy gap (ΔE) for complex **3**. Due to the lower energy gap (ΔE),[36] complex **3** will be more reactive and can easily react with the free radicals to yield a more resonance stabilized complex species.

CONCLUSION

A Schiff base ligand (7*E*)-*N*-benzylidene-2-styrylbenzenamine1,2-diamine--2,4-dihydroxy-phenol (**L**) and its novel metal derivatives of Fe(III), Co(II) and Ni(II) were synthesized and characterized by spectroscopy. The spectral data has revealed that the Schiff base acts as a tetradentate ONNO donor ligand and coordinated through phenolic oxygen and azomethine nitrogen. In FT-IR and NMR, a quite good correlation has been observed in experimental and theoretical data. Several quantum chemical calculations have been performed to achieve better insight into molecular structure, and the geometry of complexes was optimized. The bond parameters, bond distance and bond angles are slightly distorted from octahedral geometry. In oxygen-binding experiment, **1** and **2** with Fe(III) and Co(II) exhibited good oxygen-binding capacity; however, **3** with Ni(II) ion is inactive probably due to greater stability of Ni–O(H_2O) bonds. The negative values of $\Delta H°$ and $\Delta S°$ for **1** and **2** demonstrated that oxygenation reaction is thermodynamically favored for these complexes. The decrease in oxygenation constant with temperature indicates that the oxygen-binding ability of complexes decreases with an increase in temperature. In the antioxidant activity experiment, complex **3** displayed more antioxidant activity than **1**, **2** and **L**, probably due to lower ΔE.

SUPPLEMENTARY MATERIAL

Additional data and information are available electronically at the pages of journal website: https://www.shd-pub.org.rs/index.php/JSCS/article/view/10208, or from the corresponding author on request.

Acknowledgements. The authors are grateful to the Principal, Government Science College, Jabalpur and Head, Department of Chemistry, for providing necessary laboratory facilities. We sincerely thank SAIF, CDRI, Lucknow, for recording ESI-MS, ^{1}H-NMR, ^{13}C-NMR and IIT, Bombay, for recording EPR. One of us (Mohan Lal Raidas) is also grateful to the UGC-New Delhi, for financial support through RGNF (Award letter no. F1-17.1/2016-17/ /RGNF-2015-17-SC-MAD-19879/(SAIII/Website).

ИЗВОД

СИНТЕЗА, СПЕКТРОСКОПСКА КАРАКТЕРИЗАЦИЈА, DFT ПРОРАЧУНИ, ВЕЗИВАЊЕ КИСЕОНИКА И АНТИОКСИДАТИВНА АКТИВНОСТ КОМПЛЕКСА Fe(III), Co(II) И Ni(II) СА ONNO-ТЕТРАДЕНТАТНОМ ШИФОВОМ БАЗОМ КАО ЛИГАНДОМ

SATYENDRA N. SHUKLA, PRATIKSHA GAUR, MOHAN L. RAIDAS и SANJAY S. BAGRI

Coordination Chemistry Research Lab, Department of Chemistry, Govt. Science College, Jabalpur (M.P.), India

Кондензационом реакцијом између 2,4-дихидроксибензалдехида и *o*-фенилендиамина добијена је Шифова база (7*E*)-*N*-бензилиден-2-стирилбензенамин-1,2-диамин--2,4-дихирдоксифенол (**L**), која је затим у реакацији са Fe(III), Co(II) и Ni(II) солима (молски однос 1:1) употребљена као лиганд за синтезу одговарајућих комплекса (**1**–**3**). Различите аналитичке технике, као што су елементална анализа, ESI-MS, UV–Vis, FT-IR, NMR и EPR спектроскопија, а затим метода мерења моларне и магнетне проводљивости, употребљене су за структурну карактеризацију лиганда и одговарајућих комплекса метала. Применом DFT методе на бази B3LYP/3-211G^{++}/LANL2DZ теоријских прорачуна оптимизована је геометрија лиганда и комплекса метала. Нађено је да је лиганд **L** преко ONNO донорских атома тетрадентатно координован за јоне метала при чему настају комплекси октаедарске геометрије. Испитивана је способност комплекса за везивање кисеоника и слободних радикала. Комплекси Fe(III) и Co(II) (**1** и **2**) су показали реверзибилну способност везивања кисеоника. Супротно томе, комплекс **3** није показао способност везивања кисеоника. Антиоксидативна активност испитиваних једињења мењала се у низу **3** > **1** > **2** > **L**.

(Примљено 30. децембра 2020, ревидирано 14. марта, прихваћено 7. априла 2021)

REFERENCES

1. V. Tsumaki, *Bull. Chem. Soc. Jpn.* **13** (1938) 262 (https://dx.doi.org/10.1246/bcsj.13.252)
2. M. F. Perutz, *Trends Biochem. Sci.* **14** (1990) 42 (https://dx.doi.org/10.1016/0968-0004(89)90039-x)
3. M. Wirstam, S. J. Lippard, R. A. Friesner, *J. Am. Chem. Soc.* **13** (2003) 3980 (https://dx.doi.org/10.1021/ja017692r)
4. M. S. Vad, F. B. Johansson, R. K. S. Egdal, J. E. McGrady, S. M. Novikov, S. I. Bozhevolnyi, A. D. Bonda, *Dalton Trans.* **42** (2013) 9921 (https://dx.doi.org/10.1039/c3dt50617g)
5. B. M. Hoffman, D. H. Petering, *Proc. Natl. Acad. Sci. USA* **67** (1970) 627 (https://dx.doi.org/10.1073/pnas.67.2.637)
6. J. H. Bowen, N. V. Shokhirev, A. M. Raitsimring, D. H. Buttlaire, F. A. Walker, *J. Phys. Chem., B* **101** (1997) 8683 (https://dx.doi.org/10.1021/jp9711306)
7. W. R. Scheidt, J. L. Hoard, *J. Am. Chem. Soc.* **95** (1973) 8281 (https://dx.doi.org/10.1021/ja00806a013)

8. A. A. A. Emara, A. M. Ali, A. F. El-Asmy, E. M. Ragab, *J. Saudi Chem. Soc*. **18** (2011) 762 (https://dx.doi.org/10.1016/j.jscs.2011.08.002)
9. L. Liu, M. S. Alam, D. U. Lee, *Bull. Korean Chem. Soc.* **33** (2012) 3361 (http://dx.doi.org/10.5012/bkcs.2012.33.10.3361)
10. G. H. Jeffery, J. Bassett, J. Mendham, R. C. Denney, *Vogel's Textbook of Quantitative Inorganic Analysis*, 5th ed., John Wiley & Sons, Inc., New York, 1989
11. M. Montazerozohori, S.A. Musavi, A. Masoudias, A. Hojjati, A. Assoud, *Spectrochim. Acta, A* **147** (2015) 139 (http://dx.doi.org/10.1016/j.saa.2015.03.028)
12. *Gaussian-09 software package*, Gaussian Inc. Wallingford, CT, 2009
13. M. Dehestani, L. Zeidabadinejad, *J. Serb. Chem. Soc.* **80** (2015) 1008 (https://dx.doi.org/10.2298/JSC150224027Z)
14. S. N. Shukla, P. Gaur, M. L. Raidas, B. Chaurasia, *J. Mol. Struc.* **1202** (2020) 127362 (https://dx.doi.org/10.1016/j.molstruc.2019.127362)
15. A. Huber, L. Müller, H. Elias, R. Klement, M. Valko, *Euro. J. Inorg. Chem.* **8** (2005) 1459 (https://dx.doi.org/10.1002/ejic.200400888)
16. T. J. Beugelsdijk, R. S. Drago, *J. Am. Chem. Soc.* **97** (1975) 6466 (https://dx.doi.org/10.1021/ja00855a028)
17. N. J. Rose, R. S. Drago, *J. Am. Chem. Soc*. **81** (1959) 6138 (https://dx.doi.org/10.1021/ja01532a009)
18. M. Kumar, T. Padmini, K. Ponnuvel, *J. Saudi Chem. Soc.* **21** (2017) 322 (https://dx.doi.org/10.1016/j.jscs.2014.03.006)
19. W. J. Gear, *J. Coord. Chem. Rev.* **7** (1971) 81(https://dx.doi.org/10.1016/S0010-8545(00)80009-0)
20. S. N. Shukla, P. Gaur, P. Vaidya, B. Chaurasia, S. Jhariya, *J. Coord. Chem.* **71** (2018) 3912 (https://dx.doi.org/10.1080/00958972.2018.1536267)
21. S. N. Shukla, P. Gaur, S. Jhariya, B. Chaurasia, P. Vaidya, M. Azam, *J. Coord. Chem*. **72** (2019) 664 (https://dx.doi.org/10.1080/00958972.2019.1572885)
22. N. Ignjatović, S. Vranješ, Ž. Mitić, D. Janković, D. Uskoković, *J. Mat. Sci. Eng., C* **43** (2014) 439 (https://dx.doi.org/10.1016/j.msec.2014.07.046)
23. A. P. Scott, L. Radom, *J. Phys. Chem.* **100** (1996) 16502 (https://dx.doi.org/10.1021/jp960976r)
24. S. Chandra, L. K. Gupta, *Trans. Metal Chem.* **32** (2007) 558 (https://dx.doi.org/10.1007/s11243-007-0201-y)
25. F. A. Cotton, G. Wilkinson, C. A. Murillo, M. Bochmann, *Advances in Inorganic Chemistry*, Sixth ed., Wiley, New York, 1999
26. R. Mehrotra, S. N. Shukla, P. Gaur, *J. Coord. Chem.* **65** (2012) 176 (https://dx.doi.org/10.1080/00958972.2011.645814)
27. R. M. Silverstein, F. X. Webster, D. J. Kiemle, D. L. Bryce, *Spectr. Ident. Org. Com.* **1991** (1998) 226
28. P. Pietrzyk, M. Srebro, M. Radon, Z. Sojka, A. Michalak, *J. Phys. Chem., A* **115** (2011) 2316 (https://dx.doi.org/10.1021/jp109524t)
29. T. Bardakçi, M. Kumru, A. Altun, *J. Mol. Struct.* **1116** (2016) 292 (https://dx.doi.org/10.1016/j.molstruc.2016.03.023)
30. S. Sebastian, N. Sundaraganesan, *Spectrochim Acta, A* **75**(2010) 941 (https://dx.doi.org/10.1016/j.saa.2009.11.030)
31. I. Rajaei, S. N. Mirsattari, *Polyhedron* **112** (2015) 479 (https://doi.org/10.1016/j.poly.2015.10.019)

32. J. M. Mir, D. K. Rajak, R. C. Maurya, *J. Coord. Chem.* **70** (2017) 3199 (https://dx.doi.org/10.1080/00958972.2017.1374381)
33. M. R. Anneser, S. Haslinger, A. Pöthig, M. Cokoja, V. D'Elia, M. P. Högerl, J. M. Basset, F. E Kühn, *Dalton Trans.* **45** (2016) 6449 (https://dx.doi.org/10.1039/c6dt00538a)
34. M. Pająk, M. Woźniczka, A. Vogt, A. Kufelnicki, *Chem. Central J.* **11** (2017) 90 (https://dx.doi.org/10.1186/s13065-017-0319-8)
35. A. Pui, *Croat. Chem. Acta* **75** (2002) 165
36. M. S. Alam, D-U Lee, *Bull. Korean Chem. Soc.* **36** (2015) 682 (https://onlinelibrary.wiley.com/doi/full/10.1002/bkcs.10132).

Journal of the Serbian Chemical Society
JSCS@tmf.bg.ac.rs • www.shd.org.rs/JSCS
J. Serb. Chem. Soc. 86 (10) S224–S240 (2021) *Supplementary material*

SUPPLEMENTARY MATERIAL TO

Synthesis, spectroscopic characterization, DFT, oxygen binding and antioxidant activity of Fe(III), Co(II) and Ni(II) complexes with a tetradentate ONNO donor Schiff base ligand

SATYENDRA N. SHUKLA*, PRATIKSHA GAUR, MOHAN L. RAIDAS and SANJAY S. BAGRI

Coordination Chemistry Research Lab, Department of Chemistry, Govt. Science College, Jabalpur (M.P.), India

J. Serb. Chem. Soc. 86 (10) (2021) 941–954

*(7*E*)-N-benzylidene-2-styrylbenzenamine1-2-diamine-2-4-dihydroxy-phenol (**L**)*

M.p.: 285 °C; Color: Light yellow, Yield: 1.86 g (63 %); Selected infrared absorption (KBr, cm^{-1}): ν(O-H)$_{arom}$, 3204*s*; ν(C-H), 2874*m*; ν(HC=N)$_{imine}$, 1631*s*; ν(C=C), 1365*w*; ν(C-O), 1244*m*; ν(C-C), 1151*m*; γ(C-H), 754*w*; γ(O-H), 644*w*. Electronic spectra (λ_{max} / nm (ε / (mol L^{-1} cm^{-1})) in DMSO: 280(1585), 340(828). ^{1}H-NMR spectra (400 MHz, CH_3CN, δ / ppm): (O-H)$_{arom(ortho,para)}$, 13.18 (*s*, 2H), 9.91 (*s*, 2H), (HC=N)$_{imine}$, 8.81 (*s*, 2H), (Ar-H)$_{phenolic}$, 7.56 (*dd*, J_1 = 8.0, J_2 = 1.6, 2H), 7.37 (*m*, 2H), 6.36(*s*, 2H), (Ar-H)$_{phynelene}$, 6.87(*m*, 4H). ^{13}C-NMR (700 MHz, CH_3CN, δ / ppm): (C-OH), δ 173.85, (>C=N)$_{imine}$, δ 166.1, (Ar-C)$_{phenolic}$, δ 119.20, δ 116.68, δ 123.77, δ 148.14, δ 119.58, δ 117.90, δ 119.46, δ 139.44, (Ar-C)$_{benzene}$, δ 162.17, δ 158.17, δ 139.44, δ 151.95, δ 150.79, δ 128.01. ESI-Mass spectra, (*m/z*): calculated for $[C_7H_6NO_2 + H^+]^+$ = 137.0959, $[C_{13}H_{11}NO_2 + H]^+$ = 213.3582, $[C_{14}H_{11}N_2O_3 + H^+]^+$ = 240.2603, $[C_{20}H_{15}N_2O + H^+]^+$ = 332.2365, $[C_{20}H_{16}N_2O_4 + H^+]^+$ = 349.0572, observed 348.352. Combustion analysis for $C_{20}H_{16}N_2O_4$: Calculated C 68.96, H 4.63, N 8.04, O 18.37; found C 68.94, H 4.61, N 8.01, O 18.35.

*[Fe(**L**)Cl(H_2O) (**1**)*

M.p.: 340 °C; Color: light gray, Yield: 0.286 g (62 %); μ_{eff} = 5.43 B.M. Selected infrared absorption (KBr, cm^{-1}): ν(C-H), 2941*s*, ν(HC=N)$_{imine}$, 11618*s*, ν(C=C), 1351*w*, ν(C-O), 1255*m*, ν(C-C), 1190*m*, γ(C-H), 738*w*, ν(M-O), 532*s*, ν(M-N), 432*s*. Electronic spectra (λ_{max} / nm (ε / (mol^{-1} L cm^{-1})) in DMSO: Found: 340(1356); 540(389); 660(101). Molar conductance Λ_m at 25 °C (Ω^{-1} cm^2 mol^{-1}): 3 in DMSO. ESI-Mass spectra, calculated for (*m/z*): calculated for

* Corresponding author. E-mail: sns1963_1@rediffmail.com; ccrl_2004@rediffmail.com

$[C_7H_5FeNO_2 + H^+]^+$ = 191.9625, $[C_7H_7ClFeNO_3 + H^+]^+$ = 245.4582, $[C_{13}H_{11}ClFeNO_3 + H^+]^+$ = 321.5293, $[C_{14}H_{12}ClFeN_2O_3 + H^+]^+$ = 348.5546, $[C_{20}H_{15}ClFeN_2O_4 + H^+]^+$ = 439.1125, $[C_{20}H_{16}ClFeN_2O_5 + H^+]^+$ = 456.2356, observed 455.6494. Combustion analysis for $C_{20}H_{16}ClFeN_2O_5$: Calculated. C 52.72, H 3.54, N 6.15, Cl 7.78, Fe 12.26; found C 52.62, H 3.3.46, N 6.02, Cl 7.68, Fe 12.16.

*[Co(**L**)(H$_2$O)$_2$] (**2**)*

M.p.: >350 °C; Color: light green, Yield: 0.332 g (61 %); μ_{eff} = 4.52 B.M. Selected infrared absorption (KBr, cm^{-1}): *ν*(C-H), 2871*s*, *ν*(HC=N)$_{imine}$, 1583*w*, *ν*(C=C), 1315*s*, *ν*(C-O), 1249*s*, *ν*(C-C), 1180*m*, *γ*(C-H), 750*s*, *ν*(M-O), 532*s*, *ν*(M-N), 434*m*. Electronic spectra (λ_{max} / nm (ε / (mol^{-1} L cm^{-1})) in DMSO: 350(1452); 540(324); 630(48). Molar conductance Λ_m at 25 °C (Ω^{-1} cm^2 mol^{-1}): 3 in DMSO. ESI-Mass spectra, (*m/z)*: calculated for $[C_7H_5CoNO_2 + H^+]^+$ = 195.1798, $[C_7H_9CoNO_4 + H^+]^+$ = 231.2723, $[C_{13}H_{13}CoNO_4 + H^+]^+$ = 307.1128, $[C_{14}H_{14}CoN_2O_5 + 2H^+]^+$ = 349.0572, $[C_{20}H_{17}CoN_2O_5 + H^+]^+$ = 425.0930, $[C_{20}H_{18}CoN_2O_6 + H^+]^+$ = 442.1558, observed 441.2999. Combustion analysis for $C_{20}H_{18}CoN_2O_6$: Calculated. C 54.43, H 4.11, Co 13.35; found C 54.41, H 4.09, N 6.31, Co 13.30.

*[Ni(**L**)(H$_2$O)$_2$] (**3**)*

M.p.: >350 °C; Color: dark green, Yield: 0.362 g (67 %); μ_{eff} = 3.07 B.M. Selected infrared absorption (KBr, cm^{-1}): *ν*(C-H), 2837*s*, *ν*(HC=N)$_{imine}$, 1579*s*, *ν*(C=C), 1315*w*, ν(C-O), 1232*m*, *ν*(C-C), 1132*m*, *γ*(C-H), 765*w*, *ν*(M-O), 538*m*, *ν*(M-N), 455(*m*). Electronic spectra (λ_{max} / nm (ε / (mol^{-1} L cm^{-1})) in DMSO: 370(1262); 410(1449); 550(158). Molar conductance Λ_m at 25 °C (Ω^{-1} cm^2 mol^{-1}): 2 in DMSO. ESI-Mass spectra, (*m/z)*: $[C_7H_5NiNO_2 + H^+]^+$ = 194.8135, $[C_7H_9NiNO_4 + H^+]^+$ = 228.6958, $[C_{13}H_{13}NiNO_4 + H^+]^+$ = 306.6514, $[C_{14}H_{14}NiN_2O_4 + H^+]^+$ = 333.9033, $[C_{20}H_{17}NiN_2O_5 + H^+]^+$ = 424.3259, $[C_{20}H_{18}N_2NiO_6 + H^+]^+$ = 442.2542, observed 441.0601. Combustion analysis for $C_{20}H_{18}N_2NiO_6$: Calculated. C 48.86, H, 4.59, N 7.09, Ni 14.89; found C 48.46, H 4.48, N 6.95, Ni 14.71.

TABLE S-I. FT-IR correlation data of Ligand (**L**) and Complex **2**

Peak assignment	Ligand **L**				Complex **2**			
	Wavenumber, cm^{-1}			Deviation,%	Wavenumber, cm^{-1}			Deviation,%
	Experimental	Theoretical			Experimental	Theoretical		
		Unscaled	Scaled			Unscaled	Scaled	
ν(O-H)$_{Arom}$	3207.73	3239.40	3204.52	0.1	-	-	-	-
ν(C-H)	2874.03	2881.74	2871.15	0.1	2871.39	2884.28	2865.64	0.2
ν(>C=N)	1631.83	1625.98	1630.19	0.1	1583.61	1612.12	1580.44	0.2
ν(C=C)	1365.65	1352.12	1364.28	0.1	1315.50	1345.18	1312.86	0.2
ν(C-O)	1244.13	1266.33	1242.88	0.1	1249.91	1225.41	1178.10	0.2
ν(C-C)	1151.54	1155.83	1150.38	0.1	1180.47	1153.81	1160.68	0.2
γ(C-H)	754.19	755.49	753.43	0.1	750.33	755.82	748.82	0.2
γ(O-H)	659.68	636.36	659.02	0.1	-	-	-	-
ν(M-O)	-	-	-	-	532.37	532.43	531.30	0.2
ν(M-N)	-	-	-	-	434.09	444.35	433.13	0.2

TABLE S-II. DFT ^{1}H-NMR and ^{13}C-NMR correlation data of Ligand (**L**)

Ligand L ^{1}H-NMR				Ligand L ^{13}C-NMR			
Calculated (gas phase), proton No	δ / ppm			Calculated (gas phase), carbon No	δ / ppm		
	Experimental (solid phase)	Calculated (gas phase)			Experimental (solid phase)	Calculated (gas phase)	
		TMS HF[a]	TMS B3[b]			TMS HF[a]	TMS B3[b]
H 41	13.173	12.726	9.010	C7	173.83	179.10	171.58
H 42	9.908	9.725	9.009	C4	166.15	179.09	161.57
H 39	8.806	8.985	8.125	C2	162.17	178.35	160.83
H 40	7.573	7.747	7.031	C22	158.17	177.32	160.80
H 36	7.569	7.746	6.715	C11	151.95	172.15	154.63
H 35	7.166	7.131	6.415	C12	150.79	172.15	154.63
H 38	7.162	7.130	6.415	C6	148.14	161.27	143.75
H 34	6.950	6.952	6.237	C24	134.44	161.27	143.75
H 31	6.948	6.952	6.237	C14	128.01	147.42	129.90
H 30	6.788	6.384	5.669	C15	123.77	147.38	129.86
H 33	6.361	6.384	5.669	C13	119..58	144.48	126.96
H 37	6.359	5.367	4.651	C16	119.46	144.48	126.96
H 39	6.354	5.357	4.641	C5	119.20	144.27	126.75
H 32	2.515	3.109	2.394	C19	117.90	144.24	126.75
H 27	2.506	3.007	2.291	C1	116.68	128.88	115.36
H 28	2.502	2.603	1.888	C23	116.68	128.86	111.34

[a]TMS HF/6-31G(d) GIAO; [b]TMS B3LYP/6-311+G(2d,p) GIAO

TABLE S-III. Mulliken atomic charges of ligand (**L**) and complexes

Ligand **L**		Complex **1**		Complex **2**		Complex **3**	
Atom	Charge, e	Atom	Charge, e	Atom	Charge, e	Atom	Charge, e
C1	-0.028395	C1	-0.279899	C1	-0.322932	C1	-0.306675
N2	-0.278142	N2	-0.230275	N2	-0.249254	N2	-0.218530
H3	0.142925	H3	0.221662	H3	0.221162	H3	0.220057
C4	-0.115112	C4	-0.324478	C4	-0.331823	C4	-0.338667
C5	0.081922	C5	0.325814	C5	0.292318	C5	0.299563
C6	0.081973	C6	0.327865	C6	0.271380	C6	0.276403
C7	-0.115132	C7	-0.324922	C7	-0.346469	C7	-0.346174
C8	-0.146010	C8	-0.237032	C8	-0.246337	C8	-0.243885

Ligand **L**		Complex **1**		Complex **2**		Complex **3**	
Atom	Charge, e	Atom	Charge, e	Atom	Charge, e	Atom	Charge, e
C9	-0.146009	C9	-0.237502	C9	-0.258555	C9	-0.246488
H10	0.166444	H10	0.233980	H10	0.229655	H10	0.233799
H11	0.166443	H11	0.235923	H11	0.237212	H11	0.236210
H12	0.148326	H12	0.240402	H12	0.235141	H12	0.237614
H13	0.148326	H13	0.240126	H13	0.235177	H13	0.237829
N14	-0.278212	N14	-0.294654	N14	-0.319319	N14	-0.274868
C15	-0.028300	C15	-0.294654	C15	-0.399989	C15	-0.350614
H16	0.142904	H16	0.221944	H16	0.220854	H16	0.225315
C17	0.289863	C17	0.336164	C17	0.321346	C17	0.327852
C18	-0.213903	C18	-0.537853	C18	-0.550206	C18	-0.542374
C19	0.254447	C19	0.319527	C19	0.308161	C19	0.315890
C20	-0.025395	C20	0.302496	C20	0.303553	C20	0.303514
C21	-0.124779	C21	-0.343801	C21	-0.365357	C21	-0.353685
C22	-0.178644	C22	-0.390478	C22	-0.390082	C22	-0.392229
H23	0.156160	H23	0.264406	H23	0.253554	H23	0.258561
H24	0.164082	H24	0.231393	H24	0.229525	H24	0.230108
H25	0.169641	H25	0.254307	H25	0.246727	H25	0.249797
C26	-0.212183	C26	-0.526927	C26	-0.536415	C26	-0.534553
C27	0.289440	C27	0.335216	C27	0.326542	C27	0.329656
C28	-0.178308	C28	-0.386583	C28	-0.389225	C28	-0.392594
C29	-0.125144	C29	-0.343783	C29	-0.354769	C29	-0.349727
C30	-0.024687	C30	0.274928	C30	0.280329	C30	0.285695
C31	0.253547	C31	0.293275	C31	0.288878	C31	0.295498
H32	0.155256	H32	0.266886	H32	0.259093	H32	0.259823
H33	0.169622	H33	0.256006	H33	0.251180	H33	0.251036
H34	0.164075	H34	0.234151	H34	0.232076	H34	0.230932
O35	-0.537508	O35	-0.373478	O35	-0.434564	O35	-0.419015
O36	-0.538336	O36	-0.366402	O36	-0.414691	O36	-0.400433
O37	-0.538336	O37	-0.474245	O37	-0.484140	O37	-0.480142
O38	-0.626509	O38	-0.474195	O38	-0.478871	O38	-0.478260
H39	0.366892	H39	0.361192	H39	0.354386	H39	0.358803
H40	0.332135	H40	0.363998	H40	0.357967	H40	0.359064
H41	0.332970	Fe41	0.123313	O41	-0.580976	O41	-0.631998
		O42	-0.625463	H42	0.215423	H42	0.411494
		H43	0.440434	H43	0.48896	H43	0.408144
		H44	0.441293	Co44	0.292168	O44	-0.624676
		CI45	-0.138782	O45	-0.574811	H45	0.438943
				H46	0.458307	H46	0.403533
				H47	0.433172	Ni47	0.240452

TABLE S-IV. Selected natural atomic charges and electronic configurations for the complex **2**

Atoms	Natural atomic charge	Natural electronic configuration
Co44	0.57074	[core]4s(0.26)3d(7.65)4p(0.51)4d(0.02)
N2	-0.47669	[core]2s(1.30)2p(4.15)3p(0.02)

Atoms	Natural atomic charge	Natural electronic configuration
N14	-0.54181	[core]2s(1.29)2p(4.23)3p(0.02)
O35	-0.63188	[core]2s(1.70)2p(4.93)3p(0.01)
O36	-0.61051	[core]2s(1.70)2p(4.90)3p(0.01)
O37	-0.74449	[core]2s(1.70)2p(5.04)3p(0.01)
O38	-0.73920	[core]2s(1.70)2p(5.03)3p(0.01)
C4	-0.21332	[core]2s(0.96)2p(3.24)3p(0.01)
C5	0.12347	[core]2s(0.83)2p(3.03)3p(0.02)
C15	0.04377	[core]2s(0.91)2p(3.02)3p(0.02)
C17	0.33718	[core]2s(0.86)2p(2.79)3p(0.01)
C18	-0.31043	[core]2s(0.98)2p(3.31)3p(0.01)
C26	-0.30943	[core]2s(0.98)2p(3.31)3p(0.02)
C27	0.34945	[core]2s(0.86)2p(2.78)3p(0.01)
C28	-0.28239	[core]2s(0.97)2p(3.29)3p(0.02)
H3	0.18528	1s(0.81)
H10	0.21220	1s(0.79)
H11	0.21549	1s(0.78)
H39	0.48621	1s(0.51)
H43	0.48896	1s(0.46)

TABLE S-V. The second-order perturbation energies$^{(2)}$ corresponding to the most important charge transfer interactions (donor–acceptor) of complex **2** at B3LYP/LanL2DZ//6-31^{++}G(d,p)

Donor Lewis NBO (i)	Acceptor Lewis NBO (j)	Types	$E^{(2)}$ / kcal mol^{-1}	$E_{(j)} - E_{(i)}$ / a.u.	$F_{(i,j)}$ / a.u.
C1−C30	C26−C31	π→π*	2.02	1.18	0.062
C1− C30	C28−C29	π→π*	1.81	1.18	0.059
C1−C30	C29−C30	π→π*	0.58	1.18	0.033
C1−C30	C30−C31	σ→σ*	0.66	1.19	0.035
C4−C5	N2−C5	π→π*	105.65	1.16	0.469
C4− C5	C4−C9	π→π*	1.32	1.08	0.051
C4−C5	C5−C6	π→π*	0.89	1.20	0.044
C4−C9	C4−C5	π→π*	1.80	1.23	0.059
C4−C9	C8−C9	σ→σ*	0.74	1.23	0.038
C4−C9	N2−C5	π→π*	6.98	0.40	0.075
C4−C9	N2−C5	π→π*	1.05	0.89	0.041
C4−C9	C7−C8	π→π*	11.20	0.28	0.072
C5−C6	N2−C5	π→π*	0.99	1.07	0.041
C5−C6	N2−C5	σ→σ*	0.77	0.88	0.040
C5−C6	N2−C5	π→π*	4.73	1.37	0.114
C5−C6	C4−C5	σ→σ*	0.97	1.28	0.045
C5−C6	C6−C7	π→π*	2.34	1.29	0.070
C6−C7	C5−C6	π→π*	2.49	1.38	0.074
C6 −C7	C7−C8	σ→σ*	0.99	1.25	0.045
C7−C8	C8−C9	σ→σ*	0.74	1.23	0.038
C7−C8	C4−C9	π→π*	8.68	0.28	0.064

Donor Lewis NBO (i)	Acceptor Lewis NBO (j)	Types	$E^{(2)}$ / kcal mol^{-1}	$E_{(j)} - E_{(i)}$ / a.u.	$F_{(i,j)}$ / a.u.
C8−C9	C4−C9	σ→σ*	0.77	1.24	0.039
C8−C9	C7−C8	σ→σ*	0.76	1.23	0.039
C15−C20	C18−C19	π→π*	2.02	1.17	0.062
C15−C20	C19−C20	σ→σ*	0.63	1.18	0.034
C15−C20	C20−C21	σ→σ*	0.59	1.18	0.033
C15−C20	C21−C22	π→π*	1.83	1.18	0.059
C15−C20	C21−C22	π→π*	7.17	0.29	0.058
C17−C18	C17−C22	π→π*	1.31	1.26	0.051
C17−C18	C18−C19	σ→σ*	0.92	1.25	0.043
C17−C18	C21−C22	π→π*	11.10	0.29	0.073
C17−C22	C17−C18	π→π*	1.18	1.25	0.048
C17−C22	C21−C22	σ→σ*	0.84	1.26	0.041
C18−C19	C17−C18	σ→σ*	0.96	1.24	0.044
C19−C20	C15−C20	σ→σ*	0.81	1.10	0.038
C19−C20	C18−C19	π→π*	1.29	1.26	0.051
C19−C20	C20−C 21	π→π*	1.44	1.26	0.054
C20−C21	C15−C20	σ→σ*	0.75	1.08	0.036
C20−C21	C19−C20	π→π*	1.71	1.25	0.058
C20−C21	C21−C22	π→π*	0.91	1.25	0.043
C21−C22	C15−C20	π→π*	2.41	1.08	0.064
C21−C22	C17−C22	σ→σ*	0.90	1.24	0.042
C21−C22	C20−C21	σ→σ*	1.09	1.24	0.046
C21−C22	C15−C20	π→π*	13.69	0.23	0.081
C21−C22	C17−C18	π→π*	9.16	0.28	0.067
C26−C27	C26−C31	σ→σ*	0.89	1.25	0.042
C26−C27	C28−C29	π→π*	10.04	0.29	0.069
C26−C27	C30−C31	π→π*	10.50	0.29	0.073
C26−C31	C31−C30	σ→σ*	2.75	1.08	0.069
C26−C31	C26−C27	σ→σ*	0.95	1.24	0.043
C27−C28	C26−C27	π→π*	1.16	1.25	0.048
C27− C28	C28−C29	σ→σ*	0.83	1.26	0.041
C28−C29	C27−C28	σ→σ*	0.89	1.24	0.042
C28−C29	C29−C30	σ→σ*	1.10	1.24	0.047
C28−C29	C26−C27	π→π*	10.52	0.28	0.071
C28−C29	C30−C31	π→π*	8.58	0.29	0.066
C29−C30	C1−N2	π→π*	1.22	1.24	0.049
C29−C30	C1−C30	σ→σ*	0.73	1.08	0.036
C29−C30	C28−C29	σ→σ*	0.90	1.25	0.043
C29−C30	C30−C31	π→π*	1.76	1.25	0.059
C30−C31	C1−C30	σ→σ*	0.81	1.10	0.038
C30−C31	C26−C31	π→π*	1.27	1.26	0.050
C30−C31	C29−C30	π→π*	1.49	1.27	0.055

Donor Lewis NBO (i)	Acceptor Lewis NBO (j)	Types	$E^{(2)}$ / kcal mol^{-1}	$E_{(j)} - E_{(i)}$ / a.u.	$F_{(i,j)}$ / a.u.
C30−C31	C26−C27	π→π*	9.19	0.29	0.065
C30−C31	C28−C29	π→π*	11.02	0.29	0.072
C30−C31	C30−C31	π→π*	0.29	0.29	0.012
LP(1)C1	C30−C31	π→π*	17.52	0.20	0.083
LP(1)N	O36−Co44	π→π*	28.00	0.41	0.135
LP(1)C19	C15−C20	π→π*	98.94	0.09	0.126
LP(1)C19	C17−C18	π→π*	37.97	0.15	0.110
LP*(6)Co44	N2−C5	π→π*	84.91	0.11	0.209
LP*(6)Co44	C4−C5	π→π*	16.57	0.01	0.055
N2−C5	C6	π→π*	157.60	0.04	0.200
C6−N14	C15−C20	π→π*	26.71	0.05	0.052
C15−C20	C21−C22	π→π*	44.80	0.06	0.087

TABLE S-VI. Quantum chemical parameters of compounds

Compounds	Ligand **L**	Complex **1**	Complex **2**	Complex **3**
E_{HOMO} / eV	-5.80954	-5.57444	-5.45526	-5.15538
E_{LUMO} / eV	-1.67919	-2.52899	-1.90585	-2.17551
ΔE / eV	4.13035	3.04545	3.54941	2.97987
Ionization energies, eV	5.80954	5.57444	5.45526	5.15538
Electron affinities, eV	1.67919	2.52899	1.90585	2.17551
Mullikan electronegativity, eV	3.74436	4.05171	3.68055	3.66544
Global hardness, eV	2.06517	1.52272	1.77470	1.48993
Absolute softness, eV	0.48422	0.65671	0.56347	0.67117
Chemical potential, eV	-3.74436	-4.05171	-3.68055	-3.66544
Global softness, eV	0.24211	0.32835	0.28173	0.33558
Global electrophilicity, eV	3.39445	5.39046	3.81654	4.50874
Electronic charge, eV	1.81309	2.66083	2.07389	2.46013
Varial ratio	2.0033	2.0520	2.0459	2.0485
Dipole moment, D	1.9848	10.7733	6.0253	6.9248
E (TD-HF/TD-KS*) / kcal mol^{-1}	-1181.99	-1395.63	-1478.69	-1502.84

*Time dependent Hartree-Fock / Kohn-Sham energies

TABLE S-VII. Geometrically optimized bond lengths of ligand L and complexes

Bond connectivity	Bond length, Å			
	Ligand **L**	Complex **1**	Complex **2**	Complex **3**
C=N (imine)	(C15-N14) 1.293	(C15-N14) 1.287	(C15-N14) 1.288	(C15-N14) 1.288
C=N' (imine)	(C1-N2) 1.293	(C1-N2) 1.289	(C1-N2) 1.289	(C1-N2) 1.289
$C\text{-}C_{(close\ to\ imine\ C)}$	(C21-C22) 1.543	(C21-C22) 1.398	(C21-C22) 1.398	(C21-C22) 1.398
$C\text{-}C'_{(close\ to\ imine\ C)}$	(C28-C29) 1.544	(C28-C29) 1.398	(C28-C29) 1.398	(C28-C29) 1.398
C-O	(C19-O35) 1.428	(C19-O35) 1.434	(C19-O35) 1.433	(C19-O35) 1.433
C-O'	(C31-O36) 1.430	(C31-O36) 1.432	(C31-O36) 1.431	(C31-O36) 1.431
O-H	(O35-H40) 0.960	-	-	-
O-H'	(O36-H41) 0.962	-	-	-

C-N	(C6-N14) 1.474	(C6-N14) 1.455	(C6-N14) 1.458	(C6-N14) 1.458
C-N’	(C5-N2) 1.463	(C5-N2) 1.456	(C5-N2) 1.459	(C5-N2) 1.459
M-N (imine)	-	(M41-N14) 1.888	(M44-N14) 1.879	(M47-N14) 1.879
M-N’ (imine)	-	(M41-N2) 1.889	(M44-N2) 1.884	(M47-N2) 1.884
M-Cl	-	(M41-Cl45) 2.150	-	-
$M\text{-}O_{(coordination)}$	-	(M41-O35) 1.830	(M44-O35) 1.827	(M47-O35) 1.827
$M\text{-}O'_{(coordination)}$	-	(M41-O36) 1.830	(M44-O36) 1.829	(M47-O36) 1.829
$M\text{-}O_{(water)}$	-	(M41-O42) 1.820	(M44-O41) 1.810	(M47-O41) 1.800
$M\text{-}O'_{(water)}$	-	-	(M44-O45) 1.828	(M47-O44) 1.801

TABLE S-VIII. Geometrically optimized bond angles of ligand **L** and complexes

Bond connectivity	Bond angle, °			
	Ligand **L**	Complex **1**	Complex **2**	Complex **3**
∠C-N=C	(∠C6-N14-C15) 119.99	(∠C6-N14-C15) 119.20	(∠C6-N14-C15) 119.89	(∠C6-N14-C15) 119.89
∠C=C-N	(∠C7-C6-N14) 119.99	(∠C7-C6-N14) 125.82	(∠C7-C6-N14) 125.20	(∠C7-C6-N14) 125.20
∠O-C=C	(∠O35-C19-C20) 119.99	(∠O35-C19-C20) 123.84	(∠O35-C19-C20) 123.29	(∠O35-C19-C20) 123.29
∠C-O-H	(∠C19-O35-H40) 109.47	-	-	-
∠M-N=C	-	(∠M41-C14-N15) 125.73	(∠M44-C14-N15) 125.36	(∠M47-C14-N15) 125.36
∠N-M-O	-	(∠N14-M41-O35) 98.19	(∠N14-M44-O35) 98.42	(∠N14-M47-O35) 98.42
∠Cl-M-O	-	(∠Cl45-M41-O35) 89.17	-	-
∠C-N-M	-	(∠C6-N14-M41) 115.06	(∠C6-N14-M44) 114.73	(∠C6-N14-M47) 114.73

TABLE S-IX. Values of the oxygenation constant and of the thermodynamic parameters

Temperature, K	Complex 1			Complex 2		
	K_{O2}/ atm^{-1}	$\Delta H°$ / kJ mol^{-1}	$\Delta S°$ / J mol^{-1} K^{-1}	K_{O2}/ atm^{-1}	$\Delta H°$ / kJ mol^{-1}	$\Delta S°$ / J mol^{-1} K^{-1}
273	11.5	-32.6	-81.2	13.6	-28.3	-78.4
283	5.9	-32.6	-81.2	6.6	-28.3	-78.4
293	2.9	-32.6	-81.2	3.1	-28.3	-78.4
303	1.5	-32.6	-81.2	1.5	-28.3	-78.4

TABLE S-X. DPPH free radical scavenging activity of Schiff base ligand (**L**) and complexes

Compounds	Concentrations, μM			
	0.002	0.004	0.006	0.008
	Free radical scavenging activity, %			
Ascorbic acid	76.33	84.90	87.66	91.62
Ligand (**L**)	33.33	39.00	53.66	65.33

[Fe(**L**)Cl(H_2O)]; **1**	42.66	54.66	68.33	76.00
[Co(**L**)(H_2O)$_2$]; **2**	36.66	42.33	54.66	70.66
[Ni(**L**)(H_2O)$_2$]; **3**	46.33	55.33	69.66	76.33

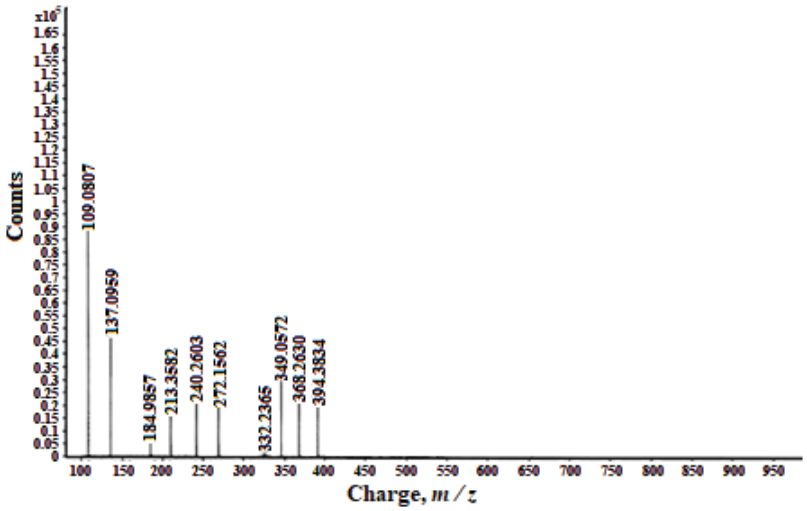

Fig. S-1. ESI-Mass spectrum of ligand **L**.

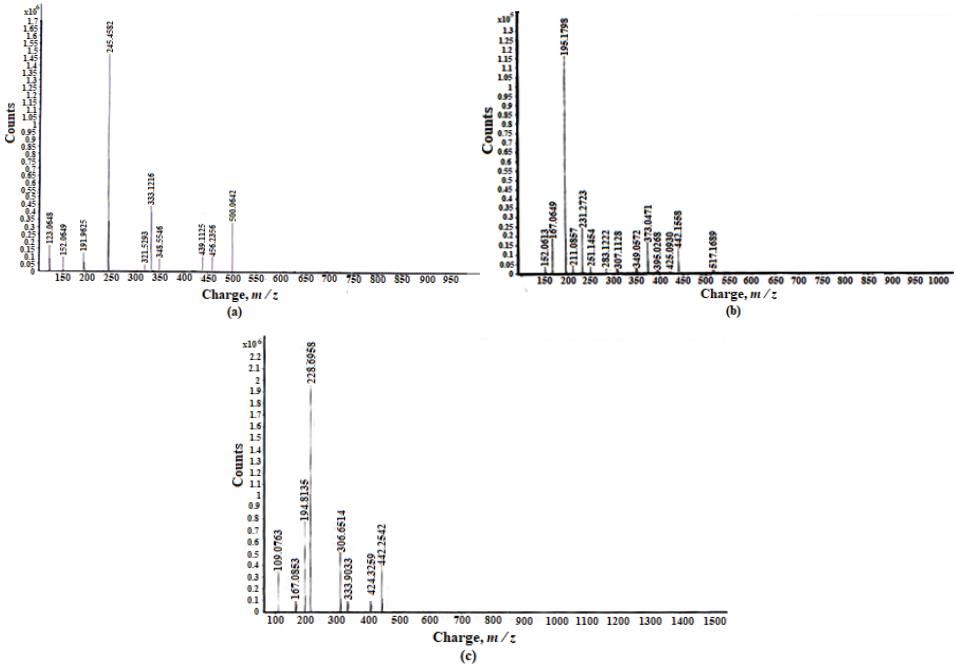

Fig. S-2. ESI-Mass spectrum of (a) complex **1**; (b) complex **2** and (c) complex **3**.

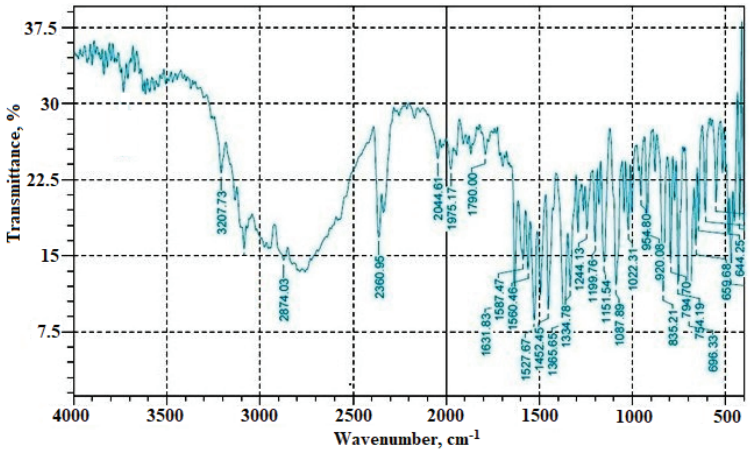

Fig. S-3. Experimental FT-IR spectrum of ligand **L**.

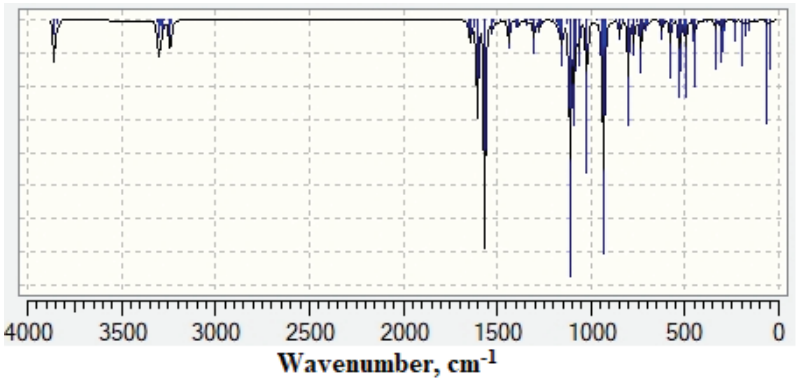

Fig. S-4. Theoretical FT-IR spectrum of ligand **L**.

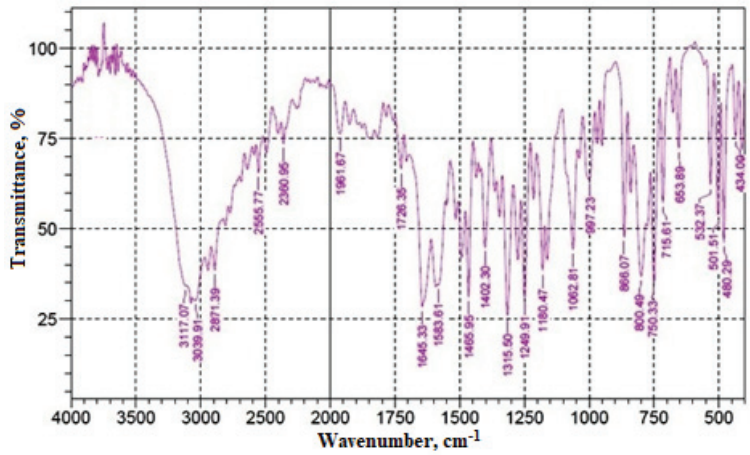

Fig. S-5. Experimental FT-IR spectrum of complex **2**.

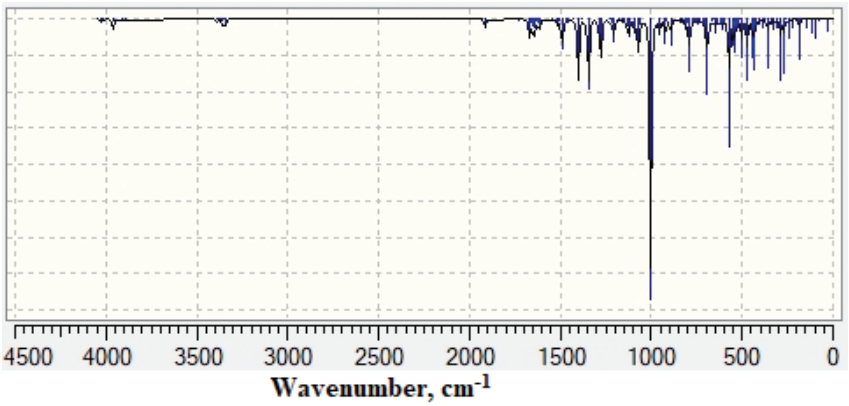

Fig. S-6. Theoretical FT-IR spectrum of complex **2**.

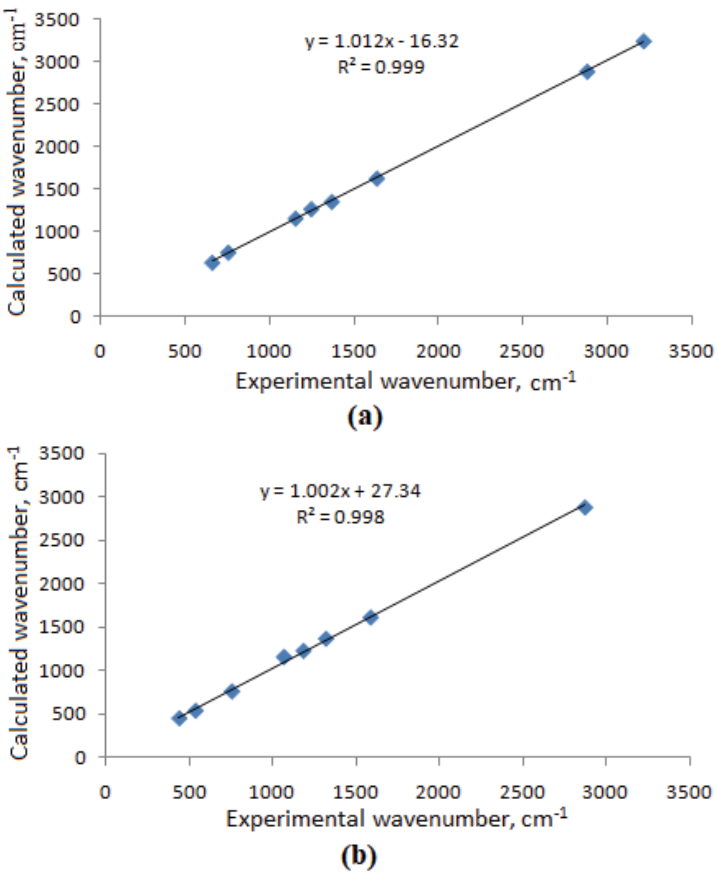

Fig. S-7. FT-IR correlation graphs of (a) ligand and (b) complex **2**.

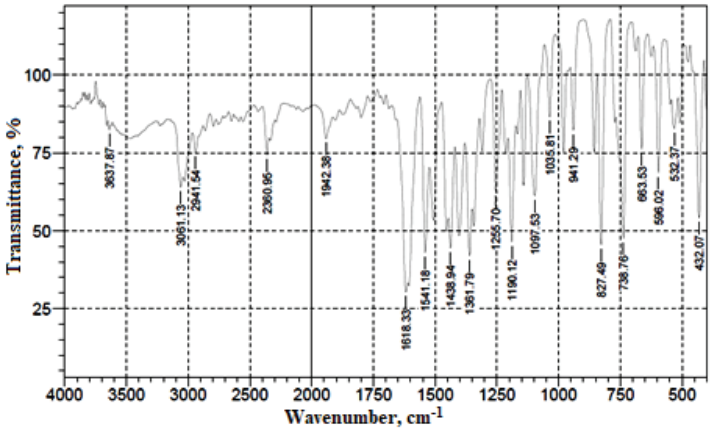

Fig. S-8. Experimental FT-IR spectrum of complex **1**.

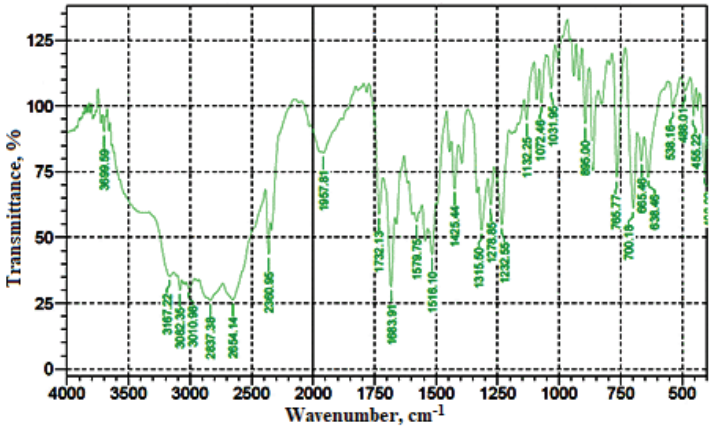

Fig. S-9. Experimental FT-IR spectrum of complex **3**.

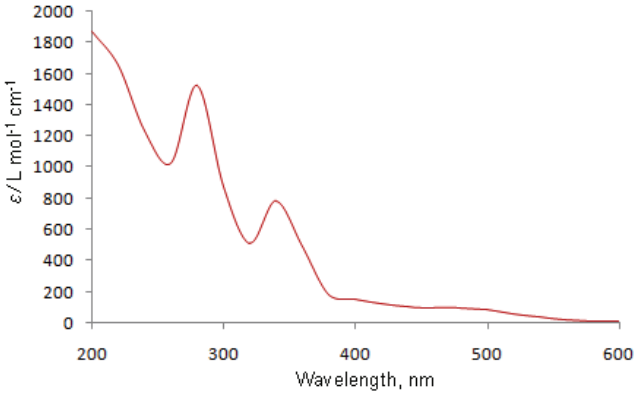

Fig. S-10. UV–Vis spectrum of Ligand **L**.

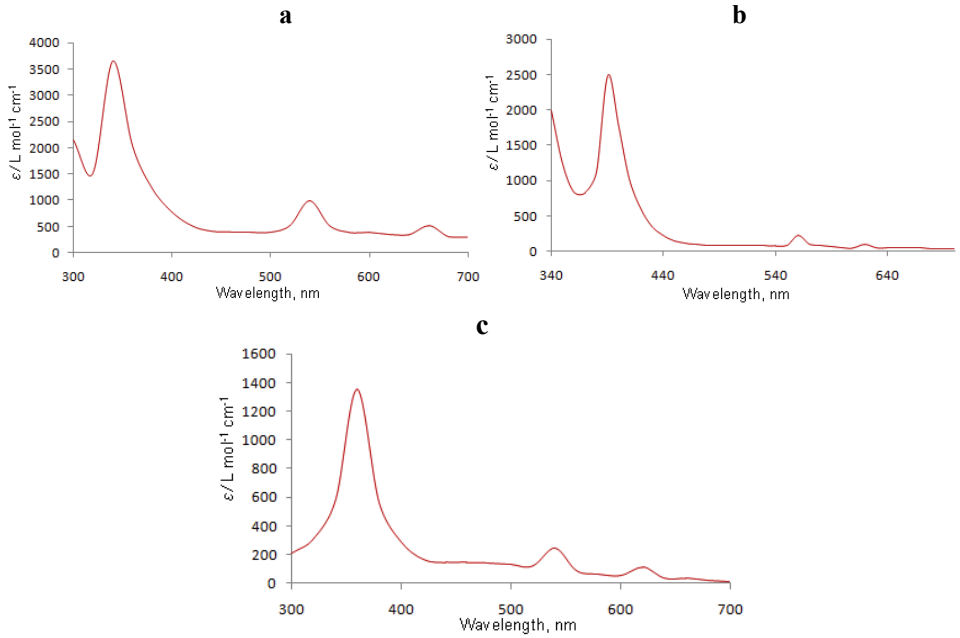

Fig. S-11. UV-Vis spectrum of: (a) complex **1**; (b) complex **2** and (c) complex **3.**

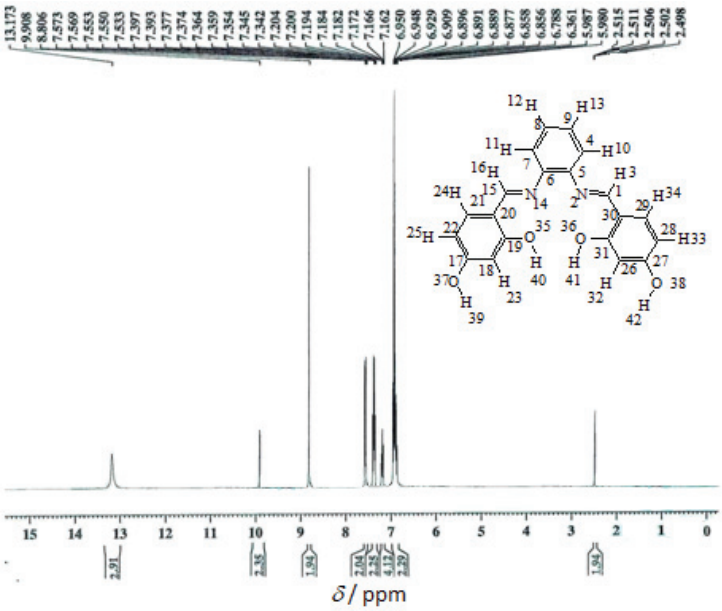

Fig. S-12. ^{1}H-NMR spectrum of Ligand **L**.

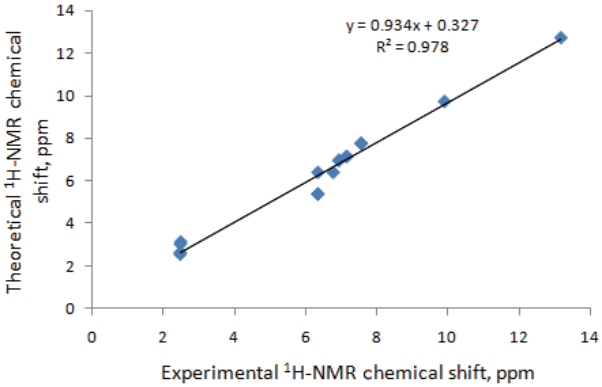

Fig. S-13. ^{1}H-NMR correlation graph of Ligand **L**.

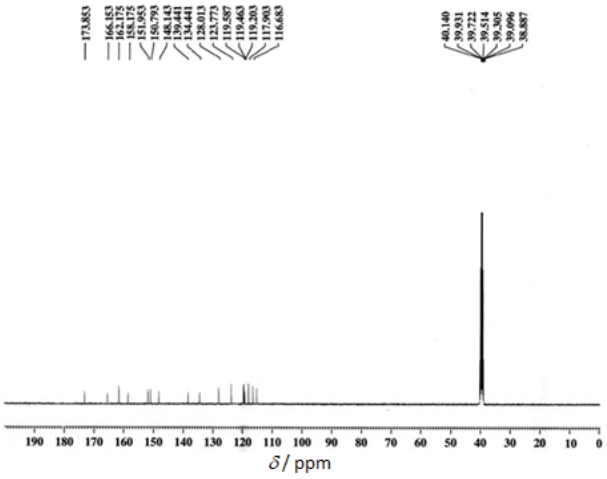

Fig. S-14. ^{13}C-NMR spectrum of Ligand **L**.

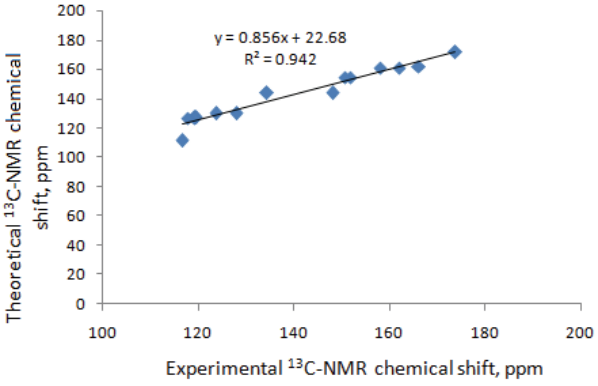

Fig. S-15. ^{13}C-NMR correlation graph of Ligand **L**.

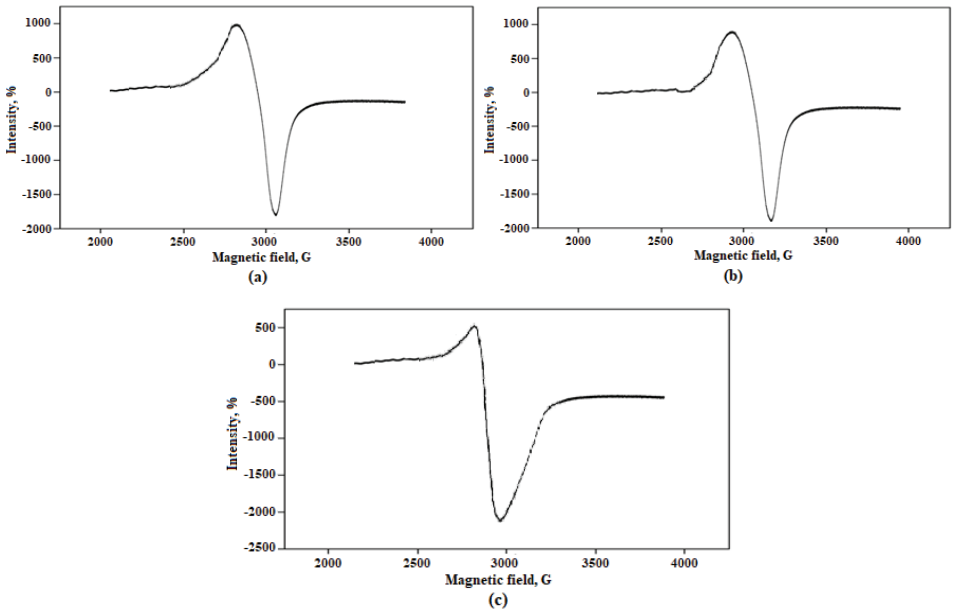

Fig. S-16. EPR spectrum of: (a) complex **1**; (b) complex **2** and (c) complex **3**.

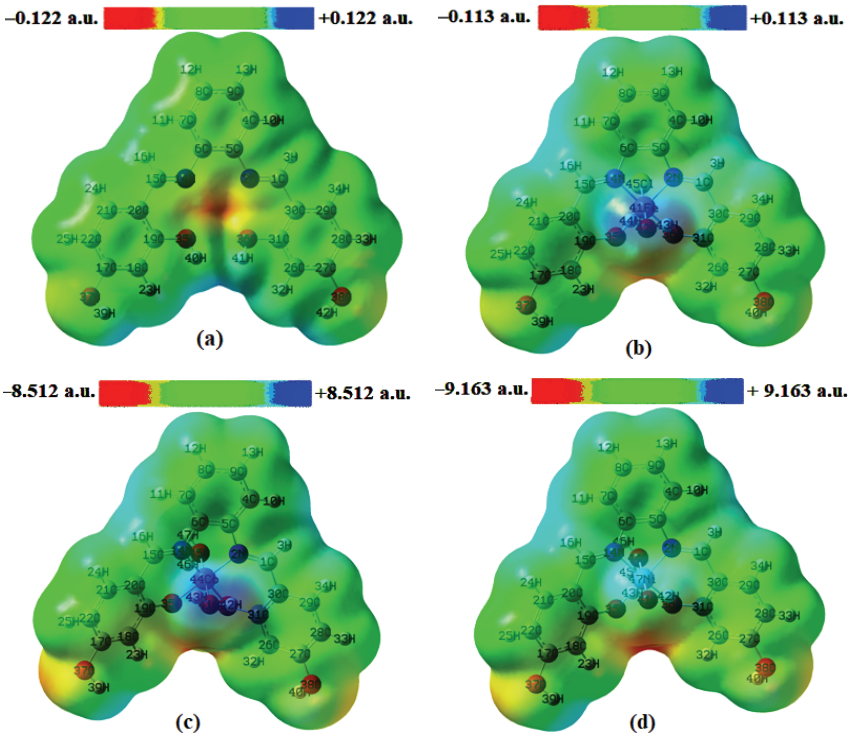

Fig. S-17. MEP of Ligand **L** (a) and complexes (b-d).

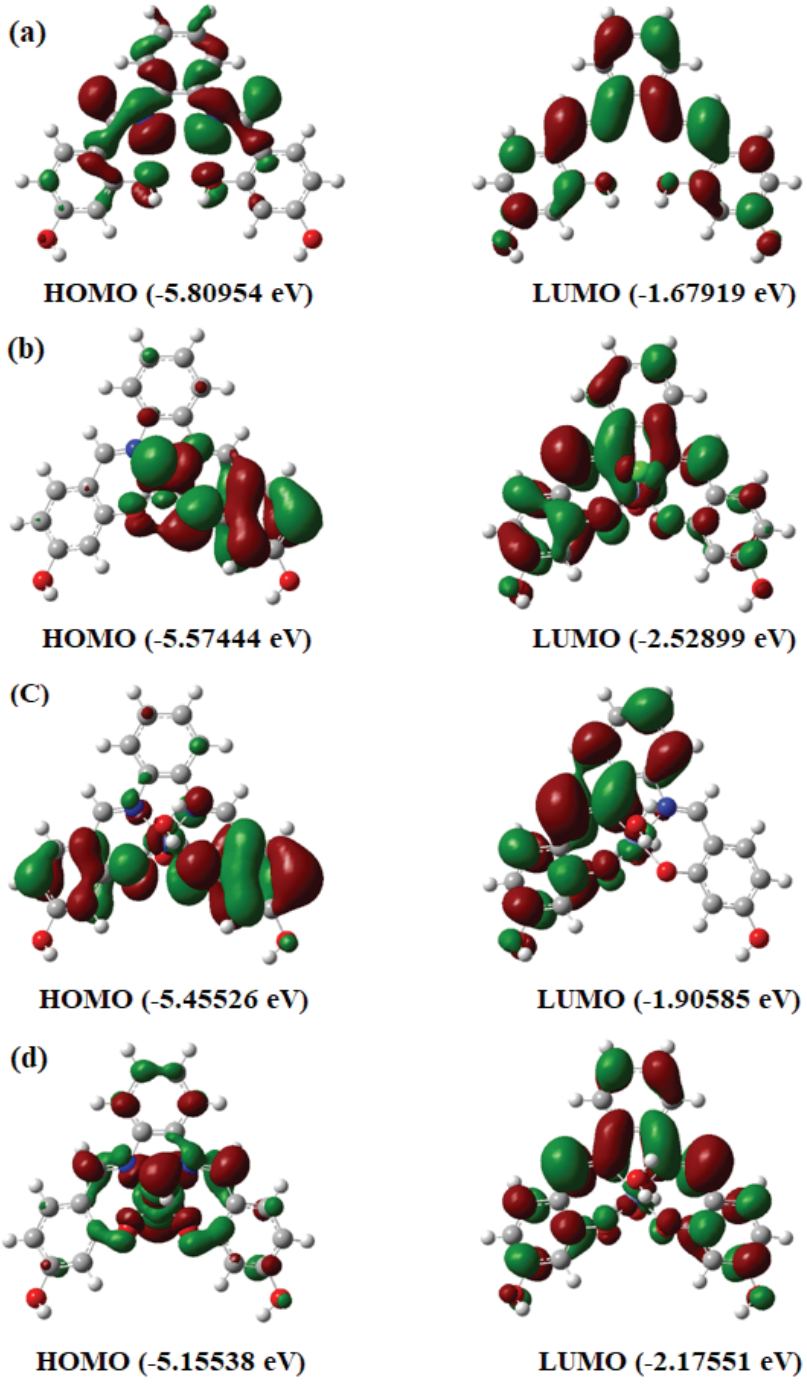

Fig. S-18. Energy level diagram of Ligand **L** (a) and Complex**es** (b-d).

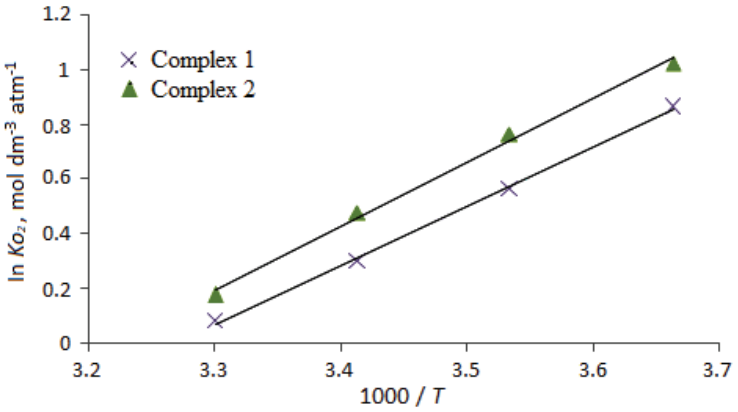

Fig. S-19. Van't Hoff diagrams for the complex **1** and **2**.

Journal of the Serbian Chemical Society
JSCS@tmf.bg.ac.rs • www.shd.org.rs/JSCS
J. Serb. Chem. Soc. *86* (10) 955–969 (2021)
JSCS–5475
Original scientific paper
Published 10 September 2021

Photodegradation kinetics of organophosphorous with hydroxyl radicals: Experimental and theoretical study

SEYDA AYDOGDU[1], ARZU HATIPOGLU[1]*, BAHAR EREN[2] and YELDA YALCIN GURKAN[2]

[1]*Yıldız Technical University, Department of Chemistry, 34220 Istanbul, Turkey and* [2]*Tekirdag Namık Kemal University, Department of Chemistry, 59030 Tekirdag, Turkey*

(Received 9 April, revised 28 June, accepted 29 June 2021)

Abstract: The presence of organophosphorus compounds (OPs) in the environmental counterparts has become an important problem because of their toxicity. In this study, the photocatalytic degradation reactions of the three OPs with hydroxyl radical were investigated by both experimental and quantum chemical methods. Photocatalytic degradation kinetics of the examined organophosphorus compounds were investigated under UV-A irradiation using TiO_2 as the photocatalyst. The effects of the initial concentrations on the degradation rate have been examined. There was an observable loss of OPs in the presence of TiO_2 photocatalyst under UV-A at 0.2 g TiO_2 per 100 mL. The quantum chemical calculations have been carried out by the density functional theory (DFT) at B3LYP/6-31g(d) level. The reaction pathways were modelled to find the most probable mechanism for OPs with the OH radical and to determine the primary intermediates. The rate constants of the eight reaction paths were calculated by the transition state theory. Conductor-like polarizable continuum model (CPCM) was used as the solvation model with the intention of understanding the water effect. The theoretical results were in agreement with experimental ones.

Keywords: UV-light; TiO_2; heterogenous catalysis; DFT; CPCM.

INTRODUCTION

Organophosphorous (OP) compounds are structurally characterized as esters or thiols derived from phosphoric, phosphonic, phosphinic or phosphoramidic acid.[1] They are mainly used as pesticides, lubricating agent, fuel additives and as warfare agents.[2] They are also used to synthesize the plasticizers.[3] The OP's mechanism of action depend on their binding properties to the enzyme acetylcholinesterase at the nerve synapse in order to inhibite the hydrolysis of the neurotransmitter acetylcholine.[4] Because of the effective properties of them as

* Corresponding author. E-mail: hatiparzu@yahoo.com
https://doi.org/10.2298/JSC210409056A

the pesticides, OPs are used in the worldwide extensively.[5] the recent studies have demonstrated that only the 1 % of utilized OP compounds from the 4 million tones of used pesticides had reached the targed pest, and the rest of them distrubuted in the different environmental parts.[6] Unfortunately, due to the widespread use, OP compunds have been detected in water, soil, even in the fruits and vegetables.[7] It has been determined that the amount of OP in water is up to 506.6 μg L^{-1}.[8] OPs pose serious threats to human health with harmful effects such as cytotoxicity, immunotoxicity, genotoxicity, and the joint effect of different OPs may become seriously toxic to health.[9] In order to protect the public health, it is important to find effective methods of removing them from the environment.

In recent years, there are many methods used to eliminate organic contaminants in water.[9] The advanced oxidation process (AOP) is the most important one of these methods. The main mechanism of this method is generating highly reactive radicals such as hydroxyl (•OH) or sulfate radicals. The most reactive one is •OH, which reacts with contaminants unselectively and fast. Their reaction is the dominant removal process of the contaminants in aquatic environment.[4] Several researchers have studied the OP degradation with using AOPs. In some works, different parameters and newly prepared photocatalyst materials effect on the degradation reactions of OP compounds have been invesitigated. These studies have demonstrated the pozitive effects of increasing temperature and TiO_2 efficiency under UV irradiation light as a photocatalysis on the degradation of OP compounds.[9–11] In the literature, there are also some studies that related the understanding of reaction mechanism and the detections of the intermediates of these reactions. With these studies, reserarchers have tried to determine the toxicity of intermediates of OP compounds degradation reactions during the different AOP process. In these studies it has been found that the toxicities of transformation intermediates can be even more dangerous than the parent compounds.[3,4,8,12,13] Though there are lots of studies about the degradation of OP compounds, it is still very limited to fully understand their reaction mechanism.

One alternative to experimental methods are the quantum chemical calculations. It is important to know the position of a radical attack on an organic molecule and how it will react.[14] However, it is difficult to find out which atom in the molecule the radical will attack by only experimental methods.[15] The quantum chemical calculations are suitable for deciding a reaction path and determining the transition states and products of the reaction by providing the correct potential energy surface.[16,17] In literature, there are some theoretical research studies on the degradation reaction of the OP with the •OH. In these studies, it has been showed that the hydrogen atom abstraction from the α carbon atom is a feasible reaction pathway.[5,16–18] To the best of our knowledge, there are no studies performed on the photo-oxidative degradation reactions of dimethyl dimethyl phosphoramidate (DDMP), diethyl phosphoramidate (DEP) and isopro-

phyl phosphorous (ISPC). The molecular structure of DDMP, DEP and ISPC are shown in the Fig. 1.

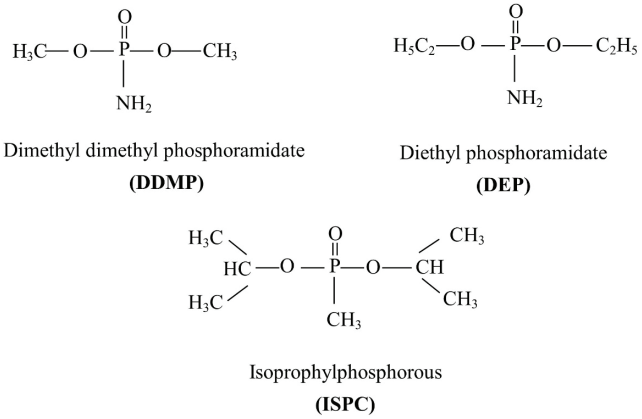

Fig. 1. Molecular structures of studied OPs.

In the experimental part of this study, the photodegradation kinetics of three OPs namely dimethyl dimethyl phosphoramidate (DDMP), diethyl phosphoramidate (DEP) and isoprophylphosphorous (ISPC) have investigated in aqueous TiO_2 suspensions under UV irradition. In the theoretical part, the calculations for all possible reaction paths have been performed by the quantum chemical density functional theory (DFT). Based on the results, the rate constants of the reactions were estimated by the transition state theory.

EXPERIMENTAL

Experimental methods

Materials. TiO_2 Degussa P25 grade with a particle size of about 21 nm and a surface area of 50 m^2 g^{-1} was used as the photocatalyst without further treatment. Degussa P25 powder, which is a mixture of anatase and rutile phases (79 % anatase, 21 % rutile) is one of the photocatalysts with high activity and has been used as a standard TiO_2 reference material. The high activity is due to a synergistic effect between the two nanocrystalline phases.[19] The OP molecules was purchased from Merck. All the chemicals that were used in the experiments were of laboratory reagent grade and used as received without further purification. The solutions were prepared with doubly distilled water.

Photocatalytic activity experiments. The performance of the OP molecules were assessed on TiO_2 by carrying out the photocatalytic degradation reactions. The photocatalytic activity experiments were carried out in a constant temperature batch-type photoreactor. 16×8 W blacklight fluorescent lamps were used as the light source. In the experiments, a stock solution of OP molecules, at a concentration of 10^{-2} mol L^{-1}, was used. The suspension was prepared by mixing definite volumes of this solution containing the desired amount of OP molecules with TiO_2 Degussa P25. The suspension was agitated in an ultrasonic bath for 15 min in the dark before introducing it into the photoreactor. The volume of the suspension was 600 mL. The amount of the photocatalyst used was 0.2 g/100 mL, which was determined as the corres-

ponding optimum photocatalyst concentration. The suspension was stirred mechanically throughout the reaction period in order to prevent TiO_2 particles from settling. Owing to continuous cooling, the temperature of the reaction solution was 22±3 °C. All the samples, each 10 mL in volume were taken intermittently for analysis. The samples were then filtered through 0.45 μm cellulose acetate filters (Millipore HA WG04751). Before analyzing, all the solutions were wrapped by aluminum foil and kept in the dark. The concentration of OP molecules were measured by a UV–Visible spectrophotometer (Perkin Elmer Lambda 25) at 318 nm which was the wavelength of maximum absorption of OP molecules. The calibration curves were prepared for a concentration range $(1.0–10.0)\times10^{-5}$ mol L^{-1}. In the experiments, the pH of the reaction solution decreased slightly. For 100 min of degradation the change in the pH was ±0.3, which did not affect the wavelength of maximum absorption in the UV spectrum of OP molecules.

Computational methodology

The geometry optimizations of the reactants, the product radicals, the pre-reactives and the transition state complexes were determined with the density functional theory (DFT) within the Gaussian 09 package.[20] The DFT calculations were performed by B3LYP method which combines HF and Becke exchange term with Lee–Yang–Parr correlation functional with 6-31G(d) level.[21,22] All the reactants, pre-reactive complexes and products confirmed as the stationary point with zero imaginary frequency. Whereas the transition states complexes were analyzed to be first order saddle points with the one negative eigenvalue that belong to the reaction coordinate by the frequency calculations. The forming O–H bond was chosen as the reaction coordinate for the determination of the transition states complexes for the OP + OH reactions. Intrinsic reaction coordinate (IRC) analysis were also carried out to prove the transition states really connected to expected reactants and the products.[23] In order to investigate the water effect the conductor-like polarizable continuum model (CPCM) was used. In this method, solute is placed in a cavity that surrounded by a polarizable continuum of solvent.[24]

Rate constants of the reactions were calculated by using transition state theory (TST) for 273.15 K:

$$k = \frac{k_B T}{h} \frac{q_{TS}}{q_{OH} q_{OP}} e^{-E_a/RT} \quad (1)$$

In this equation, k_B is Boltzman constant, h is Plank constant, E_a is the activation energy and q's are the molecular partition functions of reactants and transition states.[25] Each of the molecular partition functions are the products of translational, rotational, vibrational and electronic partition functions of all species. The overall rate constant of all investigated molecules reactions were obtained by the sum of all reaction path's rate constant.

RESULTS AND DISCUSSION

Experimental results

In this study, photocatalytic degradation reactions of OP molecules in aqueous TiO_2 suspensions were examined. When TiO_2, an n-type semiconductor, is irradiated with UV radiation, an electron from valence band (VB) jumps to the conduction band (CB), creating an electron–hole pair. Electron–hole pairs which formed in this way, can initiate oxidation and reduction reactions on the surface

of TiO_2. In aqueous suspension systems, holes react with surface –OH groups and generate •OH. •OH is very reactive to OPs and degrades them.[26]

Kinetics of DDMP, DEP and ISPC

Fig. 2 shows the disappearance kinetics of DDMP, DEP and ISPC from an initial concentration of 10^{-4} mol L^{-1} under three conditions. In non-irradiated suspensions, there was a slight loss of three OPs, ~1.0 %, due to the adsorption onto TiO_2 particles. However, in the presence of TiO_2, a rapid degradation of all of the studied OPs occurred by irradiation. The concentration change amounts to 83 and 90 % after irradiating for 90 min for DDMP and ISPC, respectively. For the DEP molecule the concentration change amounts to 87 % after irradiating for 100 min.

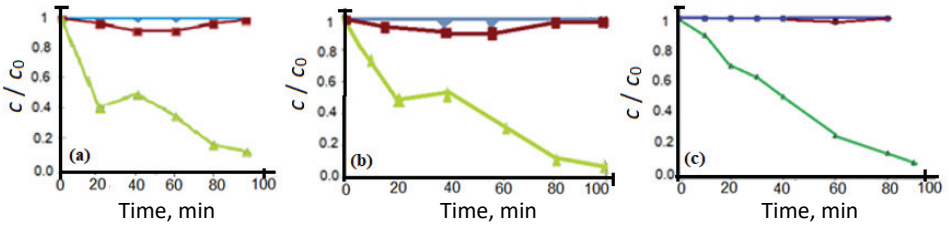

Fig. 2. Kinetics of the photocatalytic degradation of: a) DDMP, b) DEP and c) ISPC; (♦) photolysis, (■) adsorption in the dark, (►) photocatalysis.

The semilogarithmic plots of concentration data gave a straight line. The correlation constant for the fitted line for DDMP, DEP and ISPC were, r = = 0.9963, 0.9788 and 0.9821, respectively. This finding indicates that the photocatalytic degradation of OPs in aqueous TiO_2 suspensions can be described by the first-order kinetic model, $\ln c = -kt + \ln c_0$, where c_0 is the initial concentration and c is the concentration of the DDMP, DEP and ISPC at time t, respectively. Under the experimental conditions used, as explained above, the rate constant k for the degradation of DDMP, DEP and ISPC was calculated to be $(2.89\pm0.006)\times10^{-8}$, $(1.78\pm0.008)\times10^{-7}$, $(1.56\pm0.003)\times10^{-10}$ min^{-1}, respectively.

Catalyst and initial concentration effect

The effect of the catalyst on the degradation rate is shown in Fig. 3. As the concentration of TiO_2 increased, the rate of degradation also increased up to a certain value of catalyst, then begined to decrease slowly. The maximum degradation was obtained at 0.2 g $(100\ mL)^{-1}$ TiO_2 concentration.

The initial concentration has a significant effect on the photocatalytic degradation rate, so the concentrations of OPs have been studied in the range 6-14 10^{-5} mol L^{-1}. The experimental results are presented in Fig. 4 and Table I, together with the correlation coefficients for each of the fitted lines. The results show that the degradation rate depends on the initial OPs concentrations. The rate

constant *k* increases with increase in the initial concentration of DDMP, DEP and ISPC. This finding indicates that the degradation kinetics of OPs is not of simple first order but pseudo-first order.

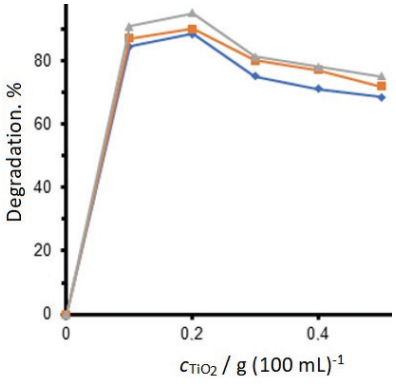

Fig. 3. The effect of TiO_2 concentration on the degradation rate, (♦) DDMP, (■) DEP, (▲) ISPC.

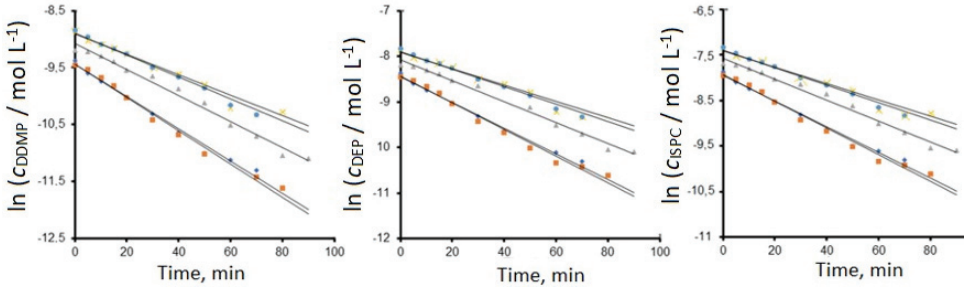

Fig. 4. Effect of the initial concentration on the degradation rate of DDMP, DEP and ISPC; (♦) 6×10^{-5}, (■) 8×10^{-5}, (►)10×10^{-5}, (**x**) 12×10^{-5}, (●) 14×10^{-5} mol L^{-1}.

TABLE I. Apparent first-order rate constants *k* and correlation constant *r* for the photocatalytic degradation of OPs

Parameter	Initial concentration, 10^{-5} mol L^{-1}				
	6.0	8.0	10.0	12.0	14.0
	DDMP				
k / 10^{-8} min^{-1}	2.152±0.001	2.274±0.005	2.893±0.006	2.650±0.002	2.493±0.003
r	0.9914	0.9865	0.9963	0.9813	0.9943
	DEP				
k / 10^{-7} min^{-1}	1.353±0.004	1.462±0.006	1.784±0.008	1.672±0.005	1.550±0.001
r	0.9763	0.9811	0.9788	0.9877	0.9987
	ISPC				
k / 10^{-10} min^{-1}	1.390±0.009	1.431±0.008	1.561±0.003	1.514±0.001	1.481±0.006
r	0.9836	0.9916	0.9821	0.9614	0.9878

As can be seen from Table I, there was a slight increase in the reaction rate as the initial concentration increased from 6×10^{-5} to 8×10^{-5} mol L^{-1}. However,

there was an observable increase in the reaction rate as the concentration increased from 8×10^{-5} to 1×10^{-4} mol L^{-1}.This indicated that the photodegradation degradation reaction occurs in solution as well as on the surface of TiO_2 particles. So, the initial concentration of OPs increases, the number of active sites on the TiO_2 surface decreases and the reaction rate changes accordingly.

Computational results

•OH is a strong electrophilic radical and it reacts with organic molecules directly.[27] It has a strong oxidizing potential with the value of E (OH/H_2O) = 2.8 V. •OH and OPs reactions occur mainly in two ways. The first one, the radical is able to abstract hydrogen from C–H and N–H bonds to form the water molecule. The second one, radical can make an addition to P=O bond.[28] In a previous study, it was found that the radical addition of organophosphorus to the P=O bond was not favourable because of the high activation energy.[29,30] Thus, in this study only hydrogen abstraction reactions of •OH were taken into consideration.

DDMP+•OH reaction

DDMP+•OH degradation reaction pathways can take place with hydrogen abstraction from methyl groups, as shown in Fig. 5, where all the hydrogen atoms of the methyl group bonded to the same C atom are equivalent.

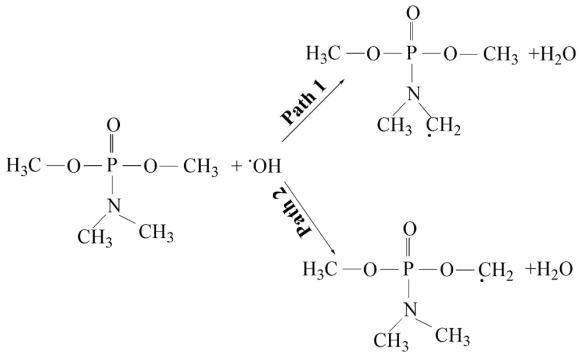

Fig. 5. Possible reaction pathways of the DDMP with •OH.

Pre-reactive complexes have important for the reaction mechanism due to the energies of the reactants. These complexes have weak van der Waals bonds. Such pre-reactive complexes affect the energy barrier of the reaction and the cleavage energies of its products as well as the kinetics.[27,31]

The structural geometries all of the pre-reactive complexes are given in Fig. 6. In DDMP+•OH reaction two different pre-reactive complexes could occurr. As it can be seen in the Fig. 6 for the PR1-DDMP structure, the oxygen atom of the hydroxyl radical approached the one of the hydrogen atom of the methyl group of DDMP molecule with the distance of 2.755 Å and the hydrogen atom of the

hydroxyl radical pointed toward the oxygen of DDMP molecule with the distance of 1.895 Å. These distances for PR2-DDMP were 2.398 and 1.806 Å, respectively. The angle of hydroxyl radical approaching to the DDMP molecule was almost 80.20° in both PR1-DDMP and PR2-DDMP.

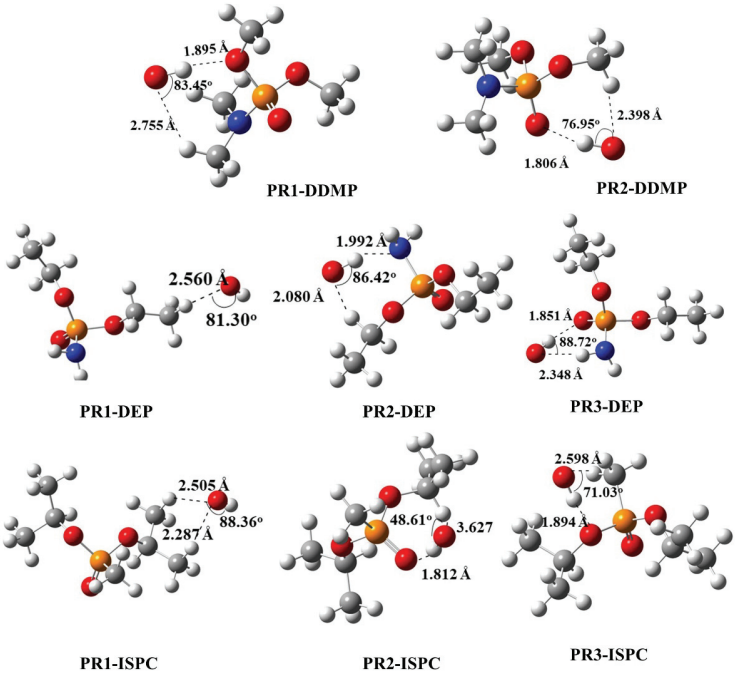

Fig. 6. The optimized structures of pre-reactive complexes at the B3LYP/6-31g(d) level.

There are two transition states for this reaction, TS1-DDMP and TS2-DDMP. The optimized geometries and the main geometrical parametres of transtion states are given in the Fig. 7. As it can be seen in the Fig. 7, the major structural changes in the transition states of DMMP geometry for the breaking of the C–H bond was elongated, whereas the others stayed same. The elongation of breaking bond length of TS1-DDMP and TS2-DDMP were 0.143 and 0.106 Å, respectively. So TS1-DDMP is the early transition state. The C–O bond is of a critical length for the formation of the of the TS complex along the reaction coordinate. The C–O bond lengths of TS1 DDMP and TS2-DDMP were 1.44 and 1.40 Å, respectively. The shortening of C–N and C–O bond lengths of TS1 and TS2 were 0.028 and 0.006 Å, respectively.

The relative energies of the DDMP and reaction are given with Fig. 8. The energies of the TS complexes were 4.39 and 3.06 kcal* mol^{-1} for gas and aqueous phase, respectively, as it can be seen in Fig. 8.

* 1 kcal = 4184 J

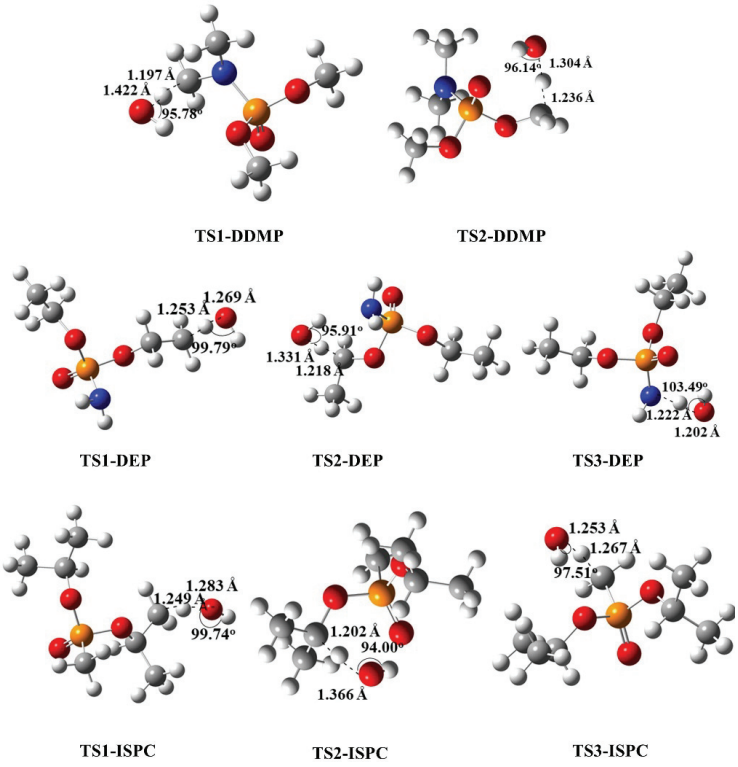

Fig. 7. The optimized structures of transition states complexes at the B3LYP/6-31g(d) level.

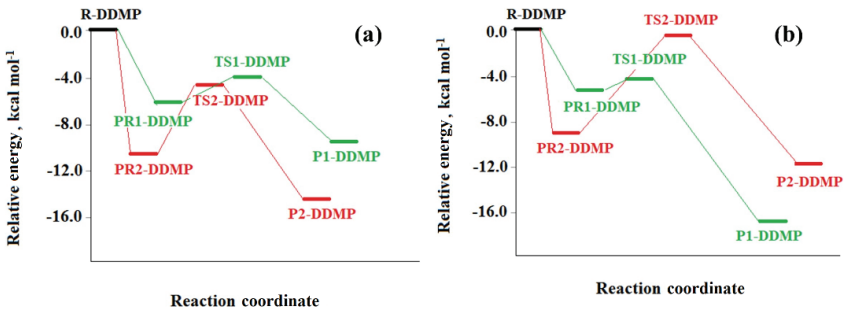

Fig. 8. Relative energies calculated at the B3LYP/6-31g(d) level of the reaction for DDMP+•OH: a) gas phase; b) aqueous medium.

In the aqueous phase the energies of TSs were decreased by around 7.98 kcal mol^{-1} for TS1-DDMP and 6.47 kcal mol^{-1} for TS2-DDMP in the gas phase. Thus, TS1 was the thermodynamically more stable complex (see Fig. 8). The energies of reactants, pre-reactive complexes, transition states and products for the all of the degradation reactions are given in the Supplementary material tothis paper, as Tables S-I–S-III for both gas and aqueous phases.

The reaction heats of all the reactions are given in the Table II for both gas and aqueous phases, and both of reaction paths are exothermic. It may be concluded that Path 1 was the more probable reaction path, with the higher exothermicity for both phases. The values in Table II showed that the activation energy of Path 1 was 6.91 and 6.38 kcal mol^{-1} lower than the Path 2, for the gas and aqueous phase, respectively. However, water has a stabilizing effect in terms of the energy barriers in aqueous solution. Energy barrier decreased 0.78 kcal mol^{-1} in aqueous solution.

TABLE II. Calculated activation energies, reaction heats and rate constants of the reactions at the B3LYP/6-31g(d) level

Path	Gas			Aqueous		
	E_a kcal mol^{-1}	ΔH kcal mol^{-1}	k cm^3 molecule^{-1} s^{-1}	E_a kcal mol^{-1}	ΔH kcal mol^{-1}	k cm^3 molecule^{-1} s^{-1}
			DDMP			
Path 1	1.32	–18.34	1.73×10^{-8}	0.81	–17.00	1.43×10^{-7}
Path 2	8.23	–14.34	2.32×10^{-14}	7.19	–12.59	3.02×10^{-12}
Overall			1.73×10^{-8}			1.43×10^{-7}
			DEP			
Path 1	3.01	–10.91	3.15×10^{-7}	4.70	–9.39	1.43×10^{-10}
Path 2	2.67	–17.62	2.53×10^{-10}	2.01	–16.20	2.49×10^{-10}
Path 3	9.78	–8.37	2.54×10^{-14}	9.39	–5.76	5.92×10^{-14}
Overall			3.15×10^{-7}			3.92×10^{-10}
			ISPC			
Path 1	3.86	–10.80	1.26×10^{-8}	3.36	–9.32	2.86×10^{-10}
Path 2	2.60	–18.45	1.12×10^{-10}	1.77	–17.30	4.19×10^{-10}
Path 3	9.33	–11.01	1.88×10^{-14}	8.91	–9.56	2.96×10^{-14}
Overall			1.27×10^{-8}			7.05×10^{-10}

DEP+•OH reaction

There are three different abstractable hydrogen atoms for the DEP molecule, two from ethoxy groups and one from amino group. The reaction paths of DEP with •OH can be seen in Supplementary Fig. S-1.

There are three different pre-reactive complexes in these reaction, PR1-DEP, PR2-DEP and PR3-DEP. The optimized structures of pre-reactive complexes can be seen in the Fig. 6. •OH approached to the DEP molecule with the an angle 85.48°, which was almost the same for all three pre-reactive structures. The distances of oxygen of hydroxyl radical and hydrogen atom that were abstracted were 2.560, 2.080 and 2.348 Å for PR1-DEP, PR2-DEP and PR3-DEP, respectively.

There are three transition states for the reaction of DEP with •OH. The optimized structures of transition states TS1-DEP, TS2-DEP, TS3-DEP can be seen in Fig. 7. The distances between the oxygen atom of •OH and hydrogen of DEP

molecule were 1.269, 1.331 and 1.222 Å for TS1-DEP, TS2-DEP, TS3-DEP, respectively. According to the Hammond's Postulate, TS2-DEP was an early transition state with 0.348 Å, which is a higher elongation of occuring bond value.[32] The calculated reaction enthalpies are listed on Table II. As seen in Table II, second reaction path was the one that prevailed with the highest exothermicity. For this reaction, the potential energy diagrams are given in Supplementary Fig. S-2 for both phases. As seen in the diagrams that the energy values of transition state structures were lower than those for the reactants for both phases, excluding TS1-DEP. This transition state's energy was approximately 3 kcal mol^{-1} higher than reactants because of steric effect. The energy decreased for TS2- DEP and TS3- DEP were 4.29 kcal mol^{-1} for gas and 3.35 kcal mol^{-1} for DEP+•OH reaction. Comparing these three paths, Path 2 had the lowest activation energy, which was compatible with the thermodynamic results of the three reaction paths.[33–35]

ISPC+•OH reaction

The degradation reaction paths of ISPC with •OH are given in Suplementary Fig. S-3. In this reaction, by the nature of the ISPC structure, hydroxyl radical could abstract three different hydrogen atoms. Thus, this reaction has three different reaction paths.

The pre-reactive complexes PR1-ISPC, PR2-ISPC and PR3-ISPC structures are given in Fig. 6. Among the pre-reactive complexes PR1-ISPC and PR3-ISPC are capable of forming a six-membered ring, while PR2-ISPC has the ability to form a seven-membered ring. This is the reason for the relative stability of these pre-reactive complexes compared to the reactant complexes. The oxygen of •OH approached to one of the hydrogen atoms of ISPC with the distances of 2.505, 3.627 and 2.598 Å for PR1-ISPC, PR2-ISPC and PR3-ISPC, respectively.

Depending on the •OH approach to ISPC, three different chemically activated transition states TS1-ISPC, TS2- ISPC and TS3- ISPC were determined. As displaced in Fig. 7, for all the transition states, •OH approached to the hydrogen atom with the angle, 99.74, 94.00 and 97.51° TS1-ISPC, TS2-ISPC and TS3--ISPC, respectively. Shortening of C–O bond in TS2-ISPC structure was 0.012 Å. There were also slight elongations of breaking bond, by around 0.109–0.175 Å, for all the transition state complexes. As can be seen in Fig. 7, among the all transition states, the longest O–H occurring bond length belonged to TS2-ISPC, while TS1-ISPC and TS3-ISPC have much lower as bond length when compared to TS2-ISPC, so, TS2-ISPC was an early transition state. The relative potential energy *versus* reaction coordinate diagrams for gas and aqueous phases are given in Supplementary Fig S-4. As seen in the diagrams, the energy values of transition state structures were higher than reactants for both phases excluding TS2--ISPC. This may be due to the branched structure of the ISPC. This transition

state complex were 9.14 and 5.56 kcal mol^{-1} lower than the reactants for gas and aqueous phases, respectively. The energies of the transition states were around 7.34 kcal mol^{-1} lower in the aqueous phase than in the gas phase. This can be attributed to the hydrogen bonds between ISPC and water molecules. Thus, the hydrogen bonding effect reduces the energies of these species. As can be seen from the Table II, the reaction paths were all exothermic and Path2 was the most exothermic one. This indicated that Path2 was the most probable hydrogen abstaction reaction from the ISPC with the lowest activation energy. This result is consistent with Zhou *et al*. result.[18]

Rate constants

The rate constant of all the studied reactions were given in the Table II. The calculated rate constants in Table II show that the highest rate constant belongs to DEP + •OH reaction. The rate constants were in the order $k_{DEP} > k_{DDMP} > k_{ISPC}$ for gas phase while in the aqueous medium order is $k_{DDMP} > k_{ISPC} > k_{DEP.}$ The calculated rate constants showed that DDMP + •OH reaction proceeded slightly faster in aqueous medium in comparison to the gas phase. However, DEP+•OH and ISPC+•OH reaction rates decreased in aqueous solution. The reason may be attributed to their branched structure and the steric effect caused by it. Due to these structures, water molecules can have a weakening effect and the attack of the •OH radical to DEP and ISPC molecules in the aqueous environment can be sterically prevented.

As it can be seen in Table II, the reaction enthalpy change values are in agreement with the activation energies. For the DDMP+•OH reaction, the enthalpy change value and the activation energy of path 1 is lower (more exothermic) and this reaction pathway is faster than Path 2. There are 3 reaction pathways in the DEP+•OH and ISPC+•OH reactions. Of these paths, the most exothermic one is path 2 for both reactions. These pathways have the lowest activation energy and are the fastest in the aqueous medium. Whereas, in the gas phase the sequence is different. Though the Path 2 has the smallest activation energy for DEP and ISPC molecules' degradation reactions, they are not the fast ones. This may be attributed to the structure of the molecules. As can be seen in Fig. 6, for Path 1, it is easier to abstract the hydrogen atom at the end of the molecule. In Path 2, it is more difficult to abstract the hydrogen atom due to the steric hindrance. However, due to the branched structure, the hydrogen which should be abstracted in Path 2 is forming hydrogen bonds with neighboring atoms so it is difficult to abstract it.

CONCLUSION

In this work, the degradation kinetics of DDMP, DEP and ISPC were investigated both experimentally and theoretically. The photocatalytic degradation of DEP, DDMP and ISPC was investigated in aqueous TiO_2 suspensions with UV

light. The best degradation rate was obtained at 10^{-4} mol L^{-1} initial concentration with UV/TiO_2. The experimental results indicated that the maximum degradation of DDMP, DEP and ISPC is due to photocatalysis at 0.2 g/100 mL TiO_2 concentration. Based on the DFT calculations results, the weakly bonded prereactive complexes were important for the degradation reactions because they were reducing the energy barrier. It has been found that the presence of a dielectric medium such as water has a stabilizing effect that reduces the total energy for this reaction system. The calculated rate constants show that for all of the reactions the rate decreases with the effect of hydrogen bonds in aqueous medium.

SUPPLEMENTARY MATERIAL

Additional data and informationare available electronically at the pages of journal website: https://www.shd-pub.org.rs/index.php/JSCS/article/view/10637, or from the corresponding author on request.

Acknowledgement. The authors of this research has greatfully acknowledgemented to financially support of Tekirdag Namık Kemal University Research Project with the project number of NKUBAP.01.GA.18.164.

ИЗВОД

КИНЕТИКА ФОТОДЕГРАДАЦИЈЕ ОРГАНОСФОСФОРНИХ ЈЕДИЊЕЊА СА ХИДРОКСИЛ РАДИКАЛИМА: ЕКСПЕРИМЕНТАЛНО И ТЕОРИЈСКО ИСПИТИВАЊЕ

SEYDA AYDOGDU[1], ARZU HATIPOGLU[1], BAHAR EREN[2] и YELDA YALCIN GURKAN[2]

[1]*Yıldız Technical University, Department of Chemistry, 34220 Istanbul, Turkey и* [2]*Tekirdag Namık Kemal University, Department of Chemistry, 59030 Tekirdag, Turkey*

Присуство органофосфорних једињења (OF) у природи је важан проблем због њихове токсичности. У овом раду испитиване су реакције фотокаталитичке разградње три OF са хидроксил-радикалима експерименталним и квантохемијским методама. Кинетика фотокаталитичке разградње OF је испитивана применом UV-A зрачења и TiO_2 фотокатализатора. Испитивани су ефекти почетних концентрација на брзину разградње. Детектовано је смањење концентрације OF у присуству TiO_2 фотокатализатора при осветљавању са UV-A зрачењем при 0,2 g TiO_2/100 mL. Квантохемијски прорачуни су извршени применом теорије функционала густине (DFT) на B3LYP/6-31g(d) нивоу. Реакције су моделоване да би се одредио највероватнији механизам деградације OF са $^{\bullet}$OH и примарни интермедијери. Константе брзина осам реакција су израчунате помоћу теорије прелазног стања. *Conductor-like polarizable continuum model* (CPCM) је коришћен као солватациони модел да би се објаснио ефекат воде. Резултати теоријских разматрања су у сагласности са резултатима добијеним експерименталним методама.

(Примљено 9. априла, ревидирано 28. јуна, прихваћено 29. јуна 2021)

REFERENCES

1. M. B. Clovic, D. Z. Krstic, T. D. Lazerevic-Pasti, A. M. Bondvic, V. M. Vasic, *Curr. Neuropharmacol.* **11**(3) (2013) 315 (https://pubmed.ncbi.nlm.nih.gov/24179466/)
2. M. Lily, A. K. Chandra, *J. Fluor. Chem.* **175** (2015) 185 (https://doi.org/10.1016/j.jfluchem.2015.04.019)

3. H. Laversin, A. El Masri, M. Al Rashidi, E. Roth, A. Chakir, *Atmos. Environ*. **126** (2016) 250 (https://doi.org/10.1016/j.atmosenv.2015.11.057)
4. A. M. Parker, Y. Lester, E. M. Spangler, U. Gunten, K. G. Linden, *Chemosphere* **182** (2017) 477 (https://doi.org/10.1016/j.chemosphere.2017.04.150)
5. Q. Zhang, X. Qu, W. Wang, *Environ. Sci. Technol.* **41** (2007) 6109 https://pubmed.ncbi.nlm.nih.gov/17937289)
6. Y. Zhou, Z. Yang, H. Yang, C. Zhang, X. liu, *J. Mol. Model.* **23** (2017) 139 (https://doi.org/10.1007/s00894-017-3277-0)
7. L. Zhang, B. Li, X. Meng, L. Huang, D. Wang, *Environ. Sci. Pollut. Res.* **22** (2015) 15104 (https://doi.org/10.1007/s11356-015-4669-2)
8. W. Li, Y. Zhao, X. Yan, J. Duan, C. P. Saint, S. Beecham, *Chemosphere* **234** (2019) 204 (https://doi.org/10.1016/j.chemosphere.2019.06.058)
9. S. Agarwal, I. Tyagi, V. Kumar Gupta, M. H. Dehghani, A. Bagheri, K. Yetilmezsoy, A. Amrane, B. Heibati, S. Rodriguez-Couto, *J. Mol. Liq.* **221** (2016) 1237 (https://doi.org/10.1016/j.molliq.2016.04.076)
10. A. Almalraj, A. Pius, *J. Water Process. Eng.* **7** (2015) 94 (https://doi.org/10.1016/J.JWPE.2015.06.002)
11. C. Wu, K. G. Linden, *Water Res.* **44** (2010) 3585 (https://doi.org/10.1016/j.watres.2010.04.011)
12. A. Ozcan, Y. Sahin, M. A. Oturan, *Water Res.* **47** (2013) 1470 (https://doi.org/10.1016/j.watres.2012.12.016)
13. E. Evgenidou, I. Konstantinou, K. Fytianos, T. Albanis, *J. Hazard. Mater.* **137** (2006) 1056 (https://doi.org/10.1016/j.jhazmat.2006.03.042)
14. Q. Mei, J. Sun, D. Han, B. Wei, Z. An, X. Wang, J. Xie, J. Zhan, M. He, *Chem. Eng. J.* **373** (2019) 668 (https://doi.org/10.1016/j.cej.2019.05.095)
15. M. B. Kralj, P. Trebse, M. Franko, *Trends Anal. Chem.* **26** (11) (2007) 1020 (https://doi.org/10.1016/j.trac.2007.09.006)
16. J. Dang, L. Ding, X. Sun, Q. Zhang, W. Wang, *Struct. Chem.* **25** (2014) 275 (https://doi.org/10.1007/s11224-013-0287-0)
17. Y. Bao, C. Zhang, W. Yang, J. Hu, X. Sun, *Sci. Total Environ.* **419** (2012) 144 (https://doi.org/10.1016/j.scitotenv.2012.01.004)
18. Q. Zhou, X. Sun, R. Gao, J. Hu, *Atmos. Environ.* **45** (2011) 3141 (https://doi.org/10.1016/j.scitotenv.2014.10.081)
19. P. Bouras, E. Stathatos, P. Lianos, *Appl. Catal., B* **73** (2007) 51 (https://doi.org/10.1016/j.apcatb.2006.06.007)
20. *Gaussian 09, Revision A.02*, Gaussian, Inc., Wallingford, CT, 2009
21. A. D. Becke, *J. Chem. Phys.* **98** (1993) 5648 (https://doi.org/10.1063/1.464913)
22. C. Lee, W. Yang, R. G. Parr, *Phys. Rev., B* **37** (1988) 785 (https://doi.org/10.1103/physrevb.37.785)
23. C. Gozalez, H. B. Schlegel, *J. Phys. Chem.* **94** (1990) 5523 (https://doi.org/10.1021/j100377a021)
24. D. C. Young, *Computational Chemistry*, 2nd ed., John Wiley & Sons, Inc., New York, 2001
25. I. N. Levine, *Physical Chemistry*, 6th ed., Mc Graw Hill Higher Education, New York, 2009
26. N. Sam, A. Hatipoğlu, G. Koçtürk, Z. Çınar, *J. Photochem. Photobiol., A* **146** (2002) 189 (https://doi.org/10.1016/S1010-6030(01)00620-7)

27. A. Hatipoglu, D. Vione, Y. Yalçın, C. Minero, Z. Çınar, *J. Photochem. Photobiol., A* **215** (2010) 59 (https://doi.org/10.1016/j.jphotochem.2010.07.021)
28. Y. Zhou, X. Liu, W. Jiang, Y. Shu, *J. Mol. Model.* **24** (2018) 44 (https://doi.org/10.1007/s00894-018-3580-4)
29. C. Li, S. Zheng, J. Chen, H. Xie, Y. Zhang, Y. Zhao, Z. Du, *Chemosphere* **201** (2018) 557 (https://doi.org/10.1016/j.chemosphere.2018.03.034)
30. Ş. Aydoğdu, A. Hatipoğlu, *J. Indian Chem. Soc.* **96** (2019) 1117
31. N. Mora-Diez, R. J. Alvarez-Idaboy, R. J. Boyd, *J. Phys. Chem., A* **105** (2001) 9034 (https://doi.org/10.1021/jp011472i)
32. B. S. Hammond, *J. Am. Chem. Soc.* **77** (1955) 334 (https://doi.org/10.1021/ja01607a027)
33. E. A. Kozlova, P. G. Smirniotis, A. V. Vorontsov, *J. Photochem. Photobiol., A* **162** (2004) 503 (https://doi.org/10.1016/S1010-6030(03)00392-7)
34. A. V. Vorontsov, D. V. Kozlov, P. G. Smirniotis, V. N. Parmon, *Kinet. Catal.* **46** (2005) 189 (https://doi.org/10.1007/s10975-005-0067-y)
35. B. Yang, Y. Wang, J. Shu, P. Zhang, W. Sun, N. Li, Y. Zhang, *Chemosphere* **138** (2015) 966 (https://doi.org/10.1016/j.chemosphere.2014.12.039).

Journal of the Serbian Chemical Society
JSCS@tmf.bg.ac.rs • www.shd.org.rs/JSCS
J. Serb. Chem. Soc. 86 (10) S241–S243 (2021) *Supplementary material*

SUPPLEMENTARY MATERIAL TO

Photodegradation kinetics of organophosphorous with hydroxyl radicals: Experimental and theoretical study

SEYDA AYDOGDU[1], ARZU HATIPOGLU[1]*, BAHAR EREN[2] and YELDA YALCIN GURKAN[2]

[1]*Yıldız Technical University, Department of Chemistry, 34220 Istanbul, Turkey and* [2]*Tekirdag Namık Kemal University, Department of Chemistry, 59030 Tekirdag, Turkey*

J. Serb. Chem. Soc. 86 (10) (2021) 955–969

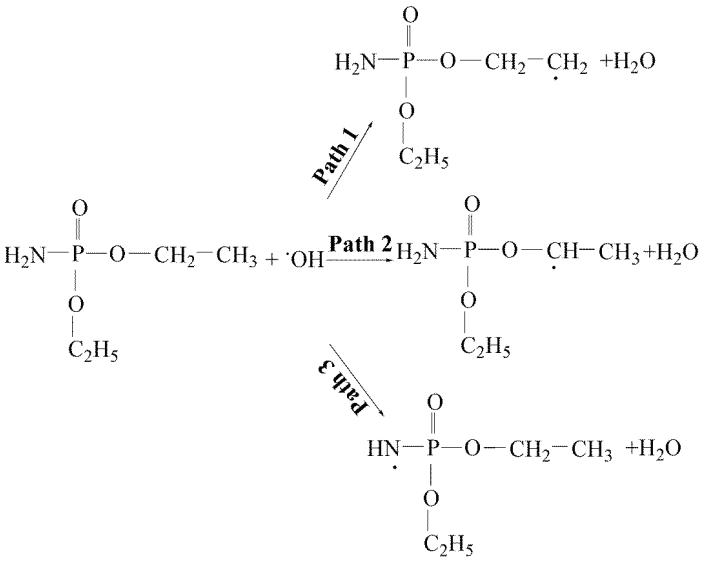

Fig. S-1. Possible reaction pathways of the DEP with •OH.

* Corresponding author. E-mail: hatiparzu@yahoo.com

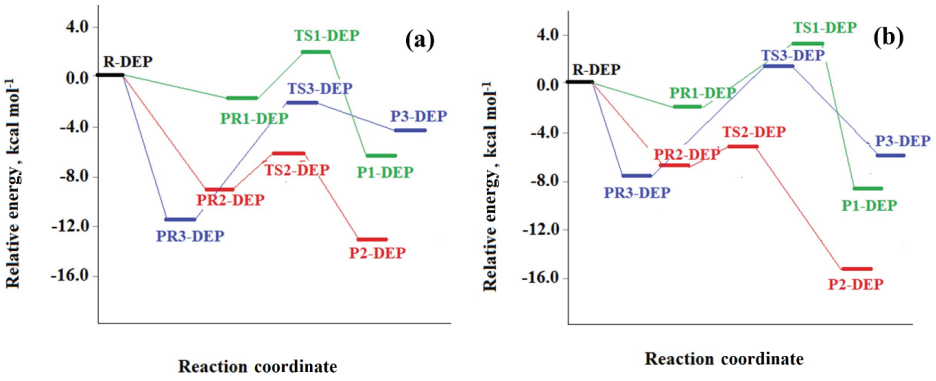

Fig. S-2. Relative energies of the reaction for DEP+•OH: a) gas phase, b) aqueous medium.

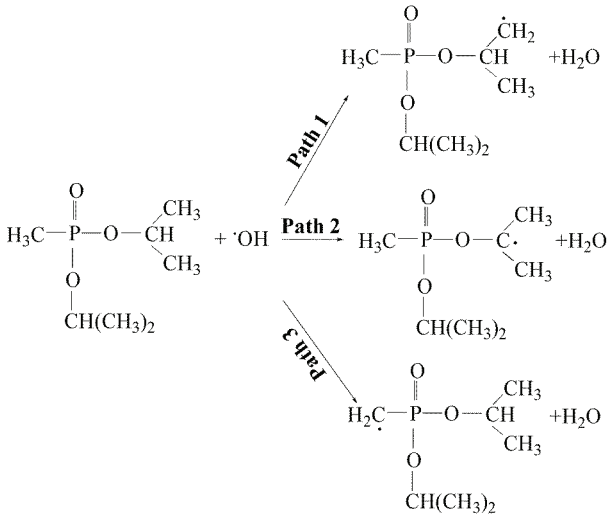

Fig. S-3. Possible reaction pathways of the ISPC with •OH.

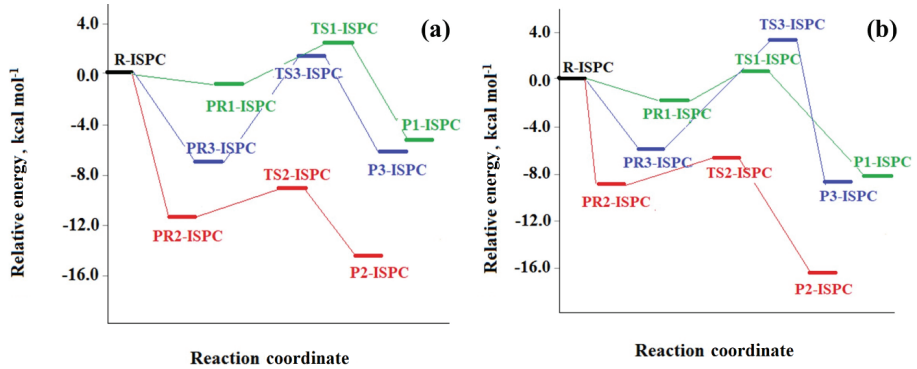

Fig. S-4. Relative energies of the reaction for ISPC+ •OH: a) gas phase, b) aqueous medium.

TABLE S-I. Energies of reactants, prereactive complexes, transition states and products for DDMP + •OH reaction

Molecule	E_h / Ha	
	Gas	Aqueous
DDMP+•OH	-857.2071	-857.2207
TS1	-857.2156	-857.2284
TS2	-857.2125	-857.2228
PR1	-857.2177	-857.2297
PR2	-857.2256	-857.2343
P1	-857.2305	-857.2471
P2	-857.2238	-857.2340

TABLE S-II. Energies of reactants, prereactive complexes, transition states and products for DEP + •OH reaction

Molecule	E_h / Ha	
	Gas	Aqueous
DEP+•OH	-857.2272	-857.2455
TS1	-857.2225	-857.2404
TS2	-857.2378	-857.2533
TS3	-857.2303	-857.2431
PR1	-857.2301	-857.2479
PR2	-857.2420	-857.2565
PR3	-857.2459	-857.2581
P1	-857.2378	-857.2588
P2	-857.2493	-857.2694
P3	-857.2346	-857.2540

TABLE S-III. Energies of reactants, prereactive complexes, transition states and products for ISPC +•OH reaction

Molecule	E_h / Ha	
	Gas	Aqueous
ISPC+•OH	-919.8349	-919.8445
TS1	-919.8175	-919.8287
TS2	-919.8232	-919.8367
TS3	-919.8390	-919.8473
PR1	-919.8324	-919.8429
PR2	-919.8309	-919.8474
PR3	-919.8440	-919.8600
P1	-919.8321	-919.8485
P2	-919.8349	-919.8445
P3	-919.8175	-919.8287

Journal of the Serbian Chemical Society
JSCS@tmf.bg.ac.rs • www.shd.org.rs/JSCS
J. Serb. Chem. Soc. *86* (10) 971–982 (2021)
JSCS–5476
Original scientific paper
Published 10 September 2021

Sodium ion chemosensor of 3-oxo-3*H*-benzo[*f*]chromene-2--carboxylic acid: An experimental and computational study

JAMALUDIN AL-ANSHORI*, ANDI RAHIM, AJAR FAFLUL ABROR, IKA WIANI HIDAYAT, TRI MAYANTI, MUHAMMAD YUSUF, JULIANDRI JULIANDRI and ACE TATANG HIDAYAT

Department of Chemistry, Faculty of Mathematics and Natural Sciences, Universitas Padjadjaran, Jl. Raya Jatinangor km.21 Bandung-Sumedang, Jatinangor, 40133, Indonesia

(Received 29 September 2020, revised 5 March, accepted 23 March 2021)

Abstract: A fluorescence compound with the typical skeleton of benzocoumarin was synthesized and its interaction with various metal ions was evaluated. The synthesis was performed *via* Knoevenagel condensation whereas identification of the product was accomplished by various spectroscopic techniques. The chemosensor test against representative metal ions was monitored by fluorescence spectrophotometry. A density functional theory calculation (DFT, functional/basis set; M06/6-31G (d, p)) was also performed to clarify the experimental results and to confirm the mechanism of interaction. 3-Oxo-3*H*-benzo-[*f*]chromene-2-carboxylic acid **1** was obtained as a yellow solid in 60 % chemical yield. Melting point; 235.6–236.7 °C and λ_{max} UV/Vis, λ_{em} and Stokes shift (MeOH, nm) of 374, 445 and 71 nm, respectively. The structure of the compound was identified based on spectroscopic data and literature comparison. Compound **1** exhibited a chelation quenched fluorescence (CHQF) phenomenon selectively toward the Na^+, with a binding stoichiometry (1:2) and *LoD* and *LoQ* of 0.14 and 0.48 mg/L, respectively. Based on DFT calculations, compound **1** chelated Na^+ through mechanism of oxidative (1:1 equivalent) and reductive (2:1 equivalent) photoinduced electron transfer (PET), correspondingly.

Keywords: benzocoumarin; fluorescence; CHQF; DFT; PET.

INTRODUCTION

Discovering new ion sensors and molecular recognition has gained increased consideration due to their prospective applications in analytical chemistry, life science, catalysis and environmental monitoring.[1–6] In particular, the ion fluorescence sensing based technique shows more prominent features than other methods, such as AAS,[7] ICP spectroscopy,[8,9] analysis based on neutron

* Corresponding author. E-mail: jamaludin.al.anshori@unpad.ac.id
https://doi.org/10.2298/JSC200929022A

activation,[10] chromatography,[11] voltammetry[12] and others[13–15] as it conserves inherent sensitivity and selectivity, low cost, handiness, spatial and temporal monitoring with instant response times.[16] Among various metal ions, sodium is predominantly attractive to current researchers, as it is one of the most abundant metals in the environment and in biology, playing critical ecological and physiological roles. To the best of our knowledge, Na^+ chemosensors based on such fluorescence platforms as BODIPY,[17] rhodol,[18] anthracene and azo,[19] ether and aza crown derivatives,[20] indole,[21] benzophosphole,[22] and calix[4]arene[23] have all been explored. A relatively unexplored class of fluorescent platform for sodium ion sensing is benzocoumarin which has better photophysical properties than basic coumarin.[24] Furthermore, the synthetic pathway is simple and straightforward through Pechmann,[25] and Knoevenagel[26] condensation. Accordingly, a known fluorescent benzocoumarin-type compound was synthesized and its chemosensory properties against sodium ion reported for the first time. In addition, a computational study of the chemosensor was performed herein.

EXPERIMENTAL

Materials and methods

P. a. grade chemicals, purchased from Sigma–Aldrich and Merck, were used. All glassware apparatus was oven-dried prior to use. ^{1}H- and ^{13}C-NMR spectra were obtained on Agilent 500 and 126 MHz spectrometers, respectively, in DMSO-d_6. The NMR signals were referenced to the residual peak of the (major) solvent. The deuterated solvents were stored over activated 3 Å molecular sieves (8–12 mesh) under dry N_2. UV/Vis absorption spectra and their molar absorptivity were measured on a Shimadzu 8400 UV/Vis spectrometer with matched 1.0 cm quartz cells. The spectra were recorded over 0.1 nm interval data. Emission spectra were recorded on an automated Fluorescence Agilent G9800A Cary Eclipse spectrometer in 1.0 cm quartz fluorescence cuvettes at 25 °C. The slit of the excitation and emission slits were set to 5 nm, while the scanning rate was 600 nm min^{-1} with interval data of 1 nm. The sample concentration was adjusted to preserve the absorbance below 0.1 at λ_{max}; each sample was measured three times and the spectra were averaged. Infrared spectra were obtained on a Perkin Elmer FTIR instrument in potassium bromide (KBr) pellets. Relative masses were recorded on a mass spectrometer (Waters high resolution-time of flight-MS Lockspray/HR-TOF-MS) in the positive and negative ion mode. The melting points were determined on an uncorrected MP55 electrothermal melting point apparatus in open-end capillary tubes. DFT calculations were performed on a PC with Processor Intel®Xeon (R) CPU E5--2650 v2@2.60 GHz ×32, RAM 16 GB. The calculations were performed using the Gaussian 09 program[27] at the M06 hybrid meta exchange correlation density functional at the 6-31G(d, p) level of theory.[28] Furthermore, the structure of chemosensor was optimized with and without M^+ to confirm their stability, by comparing their frequency values. Frontier molecular orbital analysis was accomplished to confirm the results of the experiment[43] as well as the interaction mechanism of chemosensor with the metal ion.

*Synthesis of 3-oxo-3*H*-benzo[*f*]chromene-2-carboxylic acid (**1**)*

The synthesis of compound **1** was carried out as in Scheme 1. The synthesis method was based on procedure reported by Xiao *et al.*[29] 2-Hydroxy-naphthaldehyde **2** (100 mg, 0.58

mmol) and meldrum's acid **3** (60.5 mg, 0.58 mmol) were dissolved in a two-neck, round-bottom flask with 15 mL of ethanol. A drop of pyridine was added to the mixture and then refluxed for 2–4 h at 80 °C. Afterwards, the reaction mixture was kept at ambient temperature for 24 h. The precipitated solid was filtered and washed several times with ethanol to yield a pure yellowish solid (83 mg, 60 %).

The analytical and spectral data of the compound are given in the Supplementary material to this paper.

*Method of metal ion sensing of 3-oxo-3*H*-benzo[f]chromene-2-carboxylic acid (**1**)*

The method was adopted from procedure reported by Piao *et al.*[30] and Amirnasr *et al.*[31] A stock solution of compound **1** (4.17×10^{-3} mol dm^{-3}) was prepared in methanol, while stock solution of representative metal ions ($1–10\times10^{-3}$ mol dm^{-3}) was dissolved in milli-Q water. Some metal ions such as, Na^+, Li^+, Mg^{2+}, Ni^{2+}, and Cu^{2+} were used as sulfate whereas some others like, K^+, Cd^{2+}, Ag^+, Al^{3+}, Pb^{2+}, and Cr^{3+} were used as nitrate. The stock solution of **1** was mixed with solution of various metal ions in 5 mL volumetric flask at mole ratio of 1:9 to 9:1 (**1**:metal ion) by keeping constant total concentration. Binding stoichiometry was calculated based on Job's plot experiment,[32] while selectivity experiment was accomplished by mixing 1 molar of compound **1** with 6 molar equivalents of Na^+ in the presence of each 6 molar equivalents of an interference ion. All fluorescence spectra were recorded at excitation wavelength of 361 nm and the temperature was 20 °C.

RESULTS AND DISCUSSION

*Synthesis of 3-oxo-3*H*-benzo[f]chromene-2-carboxylic acid (**1**)*

Knoevenagel condensation of **2** and **3** over basic catalyst of pyridine resulted in a 60 % chemical yield of 3-oxo-3*H*-benzo[*f*]chromene-2-carboxylic acid **1** (Scheme 1).

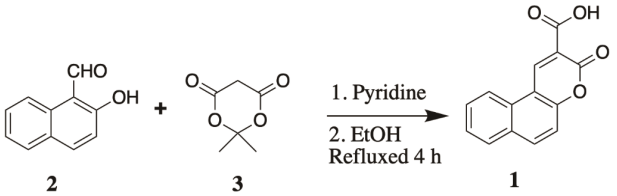

Scheme 1. Synthesis of **1**, 3-oxo-3*H*-benzo[*f*]chromene-2-carboxylic acid.

Instead of Pechmann condensation,[25] this pathway was one of the common method to form coumarin skeleton through intramolecular heterocyclization between an active hydrogen compound of meldrum's acid with an α-hydroxy aldehyde in the presence of a basic catalyst.[26] In general, the achieved product has similar properties to those obtained by Xiao *et al.*[29]

The infrared spectrum of **1** (Fig. S-1 of the Supplementary material) showed typical carboxylic acid absorbances at 3420 (broad weak) and 1750 cm^{-1} (sharp medium), which belong to stretching vibrations of the –OH and C=O moieties, respectively. The appearance of ester lactone was characterized by the vibration of C=O and C–O at 1683 and 1218 cm^{-1} (sharp strong), correspondingly. The naphthalene moiety was confirmed by the stretching vibration of C–H sp^2 (sharp

medium) at 3058 cm^{-1} and C=C aryl (sharp strong) at 1571 cm^{-1}. To clarify the data, ^{1}H-NMR and ^{13}C-NMR were recorded in aprotic solvent of DMSO-d_6 (Figs. S-2 and S-3 of the Supplementary material). Seven different types of protons were observed in the spectrum. One proton resonance at 9.34 ppm was attributed to the alkene proton of H-14 and the other six resonances at 7.59–8.57 ppm were recognized as aromatic naphthalene protons. In addition, 13 different types of carbons appeared in the ^{13}C-NMR spectrum. The signals were attributed to one olefinic carbon at 112.50 ppm, nine aryl carbons at 116.94, 117.94, 122.77, 126.88, 129.45, 129.50, 130.27, 136.30 and 144.18 ppm, one oxygenated aryl carbon at 155.49 ppm, one lactone carbonyl at 157.24 ppm, and one carboxylic acid carbonyl at 164.78 ppm. All NMR data were in agreement with those reported by Fu *et al.* (Tables S-I and S-II of the Supplementary material).[33] Finally, the molecular formula of **1** was confirmed as $C_{14}H_8O_4$ by HR-TOF-MS (ES^- and ES^+, Fig. S-4 of the Supplementary material).

*Photophysical properties of 3-oxo-3*H*-benzo[f]chromene-2-carboxylic acid (**1**)*

Compound **1** showed strong absorption (λ_{max}) and emission maximum (λ_{em}) in methanol at 374 and 445 nm, respectively (Fig. 1). The typical maxima ranged within the benzocoumarin scaffold absorption and emission spectra at 355–488 and 400–625 nm, correspondingly.[26]

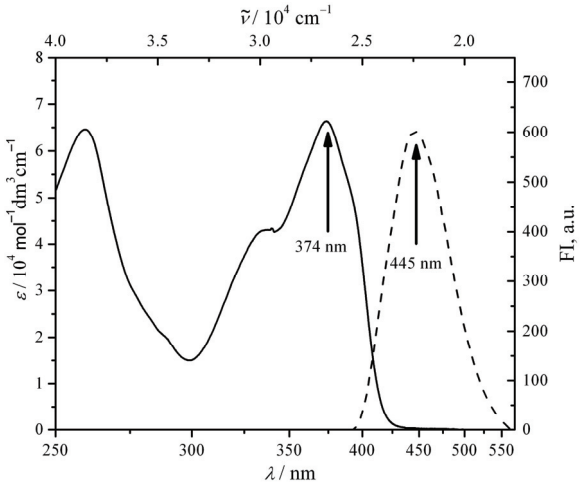

Fig. 1. Spectra of UV/Vis (solid line) and emission (dash line), λ_{ex} 361 nm, of **1** (8×10^{-6} mol dm^{-3}) in MeOH.

Compared to the spectral properties of the basic coumarin skeleton, the extended conjugated π system of **1** was not only able to shift the maxima batochromically by 20–50 nm but also increase its absorptivity by more than 10 times. In addition, intermolecular hydrogen bonding between methanol and carbonyl

moieties of such coumarine compound allowed an intramolecular charge transfer (ICT)[34] and red shifted the emission spectra of **1**.[35] Thus, the Stokes shift of compound **1** was relatively large as 71 nm. Overall, the benzocoumarin system improved optical properties of the coumarin system, which could overcome the limitations such as, photobleaching, photodamage, and shallow tissue penetration depth in bioimaging application.[36–39]

*Chemosensor properties of 3-oxo-3*H*-benzo[f]chromene-2-carboxylic acid (**1**) against various metal ions*

The interaction of **1** with representative metal ions (Li^+, Na^+, K^+, Mg^{2+}, Ag^+, Cu^{2+}, Pb^{2+}, Ni^{2+}, Cd^{2+}, Cr^{3+} and Al^{3+}) was monitored qualitatively through visual observation of the metal-induced fluorescence quenching under a 365 nm UV lamp and quantitatively by fluorescence spectrophotometry in a mixture of MeOH:H_2O (2:8 volume ratio) at room temperature. Upon addition of respective equimolar quantities of metal ions, *i.e.*, Li^+, Na^+, K^+, Mg^{2+}, Ag^+, Cu^{2+}, Pb^{2+}, Ni^{2+}, Cd^{2+}, Cr^{3+} and Al^{3+}, to a 2.28×10^{-6} mol dm^{-3} solution of **1**, it was found that only Na^+ induced blue fluorescence quenching of **1** (Figs. 2 and 3) with a binding stoichiometry of 1:2 (Fig. S-5 of the Supplementary material).

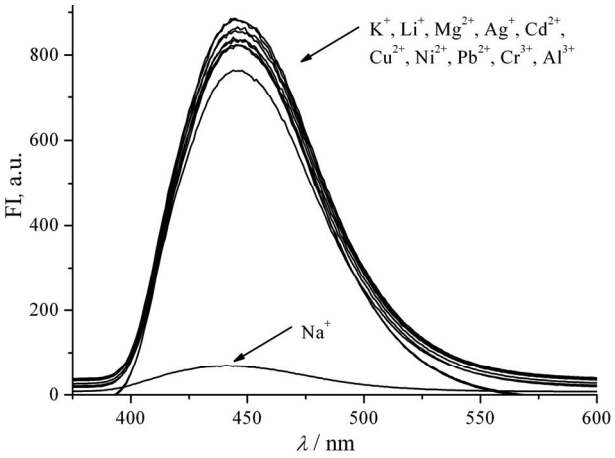

Fig. 2. Fluorescence spectra of **1** (2.28×10^{-6} mol dm^{-3}) before and after addition of 6 molar equivalents of various metal ions (λ_{ex} = 361 nm, λ_{em} = 455 nm).

Upon titration of **1** with sodium ions, red shifts of the emission spectra of the **1** + Na^+ complex were revealed up to ±10 nm compared to the original emission maxima of **1** (445 nm, Fig. 3). This implies that a dipolar interaction was formed between the complex of **1**+Na^+ and the polar solvent of MeOH:H_2O (2:8) and thus, the energy of the excited state decreased and the maxima shifted to a longer wavelength.[40] Furthermore, based on the linear equation, obtained from the calibration curve of **1** against various concentration of sodium ion (Fig. S-6 of the

Supplementary material), the *LoD* and *LoQ* of **1** were found to be 0.14 and 0.48 mg L^{-1}, respectively.

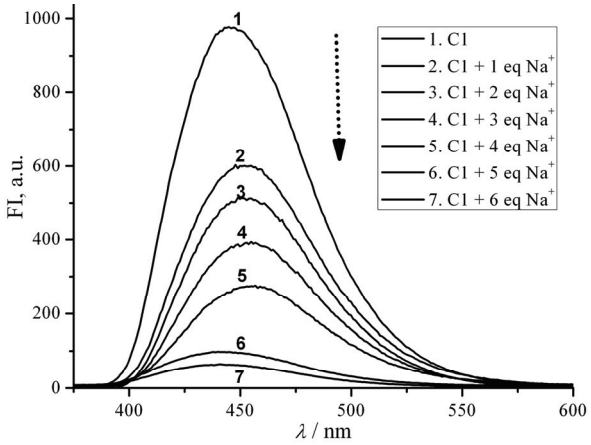

Fig. 3. The changes of fluorescence spectra of **1** (C1; 2.28×10^{-6} mol dm^{-3}) after addition of 1–6 molar equivalents of Na^+ in MeOH:H_2O (2:8, volume ratio); λ_{ex} = 361 nm, λ_{em} = 455 nm.

In fact, based on qualitative observation under UV light at 365 nm, the fluorescence intensity of **1** was actually totally quenched by other metal ions but at equimolar quantities of 15 to more than 500 (Fig. S-7 of the Supplementary material). In general, the fluorescence quenching was attributed to the metal ion chelation with the donor atom of carboxylate O in **1**, known as a chelation--quenched fluorescence (CHQF) effect. The phenomenon is due to electron transfer from the LUMO of the excited fluorophore to the vacant s-orbital of metal ion.[41] which promotes intermolecular charge transfer (ICT). The competitive experiment to further estimate selectivity of **1** against Na^+ in the presence of other metal ions including Li^+, K^+, Mg^{2+}, Ag^+, Cu^{2+}, Pb^{2+}, Ni^{2+}, Cd^{2+}, Cr^{3+}, and Al^{3+} was accomplished under the same conditions (Fig. 4). It was clearly noticeable that the presence of Na^+ among other metal ions showed immediate response in quenching of fluorescence. The result revealed that recognition of Na^+ by **1** was relatively not influenced by other competitive metal ions.

*Computational study of chemosensory mechanism of 3-oxo-3*H*-benzo[f]chromene-2-carboxylic acid (1) against sodium metal ion*

To understand selectivity of compound **1** against sodium ion and its mechanism, DFT calculations were performed and analyzed using the Gaussian 09W program. Since an intermolecular charge transfer (ICT) between a chemosensor and a metal ion plays essential role during chelating processes,[42] the calculation was pointed to the energy gap of HOMO–LUMO of compound **1** against the sodium ion.

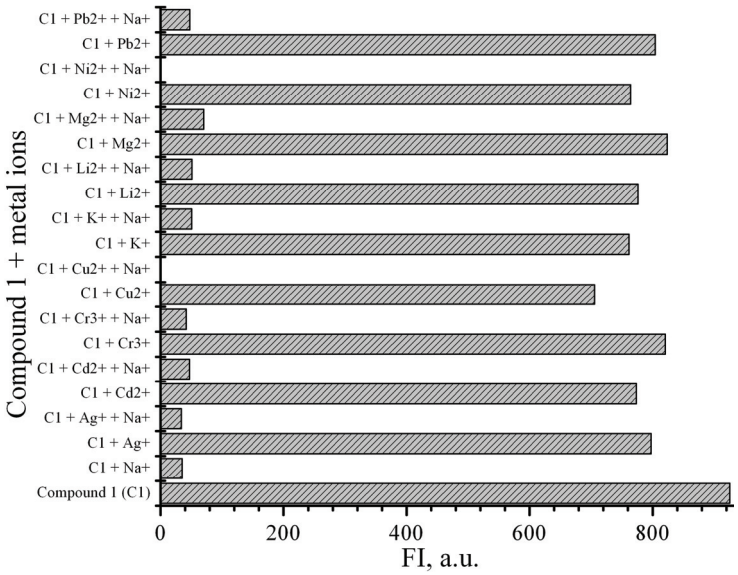

Fig. 4. Fluorescence intensity of compound **1** (C1; 2.28×10^{-6} mol dm^{-3}) with various metal ions (Ag^{+}, Cd^{2+}, Cr^{3+}, Cu^{2+}, Pb^{2+}, K^{+}, Li^{2+}, Mg^{2+}, Ni^{2+}) in MeOH:H_2O (2:8 volume ratio) in the presence of Na^{+} (1:6 molar equivalents; λ_{ex} = 361 nm, λ_{em} = 455 nm).

In geometry optimization of **1**, the minimum state was used to obtain a stable structure of the compound, which could be observed from its positive frequency value (Table S-III of the Supplementary material). Furthermore, frontier molecular orbital (FMO) analysis of optimized **1** (Fig. S-8 of the Supplementary material) confirmed that compound **1**, which has a lower E_{HOMO} of receptor than the E_{HOMO} of the fluorophore, emitted the fluorescence. On the other hand, upon chelation toward the Na^{+} (Fig. 5), compound **1** exhibited fluorescence quenching process, as described in Figs. 6 and 7.

FMO analysis of the optimized **1** against Na^{+} (purple) with ratios 1:1 and 2:1, clearly distinguished typical photoinduced electron transfer occurred in the chelating compound **1** + Na^{+}.

According to Fig. 6, when ratio of compound **1** to Na^{+} was 1:1, fluorescence quenching was allowed upon transfer of an excited electron of fluorophore to the LUMO of receptor and finally to the HOMO of the fluorophore. The electron transfer, identified as oxidative PET,[43] was plausibly occurring if the energy gap of the LUMO of the fluorophore and receptor (0.631 eV) was lower than the energy gap of the HOMO–LUMO of the fluorophore (4.347 eV).

On the other hand, when the ratio of compound **1** to Na^{+} was 2:1 (Fig. 7), quenching occurred through transfer of a HOMO electron of the receptor to the HOMO of the excited fluorophore. The process, identified as reductive PET,[42] was probably occurring if the energy gap of the HOMO of the fluorophore and

receptor (0.336 eV) was lower than the HOMO–LUMO energy gap of the fluorophore (4.362 eV).

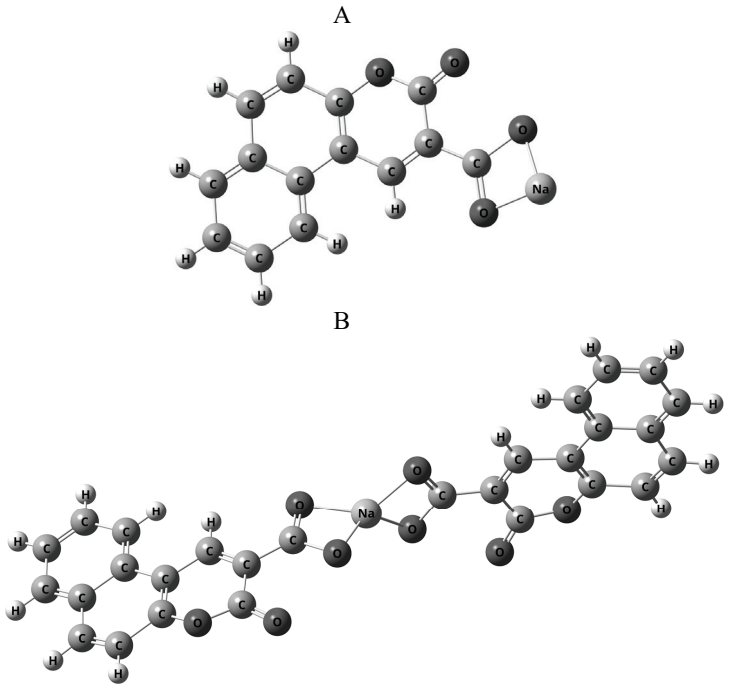

Fig. 5. Structure modeling of **1** against Na^+; A) 1:1; B) 2:1.

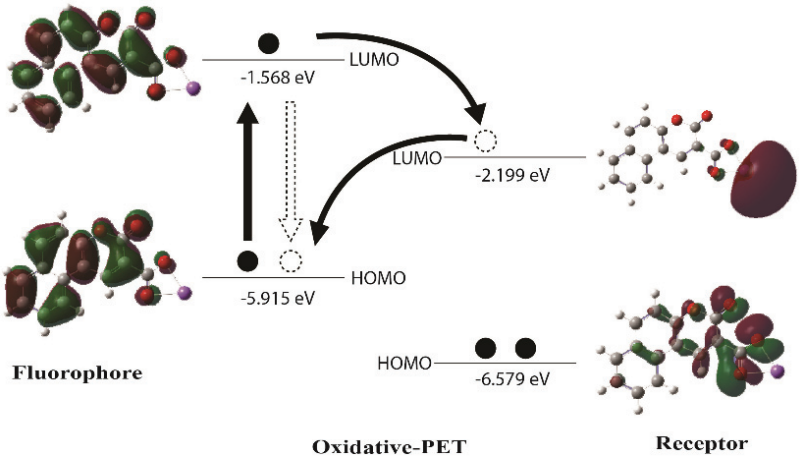

Fig. 6. Calculated frontier molecular orbitals of compound **1** + Na^+ (1:1) and the corresponding interaction of HOMO and LUMO orbital *via* oxidative-PET.

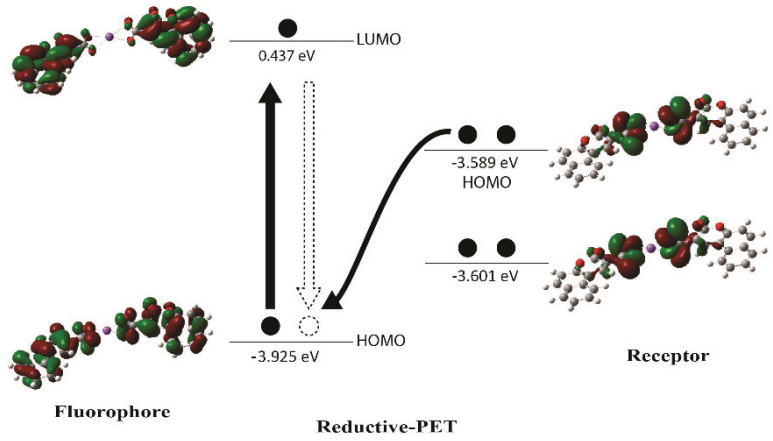

Fig. 7. Calculated frontier molecular orbitals of compound **1** + Na^+ (2:1) and the corresponding interaction of the HOMO and LUMO orbitals *via* reductive-PET.

Overall, the theoretical calculation was in accordance with the experimental results. Furthermore, the interaction mechanism was clearly resolved *in silico*.

CONCLUSIONS

The benzocoumarin typical compound, 3-oxo-3*H*-benzo[*f*]chromene-2-carboxylic acid (**1**) was successfully synthesized in 60 % chemical yield. The compound showed prominent sensory properties against Na^+ selectively through oxidative and reductive PET mechanisms. The *LoD* and *LoQ* **1** against Na^+ in MeOH:H_2O (2:8 volume ratio) were 0.14 and 0.48 mg/L, respectively. Thus, the compound was suggested as potential chemosensor of Na^+ ion in aqueous systems.

SUPPLEMENTARY MATERIAL

Additional data and information are available electronically at the pages of journal website: https://www.shd-pub.org.rs/index.php/JSCS/article/view/9945, or from the corresponding author on request.

Acknowledgements. This work was supported by KEMENRISTEK DIKTI research grant (No.1827/UN6.3.1/LT/2020) and ALG grant of Prof. Ace T. Hidayat (No.1427/UN6.3.1/LT/2020).

ИЗВОД

НАТРИЈУМСКИ ХЕМОСЕНЗОР 3-ОКСО-3*H*-БЕНЗО[*f*]ХРОМЕН-2-КАРБОКСИЛНА КИСЕЛИНА: ЕСПЕРИМЕНТАЛНА И КОМПЈУТЕРСКА СУДИЈА

JAMALUDIN AL-ANSHORI, ANDI RAHIM, AJAR FAFLUL ABROR, IKA WIANI HIDAYAT, TRI MAYANTI, MUHAMMAD YUSUF, JULIANDRI JULIANDRI и ACE TATANG HIDAYAT

Department of Chemistry, Faculty of Mathematics and Natural Sciences, Universitas Padjadjaran Jl. Raya Jatinangor km.21 Bandung-Sumedang, Jatinangor, 40133, Indonesia

Синтетисано је флуоресцентно једињење бензокумаринске структуре и иститивана је његова интеракција са различитим металима. Синтеза је изведена примером *Knoeven-*

agel кондензације, док је идентификација производа урађена примером различитих спектроскопних техника. Хемосензор је тестиран са репрезентативним јонима метала флуоресцентом спектроскопијом. Примењена је и теорија функционала густине (DFT), ради појашњавања експерименталних резултата и потврде механизме реакције. Добијена је 3-оксо-3*H*-бензо[*f*]хромен-2-карбоксилна киселина (**1**), као жута супстанца са приносом од 60 %, тачком топљења од 235,6–236,77 °C, λ_{max} UV/Vis, λ_{em} и *Stokes* померањем (MeOH, nm) на 374, 445 и 71 nm, редом. Структура једење је идентификована на основу поређења спектроскопских и података из литературе. Једињење **1** испољава феномен хелационог гашења флуоресценције (CHQF) селективно према Na^+, са стехиометријом 1:2 и лимитима детекције и квантификације од 0,14 и 0,48 mg/L. На основу DFT калкулације, једињење **1** хелира Na^+ механизмима оксидативног (1:1) и редуктивног (2:1) фотоиндукованог електронског трансфера (PET).

(Примљено 29. септембра 2020, ревидирано 5. марта, прихваћено 23. марта 2021)

REFERENCES

1. C. Zhou, N. Xiao, Y. Li, *Can. J. Chem.* **92** (2014) 1092 (https://dx.doi.org/10.1139/cjc-2014-0011)
2. J. S. Kim, D. T. Quang, *Chem. Rev.* **107** (2007) 3780 (https://dx.doi.org/10.1021/cr068046j)
3. H. N. Kim, M. H. Lee, H. J. Kim, J. S. Kim, J. Yoon, *Chem. Soc. Rev.* **37** (2008) 1465 (http://dx.doi.org/10.1039/B802497A)
4. X. Chen, T. Pradhan, F. Wang, J. S. Kim, J. Yoon, *Chem. Rev.* **112** (2012) 1910 (https://doi.org/10.1021/cr200201z)
5. J. F. Clark, D. L. Clark, G. D. Whitener, N. C. Schroeder, S. H. Strauss, *Environ. Sci. Technol.* **30** (1996) 3124 (https://dx.doi.org/10.1021/es960394n)
6. M. P. Anderson, R. J. Gregory, S. Thompson, D. W. Souza, S. Paul, R. C. Mulligan, A. E. Smith, M. J. Welsh, *Science* **80 253** (1991) 202 (https://dx.doi.org/10.1126/science.1712984)
7. Y. Yamini, N. Alizadeh, M. Shamsipur, *Anal. Chim. Acta* **355** (1997) 69 (https://dx.doi.org/10.1016/S0003-2670(97)81613-3)
8. C.F. Harrington, S.A. Merson, T. M. D. D'Silva, *Anal. Chim. Acta* **505** (2004) 247 (https://dx.doi.org/10.1016/j.aca.2003.10.046)
9. S. L. C. Ferreira, A. S. Queiroz, M. S. Fernandes, H. C. dos Santos, *Spectrochim. Acta, B* **57** (2002) 1939–1950 (https://dx.doi.org/10.1016/S0584-8547(02)00160-X)
10. J. C. Yu, J. M. Lo, C. M. Wai, *Anal. Chim. Acta* **154** (1983) 307 (https://dx.doi.org/10.1016/0003-2670(83)80032-4)
11. A. Ali, H. Shen, X. Yin, *Anal. Chim. Acta* **369** (1998) 215 (https://doi.org/10.1016/S0003-2670(98)00252-9)
12. A. Bobrowski, K. Nowak, J. Zarebski, *Anal. Bioanal. Chem.* **382** (2005) 1691 (https://dx.doi.org/10.1007/s00216-005-3313-2)
13. S. Karthikeyan, V. K. Gupta, R. Boopathy, A. Titus, G. Sekaran, *J. Mol. Liq.* **173** (2012) 153 (https://dx.doi.org/10.1016/j.molliq.2012.06.022)
14. V. K. Gupta, S. Kumar, R. Singh, L. P. Singh, S. K. Shoora, B. Sethi, *J. Mol. Liq.* **195** (2014) 65 (https://dx.doi.org/10.1016/j.molliq.2014.02.001)
15. G. Dimeski, T. Badrick, A. S. John, *Clin. Chim. Acta* **411** (2010) 309 (https://dx.doi.org/10.1016/j.cca.2009.12.005)
16. N. Mergu, A. K. Singh, V. K. Gupta, *Sensors* **15** (2015) 9097 (https://doi.org/10.3390/s150409097)

17. K. Yamada, Y. Nomura, D. Citterio, N. Iwasawa, K. Suzuki, *J. Am. Chem. Soc.* **127** (2005) 6956 (https://dx.doi.org/10.1021/ja042414o)
18. Y. M. Poronik, G. Clermont, M. Blanchard-Desce, D. T. Gryko, *J. Org. Chem.* **78** (2013) 11721 (https://dx.doi.org/10.1021/jo401653t)
19. T. Gunnlaugsson, M. Nieuwenhuyzen, L. Richard, V. Thoss, *J. Chem. Soc. Perkin Trans. 2* (2002) 141 (http://dx.doi.org/10.1039/B106474F)
20. P. Nandhikonda, M. P. Begaye, M. D. Heagy, *Tetrahedron Lett.* **50** (2009) 2459 (https://dx.doi.org/10.1016/j.tetlet.2009.02.197)
21. W. Zhou, J. Ding, J. Liu, *Nucleic Acids Res.* **44** (2016) 10377 (https://dx.doi.org/10.1093/nar/gkw845)
22. M. Taki, H. Ogasawara, H. Osaki, A. Fukazawa, Y. Sato, K. Ogasawara, T. Higashiyama, S. Yamaguchi, *Chem. Commun.* **51** (2015) 11880 (https://dx.doi.org/10.1039/c5cc03547c)
23. I. Leray, J.-P. Lefevre, J.-F. Delouis, J. Delaire, B. Valeur, *Chem. Eur. J.* **7** (2001) 4590 (https://doi.org/10.1002/1521-3765(20011105)7:21%3C4590::AID-CHEM4590%3E3.0.CO;2-A)
24. N. A. Al-Masoudi, N. J. Al-Salihi, Y. A. Marich, *J. Fluoresc.* **25** (2015) 1847 (https://dx.doi.org/10.1007/s10895-015-1677-z)
25. J. Al Anshori, D. S. Rahayu, A. T. Hidayat, I. W. Hidayat, A. Zainuddin, *Res. J. Chem. Environ.* **22** (2018) 91 (https://worldresearchersassociations.com/SpecialIssueAugust2018.aspx)
26. M. Tasior, D. Kim, S. Singha, M. Krzeszewski, K. H. Ahn, D. T. Gryko, *J. Mater. Chem. C* **3** (2015) 1421 (https://dx.doi.org/10.1039/C4TC02665A)
27. *Gaussian 16, Revision C.01,* Gaussian, Inc., Wallingford, CT, 2016 (https://gaussian.com)
28. Y. Zhao, D. G. Truhlar, *Theor. Chem. Accounts* **120** (2008) 215 (https://dx.doi.org/10.1007/s00214-007-0310-x)
29. J. M. Xiao, L. Feng, L. S. Zhou, H. Z. Gao, Y. L. Zhang, K. W. Yang, *Eur. J. Med. Chem.* **59** (2013) 150 (https://dx.doi.org/10.1016/j.ejmech.2012.11.019)
30. J. Piao, J. Lv, X. Zhou, T. Zhao, X. Wu, *Spectrochim. Acta, A* **128** (2014) 475 (https://dx.doi.org/10.1016/j.saa.2014.03.002)
31. M. Amirnasr, R. Sadeghi Erami, S. Meghdadi, *Sensors Actuators, B* **233** (2016) 355 (https://dx.doi.org/10.1016/j.snb.2016.04.077)
32. S. Goswami, S. Chakraborty, S. Paul, S. Halder, S. Panja, S. K. Mukhopadhyay, *Org. Biomol. Chem.* **12** (2014) 3037 (https://dx.doi.org/10.1039/C4OB00067F)
33. X. B. Fu, X. F. Wang, J. N. Chen, D. W. Wu, T. Li, X. C. Shen, J. K. Qin, *Molecules* **20** (2015) 18565 (https://doi.org/10.3390/molecules201018565)
34. W. Zhao, L. Pan, W. Bian, J. Wang, *Chem. Phys. Chem.* **9** (2008) 1593 (https://dx.doi.org/10.1002/cphc.200800131)
35. X. Liu, J. M. Cole, K. S. Low, *J. Phys. Chem., C* **117** (2013) 14731 (https://dx.doi.org/10.1021/jp310397z)
36. R. Wang, F. Zhang, *J. Mater. Chem., B* **2** (2014) 2422 (https://dx.doi.org/10.1039/C3TB21447H)
37. T. G. Phan, A. Bullen, *Immunol. Cell Biol.* **88** (2010) 438 (https://doi.org/10.1038/icb.2009.116)
38. B. P. Joshi, T. D. Wang, *Cancers* **2** (2010) 1251 (https://dx.doi.org/10.3390/cancers2021251)
39. J. Rao, A. Dragulescu-Andrasi, H. Yao, *Curr. Opin. Biotechnol.* **18** (2007) 17 (https://dx.doi.org/10.1016/j.copbio.2007.01.003)

40. R. Macgregor, G. Weber, *Ann. N.Y. Acad. Sci.* **366** (1981) 140 (https://doi.org/10.1111/j.1749-6632.1981.tb20751.x)
41. A. T. Afaneh, G. Schreckenbach, *J. Phys. Chem., A* **119** (2015) 8106 (https://dx.doi.org/10.1021/acs.jpca.5b04691)
42. N. Mergu, M. Kim, Y.-A. Son, *Spectrochim. Acta, A* **188** (2018) 571 (https://doi.org/10.1016/j.saa.2017.07.047)
43. T. Keawwangchai, N. Morakot, B. Wanno, *J. Mol. Model.* **19** (2013) 1435 (https://dx.doi.org/10.1007/s00894-012-1698-3).

Journal of the Serbian Chemical Society
JSCS@tmf.bg.ac.rs • www.shd.org.rs/JSCS
J. Serb. Chem. Soc. *86* (10) S244–S251 (2021) *Supplementary material*

SUPPLEMENTARY MATERIAL TO

Sodium ion chemosensor of 3-oxo-3*H*-benzo[*f*]chromene-2--carboxylic acid: An experimental and computational study

JAMALUDIN AL-ANSHORI*, ANDI RAHIM, AJAR FAFLUL ABROR, IKA WIANI HIDAYAT, TRI MAYANTI, MUHAMMAD YUSUF, JULIANDRI JULIANDRI and ACE TATANG HIDAYAT

Department of Chemistry, Faculty of Mathematics and Natural Sciences, Universitas Padjadjaran, Jl. Raya Jatinangor km.21 Bandung-Sumedang, Jatinangor, 40133, Indonesia

J. Serb. Chem. Soc. *86* (10) (2021) 971–982

ANALYTICAL AND SPECTRAL DATA FOR 3-OXO-3*H*-BENZO[*f*]CHROMENE-2--CARBOXYLIC ACID (**1**)

Yield: 83 mg, (60 %); m.p.: 235.6–236.7 °C; IR (KBr, ν / cm^{-1}): 3420 (–OH), 3058 (C–H sp^2), 1750 (C=O carboxylate), 1683 (C=O lactone), 1571 (C=C aromatic), 1218 (C–O–C ester); ^{1}H-NMR (500 MHz, DMSO-d_6, δ / ppm):) 9.34 (1H, *s*, H-14), 8.56 (1H, *d*, J = 8.4 Hz, H-8), 8.29 (1H, *d*, J = 9.0 Hz, H-7), 8.06 (1H, *d*, J = 8.0 Hz, H-3), 7.75 (1H, *t*, J = 7.7 Hz, H-2), 7.64 (1H, *t*, J = 7.5 Hz, H-1), 7.57 (1H, *d*, J = 9.0 Hz, H-6); ^{13}C-NMR (126 MHz, DMSO-d_6, δ / ppm): 164.76, 157.23, 155.48, 144.18, 136.30, 130.26, 129.48, 129.45, 126.88, 122.75, 117.66, 116.93, 112.53; (–)ESI-HRMS (*m/z*): calcd. for $[C_{14}H_8O_4 - H]^-$ 239.0344, observed 239.0293; (+)ESI-HRMS (*m/z*): calcd for $[C_{14}H_8O_4 + H]^+$ 241.0342, observed 241.0549; UV/Vis. spectra in MeOH (8×10^{-6} mol dm^{-3}): λ_{max} / nm (ε / mol^{-1} dm^3 cm^{-1}): 258 (6.5×10^4) 374 (6.7×10^4); Emission spectra in MeOH (8×10^{-6} mol dm^{-3}): λ_{ex} / nm: 361, λ_{em} / nm: 445. Stokes Shift: 71 nm.

* Corresponding author. E-mail: jamaludin.al.anshori@unpad.ac.id

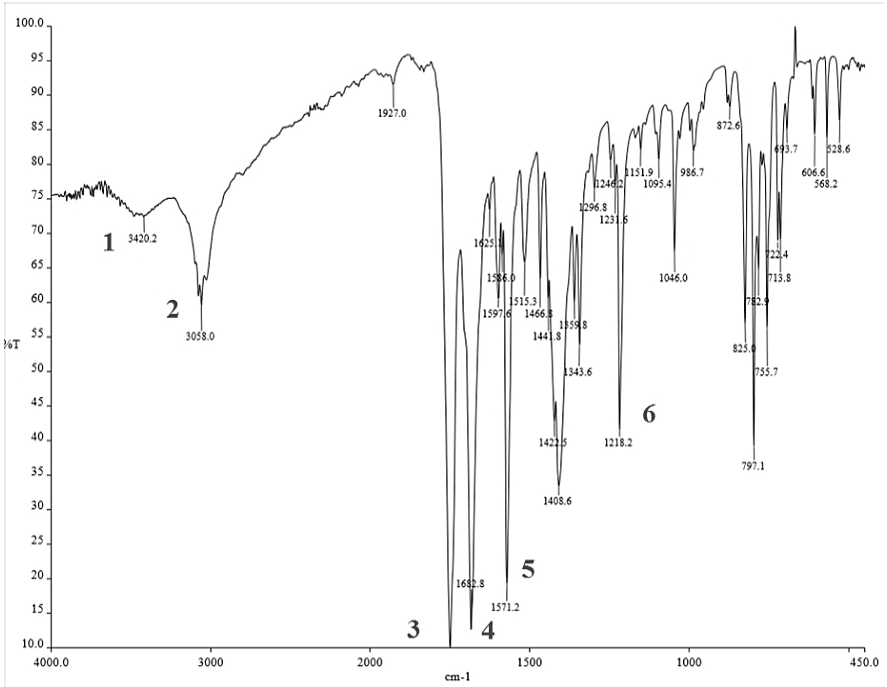

Fig. S-1. Infrared spectra of 3-oxo-3*H*-benzo[*f*]chromene-2-carboxylic acid **1** in KBr disk.

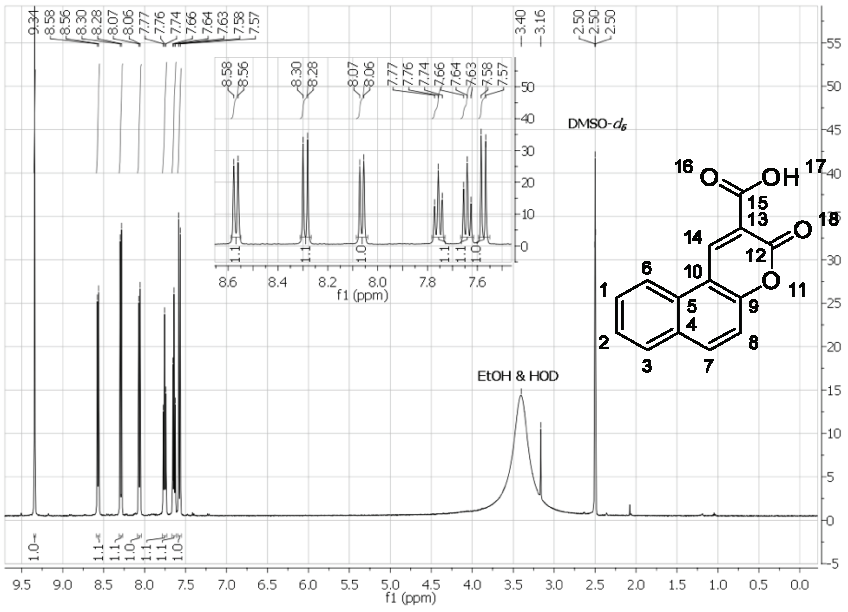

Fig. S-2. ^{1}H-NMR spectra (500 MHz) of 3-oxo-3*H*-benzo[*f*]chromene-2-carboxylic acid (**1**) in DMSO-d_6.

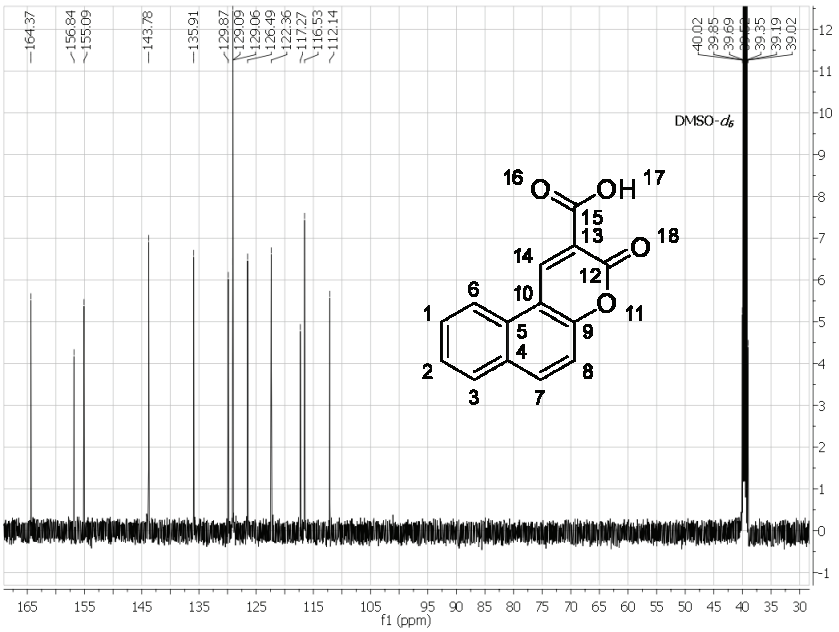

Fig. S-3. ^{13}C-NMR spectra (126 MHz) of 3-oxo-3*H*-benzo[*f*]chromene-2-carboxylic acid **1** in DMSO-d_6.

TABLE S-I. Data of ^{1}H-NMR (500 MHz) of **1** in DMSO-d_6 compared to literature data[1]

No	Compound 1 (500 MHz, DMSO-d_6)			Literature (500 MHz, DMSO-d_6)		Type of proton
	δ_H / ppm	Σ_H	Multiplicity	δ_H / ppm	Multiplicity	
1	7.57	1	Doublet (J = 9.0 Hz)	7.57	Doublet (J = 9.0 Hz)	H-6
2	7.64	1	Triplet (J = 7.5 Hz)	7.64	Triplet (J = 7.2 Hz)	H-1
3	7.75	1	Triplet (J = 7.7 Hz)	7.75	Triplet (J = 7.7 Hz)	H-2
4	8.06	1	Doublet (J = 8.0 Hz)	8.06	Doublet (J = 8.0 Hz)	H-3
5	8.29	1	Doublet (J = 9.0 Hz)	8.29	Doublet (J = 9.0 Hz)	H-7
6	8.56	1	Doublet (J = 8.4 Hz)	8.57	Doublet (J = 8.4 Hz)	H-8
7	9.34	1	Singlet	9.34	Singlet	H-14

TABLE S-II. Data of ^{13}C-NMR (126 MHz) of 1 in DMSO-d_6 compared to literature data[1]

δ_C / ppm		
Literature (126 MHz, DMSO-d_6)	Compound **1** (126 MHz, DMSO-d_6)	Type of carbon
112.55	112.14	C14
116.94	116.53	C1
117.68	117.27	C2
122.77	122.36	C3
126.88	126.49	C6
129.45	129.06	C7
129.50	129.09	C8
130.27	129.87	C4
136.30	135.91	C5
144.18	143.78	C10
155.49	155.09	C9
157.24	156.84	C12
164.78	164.37	C15

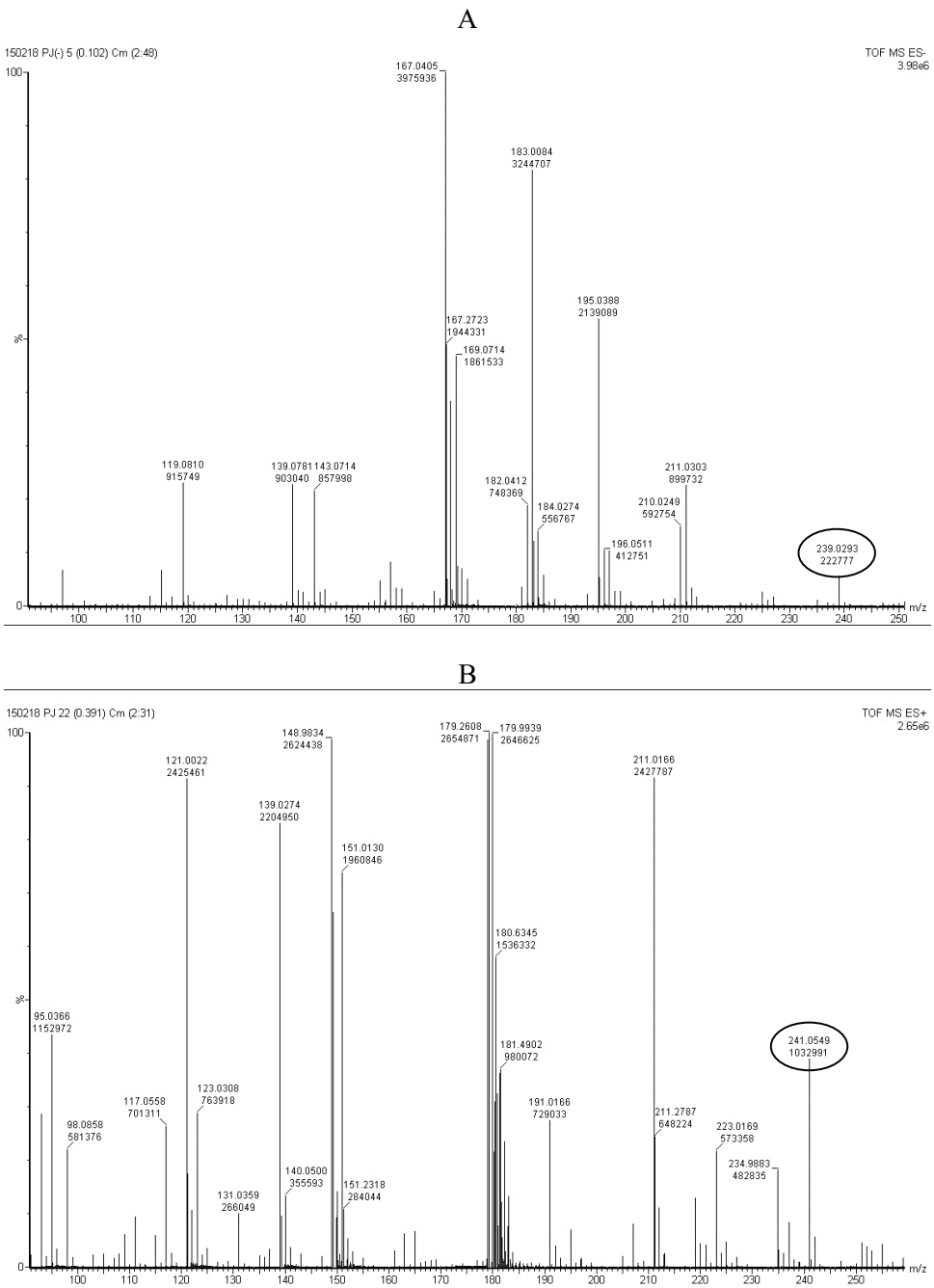

Fig. S-4. Mass spectra of 3-oxo-3*H*-benzo[*f*]chromene-2-carboxylic acid **1** (A) (–)ES and (B) (+)ES.

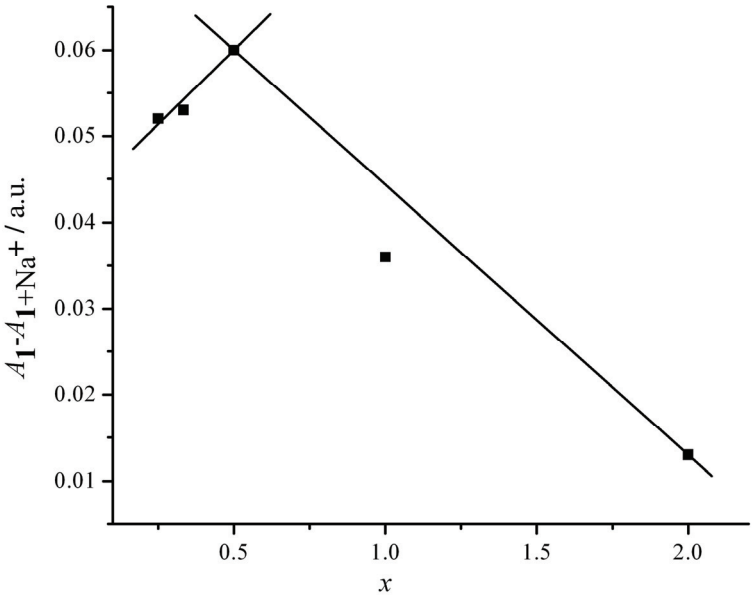

Fig. S-5. Job's Plot for the binding of **1** (1.5×10^{-5} mol dm^{-3}) with Na^+ . ΔA at 360 nm was plotted as a function of mole fraction.

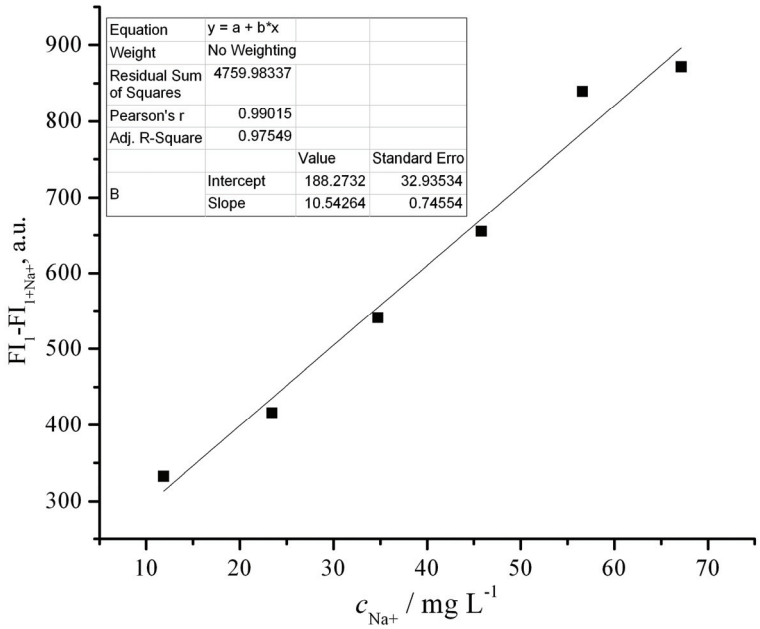

Fig. S-6. Calibration curve of **1** against various concentration of Na^+ in MeOH:H_2O (2:8 v/v)

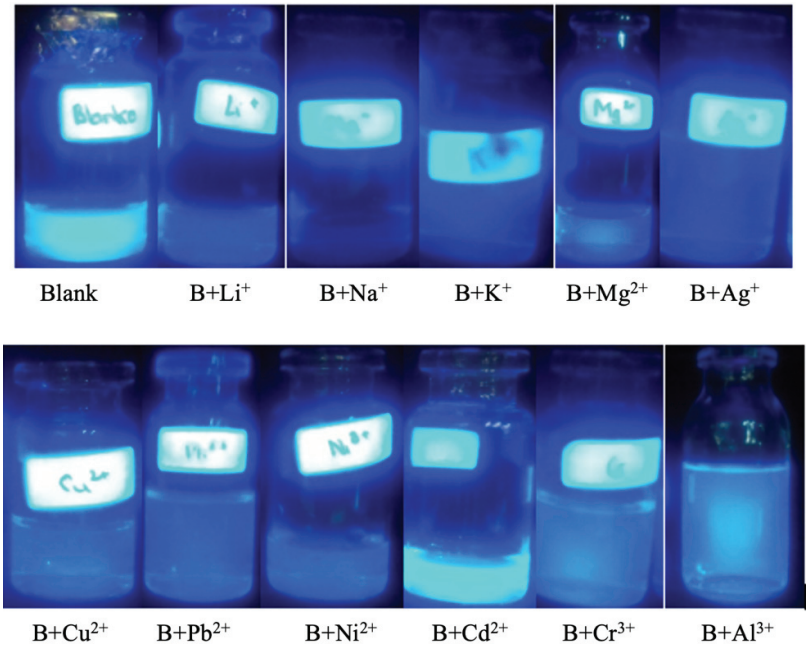

Fig. S-7. Fluorescent intensity quenching of **1** (B; 8.32×10^{-8} mol dm^{-3}) by addition of molar equivalents of various metal ions (Li^+: 100, Na^+: 6, K^+: 15, Mg^{2+}: 30, Ag^+: 500, Cu^{2+}: 15, Pb^{2+}: 170, Ni^{2+}: 60, Cd^{2+}: 500, Cr^{3+}: 400, Al^{3+}: 200), observed under UV light at 365 nm.

TABLE S-III. Calculated imaginary frequency values of vibrated atoms of compound **1**

Mode	Frequency, cm^{-1}	IR intensity, km mol^{-1}
1	55.44	0.5561
2	68.60	0.0011
3	105.12	2.6084
4	140.69	4.5864
5	159.17	0.5869
6	174.04	1.2744
7	251.91	11.1475
8	270.10	5.9061
9	323.47	1.3467
10	328.06	5.1032
11	375.91	13.8163
12	380.17	0.4003
13	431.69	2.3291
14	434.01	7.7653
15	443.01	12.0847
16	520.79	0.4615
17	534.95	2.8835
18	540.64	0.0489
19	571.60	6.6310
20	618.64	11.7080

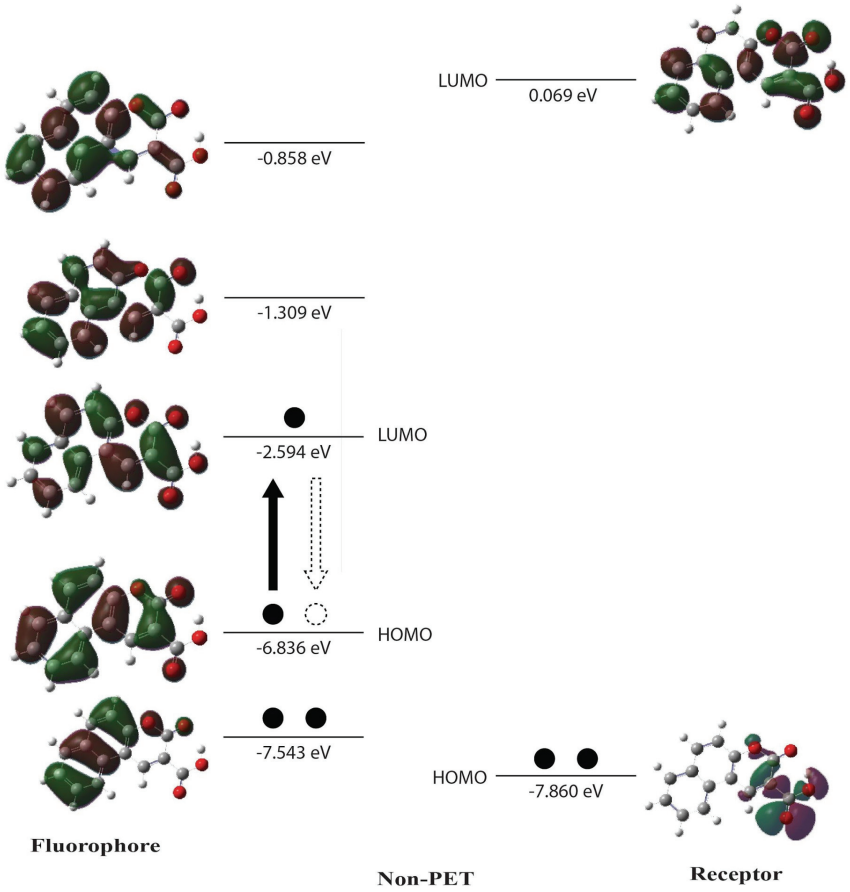

Fig. S-8. Calculated frontier molecular orbitals of compound **1** and the corresponding HOMO and LUMO orbitals.

REFERENCES

1. X. B. Fu, X. F. Wang, J. N. Chen, D. W. Wu, T. Li, X. C. Shen, J. K. Qin, *Molecules* **20** (2015) 18565 (https://doi.org/10.3390/molecules201018565).

Journal of the Serbian Chemical Society
JSCS-info@shd.org.rs • www.shd.org.rs/JSCS
J. Serb. Chem. Soc. *86* (10) 983–995 (2021)
JSCS–5477
Original scientific paper
Published 10 September 2021

Role of the lattice energy from chemical agents in the activation of highly-condensed carbons

EUMARIELYS M. ESPINOZA and LUIS F. ISERNIA*

Laboratorio de Tamices Moleculares, Universidad de Oriente, Urb. Juanico, Calle Maldonado con Florida, Maturín, Estado Monagas, Venezuela

(Received 11 December 2020, revised 22 March, accepted 7 April 2021)

Abstract: Highly condensed carbons from pet-coke were first treated with Na/K hydroxides and carbonates and then with H_2SO_4. The esterification reaction of palmitic acid reached conversions of up to 97 % on the yielded activated carbons. The results evidence the relationship between the efficacy of Na/K hydroxides and carbonates as treatment agents and their lattice potential energy. Moreover, the analysis of carbonaceous solids confirms that both surface area and acidity are primary factors promoting activity in the esterification reaction. Furthermore, the results do not indicate a direct relationship between the activity and the oxidized species (SO_x) arising from the treatment with H_2SO_4. The relatively low melting and decomposition temperature of Na/K hydroxides can improve their effect on the pet-coke matrix, leading to higher surface areas, acidities, and catalytic activities than treatment with carbonates. This supports an affinity between the carboxyl functions of the fatty acid molecules and the polar and catalytically active centers of the hydroxide-treated solid surface.

Keywords: acidity; activated carbon; delayed pet-coke; esterification.

INTRODUCTION

Pet-coke is a petroleum refinement by-product, mostly composed of highly condensed carbon species. A way to help address the amounts of pet-coke that result from heavy-petroleum refinement consists in their conversion into environmentally-friendly products with a higher aggregate value, as activated carbons. The activated carbons have been extensively studied because of their catalytic and adsorptive properties.[1–4] Moreover, their acid modifications have good activity in acid-catalyzed reactions[5,6] such as the hydrolysis of the cellulose[5] or the esterification of free fatty acids.[6]

In the industries of cosmetology, solvents, polymers, and alternative fuels, among others, esters play an important role. They mainly come from the trances-

* Corresponding author. E-mail: luis.isernia@gmail.com
https://doi.org/10.2298/JSC201211027E

terification[7] of triglycerides contained in vegetable oil and animal fats in the presence of homogeneous catalysts, such as metal hydroxides or (less frequently) inorganic acids. Likewise, in Fisher's esterification of fatty acids, inorganic acids are commonly used.

Special attention has been directed to the use of waste oils from industrial and domestic sources to avoid the use of alimentary resources. However, the high presence of fatty acids in these sources limits the efficacy of base-catalyzed transesterification because of the formation of soaps. To overcome this problem, prior esterification of fatty acids is applied in the presence of an alcohol and strongly acidic homogeneous catalysts, such as H_2SO_4 and HF, followed by transesterification.[8] Conversely, their corrosive nature and difficulties in separation from the reaction product mixture have driven the search for heterogeneous catalysts of a less corrosive nature and relatively easy separation and reutilization.[8] In this sense, several alternatives were analyzed, such as ion exchange resins,[9] superacids, mesoporous aluminosilicates, microporous solids, such as zeolites[10] and activated carbons.[1–4] Activated carbons, for example, have remarkable properties as catalysts and adsorbents.[1–4] These could be obtained by thermal treating (also called "physical treatment") between 873 and 1073 K, of organic precursors, such as sugar, wood, charcoal or asphalt, among others, in the presence of CO_2, steam, noble gases or N_2,[11] and/or by treatment with chemical reagents of diverse character.[12,13]

Among the different agents for the chemical treatment of carbonous precursors, K and Na hydroxides have gained increasing attention. Zeng *et al.*[2] reported the use of activated carbon (achieved by step treatment with KOH and H_2SO_4 of Chinese pet-coke) in oleic acid esterification with methanol. The resulting activated carbons had stronger acidity than that of SO_4^{2-}/ZrO_2 solids but were slightly weaker than pure H_2SO_4. Furthermore, their catalytic performance was close to 72 %. Lee and Choi[3] treated high sulfur petroleum coke with K and Na hydroxides between 673 and 873 K. Their investigation revealed that KOH was a more effective activating agent, leading to a surface area of 1980 $m^2\ g^{-1}$ with a metal hydroxide to coke mass ratio of 4. Similar observations were first made by Ehrburger *et al.*,[14] who reported that much more CO_2 was yielded from coal treated with KOH than with NaOH.

Lillo and coworkers[4] proposed that K and Na hydroxides are reduced by the carbon, producing a metallic element during the heat treatment:

$$4MOH + C \leftrightarrow 4M + CO_2 + 2H_2O \quad (M = K, Na) \quad (1)$$

$$6MOH+2C\leftrightarrow 2M+3H_2 +2M_2CO_3 \quad (M = K, Na) \quad (2)$$

However, there is increasing interest in the use of less aggressive or corrosives chemical activating agents. Na_2CO_3 and K_2CO_3 offer a possible alternative. In addition to their lower aggressiveness, CO_3^{2+} were proposed as central parti-

cipants in the reaction mechanisms that lead to activated carbons.[15] In this sense, various researchers have proposed[16] that carbonates could react with carbon directly by reactions (3) and (4), yielding the associated metallic element and their oxide during the heat treatment:

$$K_2CO_3 + 2C \leftrightarrow 2K + 3CO \quad (3)$$

$$K_2CO_3 + C \leftrightarrow K_2O + 2CO \quad (4)$$

Moreover, the derived metallic oxide can also be a key participant in the reaction mechanisms that lead to activated carbons:

$$K_2O + C \rightarrow 2K + CO \quad (5)$$

However, these reactions do not offer a direct explanation for the development of an acidic character in some resulting activated carbons.

Inorganic acids, such as H_3PO_4, H_2SO_4, HCl and HNO, were early employed[17] for the synthesis of activated carbons. Between them, H_2SO_4 has considerable use[2,5,6] as a sulfonation agent.[18] The incorporation of sulfuric acid into the interior carbonous matrix promotes sulfonation[18] of aromatic structures that constitute the coke and results in stable carbon structures with a higher density of $–SO_3H$ groups. In this regard, various research groups[5,6] have reported the preparation of activated carbons bearing $–SO_3H$ functions by treating several organic species with concentrated sulfuric acid.

Carbons with $–SO_3H$ groups are known for their considerable acidity, showing good activity in acid-catalyzed[5,6] reactions, such as the hydrolysis of cellulose[5] or the esterification of free fatty acids with methanol.[6]

The lattice potential energy[19] (LPE) is usually expressed in kJ $mol^{–1}$ and defined in some textbooks as the energy required for the endothermic breaking apart of an ionic solid and the conversion of its component atoms into gaseous ions, giving positive values. Another definition explains it as the reverse process, giving negative values. The direct experimental determination of lattice potential energy is difficult. Nevertheless, LPE can be calculated from other measurable energy quantities through the Born–Fajans–Haber thermochemical cycle.[20] Moreover, there are theoretical models for the calculation of lattice energies of ionic crystals based on the Born–Mayer equation[21] using the Madelung constant[22] or more approximately through the Kapustinskii equation.[23]

The LPE can be taking into account as an indicator of the relative stabilities of the treatment agents and their propensity to transformation in the chemical species that effectively perform the chemical activation of carbons. In this sense, it could be valuable to estimate the relative proneness of the activation.

Although there is substantial knowledge about the aforementioned features, the understanding of their action on issues such as acidity, substrate adsorption, or catalytic activity remains incomplete. Consequently, the present work addresses these aspects through the study of KOH, NaOH, K_2CO_3 and Na_2CO_3 acti-

vating action and the subsequent treatment with sulfuric acid on the physico-chemical properties and catalytic performance in the esterification of palmitic acid; of highly condensed carbons obtained from Venezuelan delayed pet-coke.

EXPERIMENTAL

Synthesis and characterization of activated carbons

Venezuelan delayed pet-coke from the upgrader complex "José Antonio Anzoátegui", ground and sieved to particles of about 53–500 μm, was used as the raw material. KOH, NaOH, Na_2CO_3 and K_2CO_3 were used as activating agents. To prepare each sample, 8 g of each activating agent and 2 g of pet-coke (mass ratio of 4:1) were thoroughly mixed. The samples were loaded in alumina crucibles into a horizontal tubular electric furnace under argon flow, heated at 1073 K for 30 min, and left cool down to room temperature. Alternately, the resulting materials were washed (by vacuum filtration) with a 5 % HCl solution and distilled water until reaching a neutral pH. Then solids were dried for 24 h at 343 K. The resulting four carbonaceous solids were labeled ActKOH, ActNaOH, ActK_2CO_3 and ActNa_2CO_3, according to the activating agent. Half of each dry sample was stirred with 50 vol. % H_2SO_4, using a ratio of 100 mL per gram of solid at 363 K foe 3 h. Then, each resultant solid was washed with deionized water by vacuum filtration until reaching a neutral pH value and dried for 24 h at 343 K. These solids were treated with H_2SO_4 and labeled ActKOH_Su, ActNaOH_Su, ActK_2CO_3_Su and ActNa_2CO_3_Su.

Textural properties were acquired from N_2 adsorption isotherms at 77 K on a Micromeritics TriStar 3000 adsorption analyzer, with a vacuum pre-treatment at 423 K for 24 h, following a previously published procedure.[24] The surface area (S_{BET}) was acquired by the BET model.[25] The microporous volume (V_μ) was determined by the "*t*-plot" method[25] and the "total porous volume" (V_t) by the "Gurvitsch" rule.[25]

X-Ray photoelectron spectroscopy (XPS) analysis was performed under high vacuum conditions (10^{-6} Pa) on a Specs–Leybold instrument with a Phoibos 150 electron analyzer and Al X-rays (1486.6 eV/240 W) emission source. The binding energy (*BE*) of 284.6 eV for the C 1s core level was used as an internal standard.

The superficial acidity was obtained through a wet method,[8] in which 0.1 g of each solid previously dried at 393 K for 24 h, was introduced into test tubes with airtight screw lids with 10 mL of KOH 0.01 mol L^{-1}. In addition, a blank test with only 10 mL of KOH 0.01 mol L^{-1} was prepared. Then, the mixtures were vigorously stirred every 8 h for 3 days and centrifuged for 10 min at 4000 min^{-1}. Four milliliters from each tube were titrated with 0.01 mol L^{-1} HCl using phenolphthalein as the indicator. After this, 2 mL of HCl were added and a back-titration with KOH 0.01 mol/L was performed. The acidity was estimated in mmol g^{-1}:

$$A = \frac{\left[\left(V_{\text{oHCl}} + 2\right)N_{\text{HCl}} - \left(V_{\text{oKOH}}N_{\text{KOH}}\right)\right] - \left[\left(V_{\text{iHCl}} + 2\right)N_{\text{HCl}} - \left(V_{\text{iKOH}}N_{\text{KOH}}\right)\right]}{0.4m} \quad (6)$$

where m is the mass in grams of catalyst, N_{KOH} and N_{HCl} are the concentrations of KOH and HCl in mol L^{-1}, respectively, V_{oHCl} and V_{iHCl} are the milliliters of HCl required to titrate the blank test and each particular sample, V_{oKOH} and V_{iKOH} are the milliliters of KOH required for the back titration of the blank test and each particular sample.

Catalytic activity evaluation

The catalytic behavior of each studied solid was evaluated through the Fisher esterification reaction for 24 h, using 0.150 g of catalyst and 0.500 g of palmitic acid (98 %) dissolved

in 50 mL of ethanol (99 %) in a 100 mL PARR 4593 batch reactor with a Teflon liner connected to a 4848 controller unit. A lateral port allowed syringe extraction of 3 mL aliquots from the stirred reaction mixture at programmed reaction times, at 403 K. The syringe was frozen before each extraction, and the aliquots were kept in refrigerated test tubes with airtight screw lids, to freeze the reaction and prevent evaporation. Then all test tubes were allowed to reach room temperature and centrifuged for 15 min at 4000 min^{-1}. The fatty acid concentration was determined by titration of 2 mL of the transparent supernatant solution of each test tube with ethanolic 0.02 mol L^{-1} KOH using phenolphthalein as indicator, and the conversion (X) in each reaction time was calculated by the Eq. (7):

$$X = (M_o – M)/M_o \quad (7)$$

where M_o is the initial concentration in mol L^{-1} and M is the concentration for each reaction time.

Adsorption isotherms of stearic acid

The adsorption isotherms of stearic acid at 305 K were obtained through a reported methodology,[8] in which 0.1 g of each solid was shaken with 5 mL of stearic acid 10^{-3} mol L^{-1} in hexane in sealed test tubes. After 24 h, all test tubes were centrifuged and 3 mL samples the clear supernatant solution were taken and titrated with 2-propanolic KOH 2×10^{-3} mol L^{-1}. The amount in mg of stearic acid adsorbed per gram of adsorbent after equilibrium (Qe_o), in the point P_o of the isotherm was calculated:

$$Qe_o = 5M_{SA}(C_o – Ce_o)/m \quad (8)$$

where C_o and Ce_o are the concentrations in mol L^{-1} of stearic acid before and after the equilibrium, M_{SA} is the molar mass in g mol^{-1} of stearic acid, and m is the mass in g of the adsorbent. Every new point P_i ($i > 0$) of the isotherm was obtained after the addition of 3 mL of stearic acid with a increasing concentration (Ca_i) from 2×10^{-3} to 10^{-2} mol L^{-1}, and repetition of the cycle (shaking, 24 h of waiting and titration) to calculate the next concentrations (C_i) and adsorbed amount in equilibrium (Qe_i):

$$C_i = (0.4\ Ce_{i-1} + 0.6\ Ca_i) \quad (9)$$

$$Qe_i = Qe_{i-1} + 5\ M_{SA}(C_i – Ce_i)/m \quad (10)$$

Eq. (11) represents the data of the isotherms fitted to the Langmuir model, where K_L is a constant and Qm / mg g^{-1} is the Langmuir monolayer capacity.

$$\frac{Ce}{Qe} = \frac{Ce}{Qm} + \frac{1}{K_L Qm} \quad (11)$$

RESULTS AND DISCUSSION

The data in Table I (columns 3–5) confirm that the solids treated with hydroxides (ActKOH, ActNaOH, ActKOH_Su and ActNaOH_Su) developed higher values of BET specific surface area, total V_t, and microporous V_μ volumes than those treated with carbonates ($ActK_2CO_3$, $ActNa_2CO_3$, $ActK_2CO_3$_Su and $ActNa_2CO_3$_Su). Additionally, KOH had higher effects over these textural properties than NaOH, K_2CO_3 and Na_2CO_3. Moreover, the Na/K hydroxide-treated solids suffered slight reductions of their superficial areas after H_2SO_4 treatment (3.43 and 14.18 %) unlike Na/K carbonate-treated solids (66.8 and 56.3 %). This

behavior indicates the persistence of Na/K carbonate clusters after HCl washing during treatment.

TABLE I. Catalytic performance, acidity, and textural properties of the studied solids; S_{BET} = surface area through BET model; V_t = total porous volume, estimated by the Gurvitsch rule; V_μ = microporous volume, estimated by the *t*-plot method; X = maximum conversion of palmitic acid; k = rate constant; Qm is the Langmuir monolayer capacity

Sample	Acidity mmol g^{-1}	S_{BET} m^2 g^{-1}	V_t cm^3 g^{-1}	V_μ cm^3 g^{-1}	X %	k h^{-1}	Qm mg g^{-1}
ActKOH	0.81	2713	1.2915	0.8044	96	0.777	416.7
ActKOH_Su	0.96	2620	1.2432	0.7659	97	0.361	434.8
ActNaOH	0.62	1456	0.7907	0.3988	97	0.496	238.1
ActNaOH_Su	0.86	1250	0.6958	0.3445	95	0.710	238.1
ActK_2CO_3	0.28	268	0.1238	0.0881	28	0.0272	–
ActK_2CO_3_Su	0.93	89	0.0445	0.0262	67	0.211	–
ActNa_2CO_3	–0.14	32	0.0180	0.0026	28	0.114	–
ActNa_2CO_3_Su	0.12	14	0.0079	0.0017	2.2	0.001	–
Pet-coke	0.15	18	0.0124	0.0011	19	0.0356	–
Self-catalyzed	–	–	–	–	9.7	0.007	–

The XPS spectrums of the S 2p core levels for the studied solids are shown in Fig. 1. The signal near 164.04 eV could be associated with sulfur species of thiophene compounds[26] that remained as so-called refractory thiophene[27,28] after achievement of the parental delayed pet-coke. This signal tends to decay after chemical treatment at 1073 K, as a possible result of an early decomposition (some authors mention higher temperatures[27]) with the removal of the residual volatile sulfur products. Moreover, initial studies[29] suggest that at high temperatures, Na or K hydroxides and carbonates can react with thiophene compounds, leading to M_2S salts (M = Na or K), that would dissolve during the subsequent HCl washing. Additionally, in the solids treated with H_2SO_4, a signal close to

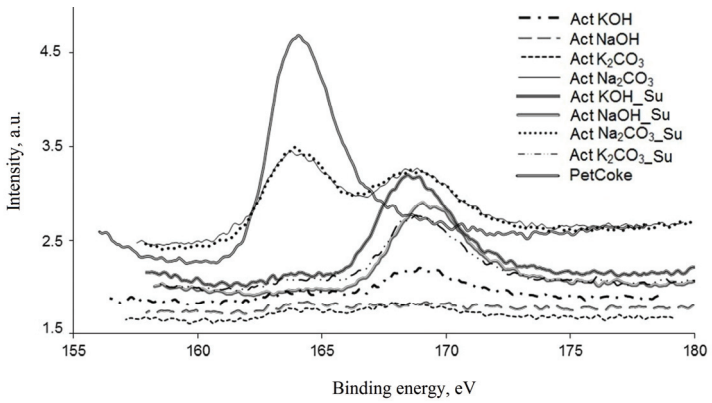

Fig. 1. XPS spectra of the S 2p region for the studied solids.

168.90 eV[30] associated with SO_x groups, indicates sulfonation[29] of the aromatic structures that constitute the coke matrix.

Treatment of pet-coke with hydroxides led to significant acidity (Table I, column 2), KOH being more effective than NaOH. However, treatment with carbonates led to poorly acidic solids, except for the ActK_2CO_3_Su, the acidity of which was similar to hydroxide-treated solids. The results also evidenced some enhancing effect of H_2SO_4 treatment over the acidity. Nevertheless, this behavior does not yield a constant increase in the activity in the esterification reaction (Table I, columns 2, 6 and 7). The low-accessibility of the fatty acid molecules to the catalytically active SO_x groups could cause this behavior.

A possible reaction between alkali metal hydroxides and halogen-substituted aromatic species[31] present in the coke matrix under the intense conditions applied in this work would explain the acidic properties of resulting solids before treatment with H_2SO_4 (Fig. 2).

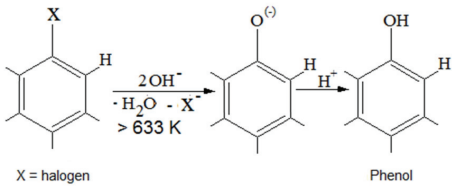

Fig. 2. The possible reaction between NaOH or KOH and halogen-substituted aromatic species during the activation process.

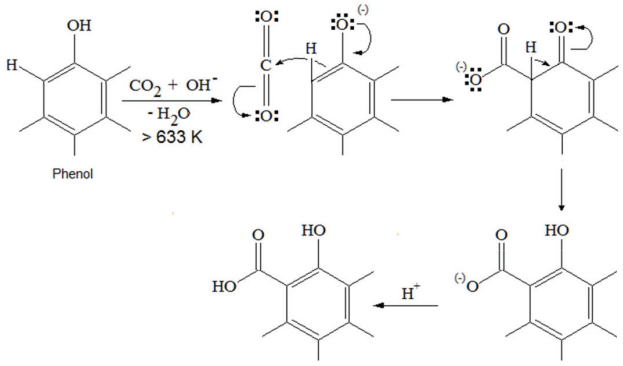

Fig. 3. The possible reaction between phenols and CO_2 generated during the activation process, leading to carboxylic groups.

Moreover, phenols could react[29] with the CO_2 generated during the activation process, yielding carboxylic groups (Fig. 3). Such a possibility concords with the similarity in the order of magnitude between the superficial chlorine concentration (by XPS Cl 2p 207 eV. Fig. 4) in pet-coke (0.75 mmol g^{-1}) and the average density of acid sites after treatment with KOH and NaOH (Table I, col-

umn 2). The combination of these acidic structures, with an adequate porosity, would act as active sites during the esterification of fatty acids. The characteristic behavior of ActK_2CO_3_Su with respect the other carbonate treated solids could originate from the smaller modulus of the lattice potential energy[19] of K_2CO_3 with respect Na_2CO_3, which promotes further thermal decomposition of K_2CO_3 and prepares the available surface of pet-coke for the subsequent action of H_2SO_4.

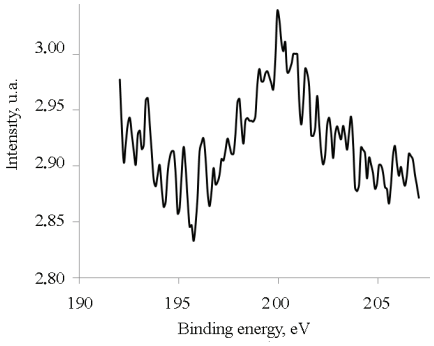

Fig. 4. XPS spectrum of the Cl 2p region of the parental delayed pet-coke.

The moderately negative acidity of ActNa_2CO_3 indicates the persistence of alkaline Na_2CO_3 clusters after HCl washing during treatment.

The adsorption isotherms of stearic acid (Fig. 5) can be separated into the A and B groups, related respectively to the hydroxide treated solids (with higher *Qe* values), and pet-coke along with the carbonate-treated solids (with lower *Qe* values).

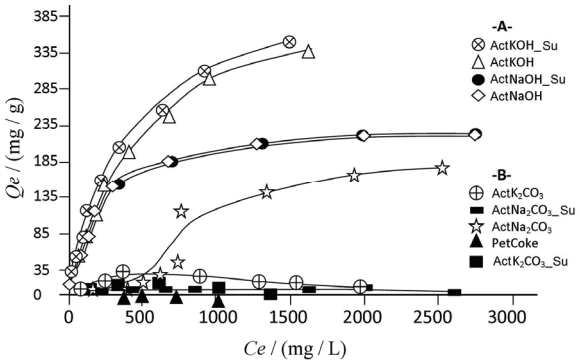

Fig. 5. Adsorption isotherms at 305 K of stearic acid on the studied solids.

The isotherms of the solids from group A fit with the linearized Langmuir model (Fig. 6), providing monolayer capacities *Qm* between 238 and 435 mg g^{-1} (Table I, column 8).

Although studies of fatty acids adsorption isotherms on activated carbons are scarce, a comparison with published values for diverse adsorbents[8,32–34] reveals

a good affinity between fatty acid molecules and the surface of the hydroxide--treated solids. Additionally, these results evidence that KOH yields activated carbons with higher *Qm* values than NaOH. On the other hand, pet-coke and group B solids do not show good agreement with this adsorption model (not displayed), probably because of the low affinity of stearic acid for their surfaces.

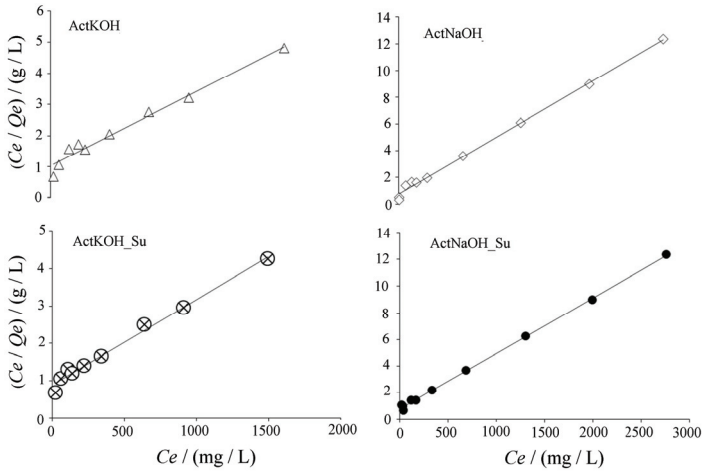

Fig. 6. Fitting of the stearic acid adsorption isotherms on the hydroxide treated solids to the linearized Langmuir model.

Moreover, treatment with H_2SO_4 did not lead to a significant increase in the *Qm* values for stearic acid adsorption, as a possible consequence of the low accessibility of the fatty acid molecules to the acidic SO_x groups. Results evidence the overall trend where solids with higher acidity and activity in the esterification reaction also show a higher affinity between their surface and fatty acid molecules (Table I, columns 2, 6–8). This suggests adsorption of fatty acid molecules with their carboxyl functions oriented to the superficial polar and catalytically active centers. The nature of the superficial polar groups is no clear. However, it would be related to carboxylic and phenolic functions resulting from the action of hydroxide over substituted aromatic rings of the carbonous matrix. Interaction with fatty acid molecules could be through hydrogen bonding, as shown in Fig. 7. The sample ActK_2CO_3_Su represents an exception. It has significant activity in the esterification reaction (Table I, columns 6 and 7), but it pertains to group B (with lower Q_e values, Fig. 5). This suggests a more complex interaction between fatty acid molecules and the superficial active sites of this solid.

The linearized representation of ln(1–*X*) as a function of the reaction time, *t*, from the data of the esterification of palmitic acid is shown in Fig. 8, which is compatible with a pseudo-first-order kinetic model:

$$\ln(1-X) = -kt \quad (12)$$

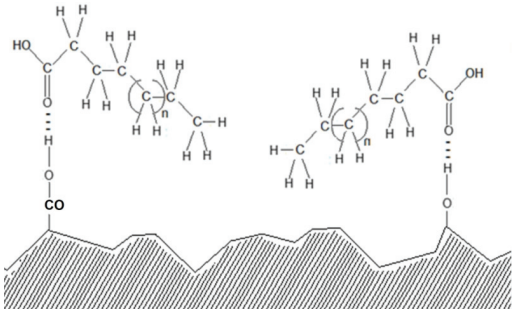

Fig. 7. Possible interaction of the superficial polar groups with the fatty acid molecules through hydrogen-bonding.

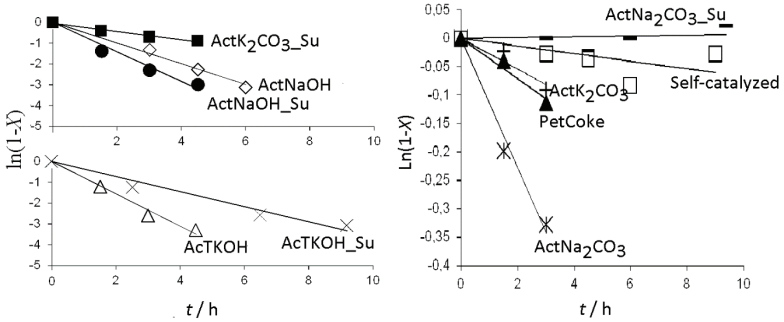

Fig. 8. Fitting of the data of the palmitic acid esterification to a pseudo-first-order kinetic model.

Then, the values of the rate constant k (Table I, column 7) reveal that hydroxide-treated catalysts are more active than their carbonate-treated counterparts, agreeing with the overall trend of both superficial area and acidity (columns 2 and 3). This behavior corroborates the fundamental role of the acid sites as catalytically active centers and the surface area.

The superior performance of hydroxides as treatment agents might be caused by the lower melting temperatures of K and Na hydroxides (591 and 683 K, respectively)[35] than their carbonate counterparts (1124 and 1178 K, respectively)[4] favoring the action of hydroxides on the pet-coke.

Finally, the results evidence a relationship between the modulus of the lattice potential energy[19] (LPE) of Na/K hydroxides and carbonates and their efficacy as treatment agents: The increase of the mean values of the properties from the derived activated carbons (resulting from the treatment with each agent) with the reduction of the LPE values are given in Table II. In this way, a lower LPE implies an easier thermal-decomposition of the treatment agents into the chemical species that perform pet-coke activation. The impact of the LPE would explain the superior efficacy of the potassium-based treatment agents in comparison with

their sodium-based counterparts, also agreeing with previous findings[14] that mention the superior effectiveness of KOH over NaOH as an activating agent.

TABLE II. Mean values of the properties from the derived activated carbons and the modulus of the lattice potential energy (LPE) of the chemical treatment agents. Mean: before and after H_2SO_4 treatment. LPE: The values[19] correspond to the "Born–Fajans Haber thermochemical cycle"

Treatment agent	Acidity mmol/g	S_{BET} $m^2\ g^{-1}$	V_t $cm^3\ g^{-1}$	V_μ $cm^3\ g^{-1}$	X %	k h^{-1}	Qm mg g^{-1}	Modulus of LPE kJ mol^{-1}
Na_2CO_3	–0.01	23.00	0.01295	0.00215	15.1	0.0575	–	2030
K_2CO_3	0.605	178.5	0.08415	0.05715	47.5	0.1191	–	1858
NaOH	0.740	1353	0.74325	0.37165	96.0	0.6030	238.1	900
KOH	0.885	2667	1.26735	0.78515	96.5	0.5690	425.8	804

CONCLUSIONS

Activated carbons of high surface acidity, obtained by treatment with K and Na hydroxides and sulfuric acid on highly condensed carbons from Venezuelan delayed pet-coke, were active in the esterification reaction of palmitic acid, reaching conversion values of up to 97 %. The analysis of the carbonaceous solids confirms that both surface area and acidity are primary factors that promote the activity in the esterification reaction. Moreover, the results do not indicate a direct relationship between oxidized (SO_x) species and activity. The relatively low melting and decomposition temperature of Na/K hydroxides could improve their effect on the pet-coke matrix, leading to higher surface areas, acidities, and catalytic activities than treatment with carbonates. This behavior matches with the affinity of the carboxyl functions of fatty acid molecules to the polar and catalytically active centers of hydroxide treated surface of solids. Likewise, the results reveal the relationship between the lattice potential energy of Na/K hydroxides and carbonates and their efficacy, where a smaller modulus of the LPE promotes their thermal decomposition into the chemical species that perform direct pet-coke activation.

Acknowledgement. The authors thank PDVSA-INTEVEP for their invaluable collaboration in materials and characterization techniques for this work.

ИЗВОД

УЛОГА ЕНЕРГИЈЕ РЕШЕТКЕ ХЕМИЈСКИХ АГЕНСА У АКТИВАЦИЈИ ВИСОКО КОНДЕНЗОВАНОГ УГЉЕНИКА

EUMARIELYS M. ESPINOZA и LUIS F. ISERNIA

Laboratorio de Tamices Moleculares, Universidad de Oriente, Urb. Juanico, Calle Maldonado con Florida, Maturín, Estado Monagas, Venezuela

Високо кондензовани угљеник добијен од петрол кокса је прво тертиран Na/K-хидроксидима или карбонатима, па затим сумпорном киселином. Реакција естерификације палмитинске киселине на угљенику активираном хидроксидима и сумпорном кисе-

лином је достигла степен конверзије 97 %. Резултати показују везу између ефикасности Na/K-хидроксида и карбоната и њихове енергије решетке. Додатно, анализа карбонизоног материјала потврђује да су и специфична површина и киселост примарни фактори који доприносе повећању активности у реакцији естерификације. Резултати не указују на директну везу између активности и оксидованих врста (SO_x) које се појављују услед третмана сумпорном киселином. Релативно ниска температура топљења и разградње Na/K-хидроксида може унапредити њихов утицај на матрикс петрол кокса, захваљући повећању специфичне површине, киселости и каталитике активности у поређењу са третманом карбонатима. Третман хидроксидима обезбеђује већи афинит поларних и каталитички активних центара површине угљеника према карбоксилним групама масних киселина.

(Примљено 11. децембра 2020, ревидирано 22. марта, прихваћено 7. априла 2021)

REFERENCES

1. G. G. Stavropoulos, A. Zabaniotou, *Fuel Process. Technol.* **90** (2009) 952 (https://doi.org/10.1016/j.fuproc.2009.04.002)
2. D. Zeng, S. Liu, W. Gong, G. Wang, J. Qiu, Y. Tian, *Catal. Commun.* **40** (2013) 5 (https://doi.org/10.1016/j.catcom.2013.05.018)
3. S. H. Lee, CS. Choi, *Fuel Process. Technol.* **64** (2000) 141 (https://doi.org/10.1016/s0378-3820(00)00070-9)
4. M. A. Lillo, D. Cazorla, A. Linares, *Carbon* **41** (2003) 267 (https://doi.org/10.1016/S0008-6223(02)00279-8)
5. A. Onda, T. Ochi, K. Yanagisawa, *Green Chem.* **10** (2008) 1033 (https://doi.org/10.1039/b808471h)
6. J. R. Kastner, J. Miller, D. P. Geller, J. Locklin, L. H. Keith, T. Johnson, *Catal. Today* **190** (2012) 122 (https://doi.org/10.1016/j.cattod.2012.02.006)
7. L. Fjerbaek, B. G. Rong, K. V. Christensen, B. Norddahl, *Comput-Aided Chem. En.* **28** (2010) 1099 (https://doi.org/10.1016/S1570-7946(10)28184-1)
8. L. F. Isernia, *Micropor. Mesopor. Mat.* **200** (2014) 19 (http://dx.doi.org/10.1016/j.micromeso.2014.08.028)
9. Y. Feng, B. He, Y. Cao, J. Li, M. Liu, F. Yan, X. Liang, *Bioresour. Technol.* **101** (2010) 1518 (https://doi.org/10.1016/j.biortech.2009.07.084)
10. K. H. Chung, D. R. Chang, B. G. Park, *Bioresour. Technol.* **99** (2008) 7438 (https://doi.org/10.1016/j.biortech.2008.02.031)
11. A. H. Jalil, *Tikrit J. Pure Sci.* **17** (2012) 1813. ISSN: 1813 – 1662
12. M. H. Kalavathy, T. Karthikeyan, S. Rajgopal, L. R. Miranda, *J. Colloid Interface Sci.* **292** (2005) 354 (http://dx.doi.org/10.1016/j.jcis.2005.05.087)
13. J. Sahira, A. Mandira, P. B. Prasad, P. R. Ram, *Res. J. Chem. Sci.* **3** (2013) 19 (ISSN 2231-606X)
14. P. Ehrburger, A. Addoun, F. Addoun, J. Donnet, *Fuel* **65** (1986)1447 (https://doi.org/10.1016/0016-2361(86)90121-3)
15. N. Rambabu, R. Azargohar, A.K. Dalai, J. Adjaye, *Fuel Process. Technol.* **106** (2013) 501 (https://doi.org/10.1016/j.fuproc.2012.09.019)
16. K.Y. Foo, B.H. Hameed, *Chem. Eng. J.* **184** (2012) 57 (http://dx.doi.org/10.1016/j.cej.2011.12.084)

17. B. S. Girgis, L. B. Khalil, T. A. M. Tawfik, *J. Chem. Technol. Biotechnol.* **61** (1994) 87 (https://doi.org/10.1002/jctb.280610113)
18. R. T. Morrison, R. N. Boyd, *Organic Chemistry* (4th ed.), Allyn and Bacon, Boston, MA, 1983 (ISBN 978-0205058389)
19. C. H. Yoder, N. J. Flora, *Am. Mineral.***90** (2005) 488 (https://doi.org/10.2138/am.2005.1537)
20. D. F. C. Morris, E. L. Short, *Nature* **224** (1969) 950 (https://doi.org/10.1038/224950a0)
21. M. Born, J. Mayer, *Z. Phys.* **75** (1932) 1 (https://doi.org/10.1007/bf01340511)
22. E. Madelung, *Phys. Z.* **19** (1918) 524
23. A. F. Kapustinskii*, Z. Phys. Chem.* **22** (1933) 257
24. L. F. Isernia, *Ciencia* **18** (2010) 43 ISSN: 1315-2076.
25. P. A. Webb, C. Orr, *Analytical Methods in Fine Particle Technology, Micrometrics* Instrument Corporation, Norcross, GA, 1997 (ISBN 096567830X)
26. J. Swanston, in: *Ullmann's Encyclopedia of Industrial Chemistry*, Wiley-VCH, Weinheim, 2006 (https://doi.org/10.1002/14356007.a26_793.pub2)
27. H. A. H. Ibrahim, M. M. Ali, *Period. Polytech-Chem.* **48** (2004) 53
28. R. Lu, J. Lin, Z. Qu, *Struct. Chem.* **24** (2013) 507 (https://doi.org/10.1007/s11224-012-0106-z)
29. B. R. Utz, S. K. Soboezenski, S. Friedman, *Prepr. Pap. Am. Chem. Soc., Div. Fuel Chem.* **30** (1985) 35
30. X. Y. Liu, M. Huang, H. L. Ma, Z. Q. Zhang, J. M. Gao, Y. L. Zhu, X. J. Han, X. Y. Guo, *Molecules* **15** (2010) 7188 (https://doi.org/10.3390/molecules15107188)
31. P. R. S. Murray, *Principles of organic chemistry: A modern and comprehensive text for schools and colleges*, Heinemann Educational, Oxford, 1999 (ISBN 0435656430)
32. A. Sari, Ö. Iþýldak, *Bull. Chem. Soc. Ethiop.* **20** (2006) 259 (https://doi.org/10.4314/bcse.v20i2.61410)
33. H. Topallar, Y. Bayrak, *Turk. J. Chem.* **23** (1999) 193
34. J. Chudoba, B. Hrnčiř, E. J. Remmelzwaal, *Acta Hydroch. Hydrob.* **6** (1978) 153 (http://dx.doi.org/10.1002/aheh.19780060208)
35. R. P. Seward, K. E. Martin, *J. Am. Chem. Soc.***71** (1949) 3564 (https://doi.org/10.1021/ja01178a530).

Journal of the Serbian Chemical Society
JSCS-info@shd.org.rs • www.shd.org.rs/JSCS
J. Serb. Chem. Soc. *86* (10) 997–1010 (2021)
JSCS–5478
Original scientific paper
Published 10 September 2021

The programme for professional development of chemistry teachers' assessment competency

BILJANA I. TOMASEVIC*[#], DRAGICA D. TRIVIC[#], VESNA D. MILANOVIC[#] and LIDIJA R. RALEVIC[#]

University of Belgrade – Faculty of Chemistry, Studentski trg 12–16, Belgrade, Serbia

(Received 10 July, accepted 19 July 2021)

Abstract: The aim of this paper is to investigate the effects of the programme for professional development of chemistry teachers on their competencies for conducting formative and summative assessment in chemistry teaching. The programme participants were 30 chemistry teachers from primary and secondary schools. Data were collected using a questionnaire at the beginning and at the end of the programme implementation. The programme included four workshops with the same structure: the introduction, group work and the discussion of the results obtained through group work. The workshops focused on: *i*) the assessment as a support for chemistry learning; *ii*) the harmonization of teaching and learning activities, formative and summative assessment, feedback from formative assessment and the criteria used to evaluate students in summative assessment; *iii*) the evaluation of the validity of tasks used for formative and summative assessment according to the curricula aims and the educational standards; *iv*) designing tasks for monitoring students' progress towards certain educational standards. Teachers' responses show the impact of the programme for the development of their competencies for assessment, particularly regarding formative and summative assessment and designing various kinds of assessment in accordance with the achievement standards.

Keywords: in-service teacher training; formative evaluation; summative evaluation.

INTRODUCTION

Teacher knowledge was first described as a symbiosis of subject content knowledge and pedagogical knowledge necessary for the transformation of teaching topics into specific classroom activities by Shulman[1] through the model of pedagogical content knowledge (PCK). Similar models were later developed, with the emphasis on subject content knowledge as a component which provides

* Corresponding author. E-mail: bsteljic@chem.bg.ac.rs
[#] Serbian Chemical Society member.
https://doi.org/10.2298/JSC210710052T

a necessary foundation and which should be integrated with pedagogical knowledge.[2] By integrating these components specific and general pedagogical context is formed.[3] Subject content knowledge plays a crucial role in the meaningful integration of the other components of teacher knowledge.[4,5] The component "assessment of scientific literacy" was introduced by Magnusson[6] *et al.* within their PCK model (1999). The component "knowledge of science assessment" includes both teacher knowledge of the dimensions of science learning and teacher knowledge of the methods used to assess students' learning within a specific topic. When introducing the component "subject matter specific pedagogical knowledge", Tamir[7] observed that testing and evaluation should also be a part of PCK. The subsequent models of PCK point out the need for better interconnection of the components which constitute PCK,[8] as well as the nature and strength of the connection among them.[9] The interconnection and mutual dependence of all PCK components indicate that the teachers who have better knowledge of teaching strategies can also better assess students' knowledge.

In the literature and research studies, a component of PCK referred to as "teachers' assessment competence or teacher competency in educational assessment" comprises the teachers' competency in the situations which require assessment of students' knowledge. Based on the understanding of competences as a measurable ability the model of teachers' assessment competence, which enables a teacher to fulfil the requirements of assessment and quantification of knowledge in a wide range of situations, was developed.[10] This model integrates cognitive judgment processes, assessment practices and the products of assessments. It is also defined as assessment literacy (AL).

The significance and complexity of teacher knowledge of student achievement assessment can be represented using the conceptual framework teacher assessment literacy in practice (TALiP), which represents the sublimation of the research studies conducted and presented in the literature in the last several decades.[11] This framework connects two aspects of research studies – educational assessment and teacher education. Six principal components through which assessment literacy (AL) should be considered are pointed out: 1. the knowledge base of assessment, 2. teacher conception of assessment, 3. institutional and socio-cultural contexts, 4. TALiP the core concept of the framework, 5. teacher learning and 6. teacher identity (re)construction as assessors.

Since education and its requirements change during every teacher's career, it is necessary for teachers to improve their competencies through the programmes of professional development and training.[12] The need for continuous teacher development is particularly important in the situation when some significant changes in the education system are introduced due to reforms or new regulations.[13,17] However, it seems that not enough attention is devoted to teachers' competences to conduct assessment of knowledge[18] within these programmes.

The complexity of the nature of knowledge assessment is caused by many inseparable educational and social functions which result from the structure and organization of the entire education system.[19,20] In a research study which investigated teachers' attitudes towards knowledge assessment, the items in the questionnaire related to four concepts of assessment: improvement, student accountability, school accountability and irrelevance.[21] There was not a statistically significant difference between the attitudes of primary and secondary school teachers towards school accountability and irrelevance. Primary school teachers agreed statistically significantly more with the statements which associated assessment activities with the potential for Improvement. Statistically significantly more secondary school teachers agreed with the significance of assessment for Student Accountability. There was a correlation of the concept of Improvement with School Accountability, but there was no correlation with Student Accountability. This means that the teachers were willing to assume the responsibility for improving school outcomes and quality and fulfilling their professional accountabilities, they were willing to include assessment in their professional responsibilities in order to improve teaching and learning process, but they were less aware of the significance of Student Accountability. The effects of assessment on teaching and learning, certification of learning and accountability of teaching were considered to have greater pedagogical-regulation significance by the primary school teachers, while they were considered to have greater societal-accreditation significance by the secondary school teachers.[19] The conducted cluster analysis showed that teachers could have different attitudes towards assessment at the same time.[22] More than half of the teachers (51 %) had moderate, average and homogenous views on different purposes of assessment which related to the attitudes that "Assessment improves teaching and learning", that "Assessment is valid for accountability" and that "Assessment is irrelevant". 28 % of teachers expressed their opinion that the most important purpose of assessment is to improve teaching and learning. Approximately 21 % of the teachers had a marked tendency to question the accuracy of assessment and believed that it had no impact on their teaching practice.

When evaluating the questionnaire items which related to the criteria of high quality assessment on an 1–5 scale, the teachers gave high grades for all ten criteria.[23] They identified "Transparency" as the most important criterion (4.50), while "Directness" (3.93) and "Reproducibility" (3.88) were considered to be the least significant. The results show that teachers consider the existing, classic assessment criteria equally important as some new ones (authenticity, cognitive complexity, costs and efficiency, directness, educational consequences and meaningfulness) which have been introduced with the orientation being shifted towards competency-based education and assessment. This finding was contrary to researchers' expectations since teachers are sometimes reluctant to accept such

changes, but this research study did not investigate whether the teachers actually appreciated and applied all assessment criteria in their teaching practice.

In view of the theoretical framework presented above, the aim of this paper was to establish the effects of the programme for professional development of chemistry teachers on their competencies for conducting formative and summative assessment in chemistry teaching. Based on the aim, the following research question was raised: How do teachers' attitudes towards the assessment in general and the formative and summative assessment of student achievements change under the influence of the programme for professional development of chemistry teachers' assessment competency?

EXPERIMENTAL

Assessment was the main focus of the two-day programme for professional development of chemistry teachers' assessment competency (PDChTAC), which was organized by the Serbian Chemical Society and the University of Belgrade – the Faculty of Chemistry. Four workshops were held in two days. The structure of all workshops was the same and they included an introduction, group work and a discussion of the results obtained through group work. The first workshop focused on assessment as a support for chemistry learning. The second workshop focused on the issue of how to harmonize teaching and learning activities, formative and summative assessment, feedback from formative assessment and the criteria by which students are evaluated in the summative assessment. Within the third workshop participants evaluated in groups the validity of tasks used for formative and summative assessment according to the curricula aims and the educational standards. In the fourth workshop the participants designed tasks for monitoring students' progress towards certain educational standards. Bearing in mind the research question, the data about the participants' attitudes towards assessment were collected using a questionnaire both before and after the programme realization. The completion of the questionnaires was on a voluntary and anonymous basis and in accordance with the Code of Conduct for Scientific Research of the University of Belgrade (http://bg.ac.rs/files/sr/univerzitet/univ-propisi/Kodeks-naucnoistrazivacki-rad-29.3.2018.pdf). The aim of the questionnaire completion was explained in several introductory sentences at the beginning of the questionnaire, and respondents were guaranteed the confidentiality of the data collected.

Sample

Thirty chemistry teachers from primary and secondary schools participated in the programme. The participants' demographic data are shown in Table I.

Out of the 30 participants, 29 were females, while one was a male. The largest number of the teachers were in 40–49 age group. Four fifths of the teachers in the sample had over 10 years of experience. University courses through which teachers could develop assessment literacy (Chemistry didactics, pedagogy and psychology) had been attended by 22 (73.3 %) participants.

Instrument

The questionnaire designed for this research study consisted of four parts: I – general information about the respondents; II – teachers' attitudes towards their usual practice of assessment of student achievements; III – teachers' general attitudes towards assessment of

student achievements; IV – teachers' attitudes towards competencies necessary for assessment of student achievements.

The questionnaire contained 59 questions altogether: 6 multiple choice questions, one open-ended question, and 52 questions in which the respondents were asked to express the level of their agreement on a Likert-type scale.

TABLE I. Background data of the sample (N = 30), C – contribution of teachers in each category

Work place[a]	C / %	Age	C / %	Length of service	C / %	Education	C / %	University faculty[b]	C / %
PS	16.7	30-39	6.7	1-5	10.0	Undergraduate studies	80.0	UBFC	70.0
GS	36.7	40-49	60.0	6-10	10.0	Undergraduate and master studies	20.0	UNSFS	6.7
VS	40.0	50-59	30.0	11-15	26.7			UBFTM	3.3
PS, GS, VS	3.3	60+	3.3	16-20	20.0			UKFS	10.0
PS, GS	3.3			20-30	30.0			UPKMFSM	3.3
				30+	3.3			UBFP	3.3
								USFES	3.3

[a]PS – primary school, GS – grammar school, VS – vocational school; [b]UBFC: University of Belgrade – Faculty of Chemistry; UNSFS: University of Novi Sad – Faculty of Sciences; UBFTM: University of Belgrade – Faculty of Technology and Metallurgy, UKFS: University of Kragujevac – Faculty of Sciences; UPKMFSM: University of Pristina, Kosovska Mitrovica – Faculty of Sciences and Mathematics; UBFP: University of Belgrade – Faculty of Physics; USFES: University of Sarajevo – Faculty of Educational Sciences

To confirm the content validity, the questionnaire was examined by the members of the Department of Chemical Education, the University of Belgrade – Faculty of Chemistry, who were familiar with the construct of interest and the research subject, but who were not involved in designing and conducting the actual research study. They also reviewed readability, clarity and comprehensiveness of the questions in the questionnaire and provided a coherent estimation of the content validity of the questionnaire.

The reliability of the questionnaire was examined by means of Cronbach's α coefficient.[24] The value of Cronbach's α coefficient in the part with Likert-type questions was 0.873 for the first application of the questionnaire, and 0.866 for the second application of the questionnaire, which indicated a satisfactory level of the internal consistency of the instrument.

RESULTS AND DISCUSSION

Teachers' evaluations of the statements in the questionnaire provide an insight into the current practice of assessing and grading student achievements in the field of chemistry in our schools (Table II).

The most frequent evaluations of chemistry teachers regarding the assessment practice in our schools (Table II) will be presented in the following part of this paper. Teachers rarely change grading criteria based on the results of written assessment of students and decision on grades based on students' suggestions and arguments. However, they more often include the effort invested by the student

in the grade and the majority of them always or almost always provide their students with an explanation for the grades awarded. The largest number of teachers sometimes or very often grade their students in the lessons during which new material is introduced, but very often or always and almost always try to make assessment contribute to further learning.

TABLE II. The teachers' attitudes towards teaching practice of assessment of student achievements: 1– never or almost never; 2 – very rarely; 3 – sometimes; 4 – very often; 5 – always or almost always

Statement	Contribution, %				
	1	2	3	4	5
1. I change the criteria for grading written assessment of knowledge after gaining insight into students' results.	6.7	40.0	16.7	30.0	6.7
2. I include the effort invested by a student in his grade.	–	3.3	30.0	30.0	36.7
3. I change my decision about the grade after students' suggestions or arguments.	16.7	23.3	40.0	16.7	–
4. I create questions for oral assessment of knowledge before the lesson.	3.3	3.3	20.0	40.0	30.0
5. I use the material designed by my colleagues for assessment of knowledge.	20.0	30.0	36.7	13.3	–
6. I grade my students in the lessons when new material is introduced.	–	10.0	36.7	46.7	6.7
7. I provide an explanation for the grades given to my students.	–	–	–	10.0	90.0
8. I attempt to make knowledge assessment contribute to further learning.	–	–	–	23.3	76.7
9. Upon unsatisfactory results of assessing knowledge of certain concepts, I explain the same concepts again.	–	6.7	13.3	50.0	30.0
10. When assessing achievements I take into account the student achievement standards.[a]	13.3	6.7	10.0	40.0	30.0
11. I design tasks for written assessment of knowledge bearing in mind the student achievement standards.[a]	6.7	6.7	6.7	43.3	36.7
12. I design tasks for oral assessment of knowledge bearing in mind the student achievement standards.[a]	6.7	6.7	13.3	53.3	20.0
13. I design tasks for practical assessment of knowledge bearing in mind the student achievement standards.[*]	10.0	3.3	20.0	53.3	13.3
14. I provide feedback on the level of achievement and recommendations for further work to each student.	–	3.3	–	33.3	63.3
15. I make my decision on the final grade based on the results of formative and summative assessment of knowledge.	–	–	3.3	33.3	60.0
16. I give my tests to colleagues so that they evaluate their quality and validity before their application in practice.	13.3	20.0	20.0	33.3	13.3
17. I include my students in defining the criteria by which their achievements will be assessed.	6.7	20.0	13.3	53.3	6.7
18. I include my students in the assessment of other students' achievements.	10.0	10.0	23.3	40.0	16.7

[a]The student achievement standards at the end of compulsory education and at the end of general secondary education

The majority of teachers very often or always and almost always explain the concepts again after unsatisfactory results of assessment of knowledge. Teachers sometimes or very rarely use materials for knowledge assessment designed by their colleagues. The majority of teachers very often or always and almost always create questions for oral assessment of knowledge before the lesson. Generally, teachers very often or always and almost always take into account the student achievement standards, mostly during the process of designing the tasks for written assessment of knowledge, to a lesser extent when designing questions for oral assessment of knowledge and least for practical assessment of knowledge. The majority of teachers very often or always and almost always provide their students with feedback on the level of achievement and recommendations for further work, and they make their decision on the final grade based on formative and summative assessment of knowledge. 40 % of the teachers very rarely or sometimes give their tests to colleagues for the evaluation of quality and validity before using them in the classroom, while 33 % of them do this very often. Slightly more than half of the teachers very often include their students in defining the criteria for evaluating achievements, while one fifth does this very rarely. 40 % percent of the teachers very often include students in the evaluation of other students' achievement, while 23 % does this sometimes.

Teachers' attitudes towards the function of assessment before the realization of the programme for PDChTAC, and after the realization of the programme can be observed from the degree of agreement with the statements presented in Table III.

Since the same group evaluated these variables, the sample is not independent, so the Wilcoxon test was used to determine whether there were any statistically significant differences between the evaluations provided by the group before and after the realization of the programme for PDChTAC. Using SPSS output, the data analysis shows that the evaluations provided by the group are statistically significantly different for 6 out of 18 variables. In the following part the results for the attitudes of teachers which are statistically significantly different compared to the attitudes which had been expressed immediately before the beginning of the development programme will be presented.

The largest percentage of teachers mainly or strongly agreed that the assessment of student achievements is as important in the teaching process as acquiring new knowledge on both occasions when their attitudes were investigated using the same question within the research study. Upon the programme completion the number of teachers who strongly agreed with the above-mentioned statement increased ($z = -2.32$, $p < 0.05$). After the development programme a larger number of teachers expressed their opinion that they mainly agreed with the statement that student achievements should be assessed in each lesson ($z = -4.42$, $p < 0.0001$). A large number of teachers changed their attitude that each assessment of achievement should result in a grade, so two thirds of the participants

stated that they strongly or mainly disagreed with this attitude ($z = -2.26$, $p < 0.05$). After the programme the number of teachers who strongly agreed that the result of formative assessment enables a student to gain an insight into his current level of achievement increased ($z = -2.30$, $p < 0.05$), while none of the teachers expressed disagreement with this attitude anymore.

TABLE III. Teachers' attitudes towards the assessment of student achievements; i – at the beginning of the programme realization; f – at the end of the programme realization: 1 – strongly disagree; 2 – mainly disagree; 3 – both agree and disagree; 4 – mainly agree; 5 – strongly agree

Statement		Contribution, %				
		1	2	3	4	5
1. Assessment of student achievements and acquiring knowledge are equally important parts of the teaching process.	i	–	–	3.3	36.7	60.0
	f	–	–	–	13.3	86.7
2. Student achievements should be assessed in every lesson.	i	–	–	23.3	30.0	46.7
	f	–	–	6.7	46.7	46.7
3. The outcome of each assessment should be a grade.	i	13.3	16.7	50.0	20.0	
	f	23.3	43.3	26.7	6.7	–
4. Written, oral and practical assessment can provide the same kind of feedback on student achievements.	i	6.7	20.0	33.3	33.3	6.7
	f	13.3	30.0	26.7	23.3	6.7
5. One kind of assessment is sufficient to gain an insight into student achievements.	i	50.0	40.0	6.7	–	3.3
	f	76.7	20.0	3.3	–	–
6. The results of formative assessment provide a student with an insight into the current level of his achievements.	i	3.3	6.7	13.3	63.3	13.3
	f	–	–	13.3	43.3	43.3
7. Being familiar with the assessment criteria contributes to better student achievements.	i	–	3.3	3.3	53.3	40.0
	f	–	–	3.3	40.0	56.7
8. Providing an explanation for the grade has a positive impact on student's subsequent work.	i	–	–	6.7	30.0	63.3
	f	–	–	–	36.7	63.3
9. Students learn through the process of achievement assessment.	i	–	–	13.3	50.0	33.3
	f	–	–	13.3	36.7	50.0
10. The results of achievement assessment depend on the type of assessment applied.	i	–	10.0	30.0	46.7	10.0
	f	–	–	43.3	43.3	13.3
11. Good practice in achievement assessment includes a discussion on the level of knowledge achieved by students.	i	–	–	13.3	36.7	50.0
	f	–	–	10.0	43.3	46.7
12. Unannounced assessment of knowledge leads to worse results than announced assessment.	i	–	3.3	36.7	30.0	30.0
	f	–	13.3	36.7	26.7	23.3
13. Formative assessment of knowledge requires special preparation and analysis.	i	–	3.3	26.7	46.7	23.3
	f	–	10.0	20.0	36.7	33.3
14. Knowledge assessment should present learning in a new context.	i	–	3.3	10.0	76.7	6.7
	f	–	6.7	10.0	40.0	43.3
15. Knowledge assessment should enable the improvement of learning strategies.	i	–	–	–	53.3	43.3
	f	–	–	6.7	43.3	50.0
16. Students can draw conclusions about the level of their achievements based on their grade.	i	–	3.3	43.3	40.0	13.3
	f	–	–	20.0	56.7	23.3
17. A grade higher than the current level of achievement has a positive effect on student's further progress.	i	–	10.0	43.3	36.7	10.0
	f	–	13.3	33.3	40.0	13.3
18. Formative assessment excludes summative assessment.	i	23.3	23.3	43.3	6.7	3.3
	f	53.3	26.7	13.3	3.3	3.3

Furthermore, the number of teachers who mainly or strongly agreed with the statement that students can draw a conclusion about the level of their achievement based on the grade increased ($z = -2.83$, $p < 0.01$). There was a statistically significant difference in the number of teachers who had previously been undecided, but who expressed their opinion that they strongly or mainly disagreed with the statement that formative assessment excludes summative assessment after the programme completion ($z = -2.40$, $p < 0.05$).

There were no statistically significant differences in the teachers' attitudes for the other 12 statements after the programme completion, but the results show that there were certain shifts and changes. A higher percentage of teachers expressed their attitude that they strongly or mainly disagreed with the statements that written, oral and practical assessment can provide the same kind of feedback on student achievements and that one kind of assessment is sufficient to gain an insight into student achievements. Furthermore, a higher percentage of teachers mainly or strongly agreed that being familiar with the assessment criteria contributes to better student achievements, which providing an explanation for a grade has a positive impact on students' subsequent work and that students learn through the process of assessment of achievement.

The questionnaire was also used to investigate the teachers' attitudes towards their competencies for assessing student achievements. The results obtained through their responses are presented in Table IV.

The Wilcoxon test was used to determine whether there were any statistically significant differences in the evaluations obtained from the group. Using SPSS output, the data analysis shows that the evaluations obtained from the group is statistically significantly different for 8 variables. In the following part the results for teachers' attitudes between which there was a statistically significant difference after the realization of the programme for PDChTAC are presented. In comparison with the initial evaluations, a higher percentage of teachers strongly agreed that they could monitor and evaluate the effectiveness of their work based on the results obtained through knowledge assessment ($z = -2.97$, $p < 0.005$) and that they understood the concepts of formative and summative assessment ($z = -3.54$, $p < 0.001$). Almost all teachers mainly or strongly agreed that they were competent to design and realize formative assessment of knowledge ($z = -2.37$, $p < 0.05$) and summative assessment of knowledge ($z = -2.99$, $p < 0.05$).

The number of teachers who considered that they were competent to design and conduct written assessment in accordance with the achievement standards also increased ($z = -2.07$, $p < 0.05$) after the development programme, and none of the teachers expressed disagreement with this statement.

TABLE IV. The teachers' attitudes towards the competencies for assessing student achievements; i – at the beginning of the programme realization; f – at the end of the programme realization: 1 – I strongly disagree; 2 – I mainly disagree; 3 – I both agree and disagree; 4 – I mainly agree; 5 – I strongly agree

Statement		Contribution, %				
		1	2	3	4	5
1. I meet the competency standards for the teaching profession.	i	–	–	–	36.7	63.3
	f	–	–	3.3	46.7	50.0
2. I am competent to design and conduct knowledge assessment in accordance with the student achievement standards.	i	–	–	16.7	43.3	36.7
	f	–	–	6.7	60.0	33.3
3. I successfully adapt knowledge assessment to students' individual abilities.	i	–	6.7	30.0	40.0	23.3
	f	–	–	26.7	60.0	13.3
4. I can monitor and evaluate the effectiveness of my work based on the results obtained through knowledge assessment.	i	–	–	23.3	66.7	10.0
	f	–	–	10.0	53.3	36.7
5. I am competent to assess student achievements using various types of assessment.	i	–	–	6.7	50.0	40.0
	f	–	–	3.3	56.7	36.7
6. I understand the concepts of formative and summative assessment.	i	3.3	6.7	30.0	36.7	20.0
	f	–	–	3.3	33.3	63.3
7. I am competent to design and conduct formative assessment of knowledge.	i	–	3.3	30.0	40.0	26.7
	f	–	–	3.3	56.7	40.0
8. I am competent to design and conduct summative assessment of knowledge.	i	–	6.7	30.0	36.7	26.7
	f	–	–	–	50.0	50.0
9. I am competent to design and conduct written assessment of knowledge in accordance with the goals of chemistry education.	i	–	–	6.7	36.7	56.7
	f	–	–	–	43.3	56.7
10. I am competent to design and conduct oral assessment of knowledge in accordance with the goals of chemistry education.	i	–	–	–	50.0	50.0
	f	–	–	–	40.0	60.0
11. I am competent to design and conduct practical assessment of knowledge in accordance with the goals of chemistry education.	i	3.3	–	6.7	63.3	26.7
	f	–	3.3	10.0	40.0	46.7
12. I am competent to design and conduct written assessment of knowledge in accordance with the achievement standards.	i	3.3	3.3	13.3	46.7	33.3
	f	–	–	10.0	43.3	46.7
13. I am competent to design and conduct oral assessment of knowledge in accordance with the achievement standards.	i	3.3	3.3	20.0	36.7	36.7
	f	–	–	6.7	43.3	50.0
14. I am competent to design practical assessment of knowledge in accordance with the achievement standards.	i	6.7	3.3	26.7	36.7	26.7
	f	–	3.3	16.7	46.7	33.3
15. I have improved my competencies for monitoring and evaluating student achievements through professional development programmes.	i	10.0	3.3	20.0	30.0	36.7
	f	–	–	6.7	40.0	53.3
16. I have improved my competencies for monitoring and evaluating student achievements by reading specialized and scientific publications.	i	6.7	6.7	6.7	53.3	23.3
	f	–	–	10.0	56.7	33.3

A considerably higher percentage of teachers mainly or strongly agreed that they were competent to design and conduct oral assessment of knowledge ($z = -2.54$, $p < 0.05$) and practical assessment of knowledge ($z = -2.05$, $p < 0.05$) in accordance with the achievement standards. Responding to the statement which referred to the previous improvement of competencies for monitoring and evaluating student achievements through professional development programmes, the teachers obviously included their experience of attending the programme for PDChTAC ($z = -2.50$, $p < 0.05$).

As far as the other statements are concerned, there was no statistically significant difference between the responses given before and after the development programme, but a higher percentage of teachers mainly or strongly agreed with the statement that they were competent to design and conduct knowledge assessment in accordance with the student achievement standards and that they adapted knowledge assessment to individual abilities of their students.

CONCLUSION

Teachers' responses regarding their assessment practice, *i.e.*, how it is conducted in schools, indicate that teachers attempt to harmonize it with the requirements prescribed by primary and secondary school regulations (they provide their students with an explanation for their grades, they attempt to make assessment contribute to further learning, they make their decisions about final grade based on the results of formative and summative assessment, they provide their students with feedback and guidelines for subsequent work, they explain the material again in case their students failed to learn it, they take into account students' effort when assessing them, they plan assessment in accordance with the student achievement standards). However, they more rarely consider the criteria which they use to decide upon grades and they more rarely consider grades in the light of students' arguments. Based on teachers' responses it can be observed that they do not cooperate enough with their colleagues as far as assessment is concerned, both regarding the use of material developed by others and asking their colleagues' opinion about the quality and validity of the instruments they use to assess student achievements.

The two-day professional development programme for chemistry teachers, which focused on strengthening their competencies for assessment, influenced the teachers in such a way that there were statistically significant differences regarding their more positive attitudes towards the following statements:

– knowledge assessment and learning are equally important segments of teaching;
– knowledge assessment should be conducted continually (in every lesson);
– formative assessment helps a student gain an insight into his current level of his achievements;

– grades enable students to gain an insight into their level of achievements.

In addition to this, the programme has caused a statistically significant increase in the number of teachers who disagree with the statements that each assessment of achievement should result in a grade and that formative assessment excludes summative assessment.

As far as the statements which refer to the competencies for assessment are concerned, after the programme, a statistically significant percentage of teachers have a more positive attitude towards the following statements:

– they can monitor and evaluate the effectiveness of their work based on the results of knowledge assessment;

– they understand the concepts of formative and summative assessment;

– they are competent to design and conduct formative and summative assessment of knowledge.

Upon the programme completion, there was a statistically significant increase in the number of teachers who evaluated that they were more competent to design and conduct written, oral and practical assessment based on the achievement standards.

Teachers' responses show the impact of the programme for the development of their competencies for assessment, particularly regarding formative and summative assessment and designing various kinds of assessment in accordance with the achievement standards. This is a unique teacher development programme in our education system which has changes identified in the knowledge, skills and attitudes of the teachers upon its realization.

Acknowledgement. Ministry of Education, Science and Technological Development of the Republic of Serbia, Contract number: 451-03-9/2021-14/200168.

ИЗВОД

ПРОГРАМ ПРОФЕСИОНАЛНОГ РАЗВОЈА КОМПЕТЕНЦИЈА НАСТАВНИКА ХЕМИЈЕ ЗА ПРОВЕРУ ЗНАЊА

БИЉАНА И. ТОМАШЕВИЋ, ДРАГИЦА Д. ТРИВИЋ, ВЕСНА Д. МИЛАНОВИЋ и ЛИДИЈА Р. РАЛЕВИЋ

Универзитет у Београду – Хемијски факултет, Студентски трг 12-16, Београд

Циљ овог рада је испитивање ефеката програма за професионални развој наставника хемије на њихове компетенције за извођење формативног и сумативног оцењивања у настави хемије. У програму је учествовало 30 наставника хемије из основних и средњих школа. Подаци су прикупљени помоћу упитника, примењеног на почетку и на крају реализације програма. Програм се састојао од четири радионице са истом структуром рада: увод, групни рад и дискусија резултата групног рада. Радионице су биле посвећене: 1) оцењивању као подршци учењу хемије; 2) усклађености активности наставе и учења, формативног и сумативног оцењивања, повратних информација формативног оцењивања и критеријума за сумативно оцењивање; 3) процени ваљаности задатака за формативно и сумативно оцењивање у складу с циљевима наставних програма и образовним стандардима; 4) припреми задатака за праћење напретка ученика

према одређеним образовним стандардима. Одговори наставника показују допринос програма развоју њихових компетенција за праћење и проверавање ученичких постигнућа, посебно у вези с формативним и сумативним проверавањем и припремањем различитих начина проверавања усклађено са стандардима постигнућа.

(Примљено 10. јула, прихваћено 19. јула 2021)

REFERENCES

1. L. S. Shulman, *Educ. Res*. **15** (1986) 4 (https://doi.org/10.2307/1175860)
2. N. Geddis, *Int. J. Sci. Educ.* **15** (1993) 673 (https://doi.org/10.1080/0950069930150605)
3. W. S. Carlsen, in *Examining Pedagogical Content Knowledge: The Construct and its Implications for Science Education*, J. Gess-Newsome, N. Lederman, Eds., Kluwer Academic, Springer, Dordrecht, 1999, p. 133 (ISBN: 978-0-7923-5903-6)
4. H. Borko, *Educ. Res*. **33** (2004) 3 (https://doi.org/10.3102/0013189X033008003)
5. J. H. Van Driel, O. De Jong, N. Verloop, *Sci. Educ.* **86** (2002) 572 (https://doi.org/10.1002/sce.10010)
6. S. Magnusson, J. Krajcik, H. Borko, in *Examining Pedagogical Content Knowledge: The Construct and its Implications for Science*, J. Gess-Newsome, N. Lederman, Eds., Kluwer Academic, Springer, Dordrecht, 1999, p. 95 (ISBN : 978-0-7923-5903-6)
7. P. Tamir, *Teach. Teach. Educ*. **4** (1988) 99 (https://doi.org/10.1016/0742-051X(88)90011-X)
8. S. Park, Y. Chen, *J. Res. Sci. Teach*. **49** (2012) 922 (https://doi.org/10.1002/tea.21022)
9. S. Aydin, Y. Boz, *Chem. Educ. Res. Pract*. **14** (2013) 615 (https://doi.org/10.1039/C3RP00095H)
10. S. Herppich, A. K. Praetorius, N. Förster, I. Glogger-Frey, K. Karst, D. Leutner, L. Behrmann, M. Böhmer, S. Ufer, J. Klug, A. Hetmanek, A. Ohle, I. Böhmer, C. Karing, J. Kaiser, A. Südkamp, *Teach. Teach. Educ*. **76** (2018) 181 (https://doi.org/10.1016/j.tate.2017.12.001)
11. Y. Xu, G. T. L. Brown, *Teach. Teach. Educ*. **58** (2016) 149 (https://doi.org/10.1016/J.TATE.2016.05.010)
12. W. J. Popham, *Theory Pract*. **48** (2009) 4 (http://www.jstor.org/stable/40071570)
13. T. C. Visser, F. G. M. Coenders, J. M. Pieters, C. Terlouw, *J. Sci. Educ. Technol.* **22** (2013) 807 (https://doi.org/10.1007/s10956-012-9432-6)
14. Hofstein, *Chem. Educ. Int.* **6** (2005) 1 (https://old.iupac.org/publications/cei/vol6/13_Hofstein.pdf)
15. M. J. Stolk, A. M.W. Bulte, O. De Jong, A. Pilot, *Chem. Educ. Res. Pract*. **10** (2009) 154 (https://doi.org/10.1039/B908252M)
16. E. J. Yezierskia, D. G. Herrington, *Chem. Educ. Res. Pract*. **12** (2011) 344 (https://doi.org/10.1039/C1RP90041B)
17. M. J. Stolk, A. M. W. Bulte, O. de Jong, A. Pilot, *Chem. Educ. Res. Pract*. **10** (2009) 164 (https://doi.org/10.1039/B908255G)
18. T. Holme, S. L. Bretz, M. Cooper, J. Lewis, P. Paek, N. Pienta, A. Stacy, R. Stevens, M.Towns, *Chem. Educ. Res. Pract*. **11** (2010) 92 (https://doi.org/10.1039/C005352J)
19. Remesal, *Teach. Teach. Educ*. **27** (2011) 472 (https://doi.org/10.1016/j.tate.2010.09.017)
20. N. Pope, S. K. Green , R. L. Johnson, M. Mitchell, *Teach. Teach. Educ*. **25** (2009) 778 (https://doi.org/10.1016/j.tate.2008.11.013)

21. G. T. L. Brown, R. Lake, G. Matters, *Teach. Teach. Educ*. **27** (2011) 210 (https://doi.org/10.1016/j.tate.2010.08.003)
22. N. Barnes, H. Fives, C. M. Dacey, *Teach. Teach. Educ*. **65** (2017) 107 (http://dx.doi.org/10.1016/j.tate.2017.02.017)
23. L. K. J. Baartman, T. J. Bastiaens, P. A. Kirschner, C. P. M. Van der Vleuten, *Teach. Teach. Educ*. **23** (2007) 857 (https://doi.org/10.1016/j.tate.2006.04.043)
24. L. Cohen, L. Manion, K. Morrison, *Research methods in education*, Routledge, London, 2007, p. 506 (ISBN-13: 978-0415368780).

Errata
(Printed version only)

1. Volume 86, Issue 9, Cover Page, first line from the top should read:

JSCSEN 86(9)781–899(2021)

2. Volume 86, Issue 9, Page 899 should read:

J. Serb. Chem. Soc. 86 (9) 899 (2021) *Note*
JSCS–5470 Published 17 August, 2021

Retracting Note

Paper entitled "Bioleaching of copper, zinc and gold from a polymetallic ore flotation concentrate from Čoka Marin deposite (Serbia)", by J. Avdalović *et al.* https://doi.org/10.2298/JSC210127016A, published on August 1, 2021 in the OnLine First section of the Journal of the Serbian Chemical Society has been retracted and withdrawn since the authors (corresponding author) did not approve galley proof prepared by Editorial office.

Retracted manuscript was deposited in the DoiSerbia quarantine, Repository service of the National Library of Serbia: http://doiserbia.nb.rs/issue.aspx?issueid=1981

https://doi.org/10.2298/JSC210817062R